

Power in wheelchair propulsion

Advancing the use of wearable sensors for wheelchair sports practice

van Dijk, M.P.

DOI

[10.4233/uuid:b8f6bc3e-1d8d-496c-8e60-35acd1763c57](https://doi.org/10.4233/uuid:b8f6bc3e-1d8d-496c-8e60-35acd1763c57)

Publication date

2024

Document Version

Final published version

Citation (APA)

van Dijk, M. P. (2024). *Power in wheelchair propulsion: Advancing the use of wearable sensors for wheelchair sports practice*. [Dissertation (TU Delft), Delft University of Technology].
<https://doi.org/10.4233/uuid:b8f6bc3e-1d8d-496c-8e60-35acd1763c57>

Important note

To cite this publication, please use the final published version (if applicable).
Please check the document version above.

Copyright

Other than for strictly personal use, it is not permitted to download, forward or distribute the text or part of it, without the consent of the author(s) and/or copyright holder(s), unless the work is under an open content license such as Creative Commons.

Takedown policy

Please contact us and provide details if you believe this document breaches copyrights.
We will remove access to the work immediately and investigate your claim.

POWER IN WHEELCHAIR PROPULSION

Advancing the use of wearable sensors
for wheelchair sports practice

MARIT VAN DIJK



POWER IN WHEELCHAIR PROPULSION

Advancing the use of wearable sensors for
wheelchair sports practice

Marit van Dijk

This work was supported by ZonMw under project number 546003002. This project, named WheelPower: wheelchair sports and data science push it to the limit is a cooperative effort between TU Delft, VU Amsterdam, THUAS, UMCG and is in cooperation with several sports federations collected under the umbrella of NOC*NSF.

Printing of this dissertation was generously and non-commercially sponsored by the Department of Biomechanical Engineering.

ISBN: 978-94-6384-571-7

Cover & Elementen: Wendy Schoneveld

Layout: Marit van Dijk

Printed by: proefschriftmaken.nl

© Marit van Dijk, 2024

All rights reserved. No part of this thesis may be reproduced, stored or transmitted in any form or by any means without prior permission of the author, or the copyright-owning journals for previously published chapters.

An electronic version of this dissertation is available at <https://repository.tudelft.nl/>

Power in wheelchair propulsion

Advancing the use of wearable sensors for wheelchair sports practice

Proefschrift

ter verkrijging van de graad van doctor
aan de Technische Universiteit Delft,
op gezag van de Rector Magnificus prof.dr.ir. T.H.J.J. van der Hagen;
voorzitter van het College voor Promoties,
in het openbaar te verdedigen op
woensdag 29 mei 2024 om 17:30 uur

door

Maria Petronella VAN DIJK
Master of Science in Artificial Intelligence
Master of Science in Human Movement Sciences
Vrije Universiteit Amsterdam, Nederland,
geboren te Rotterdam, Nederland

Dit proefschrift is goedgekeurd door de promotoren.

De promotiecommissie bestaat uit de volgende samenstelling:

Rector magnificus	voorzitter
Prof.dr. H.E.J. Veeger	Delft University of Technology, promotor
Dr. M.J.M. Hoozemans	Vrije Universiteit Amsterdam, promotor
Dr. M.A.M. Berger	The Hague University of Applied Sciences, copromotor

Onafhankelijke leden:	
Prof. dr. F.C.T. van der Helm	Delft University of Technology
Prof. dr. ir. G. Jongbloed	Delft University of Technology
Dr. M. Kok	Delft University of Technology
Dr. Eng. D. Paez-Granados	Eidgenössische Technische Hochschule Zürich
Prof. dr. J. Dankelman	Delft University of Technology (reserve member)

Geloof niet alles wat je denkt

TABLE OF CONTENTS

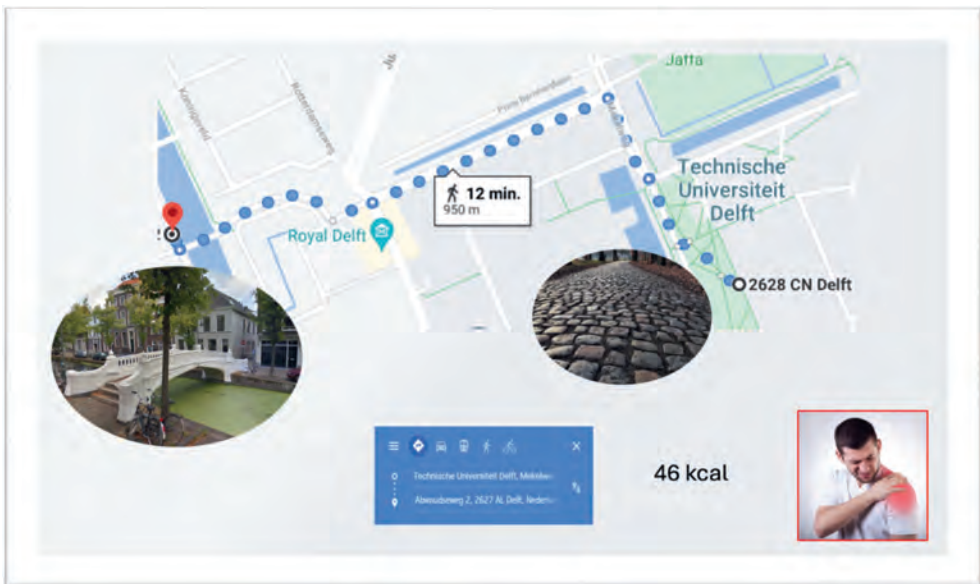
Chapter 1	General Introduction	11
	Part I From theory to practice: Estimating mechanical power during in-field wheelchair propulsion	
Chapter 2	Using wearable sensors to estimate mechanical power output in cyclical sports other than cycling - A review	23
Chapter 3	From theory to practice: monitoring mechanical power output during wheelchair field and court sports using inertial measurement units	43
	Part II Pushing further: The role of trunk motion on estimating power during wheelchair propulsion	
Chapter 4	Machine learning to improve orientation estimation in sports situations challenging for inertial sensor use	65
Chapter 5	Trunk motion influences mechanical power estimates during wheelchair propulsion	85
	Part III Power for all: Meeting the demands of different wheelchair user populations	
Chapter 6	Towards an accurate rolling resistance: Estimating intra-cycle load distribution between front- and rear wheels during wheelchair propulsion from inertial sensors	103
Chapter 7	The combined strength of standardized lab sprint testing and wheelchair mobility field testing among wheelchair tennis players	121
Chapter 8	Obtaining wheelchair kinematics with one sensor only? The trade-off between number of inertial sensors and accuracy for measuring wheelchair mobility performance in sports	139
Chapter 9	Rim Hit DEtection system: an accessible and easy applicable device to monitor push technique during overground wheelchair propulsion	151
Chapter 10	General Discussion	159
	Summary	174
	Samenvatting	176
	Dankwoord	178
	List of publications	182
	Curriculum Vitae	185

Wheelchair power to the people

'Imagine that you just drove your wheelchair for half an hour over bumpy roads and some grassy spots (Google Maps told you that this would be the shortest way). While taking a short break, you feel sweaty. Your shoulders hurt. Your smartwatch informs you that you took only 50 steps, burned virtually no calories and that it's "time to stand up".' Wearable sensors have become more and more part of our daily lives and are widely used to encourage a healthy lifestyle. However, despite rapid developments in this field, these systems are obviously not well adjusted for every type of user yet.

This dissertation outlines the possibilities of monitoring power during daily wheelchair (sports) practice. Although the dissertation focuses on estimating power, i.e., calories per second, in wheelchair sports, this could be the start of a wheelchair-specific smartwatch that allows wheelchair athletes and users to self-track their activities, to get warned when they tend to overuse their shoulders, and to eventually take over Strava. With all data that will be collected in this way, Google Maps may suggest wheelchair accessible routes, municipalities gain insight into the wheelchair (in)accessibility of their public areas, and wheelchair design can be optimized. Starting with 'wheelchair power to the people', I hope that this dissertation will ultimately bring some ...

Power to the wheelchair people





CHAPTER 1

General introduction

Introduction

The power of monitoring power

‘Imagine a beautiful sunny day in September. You are cycling home from work. While you cycle with exactly the same speed as in the morning, the ride in the afternoon feels much tougher. This may be caused by the long working day at which you have struggled with writing a proper start of your dissertation. However, it may also be that you are facing a strong head wind on the way back, that you have a flat tire, or that your house is located on a hill. In this case, although the speed and duration of your ride is the same, the energy you use to maintain this speed is much higher on the way back. Each of the mentioned factors, or external forces (such as air resistance, rolling resistance or gravity), require a higher power to produce on your bike when returning home.’ The example clarifies that power is a more valid measure of intensity, i.e. amount of effort, required in a certain period than speed. Besides speed, this also applies to other subjective measures such as number of steps or minutes performing an activity.

In everyday life, however, we do not often come across the term power. Instead, we talk about energy expenditure (e.g. expressed in kcal) over a certain period of time. The last decades, energy expenditure or power has been related to many societal health factors, such as mental and physical well-being. For example, the university of Kansas reported that recent studies ‘show that walking 10,000 steps can improve cardiovascular health and reduce risks of both dementia and cancer better than any pill or injection currently available’ [1–4]. In addition, an increased energy expenditure was reported to be strongly associated with a lower risk of mortality in healthy older adults [5], and ‘physical activity’ has been found to reduce chronic disease risk and enhances functional capacity [6]. Monitoring power production or energy expenditure is therefore an important first step towards overall health benefits.

For wheelchair users, the relevance of power monitoring may be even larger. Wheelchair users, in general, have a higher risk for diseases and cardiovascular events [7], and are more prone to - mainly shoulder - injuries compared to non-wheelchair users [8]. Monitoring power of wheelchair users may help to prevent injuries, and to design specific ‘physical activity’ guidelines for wheelchair users [9]. In addition, monitoring and giving feedback on power may be used to stimulate wheelchair users in performing physical activity such as taking a ride or performing wheelchair sports, to study aspects of different propulsion techniques [10–13], to investigate a person’s physical capacity [14, 15], to analyze sport performance [16, 17] or as an extra measurement tool to evaluate wheelchair design [15]. Monitoring power has thus many benefits for both non-active, active and ‘athletic’ wheelchair users.

What is power?

The previous paragraphs clarified that power is considered a useful measure. But what is power? Power is the energy transferred or converted per unit of time, usually expressed in Watts or normalized to Watts per kg. It is a broad concept which is all around in our daily lives. Think of a light bulb that converts oil (or electricity) into light, the water boiler that converts electricity into heat and your car that converts gasoline into wheel rotation. The human body works in a similar way albeit using other power sources. In human locomotion, metabolic energy (originating from food) is converted into muscle power (to generate muscle force). Subsequently, muscle force enables body segments to overcome internal and external friction to, eventually, produce locomotion (by propelling the push-rims of a wheelchair for instance). In the present dissertation I will focus on ‘locomotion power’, also called ‘power output’, which is the power that is transferred between a – in this case - wheelchair user and the environment. This type of power

be approached purely mechanical, as it equals the sum of the user's forces multiplied by the linear velocities of (the points of application of) these forces; and the sum of the user's moments multiplied by their angular velocities (see Eq. 1.1). We therefore refer to it as 'mechanical power'.

$$P_{user} = \sum \mathbf{F}_{user} * \mathbf{v}_{F,user} + \sum \mathbf{M}_{user} * \boldsymbol{\omega}_{M,user} \quad (1.1)$$

(Im)possibilities for measuring power in wheelchair propulsion

When force (and/or moment) and (angular) velocity is known, mechanical power can be obtained. Determining wheelchair velocity during (overground) wheelchair propulsion is relatively straight-forward and is done for decades [18, 19]. The force applied on the push-rims of a wheelchair, on the other hand, can only be measured with specialized equipment [15].

Wheelchair propulsion laboratories have been used to measure wheelchair propulsion forces and moments, and to gain insights into wheelchair propulsion techniques [20, 21]. So-called wheelchair ergometers have been measuring mechanical power for several years [14, 22]. Whereas the wheelchair was previously integrated in the wheelchair ergometer, such that all experiments were done on the same (adjustable) chair [11, 15], a new ergometer has been developed recently, allowing wheelchair users to be measured in their own wheelchair [23]. With these ergometers, the gap between lab and field has already narrowed. However, the ecological validity of such a system is still low. To understand this, some crucial aspects of wheelchair dynamics will be explained below.

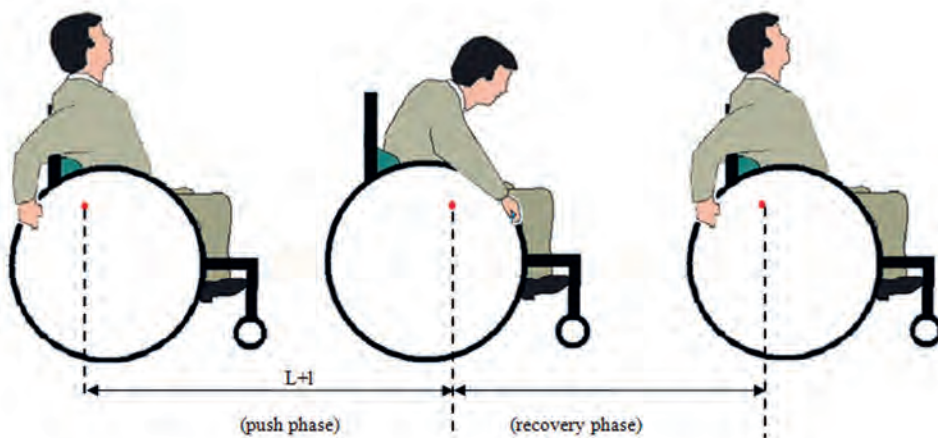


Figure 1.1. A propulsion cycle with the 'push' phase and the 'recovery' phase and corresponding (common) upper body moments (obtained from Salimi and Ferguson-Pell [24]).

Look mummy, no hands! Some background on wheelchair propulsion dynamics

Contrary to many other locomotion activities, during wheelchair propulsion, the wheelchair is not propelled continuously. A propulsion cycle is commonly subdivided into a 'push' phase and a 'recovery' phase (see Fig. 1.2). During the push phase, a wheelchair user applies force to the rim of the wheelchair. If a wheelchair user has sufficient upper body function, this movement is often accompanied by inclining the upper body, such that the range of motion of the arms and hands is increased, and a longer push can be obtained. After the push phase, the wheelchair user returns to the initial position, which is called the 'recovery phase'. When the upper body accelerates backwards (e.g., to return its initial position), the user unconsciously pushes the wheelchair forward (without using his/her hands) [25]. This is visible in a forward acceleration of the wheelchair. In our paper 'Look mummy, no hands! The effect of trunk motion on forward wheelchair propulsion', this phenomenon was further investigated in which upper body motion was represented by the movements of the trunk. The interaction between trunk motion and wheelchair acceleration is visible in Figure 1.2. Here, the trunk angle, wheelchair acceleration, hand contact (push phase) and hand release (recovery phase) are presented during a propulsion cycle at normal intensity (left figure) and during a propulsion cycle at maximal intensity (right figure). As is visible in Figure 1.2, the wheelchair is 'propelled' (i.e., accelerated) not only during the push phase, but also during a part of the recovery phase.

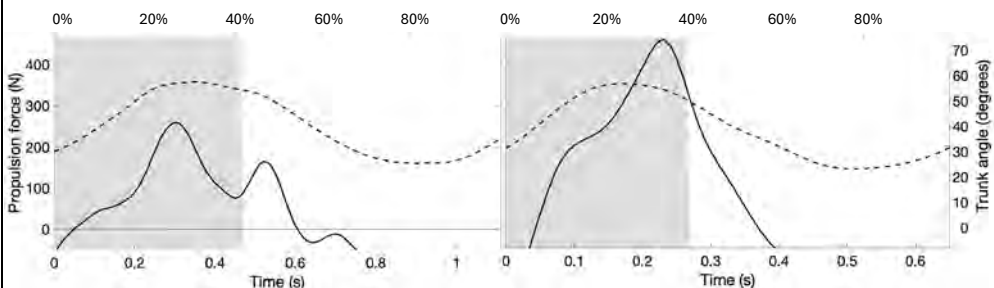


Figure 1.2. Example of propulsion force (N; solid line) and trunk angle (degrees, with respect to the vertical; dashed line) over time for one push cycle at normal intensity (left) and one push cycle at high intensity (right). The grey surface indicates the push phase, the white surface indicates the recovery phase [25].

Given some background on wheelchair propulsion dynamics, it may be clear that measuring power with a wheelchair ergometer (see Fig. 1.3) has limited ecological validity. First, on a wheelchair ergometer, the (own) wheelchair is fixed to an ergometer device positioned in the lab, such that the wheelchair dynamics differ from overground propulsion (i.e., no wheelchair acceleration/deceleration during recovery) and forces that are exerted on the wheelchair seat will be neglected. Second, resistive forces, like air resistance and rolling resistance will not be realistic on wheelchair ergometers. Whereas air resistance depends on the air velocity relative to the athlete-wheelchair system (which is near zero on a lab-based ergometer), rolling resistance is commonly imposed by the ergometer as a constant force [23]. However, rolling resistance for overground wheelchair propulsion usually varies within a stroke cycle due to

trunk-motion induced upper body movements [26, 27]. Therefore, while the force applied on the push-rims of a wheelchair can be measured with a wheelchair ergometer, the translation of ergometer-based power values to real-life situations is complex and error-prone.

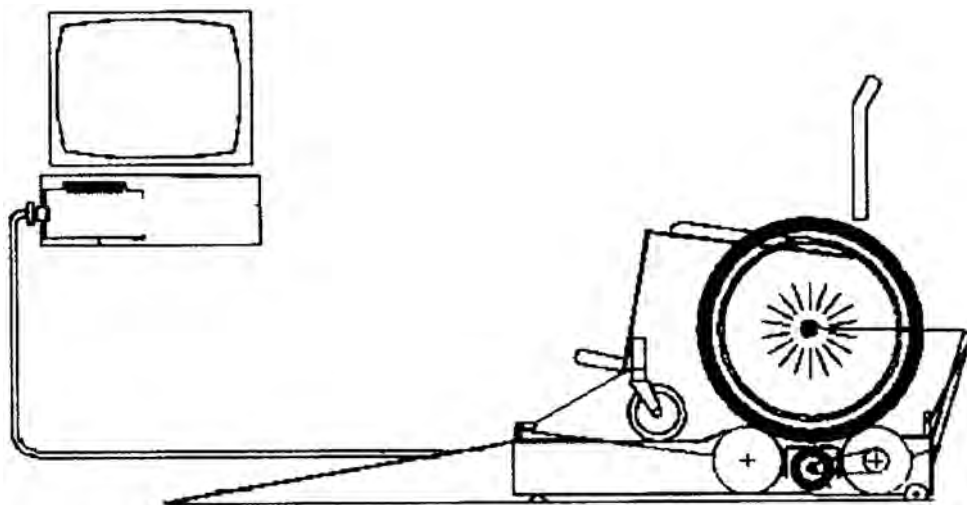


Figure 1.3. Wheelchair fixed on a wheelchair ergometer (obtained from Bougenot et al. [28])

An ambulatory system that measures force on the push-rims was first reported in 1993 [29]. Similar to power meters in for example road cycling and rowing, force sensors can be integrated in the push-rims of a wheelchair to measure the force or torque applied on the push-rims. These force-instrumented push-rims have been used to analyze wheelchair propulsion techniques, to study force applications and to assess propulsion technique changes with fatigue [30]. However, one major drawback is that force-instrumented push-rims nowadays weight about 6-9 kg [31], such that it adds 60-90% to the average mass of a wheelchair and has therefore a large impact on the wheelchair dynamics and propulsion technique. Moreover, force-instrumented push-rims are expensive and not sufficiently robust to be used during everyday wheelchair use or wheelchair sports. At present, force-instrumented push-rims are thus not feasible to monitor propulsive force and power in wheelchair sport practice.

Power in wheelchair sports

In wheelchair sports, on-field monitoring of mechanical power is requested by coaches, athletes and sports scientists. When power is monitored during, for instance, every training session or competition, valuable information can be gained on the athlete's performance ('Can my athlete produce more power on the racing wheelchair than one month ago?') and on their fitness level ('The heartrate is higher, while power produced is the same as yesterday, maybe I am fatigued and should take some rest'). Moreover, when the power values are lower than expected, overuse or fatigue can be identified in an early stage such that coaches or athletes can act upon this and reduce the risk of injuries. After recovery of an injury or period of rest, power can again be used to specify and individualize training programs to bring the athlete back on its elite level. Lastly, power can be used to optimize wheelchair settings. If, for example, an athlete maintains a

certain power output, but reaches a higher speed in Wheelchair A than in Wheelchair B, than the first one will be the best choice.

As power in sports is used more and more to enhance performance and to reduce the risks of injuries in a variety of sports disciplines [16, 32–34], much knowledge has already been accumulated. Monitoring power during daily wheelchair sports practice would thus provide many opportunities for both wheelchair field and court sports (such as wheelchair basketball, rugby, tennis) as well as wheelchair racing (from 100m sprints to marathon or triathlon disciplines). To provide coaches and athletes with feedback on power during regular training sessions and in match-like situations, without interrupting their daily training routine, a non-invasive ambulatory method to monitor power should be developed.

Problem statement and research aim:

In wheelchair sports, on-field power monitoring is essential to enhance performance and reduce injury risk. However, a non-invasive and inexpensive method to determine mechanical power during wheelchair sports is not yet available. Therefore, the aim of this dissertation is to enable non-invasive and inexpensive mechanical power monitoring during overground hand-rim wheelchair propulsion, mainly in the context of wheelchair sports.

In unmotorized wheelchairs, athletes' mechanical power is used to change the speed and direction of the wheelchair. In addition, in wheelchair field and court sports, power is also used to change the speed and direction of the ball (with or without racket or stick). Even though determining power during all these activities would provide the most complete overview, the demand from wheelchair sports practice is mainly focused on the propulsive part instead of power loss due to ball handling. Moreover, as turning may involve additional unknown and complex factors such as rotational inertia and increased rolling resistance, this dissertation focuses on straight-line wheelchair propulsion.

Outline of the dissertation

The present dissertation is subdivided in three sub-sections. Below, the different aims of the subsections are explained.

From theory to practice: Estimating mechanical power during on-field wheelchair propulsion

The main aim of this subsection is to identify an ambulatory method to estimate mechanical power during wheelchair propulsion. As wheelchair propulsion can be seen as a cyclic sport, Chapter 2 reviews the present literature on using wearable sensors to estimate mechanical power in different cyclical sports. Inspired by this, Chapter 3 presents a theoretical framework for modelling the mechanical power transferred between the athlete-wheelchair combination and the environment, and validates mechanical power derived from inertial sensors against a reference.

Pushing further: The role of trunk motion on estimating power during wheelchair propulsion

As several studies reported on the interaction between trunk motion and wheelchair dynamics [25–27, 35], the second sub-section investigates the role of trunk motion on power prediction in hand-rim wheelchair propulsion. Therefore, in Chapter 4, a method is developed that measures instantaneous trunk inclination during on-field wheelchair propulsion. Chapter 5 investigates how trunk motion influences the mechanical power estimations during wheelchair propulsion.

Power for all: Meeting the demands of different wheelchair user populations

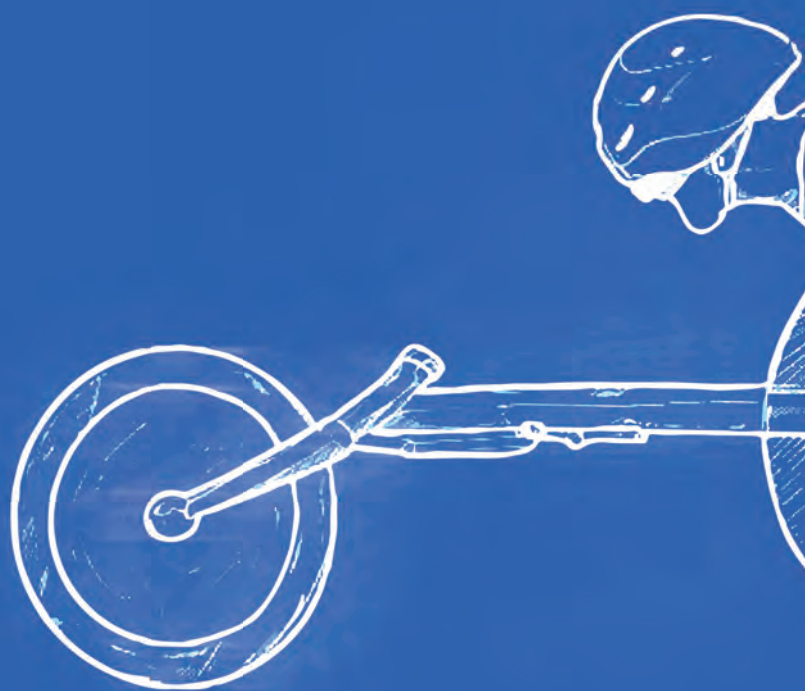
Besides elite athletes, recreational athletes and daily wheelchair users may benefit from monitoring power as well (see ‘The power of monitoring power’). However, the demands of a daily wheelchair user with respect to a power monitoring device (cheap, simple) may differ from those of a recreational athlete (accurate but feasible) or an elite athlete (high accuracy, peak powers). Moreover, demands for elite athletes may differ during the day or week as well. To this end, section 3 specializes towards the different user requirements. On the one hand, Chapter 6 focuses on the elite athlete by further improving the accuracy of power estimates based on the prediction of mass distribution between the front- and rear wheels. In Chapter 7 this is followed by the application of the improved power estimates during overground wheelchair tennis sprints. On the other hand, Chapter 8 investigates to what extent decreasing the number of inertial sensors would affect the accuracy of wheelchair kinematics, such that power monitoring becomes more accessible to the daily wheelchair users and/or recreational athlete. Lastly, a novel RHIDE (Rim HIt DEtection) system is presented in Chapter 9, that – in addition to wheelchair kinematics - identifies time and location of hand contact, and might be used to monitor push technique and as an activity tracker suitable for all wheelchair users.

References

1. Del Pozo Cruz B, Ahmadi MN, Lee I-M, Stamatakis E (2022) Prospective Associations of Daily Step Counts and Intensity With Cancer and Cardiovascular Disease Incidence and Mortality and All-Cause Mortality. *JAMA Intern Med* 182:1139
2. Master H (2022) Association of step counts over time with the risk of chronic disease in the All of Us Research Program. *Nat. Med.* 28:
3. Lee I-M, Shiroma EJ, Kamada M, Bassett DR, Matthews CE, Buring JE (2019) Association of Step Volume and Intensity With All-Cause Mortality in Older Women.
4. Hawes K (2022) Studies in JAMA show that walking 10,000 steps can improve cardiovascular health and reduce risks of both dementia and cancer better than any pill or injection currently available. *KU Med. Cent.*
5. Manini TM, Everhart JE, Patel KV, Schoeller DA, Colbert LH, Visser M, Tylavsky F, Bauer DC, Goodpaster BH, Harris TB (2006) Daily Activity Energy Expenditure and Mortality Among Older Adults. *JAMA* 296:171
6. Haskell WL, Blair SN, Hill JO (2009) Physical activity: Health outcomes and importance for public health policy. *Prev Med* 49:280–282
7. (2019) Can Physical Activity Improve the Health of Wheelchair Users? A Systematic Review. Agency for Healthcare Research and Quality
8. Liampas A, Neophytou P, Sokratous M, Varrassi G, Ioannou C, Hadjigeorgiou GM, Zis P (2021) Musculoskeletal Pain Due to Wheelchair Use: A Systematic Review and Meta-Analysis. *Pain Ther* 10:973–984
9. Nightingale TE, Rouse PC, Thompson D, Bilzon JLJ (2017) Measurement of physical activity and energy expenditure in wheelchair users: Methods, considerations and future directions. *Sports Med - Open*. <https://doi.org/10.1186/s40798-017-0077-0>
10. Roeleveld K, Lute E, Veeger D, Woude LVD, Gwinn T (1994) Power Output and Technique of Wheelchair Athletes. *Adapt Phys Act Q* 11:71–85

11. Veeger HEJ, Lute EMC, Roeleveld K, Van Der Woude LHV (1992) Differences in performance between trained and untrained subjects during a 30-s sprint test in a wheelchair ergometer. *Eur J Appl Physiol* 64:158–164
12. Veeger, H.E.J., van der Woude, L.H.V., Rozendal, R.H. (1991) Effect of handrim velocity on mechanical efficiency in wheelchair propulsion. *Med. Sci. Sports Exerc.* 24:
13. Wu H-W, Berglund LJ, Su F-C, Yu B, Westreich A, Kim K-J, An K-N (1998) An Instrumented Wheel for Kinetic Analysis of Wheelchair Propulsion. *J Biomech Eng* 120:533–535
14. Janssen RJF, Vegter RJK, Houdijk H, Van Der Woude LHV, De Groot S (2022) Evaluation of a standardized test protocol to measure wheelchair-specific anaerobic and aerobic exercise capacity in healthy novices on an instrumented roller ergometer. *PLOS ONE* 17:e0274255
15. van der Woude LHV, Veeger HEJ, Dallmeijer AJ, Janssen TWJ, Rozendaal LA (2001) Biomechanics and physiology in active manual wheelchair propulsion. *Med Eng Phys* 23:713–733
16. Leo P, Spragg J, Podlogar T, Lawley JS, Mujika I (2022) Power profiling and the power-duration relationship in cycling: a narrative review. *Eur J Appl Physiol* 122:301–316
17. Tlukdar K, Cronin J, Zois J, Sharp AP (2015) The Role of Rotational Mobility and Power on Throwing Velocity. *J Strength Cond Res* 29:905–911
18. Mattison, P.G., Hunter, J., Spence, S. (1989) Development of a realistic method to assess wheelchair propulsion by disabled people. *Int J Rehabil Res* 12:137–145
19. Vanlandewijck, Y.C., Daly, D.J., Theisen, D.M. (1999) Field Test Evaluation of Aerobic, Anaerobic, and Wheelchair Basketball Skill Performances. *Int J Sports Med* 20:548–554
20. van der Woude LHV, Veeger HEJ, Rozendal RH (1989) Propulsion technique in hand rim wheelchair ambulation. *J Med Eng Technol* 13:136–141
21. Veeger HEJ, Van Der Woude LHV, Rozendal RH (1992) The effect of handrim velocity on mechanical efficiency in wheelchair propulsion. *Med Sci Sports Exerc* 24:100–107
22. de Klerk R, Vegter RJK, Leving MT, De Groot S, Veeger DHEJ, Van Der Woude LHV (2020) Determining and Controlling External Power Output During Regular Handrim Wheelchair Propulsion. *J Vis Exp* 60492
23. de Klerk R, Vegter RJK, Veeger HEJ, Van Der Woude LHV (2020) Technical Note: A Novel Servo-Driven Dual-Roller Handrim Wheelchair Ergometer. *IEEE Trans Neural Syst Rehabil Eng* 28:953–960
24. Salimi Z, Ferguson-Pell MW (2013) Ergometers Can Now Biomechanically Replicate Straight-Line Floor Wheelchair Propulsion: Three Models Are Presented. In: Vol. 3A Biomed. Biotechnol. Eng. American Society of Mechanical Engineers, San Diego, California, USA, p V03AT03A045
25. van Dijk MP, van der Slikke, R.M.A., Berger, M.A.M., Hoozemans, M.J.M., Veeger HEJ (2021) Look mummy, no hands! The effect of trunk motion on forward wheelchair propulsion. 39th ISBS Conf 4
26. Poulet Y, Brassart F, Simonetti E, Pillet H, Faupin A, Sauret C (2022) Analyzing Intra-Cycle Velocity Profile and Trunk Inclination during Wheelchair Racing Propulsion. *Sensors* 23:58
27. Sauret C, Vaslin P, Lavaste F, de Saint Remy N, Cid M (2013) Effects of user's actions on rolling resistance and wheelchair stability during handrim wheelchair propulsion in the field. *Med Eng Phys* 35:289–297
28. Bougenot M-P, Tordi N, Betik AC, Martin X, Le Foll D, Parratte B, Lonsdorfer J, Rouillon JD (2003) Effects of a wheelchair ergometer training programme on spinal cord-injured persons. *Spinal Cord* 41:451–456

29. Asato KT, Cooper RA, Robertson RN, Ster JF (1993) SMARTWheels: Development and testing of a system for measuring manual wheelchair propulsion dynamics. *IEEE Trans Biomed Eng* 40:1320–1324
30. Rodgers MM, Gayle GW, Figoni SF, Kobayashi M, Lieh J, Glaser RM (1994) Biomechanics of wheelchair propulsion during fatigue. *Arch Phys Med Rehabil* 75:85–93
31. de Groot S, Vegter R, Vuijk C, Dijk F, Plaggenmarsch C, Sloots M, Stolwijk-Swaeste J, Woldring F, Tepper M, Woude L (2014) WHEEL-I: Development of a wheelchair propulsion laboratory for rehabilitation. *J Rehabil Med* 46:493–503
32. Gløersen Ø, Losnegard T, Malthe-Sørensen A, Dysthe DK, Gilgien M (2018) Propulsive Power in Cross-Country Skiing: Application and Limitations of a Novel Wearable Sensor-Based Method During Roller Skiing. *Front Physiol* 9:1631
33. Hofmijster MJ, Lintmeijer LL, Beek PJ, van Soest AJK (2018) Mechanical power output in rowing should not be determined from oar forces and oar motion alone. *J Sports Sci* 36:2147–2153
34. West DJ, Owen NJ, Cunningham DJ, Cook CJ, Kilduff LP (2011) Strength and power predictors of swimming starts in international sprint swimmers. *J Strength Cond Res* 25:950–955
35. Chenier F, Gagnon DH, Blouin M, Aissaoui R (2016) A Simplified Upper-Body Model to Improve the External Validity of Wheelchair Simulators. *IEEEASME Trans Mechatron* 21:1641–1649



Abstract

More insight into in-field mechanical power in cyclical sports is useful for coaches, sport scientists, and athletes for various reasons. To estimate in-field mechanical power, the use of wearable sensors can be a convenient solution. However, as many model options and approaches for mechanical power estimation using wearable sensors exist, and the optimal combination differs between sports and depends on the intended aim, determining the best setup for a given sport can be challenging. This review aims to provide an overview and discussion of the present methods to estimate in-field mechanical power in different cyclical sports. Overall, in-field mechanical power estimation can be complex, such that methods are often simplified to improve feasibility. For example, for some sports, power meters exist that use the main propulsive force for mechanical power estimation. Another non-invasive method usable for in-field mechanical power estimation is the use of inertial measurement units (IMUs). These wearable sensors can either be used as stand-alone approach or in combination with force sensors. However, every method has consequences for interpretation of power values. Based on the findings of this review, recommendations for mechanical power measurement and interpretation in kayaking, rowing, wheelchair propulsion, speed skating, and cross-country skiing are done.

Introduction

Mechanical power is a useful and objective variable to monitor in cyclical endurance sports for several purposes. First of all, it can be used as a performance measure since the average velocity, and therefore performance, largely depends on the mechanical power sustained for a given distance [1]. In addition, mechanical power includes environmental factors such as wind velocity, which makes it an objective measure to assess the external load of a training or competition [2,3]. Furthermore, mechanical power can be used for fitness and fatigue assessments [3], and consequently, for prevention of overtraining and training periodization [4]. Therefore, estimations of mechanical power may be of great value for coaches, sport scientists, and athletes.

Most of the applications of mechanical power require day-to-day monitoring of mechanical power in an ecological valid environment. Therefore, in-field mechanical power estimation might be favorable for coaches and athletes as opposed to laboratory-based mechanical power estimation. Accordingly, in-field estimation of mechanical power in cycling is well-integrated in various cycling power meters, which are widely used by coaches, sport scientists, and athletes [5–7]. In cycling, power meters are often used to gain insight in power profiling, training load, and performance assessments and for establishing training zones [7]. As these applications of power are successfully developed in both professional and recreational cycling, the use of cycling power meters is an inspiration to provide methods for mechanical power estimation in other cyclical sports as well. However, having access to a commercially available power meter or a properly defined method to estimate mechanical power is not as common in any given cyclical sport as it is in cycling.

To estimate mechanical power in any sport of interest, it is important to understand its principle. In physics, power is defined as the rate of transferring energy from or to an object (i.e., doing work) with respect to time. Power associated with a force is calculated as the scalar product of the force vector and the velocity vector of its point of application, or $\mathbf{F} \cdot \mathbf{v}$. In sports, mechanical power can be defined as the power transferred by the athlete to the environment, which is the main focus of this review. Mechanical power in sports can be estimated by solving the power equation while treating the human body as a chain of a number of linked rigid bodies [1]. Van der Kruk et al. [8] defined this power equation based on five terms: joint power, kinetic power, gravitational power, environmental power, and frictional power [8], with the following relationship:

$$P_j = P_k + P_f - P_g - P_e \quad (2.1)$$

where P_j is joint power, P_k is kinetic power, P_f is frictional power, P_g is gravitational power, and P_e is environmental power. Translated into words, an athlete generates power (P_j) to (partially) overcome power losses due to resistive forces (P_f , P_g and P_e) resulting in velocity and acceleration of the athlete (P_k).

According to van Ingen Schenau and Cavanagh [1] and van der Kruk et al. [8], mechanical power generated by an athlete can either be estimated by estimating the joint power (left-hand-side of Equation (2.1)) or through the sum of the kinetic power and power losses due to resistive forces (right-hand-side of Equation (2.1)). Joint power is calculated as the sum of the scalar products of joint moments and angular velocity per joint ($\sum \mathbf{M}_j \cdot \boldsymbol{\omega}_j$) using inverse dynamics [1]. The power associated with resistive forces is calculated through the scalar product of the force and the velocity of its point of application. Hence, the right-hand-side of Equation (2.1), considering every acting force as an external force, simplifies to $\sum \left(\frac{dE_{kin}}{dt} \right) - \sum \mathbf{F}_e \cdot \mathbf{v}_e - \sum \mathbf{M}_e \cdot \boldsymbol{\omega}_e$ [1]. Therefore, the equation in Equation (2.1) can be rewritten as:

$$\sum \mathbf{M}_j \cdot \boldsymbol{\omega}_j = \sum \frac{dE_{kin}}{dt} - \sum \mathbf{F}_e \cdot \mathbf{v}_e - \sum \mathbf{M}_e \cdot \boldsymbol{\omega}_e \quad (2.2)$$

Obtaining an estimation of the power transferred from the athlete to its environment (e.g., rower on oar or boat, athlete to the wheelchair) using Equation (2.2), however, can be a very laborious procedure due to the number of variables that have to be measured and processed. Therefore, to increase feasibility for mechanical power estimation, simplifications of the power equation (Equation (2.2)) are often made. Frequently used simplifications and their consequences are extensively discussed by van der Kruk et al. [8]. One of these simplifications is using a single-body model in which the athlete is treated as a point mass located at the center of mass (CoM). Another simplification is the neglect of parts of the power equation: for example, by only taking what is considered as the main propulsion force into account for mechanical power estimation.

Using the power equation (Equation (2.2)) with or without simplification to obtain an in-field estimation of the power transferred from the athlete to its environment, requires wearable devices or sensors, such as strain gauges for force measurement or inertial measurement units (IMU) for measuring body segment kinematics [5,9]. IMUs are small and lightweight sensors that typically consist of an accelerometer, gyroscope, and magnetometer, which measure linear acceleration, angular velocity, and local magnetic field, respectively. With these outputs, IMUs can be used to determine segment kinematics such as orientation and angular velocity [9]. IMUs can also be useful for estimation of external forces [9], such that they could be used as a standalone approach for in-field mechanical power estimations. As many options and combinations for power estimation exist, and the optimal solution differs between sports, a sport-specific method is needed.

To summarize, a lot of possibilities exist for estimating mechanical power during in-field cyclical sports. There are different methods (P_j or $P_k + P_{resistive}$) and multiple simplifications that can be made. Many decisions have to be made to establish a power model for a sport of interest, which can be challenging for coaches or sport scientists. To date, no overview of the methods to estimate mechanical power in different cyclic sports exists. Therefore, the aim of this review is to evaluate the literature on chosen approaches for estimating mechanical power, including the methods, devices and assumptions. By providing an overview and discussion of the existing methods, this review intends to guide coaches and sport scientists to form a well-founded model for mechanical power estimation in line with their intended aim.

As several reviews discuss the application of power meters in cycling [5–7], cycling will be omitted from this review.

2. Method

2.1. Literature Search

For this search, Scopus and PubMed were used. The last search was performed in May 2022. The complete search consisted of three search strings. The first search string included the following terms: mechanical power OR external power OR power output OR mechanical energy expenditure OR joint power OR internal power OR work rate. The second search included the following terms: cyclic sport OR swim * OR wheelchair OR kano * OR cross-country skiing OR speed skating OR skating OR rowing OR kayak. The third string included: IMU OR inertial sens * OR inertial measurement unit OR wearable sens * OR 3D acceler * OR force sens * OR power meter OR wearable devices OR wearable tech*. The strings were then combined using the AND modifier.

2.2. Selection of Studies

After removing duplicates, this search resulted in 16 records (Fig. 2.1). Titles and abstracts were read to inspect whether the record was suitable for the current review. Records were included if they were focused on the method of estimation of mechanical power or any of the terms that are essential to estimation of mechanical power output and used healthy participants, with healthy meaning within the scope of the sport-specific requirements.

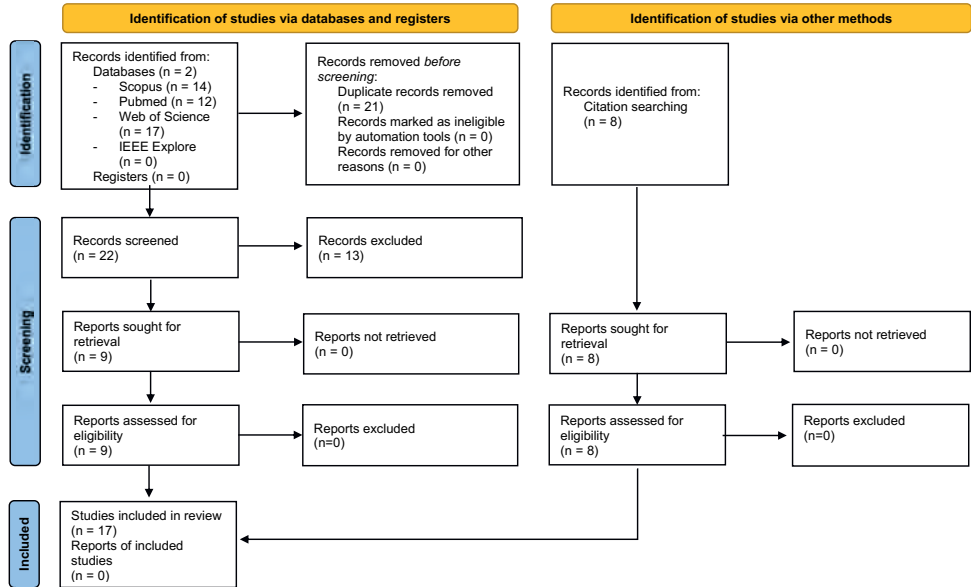


Figure 2.1. PRISMA diagram of included studies.

Records were excluded if one of the following exclusion criteria were present: published before the year 2000, focusing on non-cyclical sports, proposing methods that include energy harvesting of human locomotion, and not written in English. Applying the inclusion and exclusion criteria resulted in 8 relevant studies. Reference lists and citations of the selected studies were inspected for additional relevant reports, resulting in a total of 17 studies. The number of published studies over the years is shown in Fig. 2.2.

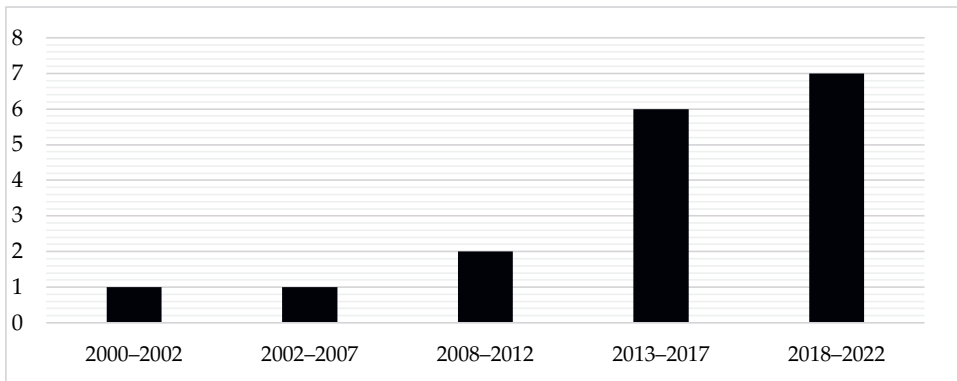


Figure 2.2. The number of published studies plotted against the year of publication.

3. Overview

An overview of the literature that estimated mechanical power using wearable devices is provided in Tables 2.1 and 2.2. To identify the acting forces on a rigid body, drawing a free body diagram of that rigid body is a useful tool. The column ‘rigid body definition’ clarifies the boundaries of the rigid body that is used and therefore designating the forces and torques to consider. The studies of interest mainly estimate mechanical power as output (see Table 2.1). However, some studies in Table 2.2 estimated only subparts of the power equation, such as the acceleration of the center of mass [10] or push-off force [11,12]. These subparts are useful for future estimation of mechanical power and need to be accurately estimated as a first step towards mechanical power estimation in, respectively, rowing, speed skating, and cross-country skiing. Whichever term is estimated is displayed in the ‘estimated term’ column. Force or torque from a source acting on an object is displayed as $F_{source,object}$ or $M_{source,object}$ in the column ‘force measurement’. The kinematics of an object relative to a reference frame such as the linear velocity or angular velocity is displayed as $v_{object/ref}$ or $\omega_{object/ref}$, respectively, in the column ‘kinematic measurement’. If known, the type of sensor used to measure the force and/or velocity component is given between brackets. If the type of sensor used to measure the force and/or velocity component is unknown, it is displayed as (-). In Table 2.1, if a measuring system is commercially available, the name of the system is given.

3.1. Model

The studies are divided in two main categories based on the used rigid body: transportation object as a rigid body (Section 3.1.1) and athlete as a rigid body (Section 3.1.2). In one case, a combination of the transportation object and athlete is used as a rigid body [13].

3.1.1. Transportation Object as the Rigid Body

Nine studies estimated mechanical power by multiplying what is considered as the main propulsion force or torque with the corresponding linear or angular velocity (see Table 2.1) [14–23].

For kayaking and rowing, the paddle or oar, respectively, were chosen as the rigid body (see Fig. 2.A1) [14–18]. These studies considered the propulsive force as the force of the hands on the paddle or oar perpendicular to the oar or paddle ($F_{hand,paddle}$ or $F_{hand,oar}$) and multiplied this with the corresponding linear velocity of the hand relative to the world ($v_{hand/world}$) to obtain mechanical power. In rowing, $F_{hand,oar}$ can directly be measured at the hand placement on the oar [16,18]. Alternatively, it can be derived from the normal force in the oarlock ($F_{oar,oarlock}$), combined with the inboard and outboard length of the oar (respectively, l_{in} and l_{out}) [16,17]. By assuming that the blade is a stationary point and the oar mass is negligible, this results in the following relation:

$$F_{hands,oar} = F_{oarlock,oar} \cdot \frac{l_{out}}{l_{in} + l_{out}} \quad (2.3)$$

The linear hand velocity ($v_{hand/world}$) was derived by multiplying the inboard length with either the change in angle of the oar relative to the oar pin on the boat ($\phi_{oar/boat}$) divided by the corresponding change in time or the angular velocity of the oar relative to the oar pin on the boat ($\omega_{oar/boat}$) [16–18]. Holt et al. [18] did not specify how the state-measured variables were derived. Since the PowerLine (Peach Innovations, Cambridge, UK) and EmPower (Nielsen-Kellerman, Boothwyn, PA, USA) measure $F_{oarlock,oar}$ [18], it is most likely that $F_{hands,oar}$ is derived using Equation (2.3), whereas $v_{hand/world}$ was derived similar to [16,17]. For the OarPowerMeter (Weba Sport, Wien, Austria), $F_{hands,oar}$ was directly measured and $\omega_{oar/boat}$ is likely multiplied with inboard length to obtain linear hand velocity [18].

Table 2.1.

Overview of studies that estimated mechanical power output by using a part of the transportation object (i.e., paddle, oar, or wheel) as a system.

Sport	Study	Rigid Body Definition	Force Measurement (Sensor Type)	Kinematic Measurement (Sensor Type)	Commercially Available (Name)
Kayaking	Hogan et al. [14] Macdermid and Fink [15]	Paddle	$F_{hand,paddle}$ (SG)	$\mathbf{a}_{shaft/world}$ and $\boldsymbol{\omega}_{shaft/world}$ (IMU)	Yes (Kayak Power Meter)
	Baudouin and Hawkins [16]	Oar	$F_{hand,oar}$ (SG)	$\phi_{oar/boat}$ (POT)	No
	Doyle et al. [17]	Oar	$F_{oar,oarlock}$ (2D load transducers)	$\phi_{oar/boat}$ (POT) and $a_{boat/world}$ (ACC)	No
Rowing	Holt et al. [18]	Oar	PowerLine: $F_{oar,oarlock}$ EmPower: $F_{oar,oarlock}$ OarPowerMeter: $F_{hand,oar}$	PowerLine: $\omega_{oar/boat}$ EmPower: $\phi_{oar/boat}$ OarPowerMeter: $\phi_{oar/boat}$	Yes (PowerLine, EmPower, Oar-PowerMeter)
	Conger et al. [19]	Wheel	$M_{F_{hand,rim}}$ (SG)	$\omega_{rearwheel/WC}$	Yes (PowerTap SL+ Track Hub)
Wheelchair propulsion	de Groot et al. [20]	Wheel	$M_{F_{hand,rim}}$	$\omega_{rearwheel/WC}$	Yes (OptiPush, SMARTWheel)
	de Klerk et al. [21]				
	van der Scheer et al. [22]	Wheel	$M_{F_{hand,rim}}$	$\omega_{rearwheel/WC}$	Yes (OptiPush)
	Mason et al. [23]	Wheel	$M_{F_{hand,rim}}$	$\omega_{rearwheel/WC}$	Yes (SMARTWheel)

ACC = accelerometer, IMU = inertial measurement unit, POT = potentiometer, SG = strain gauge, WC = wheelchair

In kayaking, the normal force of the hand on the paddle ($F_{hand,paddle}$) was measured at the hand placement on the oar [14,15]. The hand velocity was derived using shaft acceleration ($\mathbf{a}_{shaft/world}$), angular velocity of the shaft ($\boldsymbol{\omega}_{shaft/world}$), and the hand placements [14,15].

In wheelchair propulsion, the wheel is chosen as a rigid body and the main propulsive force is considered the force of the hands on the rim tangential to the rim ($F_{hand,rim}$), resulting in a torque around the rear wheel axis ($M_{F_{hand,rim}}$) [19–23]. This torque is then multiplied with the angular velocity of the rear wheel around the rear wheel axis ($\omega_{rearwheel/WC}$) to obtain mechanical power.

3.1.2. Athlete as the Rigid Body

Alternatively, six studies estimated power using all forces acting on the athlete as a single or multibody model (see Table 2.2) [10–12,24–26]. One study estimated mechanical power by considering the athlete and transportation object as a single rigid body (see Table 2.2) [13].

A multibody model is used by both Kleshnev [24] and Lintmeijer et al. [10] in rowing. Kleshnev [24] determined all forces acting on the rower and their corresponding velocities to estimate mechanical power generated by the athlete (see Fig. 2.A2). The force of the foot stretcher on the feet in the propulsive direction ($F_{feet,footstretcher}$) was measured in the foot stretcher and $F_{oar,hand}$ was derived as $F_{oar,oarlock}$. The velocity of the feet is equal to boat velocity ($v_{boat/world}$) and $v_{hands/world}$ is derived using $\phi_{oar/boat}$ [24].

Table 2.2.

Overview of studies that estimated mechanical power or another essential term by using the athlete as a rigid body. In some estimations, a single body (SB) is used.

Sport	Study	Rigid Body Definition	Estimate d Term	Force Measurement (Sensor type)	Kinematic Measurement (Sensor Type)
Rowing	Kleshnev [24]	Rower	PO	$F_{oar,oarlock}$ (instrumented gates) $F_{feet,footstretcher}$ (SG)	$v_{seat/boat}, v_{trunk/boat},$ $\phi_{oar/boat}$ (POT), $v_{boat/world}$ (other), $a_{boat/world}$ (ACC)
	Lintmeijer et al. [10]	Rower		$a_{CoM/boat}$	$a_{seg/world}$ * (IMU)
Speed skating	van der Kruk et al. [11]	Skater	$F_{GR,feet}$	$F_{GR,feet}$ (3D force sensors)	-
Cross-country skiing	Gloersen et al. [25]	Skier (SB)	PO	$F_{GR,ath} = (m_{tot} a_{CoM} - F_g - F_d - F_f) \cdot \frac{v}{ v }$	$v_{CoM/world}$ (IMU)
	Ohtonen et al. [12]	Skier	$F_{GR,feet}$	$F_{GR,feet}$ (SG)	-
	Uddin et al. [26]	Skier (SB)	PO	-	$a_{seg/world}$ ** (IMU)
Wheelchair propulsion	Rietveld et al. [13]	Wheelchair + athlete (SB)	PO	$F_{drag,ath} = m_{tot} \cdot a_{WC/world}$ (IMU)	$v_{WC/world}$ (IMU)

ACC = accelerometer, IMU = inertial measurement unit, POT = potentiometer, SG = strain gauge, PO = mechanical power, SB = single-body model, WC = wheelchair. * seg = pelvis, abdomen plus thorax, head, the left and right thighs, shanks, feet, upper arms and the forearms plus hand. ** seg = chest, upper and lower back, left and right wrists, left and right skate

Based on a preliminary study of Hofmijster et al. [27], Lintmeijer et al. [10] determined the acceleration of the CoM of the rower relative to the boat ($a_{CoM/boat}$) in anterior-posterior direction. Multiplying $a_{CoM/boat}$ with the mass of the rower and the velocity of the boat and adding this to the power generated by the hands on the oar, results in an alternative mechanical power estimation for the rower, that, according to the authors, does not neglect any force in accordance with Equation (2.2).

Gloersen et al. [25] and Uddin et al. [26] used a single-body model of the athlete to improve the feasibility of mechanical power estimation in cross-country skiing, which was imitated with roller ski skating (see Fig. 2.A3). To further simplify the approach, both studies only used kinematic data and estimated the resistive forces to estimate mechanical power. Gloersen et al. [25] estimated the propulsive force of the ground on the athlete in the skiing direction ($F_{GR,ath}$) as the total mass of the athlete multiplied by the acceleration of the CoM of the athlete ($m_{tot} a_{CoM}$) minus the sum of power associated with gravity (F_g), rolling resistance (F_f), and aerodynamic drag (F_d) (right-hand-side of Equation (2.2)). An air drag model and rolling resistance coefficients were used to estimate the corresponding forces. The propulsive force ($F_{GR,ath}$) was multiplied with the velocity of the CoM to obtain a mechanical power estimation.

Uddin et al. [26] performed their experiments on a treadmill, eliminating air drag. Mechanical power was calculated as the sum of power against gravity and rolling resistance. After obtaining an estimation of mechanical power, Uddin et al. [26] used a Long Short-Term Memory neural network to estimate the mechanical power during in-field roller ski skating based on data of seven IMUs, treadmill incline, and velocity and body mass. The relative error of the user-dependent model was 3.5%, while the relative error of the user-independent model was 11.6%. Considering this, the user-independent model is less accurate in estimating mechanical power, but it might be useful to recreational skiers.

Two studies determined the push-off force (i.e., the force of the ground on the athlete; $F_{GR,athlete}$) exerted by the athlete in speed skating and cross-country skiing (see Fig. 2.A3) [11,12]. These push-off forces are essential for mechanical power estimation and can be used in combination with kinematics to obtain a mechanical power estimation.

Only one study used a combination of athlete and transportation object as a rigid body [13]. Rietveld et al. [13] modelled the wheelchair with the athlete as a single body located at a point on the wheelchair. They assumed that the total CoM of this body is located at the wheelchair, which is rather acceptable over a push cycle. Mean drag forces were estimated based on the deceleration of the wheelchair during the non-push phase of wheelchair propulsion. However, in the non-push phase, the deceleration of the wheelchair is not necessarily equal to the deceleration of the CoM of the athlete plus the wheelchair since the upper body moves relative to the wheelchair in this phase. To obtain mechanical power, the mean drag force obtained in the non-push phase was multiplied with the velocity of the wheelchair [13]. However, Rietveld et al. [13] concluded that this method for mechanical power estimation is not yet suitable in wheelchair sprinting, due to the relative CoM movement, which is not taken into account.

3.2. Sensors

The sensors that were used in the considered literature can be divided into two main categories. The first category involves sensors that are able to directly measure mechanical power (Section 3.2.1.), such as power meters. The second category uses separate kinematic and/or force sensors to obtain mechanical power (Section 3.2.2.).

3.2.1. Direct Mechanical Power Measurement

Seven studies used commercially available systems that are able to directly provide mechanical power (see Table 2.1) [14,15,18–23].

For kayaking, the Kayak Power Meter (One Giant Leap, Nelson, New Zealand) is designed and is reported to be applicable to both flat-water slalom and sprint kayaking. This power meter is validated by comparing mechanical power to the velocity of the kayak relative to water cubed ($v_{kayak/water}^3$) or to the velocity of the kayak relative to land cubed ($v_{kayak/land}^3$) in flat water conditions [14,15].

For rowing, three power meters are commercially available: the PowerLine, the OarPowerMeter and the EmPower. Holt et al. [18] recommended to use the PowerLine for measurement of mean and stroke-to-stroke mechanical power in rowing because of the higher sensitivity compared to the other two power meters.

Lastly, for wheelchair propulsion, three systems are available that can be used for mechanical power estimation. The OptiPush (Max Mobility, LLC, Antioch, TN, USA) and SMARTWheel (Three Rivers Holdings, Mesa, AZ, USA) were specifically designed for wheelchair propulsion. These two systems are not designed for mechanical power estimation; however, they provide the variables allowing for mechanical power estimation. The third system used in

wheelchair propulsion is the PowerTap SL+ Track Hub (Saris Cycling Group, Madison, WI, USA), which is a power meter originally designed for cycling but modified to fit on a wheelchair.

To date, based on the current literature search, no commercially available power meter for speed skating and cross-country skiing exist.

3.2.2. Force and Kinematic Measurement

For force measurement, mostly strain gauges were used, as can be seen in Tables 2.1 and 2.2 [12,14–16,24]. Van der Kruk et al. [11] used three-dimensional piezoresistive force sensors to measure push-off force in speed skating (see Table 2.2). Several studies did not specify whatever type of force-measuring sensor was used [18,20–23]. Others modelled force as a function of other known components, such as acceleration [13,24].

For kinematic measurements after the year 2010, mainly IMUs were used (see Tables 2.1 and 2.2) [10,12,13,15,25,26]. Before the year 2010, mainly potentiometers, occasionally in combination with accelerometers, were used [16,17,24]. Nowadays, these studies can be performed by replacing the potentiometers, used with or without accelerometers, with IMUs. For the studies in Table 2.2 which are not using commercially available power meters but are only using IMUs [10,13,25,26], any IMU can be used.

4. Discussion

The aim of the present review was to provide an overview and discussion of the present methods to estimate in-field mechanical power in different cyclical sports. Based on the sixteen studies considered in this review, the differences and similarities of the used mechanical power estimation methods were identified for application in kayaking, rowing, wheelchair propulsion, speed skating and cross-country skiing. By providing an overview of the current possibilities in mechanical power estimation in cyclical sports, this paper can be used as a guideline for coaches, sport scientists, and those interested in making well-informed decisions for estimation and interpretation of mechanical power.

The most extensive approach to estimate mechanical power is the joint power method (left-hand-side of Equation (2.2)) as discussed by van Ingen Schenau and Cavanagh [1] and van der Kruk et al. [8]. As this approach involves analyzing the full-body kinematics, the obtained mechanical power can be used as a measure of mechanical energy expenditure. However, this joint power method is quite laborious, which causes it to be less practical for coaches. In addition, if the aim is to obtain an accurate measure for an energy expenditure, doing a full-body kinematic analysis may defeat its purpose. It is probably more convenient to obtain an energy expenditure measure by directly measuring oxygen uptake with a wearable respiratory gas analysis device (e.g., Cosmed K5). Moreover, measuring oxygen uptake is a more accurate parameter for energy expenditure than mechanical power. Alternatively, heart rate can be used to indirectly estimate the oxygen uptake. This is, however, not recommended as the accuracy is low. Therefore, if the aim is to obtain an accurate measure for energy expenditure, direct measurement of oxygen uptake might be more favorable than using the joint power method.

Every other method to estimate mechanical power can be considered as a simplification of the joint power method to improve feasibility, such as the often-used main propulsion method. This method revolves around using the main propulsion force or torque in the specific sport, such as the force of the hands on the oar, paddle, or wheel. The main propulsion method is widely used in cycling power meters, where the force of the feet on the paddles is considered as the main propulsion force [5–7]. By multiplying the main propulsion force or torque with the corresponding linear or angular velocity vector, one obtains the mechanical power responsible for most of the propulsion. The main propulsion method is therefore useful when mechanical power is obtained to gain insights about performance.

Simplifications, however, are mostly accompanied by assumptions and implications to consider. For example, in rowing and wheelchair propulsion, there is a CoM movement of the athlete relative to the transportation object causing possible mechanical power transfer of the athlete to the transportation object, which is not accounted for with the main propulsion method. A simple thought experiment can clarify this: consider an athlete in a wheelchair moving his upper body in a periodic manner without applying force to the push rims. By doing so, the wheelchair is also moved periodically in a direction opposed to the trunk [28]. Since the wheelchair is moving, there is power loss due to rolling resistance. However, since there is no mechanical power input from the hands on the push rims, there has to be another location where mechanical power is added to the wheelchair. This situation was also explained by Hofmijster et al. [27] for rowing, where it presents itself when a rower in a boat only moves its body relative to the boat. However, over a cycle, it may be that the influence of this power input towards propulsion and therefore towards performance has no net contribution. The influence of other forces should be examined per sport in order to assess whether the main propulsion force method is sufficient or that other kinematics or forces should be measured.

If a sport, therefore, involves a transportation object and the intended aim is to obtain a mechanical power as a performance measure, it is advised to determine it with the main propulsion force. If the sport involves a transportation object and the intended aim is to obtain a measure for energy expenditure, consider using a respiratory gas analysis device instead of determining mechanical power using the joint power method. If a sport does not involve a transportation object and a measure for performance is desired, consider whether a simplification of the athlete such as a single-body model is sufficient. By doing so, the power associated with relative segment movements is neglected. However, it can provide information about general performance. If a sport does not involve a transportation object and a measure for energy expenditure is desired, again consider using a respiratory gas analysis device instead of determining mechanical power using the joint power method. A schematic overview to assist practitioners in the selection of a suitable power measurement method given their intended aim and type of sport is given in Fig. 2.B1.

If the main propulsion method is considered suitable for the set purpose, some commercially available power meters for kayaking, rowing, and wheelchair propulsion can be used. Although power meters are ambulatory and need almost no post-processing, the suitability of a power meter differs between sports. For kayaking and rowing, power meters are lightweight and thus, there is no influence on moving the equipment + power meter. However, for wheelchair propulsion, using the OptiPush or SMARTWheel for estimating mechanical power implies adding a considerable extra mass (7–9 kg per wheelchair). Chenier et al. [29] designed an instrumented wheel for wheelchair racing, which also adds 5.6 kg to an already lightweight racing wheelchair (8–10 kg). As those instrumented wheels increase the total weight of the wheelchair with ~50–90%, they will influence wheelchair dynamics. On top of that, these instrumented wheels may not be robust to collisions, making them not suitable for wheelchair field sports. To summarize, although instrumented wheels may be of use for assessing wheelchair biomechanics, the power measurements may not be convenient for daily wheelchair sport situations.

If power meters are not available or not practical, the appropriate kinematics and forces can be measured by means of IMUs or strain gauges. The future perspectives on using IMUs for mechanical power estimation are especially promising. Moreover, in some cases, measuring forces might be redundant with the use of IMUs. For instance, in wheelchair propulsion, it might be possible to estimate rolling resistance by placing an IMU on the wheelchair and one on the trunk [30]. Force on the rear and caster wheels could be modelled as a function of trunk angle and in combination with coast down tests for rolling resistance coefficients, rolling resistance could be estimated. Consequently, mechanical power can be estimated with the power lost to

rolling resistance in combination with the estimation of the kinetic power (right-hand-side of Equation (2.2)). Power lost to air drag is then neglected, which is acceptable for low-speed indoor wheelchair sports, such as wheelchair basketball. Another option with IMUs is to use machine learning to estimate forces. For example, Uddin et al. [26] already used a Long Short-Term Memory neural network to estimate the mechanical power during roller ski skating by only using IMUs. This could also be an option for similar sports, such as speed skating or roller blade skating. Although some improvement is needed to make the method of Uddin et al. [26] suitable to implement on elite sport levels, this shows that IMUs in combination with machine learning have the potential to estimate mechanical power.

Lastly, the cost-effectiveness of estimating in-field mechanical power is useful to take into account when choosing the most appropriate approach. For equipment that can be used by multiple athletes or teams, such as a rowing boat, acquiring expensive power meters is soon affordable. In addition, once installed, the devices can remain on the boat. On the contrary, for wheelchair sports of speed skating, equipment should be purchased and installed for each individual wheelchair or skate. As athletes commonly have their own personalized equipment, using instrumented equipment for all athletes of a team will be both money- and time-consuming. Therefore, for sports with individualized equipment, non-invasive and cheaper solutions such as IMUs may be more feasible.

Although this literature review discusses the theory and practical implications of different in-field power measurement methods across different sports, some limitations should be noted. First of all, as this review was based on reported power measurement methods in kayaking, rowing, wheelchair propulsion, speed skating, and cross-country skiing, the most prominent pitfalls of those sports were discussed. Pitfalls of other sports may exist as well. However, as the concepts discussed in this review can be used as a guideline for mechanical power estimation in any other cyclical sport of interest, for example, swimming, canoeing, or roller blade skating, the main pitfalls of any other sport can be reasoned based on this review as well. Second, running was not taken into account in the present review. As the main focus of this review was defined by the power transferred from the athlete to the environment, which is only a fraction of the total mechanical power produced in running [1], running was considered beyond the scope of this review.

In conclusion, the most appropriate method to obtain mechanical power in cyclical sports differs for sports with transportation object compared to sports without a transportation object, and depends on whether performance or energy expenditure is the main interest. On top of that, the availability of a power meter, financial incentives, and mass of measurement equipment may influence the choice of a specific approach. This review provides useful handles to choose the most appropriate power measurement method for a given aim and type of sport, and explains the biomechanical underpinnings behind the different methods. A schematic overview to assist in selecting the proper power estimation method is given in Appendix A. With these insights, coaches, sport scientists, or any other person interested in measuring mechanical power can make their own, well-founded choices for measuring in-field mechanical power in any sport of interest.

5. Author Contributions

Conceptualization, M.P.v.D. and H.E.J.V.; methodology, V.G.d.V.; writing—original draft preparation, V.G.d.V.; writing—review and editing, M.P.v.D. and H.E.J.V.; supervision, M.P.v.D. and H.E.J.V. All authors have read and agreed to the published version of the manuscript.

6. Funding

This work was supported by ZonMw under project number 546003002. This project, named WheelPower: wheelchair sports and data science push it to the limit is a cooperative effort

between TU Delft, UMCG, THUAS, VU Amsterdam and is in cooperation with several sports federations collected under the umbrella of NOC * NSF.

7. Conflicts of Interest

The authors declare no conflicts of interest.

8. References

1. van Ingen Schenau, G.J.; Cavanagh, P.R. Power Equations in Endurance Sports. *J. Biomech.* **1990**, *23*, 865–881. [https://doi.org/10.1016/0021-9290\(90\)90352-4](https://doi.org/10.1016/0021-9290(90)90352-4).
2. Halson, S.L. Monitoring Training Load to Understand Fatigue in Athletes. *Sports Med.* **2014**, *44*, 139–147. <https://doi.org/10.1007/s40279-014-0253-z>.
3. Mujika, I. Quantification of Training and Competition Loads in Endurance Sports: Methods and Applications. *Int. J. Sports Physiol. Perform.* **2017**, *12*, S2-9–S2-17. <https://doi.org/10.1123/ijsp.2016-0403>.
4. Soligard, T.; Schwelunus, M.; Alonso, J.-M.; Bahr, R.; Clarsen, B.; Dijkstra, H.P.; Gabbett, T.; Gleeson, M.; Häggglund, M.; Hutchinson, M.R.; et al. How Much Is Too Much? (Part 1) International Olympic Committee Consensus Statement on Load in Sport and Risk of Injury. *Br. J. Sports Med.* **2016**, *50*, 1030–1041. <https://doi.org/10.1136/bjsports-2016-096581>.
5. Bini, R.; Diefenthaler, F.; Carpes, F. Determining Force and Power in Cycling: A Review of Methods and Instruments for Pedal Force and Crank Torque Measurements. *Int. SportsMed J.* **2014**, *15*, 96–112.
6. Bouillod, A.; Soto-Romero, G.; Grappe, F.; Bertucci, W.; Brunet, E.; Cassirame, J. Caveats and Recommendations to Assess the Validity and Reliability of Cycling Power Meters: A Systematic Scoping Review. *Sensors* **2022**, *22*, 386. <https://doi.org/10.3390/s22010386>.
7. Sitko, S.; Cirer-Sastre, R.; Corbi, F.; López, I. Power Assessment in Road Cycling: A Narrative Review. *Sustainability* **2020**, *12*, 5216. <https://doi.org/10.3390/su12125216>.
8. van der Kruk, E.; van der Helm, F.C.T.; Veeger, H.E.J.; Schwab, A.L. Power in Sports: A Literature Review on the Application, Assumptions, and Terminology of Mechanical Power in Sport Research. *J. Biomech.* **2018**, *79*, 1–14. <https://doi.org/10.1016/j.jbiomech.2018.08.031>.
9. Camomilla, V.; Bergamini, E.; Fantozzi, S.; Vannozzi, G. Trends Supporting the In-Field Use of Wearable Inertial Sensors for Sport Performance Evaluation: A Systematic Review. *Sensors* **2018**, *18*, 873. <https://doi.org/10.3390/s18030873>.
10. Lintmeijer, L.L.; Faber, G.S.; Kruk, H.R.; van Soest, A.J.; Hofmijster, M.J. An Accurate Estimation of the Horizontal Acceleration of a Rower's Centre of Mass Using Inertial Sensors: A Validation. *Eur. J. Sport Sci.* **2018**, *18*, 940–946. <https://doi.org/10.1080/17461391.2018.1465126>.
11. van der Kruk, E.; den Braver, O.; Schwab, A.L.; van der Helm, F.C.T.; Veeger, H.E.J. Wireless Instrumented Klapskates for Long-Track Speed Skating. *Sport. Eng.* **2016**, *19*, 273–281. <https://doi.org/10.1007/s12283-016-0208-8>.
12. Ohtonen, O.; Lindinger, S.; Lemmettylä, T.; Seppälä, S.; Linnamo, V. Validation of PorTable 2D Force Binding Systems for Cross-Country Skiing. *Sport. Eng.* **2013**, *16*, 281–296. <https://doi.org/10.1007/s12283-013-0136-9>.
13. Rietveld, T.; Mason, B.S.; Goosey-Tolfrey, V.L.; van der Woude, L.H.V.; de Groot, S.; Vegter, R.J.K. Inertial Measurement Units to Estimate Drag Forces and Power Output during Standardised Wheelchair Tennis Coast-down and Sprint Tests. *Sports Biomech.* **2021**, *1*–19. <https://doi.org/10.1080/14763141.2021.1902555>.

14. Hogan, C.; Binnie, M.J.; Doyle, M.; Peeling, P. Quantifying Sprint Kayak Training on a Flowing River: Exploring the Utility of Novel Power Measures and Its Relationship to Measures of Relative Boat Speed. *Eur. J. Sport Sci.* **2022**, *22*, 1668–1677. <https://doi.org/10.1080/17461391.2021.1977393>.
15. Macdermid, P.; Fink, P. The Validation of a Paddle Power Meter for Slalom Kayaking. *Sports Med. Int. Open* **2017**, *1*, E50–E57. <https://doi.org/10.1055/s-0043-100380>.
16. Baudouin, A.; Hawkins, D. Investigation of Biomechanical Factors Affecting Rowing Performance. *J. Biomech.* **2004**, *37*, 969–976. <https://doi.org/10.1016/j.jbiomech.2003.11.011>.
17. Doyle, M.M.; Lyttle, A.; Elliott, B. Comparison of Force-Related Performance Indicators between Heavyweight and Lightweight Rowers. *Sports Biomech.* **2010**, *9*, 178–192. <https://doi.org/10.1080/14763141.2010.511678>.
18. Holt, A.C.; Hopkins, W.G.; Aughey, R.J.; Siegel, R.; Rouillard, V.; Ball, K. Concurrent Validity of Power from Three On-Water Rowing Instrumentation Systems and a Concept2 Ergometer. *Front. Physiol.* **2021**, *12*, 1960. <https://doi.org/10.3389/fphys.2021.758015>.
19. Conger, S.A.; Scott, S.N.; Bassett, D.R. Predicting Energy Expenditure through Hand Rim Propulsion Power Output in Individuals Who Use Wheelchairs. *Br. J. Sports Med.* **2014**, *48*, 1048–1053. <https://doi.org/10.1136/bjsports-2014-093540>.
20. de Groot, S.; Vegter, R.J.K.; van der Woude, L.H.V. Effect of Wheelchair Mass, Tire Type and Tire Pressure on Physical Strain and Wheelchair Propulsion Technique. *Med. Eng. Phys.* **2013**, *35*, 1476–1482. <https://doi.org/10.1016/j.medengphy.2013.03.019>.
21. de Klerk, R.; Vegter, R.J.K.; Leving, M.T.; de Groot, S.; Veeger, D.H.E.J.; van der Woude, L.H.V. Determining and Controlling External Power Output during Regular Handrim Wheelchair Propulsion. *J. Vis. Exp.* **2020**, e60492. <https://doi.org/10.3791/60492>.
22. van der Scheer, J.W.; de Groot, S.; Vegter, R.J.K.; Veeger, D.; van der Woude, L.H.V. Can a 15 M-Overground Wheelchair Sprint Be Used to Assess Wheelchair-Specific Anaerobic Work Capacity? *Med. Eng. Phys.* **2014**, *36*, 432–438. <https://doi.org/10.1016/j.medengphy.2014.01.003>.
23. Mason, B.S.; van der Woude, L.H.V.; Tolfrey, K.; Lenton, J.P.; Goosey-Tolfrey, V.L. Effects of Wheel and Hand-Rim Size on Submaximal Propulsion in Wheelchair Athletes. *Med. Sci. Sports Exerc.* **2012**, *44*, 126–134. <https://doi.org/10.1249/MSS.0b013e31822a2df0>.
24. Kleshnev, V. Power in Rowing. 18 International Symposium on Biomechanics in Sport, Hong Kong, China, June 25–30, 2000.
25. Gløersen, Ø.; Losnegard, T.; Malthe-Sørensen, A.; Dysthe, D.K.; Gilgien, M. Propulsive Power in Cross-Country Skiing: Application and Limitations of a Novel Wearable Sensor-Based Method during Roller Skiing. *Front. Physiol.* **2018**, *9*, 1631. <https://doi.org/10.3389/fphys.2018.01631>.
26. Uddin, M.Z.; Seeberg, T.M.; Kocbach, J.; Liverud, A.E.; Gonzalez, V.; Sandbakk, Ø.; Meyer, F. Estimation of Mechanical Power Output Employing Deep Learning on Inertial Measurement Data in Roller Ski Skating. *Sensors* **2021**, *21*, 6500. <https://doi.org/10.3390/s21196500>.
27. Hofmijster, M.J.; Lintmeijer, L.L.; Beek, P.J.; van Soest, A.J. Mechanical Power Output in Rowing Should Not Be Determined from Oar Forces and Oar Motion Alone. *J. Sports Sci.* **2018**, *36*, 2147–2153. <https://doi.org/10.1080/02640414.2018.1439346>.
28. van Dijk, M.P.; van der Slikke, R.M.A.; Berger, M.A.M.; Hoozemans, M.J.M.; Veeger, D.H.E.J. Look Mummy, No Hands! The Effect of Trunkmotion on Forward Wheelchair Propulsion. *ISBS Proc. Arch.* **2021**, *39*, 312.
29. Chénier, F.; Pelland-Leblanc, J.-P.; Parrinello, A.; Marquis, E.; Rancourt, D. A High Sample Rate, Wireless Instrumented Wheel for Measuring 3D Pushrim Kinetics of a Racing Wheelchair. *Med. Eng. Phys.* **2021**, *87*, 30–37. <https://doi.org/10.1016/j.medengphy.2020.11.008>.

30. van Dijk, M.P.; Kok, M.; Berger, M.A.M.; Hoozemans, M.J.M.; Veeger, H.E.J. Machine Learning to Improve Orientation Estimation in Sports Situations Challenging for Inertial Sensor Use. *Front. Sports Act. Living* **2021**, *3*, 670263. <https://doi.org/10.3389/fspor.2021.670263>.
31. Noordhof, D.A.; Foster, C.; Hoozemans, M.J.M.; de Koning, J.J. Changes in Speed Skating Velocity in Relation to Push-Off Effectiveness. *Int. J. Sports Physiol. Perform.* **2013**, *8*, 188–194. <https://doi.org/10.1123/ijspp.8.2.188>

Appendix A

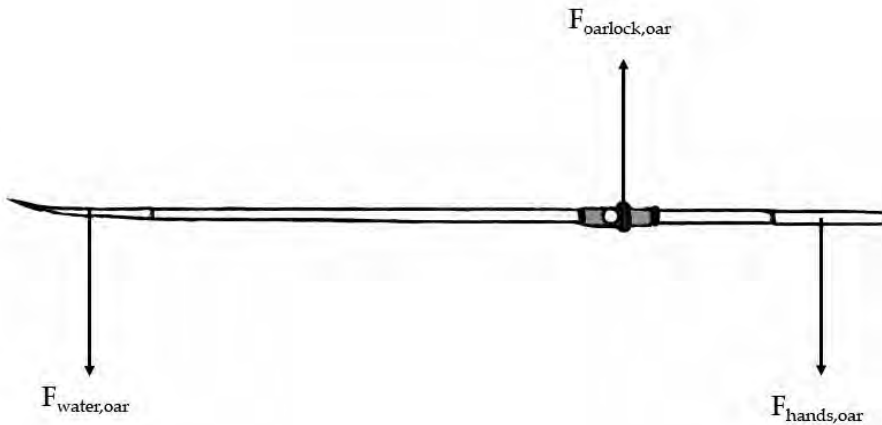


Figure 2.A1. The oar as a rigid body. The force of the hands on the oar is displayed as $F_{\text{hands,oar}}$, the force of the oarlock on the oar is displayed as $F_{\text{oarlock,oar}}$ and the force of the water on the oar is displayed as $F_{\text{water,oar}}$. This figure can also be used for kayaking. With the paddle as rigid body, the word oar can be replaced with paddle. $F_{\text{hands,oar}}$ must then be replaced with force of the top hand on the paddle and the force of the bottom hand on the paddle replaces $F_{\text{oarlock,oar}}$. This figure is adapted from Hofmijster et al. [27].

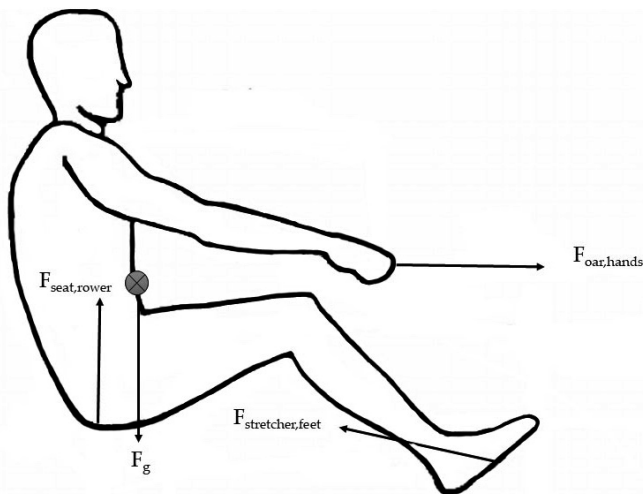


Figure 2.A2. The rower as a rigid body. The force of the oar on the hand is displayed as $F_{\text{oar,hands}}$, the force of the stretcher on the feet is displayed as $F_{\text{stretcher,feet}}$, the force of the seat on the rowers is displayed as $F_{\text{seat,rower}}$ and the gravitational force is displayed as F_g . This figure is also applicable for kayakers if the rower is replaced by kayaker and oar is replaced by paddle. This figure is adapted from Hofmijster et al. [27].

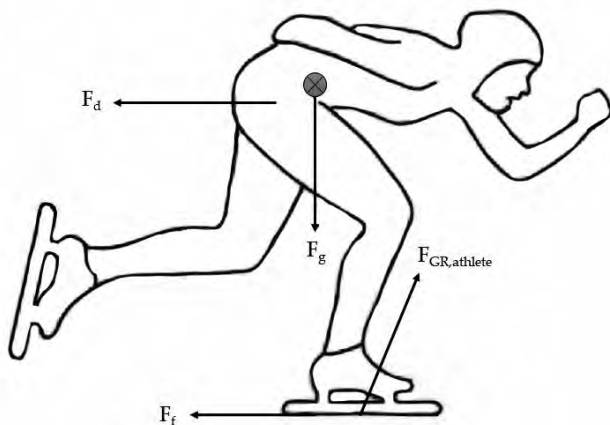


Figure 2.A3. The speed skater as a rigid body. The drag force is displayed as F_d , the gravitational force is displayed as F_g , the frictional force of the skates with the surface as F_i and the push-off force is displayed as $F_{GR,athlete}$. This figure is also applicable for cross-country skiing. This figure is adapted from Noordhof et al. [31].

Appendix B

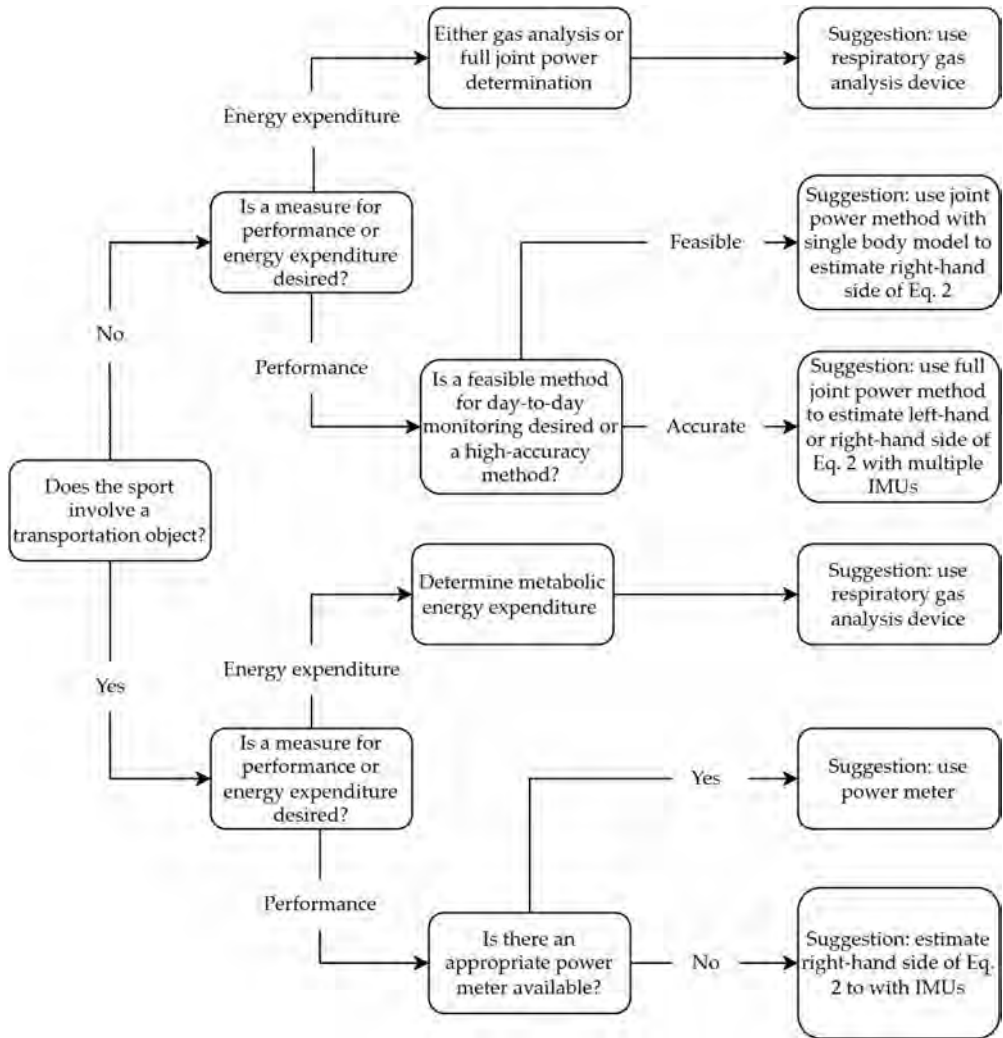


Figure 2.B1. A schematic overview to assist in the selection of a suitable power measurement method given their intended aim and type of sport.



Abstract

An important performance determinant in wheelchair sports is the power exchanged between the athlete-wheelchair combination and the environment, in short, mechanical power. Inertial measurement units (IMUs) might be used to estimate the exchanged mechanical power during wheelchair sports practice. However, to validly apply IMUs for mechanical power assessment in wheelchair sports, a well-founded and unambiguous theoretical framework is required that follows the dynamics of manual wheelchair propulsion. Therefore, this research has two goals. First, to present a theoretical framework that supports the use of IMUs to estimate power output via power balance equations. Second, to demonstrate the use of the IMU-based power estimates during wheelchair propulsion based on experimental data. Mechanical power during straight-line wheelchair propulsion on a treadmill was estimated using a wheel mounted IMU and was subsequently compared to optical motion capture data serving as a reference. IMU-based power was calculated from rolling resistance (estimated from drag tests) and change in kinetic energy (estimated using wheelchair velocity and wheelchair acceleration). The results reveal no significant difference between reference power values and the proposed IMU-based power (1.8% mean difference, N.S.). As the estimated rolling resistance shows a 0.9-1.7% underestimation, over time, IMU-based power will be slightly underestimated as well. To conclude, the theoretical framework and the resulting IMU model seems to provide acceptable estimates of mechanical power during straight-line wheelchair propulsion in wheelchair (sports) practice, and it is an important first step towards feasible power estimations in all wheelchair sports situations.

Table 3.1. Table of definitions

i	Point of application
$F_{ext,i}$	External force(s) acting on i
$M_{ext,i}$	External moment(s) acting on i
$F_{roll,i}$	Rolling resistance of i
$F_{air,i}$	Air resistance of i
$F_{g,i}$	Gravity of i
$F_{propulsion}$	Propulsive force
$F_{N,j}$	Normal force acting on wheel j
$F_{source,i}$	Force of source on i
a_i	Acceleration of i
\bar{a}_i	Cycle-average acceleration of i
ω_i	Angular velocity of i
v_i	Linear velocity of i
\bar{v}_i	Cycle-average linear velocity of i
$v_{i/ref}$	Velocity of i relative to reference
P_i	Power generated or dissipated by i (i can be a model or a source)
\bar{P}_{model}	Cycle average power according to defined model
dE_{kin}/dt	Change in kinetic energy of the chosen system
θ_j	Inclination angle of object j with respect to the horizontal
μ_j	Rolling resistance coefficient of wheel j
$c_{air,j}$	Air resistance coefficient of object j

Introduction

Wheelchair sports have become increasingly popular over the last decades (Cooper and De Luigi 2014; vanLandewijck and Thompson 2011). In line with their popularity, monitoring performance in wheelchair sports is becoming more common. Wheelchair sport performance can be monitored by recording time and velocity (Goosey-Tolfrey and Moss 2005; van der Slikke et al. 2016; de Witte et al. 2018). However, velocity can be biased as a measure of exercise intensity. A large head wind or uneven surface, for example, will generally decrease the velocity, while exercise intensity may be equal. In contrast, the mechanical power exchanged between the athlete-wheelchair combination and the environment, here referred to as mechanical power, is a more objective measure for exercise intensity as not only velocity but also forces are included (van Ingen-Schenau and Cavanagh 1990). For this reason, mechanical power is often used to provide information on, for instance, training load, physical and physiological capacity, and fatigue, which may support coaches and athletes to reduce injury risks and improve performance (Halson 2014; Mujika 2017; Soligard et al. 2016). It should therefore be monitored during wheelchair sports.

In contrast to the well-integrated power meters in professional cycling, obtaining mechanical power during in-field wheelchair sports is challenging. While bicycles can be equipped with power meters integrated into cranksets or pedals, directly measuring mechanical power in wheelchairs would involve force-instrumented push-rims (de Groot et al., 2014). However, as these systems are expensive, heavy and not sufficiently robust to be used during court sports such as wheelchair basketball or rugby, a non-invasive and inexpensive method to monitor power during wheelchair sports is needed.

One possible method is the use of inertial measurement units (IMUs). IMUs are small wearable sensors that generally contain an accelerometer, gyroscope, and magnetometer, to measure three-dimensional linear acceleration, angular velocity, and the magnetic field, respectively. IMUs can easily be attached to body parts or wheelchair segments and have been used to estimate mechanical power in sports like rowing and cross-country skiing (Gløersen et al. 2018; Uddin et al. 2021; de Vette, Veeger, and van Dijk 2022). As IMUs are used to monitor velocity, acceleration and rotations in wheelchair practice (Bakatchina et al. 2021; Poulet et al. 2022; Rupf et al. 2021; van der Slikke et al. 2015; de Vries et al. 2023), it would be possible to use IMUs for power monitoring as well.

To validly apply IMUs for mechanical power assessment in wheelchair sports, a well-founded and unambiguous theoretical framework is required that follows the dynamics of manual wheelchair propulsion. Although several wheelchair models have been reported previously, they are focused on specific aspects of wheelchair propulsion (e.g. rolling resistance (Cooper 1990; Sauret et al. 2009; Silva et al. 2017; Teran and Ueda 2017), athlete/user dynamics (Chénier et al. 2016; Cooper 1990; Schnorenberg et al. 2014; Veeger, Rozendaal, and Van Der Helm 2002; Veeger, van der Woude, and Rozendal 1991), or roller systems (Chénier, Bigras, and Aissaoui 2015; Cooper 1990) and are, therefore, incomplete or too extensive.

Therefore, the present paper has two goals. First, to present a theoretical framework that supports the use of IMUs to estimate mechanical power via power balance equations. Second, to demonstrate the use of the IMU-based power estimates during wheelchair propulsion based on experimental data.

Theoretical framework

Definition(s) of power

Power is the energy transferred or converted per unit of time and is expressed in Watts. In human locomotion, metabolic energy is converted into muscle power. Subsequently, muscle power enables body segments to overcome internal friction to, eventually, produce external power (e.g., on the push-rims of a wheelchair). However, not all power liberated from metabolic energy is available for locomotion. As energy is required to, for instance, operate the cardio-respiratory system, produce heat, and stabilize the human body, the (metabolic) power input differs from the (mechanical) power output. Power input is essentially equal to the metabolic rate (van Ingen-Schenau and Cavanagh 1990) and is often measured with respiratory gas analysis systems. Power output is transferred from a – in this case - wheelchair athlete to the environment and it can be approached purely mechanical (see Eq. 3.1). We therefore refer to power output as ‘mechanical power’. Power can be measured with a wheelchair ergometer, a force-instrumented push-rim, or estimated from kinematic data.

The power balance for wheelchair propulsion

Following the classic ‘power equations in endurance sports’ of van Ingen-Schenau & Cavanagh (1990), the mechanical power balance of an athlete equals:

$$P_{athlete} = -\sum F_{ext,athlete} * v_{ext,athlete} - \sum M_{ext,athlete} * \omega_{ext,athlete} + \sum dE_{kin}/dt \quad (3.1)$$

$$P_{athlete} = -P_{friction} - P_{gravity} - P_{environmental} + P_{kinetic} \quad (3.2)$$

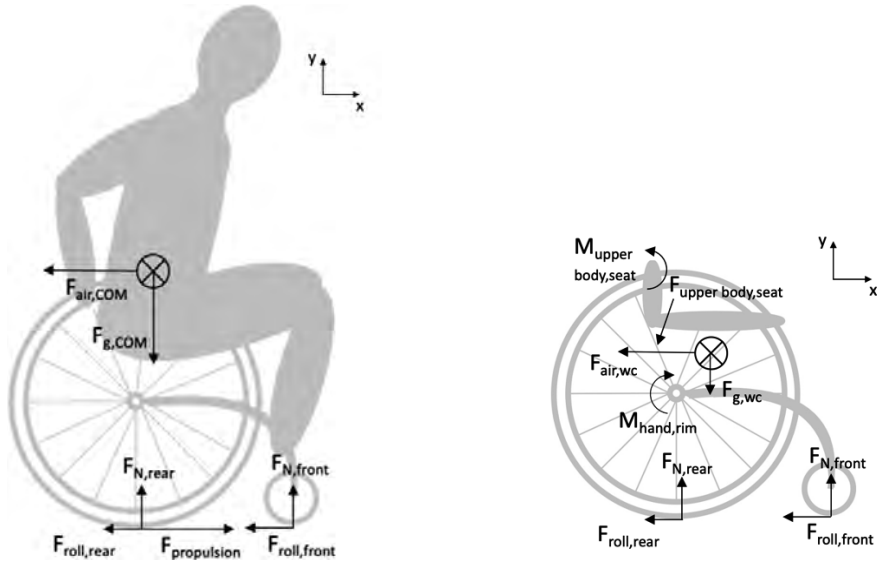


Fig. 3.1a-b. Rigid body diagrams with forces acting on the segments. The left figure (a) shows the athlete-wheelchair model. The right figure (b) shows the wheelchair model. Note that the actual direction of the force vectors may differ from the directions as drawn here. Note also that $M_{hand,rim}$ is drawn at the wheel axes as it represents the moment that the athlete applies on the push-rims around the wheel axes. However, $M_{hand,rim}$ will also apply a moment from the hands on the push-rims around the hand which is described by Van Der Woude et al. (2001) as the ‘hand moment’. As this moment is assumed to produce no power, we drew, $M_{hand,rim}$ around the wheel axes.

In Eq. 3.1, the effects of gravity are included as an external force (van Ingen-Schenau and Cavanagh 1990). An alternative way to represent the power equation is given in Eq. 3.2 (van der Kruk et al. 2018), in which the athlete generates power ($P_{athlete}$) to (partially) overcome power losses due to resistive forces ($P_{friction}$, $P_{gravity}$ and $P_{environmental}$) resulting in a (changing) velocity of the athlete ($P_{kinetic}$). To apply the power balance to a wheelchair athlete, a suitable system must be defined. Two complete yet concise model options are presented below.

Athlete-wheelchair model

The simplest approach is to consider the athlete-wheelchair combination as a single rigid body. The free body diagram corresponding to this ‘athlete-wheelchair model’ is presented in Fig. 3.1a. The external forces acting on the athlete-wheelchair model are normal forces ($\mathbf{F}_{N,i}$), rolling resistance ($\mathbf{F}_{roll,i}$), air resistance ($\mathbf{F}_{air,i}$), and gravity ($\mathbf{F}_{g,i}$). Throughout this article, internal resistance is considered part of the rolling resistance. No external moments are identified. In the power balance corresponding to the free body diagram, $\mathbf{F}_{roll,rear}$ and $\mathbf{F}_{roll,front}$ are summarized by $\mathbf{F}_{roll,i}$ (see Eq. 3.3). As normal force is perpendicular to the movement direction of its point of application, it does not produce power and is not included in the power balance. As the rigid bodies are assumed to have no rotations, rotational kinetic energy is not included. Note that the left hand-side of Eq. 3.3 could be replaced by $\mathbf{F}_{propulsion,COM} * \mathbf{v}_{COM}$ (see Eq. 3.4). In all equations, COM refers to the center of mass of the athlete-wheelchair combination (AW). In the text, COM_{AW} is used to avoid confusion.

$$P_{AW} = -\mathbf{F}_{roll,COM} * \mathbf{v}_{COM} - \mathbf{F}_{air,COM} * \mathbf{v}_{COM} - \mathbf{F}_{g,COM} * \mathbf{v}_{COM} + \frac{1}{dt} (0.5 * m_{AW} * \mathbf{v}_{COM}^2) \quad (3.3)$$

$$P_{AW} = \mathbf{F}_{propulsion,COM} * \mathbf{v}_{COM} \quad (3.4)$$

Wheelchair model

An alternative approach is to model all forces, moments, and corresponding (angular) velocities, acting on the transportation object, in this case the manual wheelchair (W), see Eq. 3.5. This approach is often used in rowing and kayaking (Doyle, Lyttle, and Elliott 2010; Hogan et al. 2022; Holt et al. 2021; Macdermid and Fink 2017). For wheelchair propulsion, Chenier et al. (2016) used a similar model to predict instantaneous wheelchair velocity from net force (consisting of average rolling resistance, measured propulsion forces and upper body mass and acceleration). The free body diagram representing this ‘wheelchair model’ is presented in Fig. 3.1b. With respect to Fig. 3.1a, four additional terms are introduced: $\mathbf{F}_{upper\ body,seat}$ and $\mathbf{M}_{upper\ body,seat}$ representing the force and moment of the upper body on the wheelchair seat induced by upper body movements, $\mathbf{M}_{hand,rim}$ representing the moment that the athlete applies on the push-rims around the wheel axes (consisting of both the ‘pure’ moment *and* the tangential force applied by the hands to the push-rim), and ω_{wheel} representing the wheel angular velocity. As the wheelchair is assumed to have no angular velocity in the sagittal plane, $\mathbf{M}_{upper\ body,seat}$ produces no power. Consequently, the power produced by the athlete consists of two terms (see Eq. 3.6).

$$P_W = -\mathbf{F}_{roll,W} * \mathbf{v}_W - \mathbf{F}_{air,W} * \mathbf{v}_W - \mathbf{F}_{g,W} * \mathbf{v}_W + \frac{1}{dt} (0.5 * m_W * \mathbf{v}_W^2) \quad (3.5)$$

$$P_W = \mathbf{M}_{hand,rim} * \omega_{wheel} + \mathbf{F}_{upper\ body,seat} * \mathbf{v}_W \quad (3.6)$$

Model comparisons

Although the instantaneous power graphs of the two models will generally differ from each other, the models are based on the same mechanical principles and can both be used to estimate wheelchair athlete power. To understand the differences between the models, let's assume that upper body movements produce no net power on the wheelchair seat (see Appendix A for the situation in which upper body movements *do* produce net mechanical power). In this case, P_{AW} will be non-zero when the hands propel the push-rims, and zero otherwise. Therefore, P_{AW} may be easier to interpret and the instantaneous power graph will be similar to that of a force-instrumented push-rim or ergometer (de Groot et al. 2014); note, however, that P_{AW} will slightly differ from power measured by force-instrumented push rims as force-instrumented push-rims assume that the wheelchair velocity equals the velocity of the COM_{AW} which is not a valid assumption. In the wheelchair model instead, $F_{upper\ body, seat}$ is included as a force exerted by the athlete as well. Although $F_{upper\ body, seat}$ is zero on average, this force fluctuates within a stroke cycle due to mass displacements of the upper body. Consequently, P_W fluctuates more within a stroke cycle than P_{AW} . However, as P_W consists of mainly wheelchair kinematics (instead of COM_{AW} kinematics, see Eq. 3.3 and 3.5), P_W may be easier to approach with IMU data. Because both models have advantages, both were used to underpin and compare with IMU-based power estimates.

Power output assessment during wheelchair propulsion with IMU's – from theoretical framework to wheelchair sports practice

In this section, four assumptions are presented to explain how IMU data can be used to approach the different components of the above-mentioned power balance equations.

Assumptions for power monitoring using IMUs

Assumption 1: Mechanical power during wheelchair propulsion can be assessed by monitoring the cycle-average power: cycle-average velocity thus suffices

To estimate power output from IMU data, the velocity of the COM_{AW} (Eq. 3.3) or the velocity of the wheelchair (Eq. 3.5), should be determined. Whereas wheelchair velocity and acceleration can already be measured accurately with an IMU attached to the wheelchair (van Dijk et al. 2022; van der Slikke et al. 2015), obtaining the instantaneous velocity and acceleration of the COM_{AW} is complex. During propulsion, the COM_{AW} moves with respect to the wheelchair due to trunk, head and arm movements (van Dijk et al., 2021). Chenier et al. (2016), accurately modeled the kinematics of the upper body COM with one IMU on the upper arm. However, they assumed trunk dynamics to be negligible in their spinal cord injury population, which is not reasonable for all wheelchair athletes. Given the differences in movement pattern and heterogeneity of wheelchair athletes, establishing a model that accurately estimates COM_{AW} kinematics from IMU data during wheelchair propulsion is complicated and requires multiple body-worn IMUs (Gløersen et al. 2018; Refai et al. 2020).

However, determining the instantaneous COM_{AW} velocity and acceleration may not be necessary. Many applications in cyclical sports use average power output per push to monitor athletes (Holt et al. 2021; Leo et al. 2022), and this may suffice for wheelchair sports as well. As athletes remain in their wheelchairs during propulsion, one can assume that $\overline{v_{COM}} = \overline{v_{WC}}$ over multiple propulsion cycles, in which \overline{v}_i represents cycle average velocity.

Assumption 2: Air resistance can be neglected during indoor wheelchair field and court sports

During wheelchair propulsion, one resistive force acting on the athlete-wheelchair combination is air resistance (see Eq. 3.3 and 3.5). To determine air resistance, both the air velocity relative to the wheelchair ($\mathbf{v}_{wc/air}$) and the air resistance coefficient ($c_{air,wc}$) should be known (see Eq. 3.7, Coe 1979; Forte et al. 2018). As $\mathbf{v}_{wc/air}$ varies with wind and wheelchair velocity, and with ‘relative’ movement direction; and $c_{air,wc}$ depends on air density, streamline and frontal area (de Koning et al. 2005), the information required to calculate air resistance cannot be derived from IMU data. However, in the present paper we focus on indoor wheelchair court sports. As these sports consist of short sprints and lots of braking, the wheelchair velocities are generally below 2.5 m/s (Chénier et al. 2022; van der Slikke et al. 2020). In addition, we assume that air velocity is zero indoors. In these circumstances, the proportion of air resistance is around 5% of the total resistance force (Barbosa et al. 2014). Therefore, $\mathbf{v}_{i/air}$ can be assumed negligible for indoor wheelchair field and court sports.

$$\mathbf{F}_{air,i} = c_{air,i} * \mathbf{v}_{i/air} * |\mathbf{v}_{i/air}| \quad (3.7)$$

Assumption 3: The rolling resistance force during wheelchair propulsion can be determined by a deceleration test

During indoor wheelchair field and court sports, rolling resistance is the main resistive force (van der Woude et al. 2001). This force can be calculated from the normal forces acting on the rear- and front wheels, and the rolling resistance coefficients of the wheels (see Eq. 3.8). However, as rolling resistance is influenced by factors such as tire pressure and surface characteristics (Ott and Pearlman 2021), rolling resistance coefficients may differ for each wheelchair and surface. In addition, the normal force may vary within a propulsion cycle. Sauret et al. (2013) assessed the instantaneous normal force acting on the wheelchair wheels and reported that the total normal force varied between 80-130% of the gravitational force. Also, they reported that the normal force at the front wheels fluctuated from 24-31% (minimal values) to 61-83% (maximal values) of the total load within each push cycle, which might be caused by upper body motions (van Dijk et al., 2021). As, in court sports, the front wheels generally have higher rolling resistance coefficients (μ_{front}) compared to the rear wheels (μ_{rear}), this causes intra-cyclical variations in rolling resistance force. To account for these variations, rolling resistance coefficients of each pair of (front or rear) wheels should be determined, and instantaneous normal forces should be known. Unfortunately, normal forces cannot yet be derived from IMU data as this requires information about the COM_{AW} position and vertical acceleration.

Most studies, however, assume the rolling resistance to be a constant (Chénier et al. 2015; De Groot et al. 2006; Rietveld et al. 2021), that can be determined by a deceleration test (Hoffman et al. 2003; Sauret et al. 2013). During this test, the wheelchair is decelerated from an initial velocity [at which air resistance is assumed negligible, i.e., < 2.5 m/s], at a horizontal surface and while the wheelchair athlete keeps a static posture. Consequently, the resistance force can be calculated from the total mass times the (IMU-based) wheelchair acceleration. During wheelchair propulsion, rolling resistance may thus be estimated by a deceleration test. Note that this test should be repeated once the user, wheelchair (tires) or surface has changed.

$$\mathbf{F}_{roll,i} = \mathbf{F}_{N,front} * \mu_{front} + \mathbf{F}_{N,rear} * \mu_{rear} \quad (3.8)$$

Assumption 4: The role of gravity can be determined from a wheel(chair)-mounted IMU

If the surface has a slope, power is transferred to potential energy and should thus be considered in the power balance (see Eq. 3.3 and 3.5). The gravitational force ($F_{g,i}$) can be determined from the inclination angle of the wheelchair with respect to the horizontal (θ) and the total mass (according to Eq. 3.9). With an IMU on the wheelchair frame or wheel and a sensor fusion algorithm that calculates the angle of the wheelchair with respect to the direction of the gravity vector (van Dijk et al., 2021), θ can be determined with relative ease. For indoor wheelchair court sports, θ (and thus $F_{g,AW}$) can be considered zero.

$$F_{g,i} = m_i * 9.81 * \sin(\theta_i) \quad (3.9)$$

Implication of assumptions: Simplified power balance for IMU-based estimates

Considering above-mentioned assumptions for wheelchair field and court sports, mean power exchanged between the athlete-wheelchair combination and the environment over multiple stroke cycles can be estimated using one wheel-mounted IMU. Consequently, the power balance for IMU-based power is given in Eq. 3.10. Here, T is the duration of one complete stroke cycle in seconds. If the assumptions are valid and the wheelchair is unmotorized, the cycle average power output derived from IMU data ($\overline{P_{IMU}}$) should be similar for the athlete-wheelchair model ($\overline{P_{AW}}$) and the wheelchair model ($\overline{P_W}$), see Eq. 3.11.

$$\overline{P_{IMU}} = (1/T) * \int_0^T -F_{roll,W} * v_W + \frac{1}{dt} (0.5 * m_{AW} * v_W^2) \quad (3.10)$$

$$\overline{P_{IMU}} \approx \overline{P_{AW}} \approx \overline{P_W} \quad (3.11)$$

Monitoring power using IMUs in practice

To demonstrate the use of IMU-based power estimates, power was estimated from IMU data (i.e., $\overline{P_{IMU}}$) during wheelchair propulsion and compared to the power estimated according to the two proposed models (i.e., $\overline{P_{AW}}$ and $\overline{P_W}$) using optical motion capture (MOCAP) data. Although demonstrating this during overground wheelchair propulsion - including curves and turns - would be ideal, the measurement area is limited when using MOCAP and rolling resistance cannot be determined accurately during curves and turns. Therefore, experiments were performed on a large (3.0 x 5.0 m) treadmill. We consider all velocities and accelerations relative to the treadmill belt.

Methods

This study was approved by the ethical committee of Delft University of Technology (Nr. 1530) and written informed consent was obtained from all participants prior to data collection. Eleven participants (8 female, mean age=30±9 years, mean body mass=72±8 kg) without wheelchair experience received a 10-minute training protocol for both overground and treadmill wheelchair propulsion to familiarize with the measurement setup. An IMU (NGIMU, X-io Technologies, Colorado Springs, United States; 100 Hz) was attached to the wheelchair right wheel axle, and marker clusters (Optotrak Certus, Northern Digital, Waterloo, Canada; 100 Hz) were attached to the wheelchair, and participants' body segments (see Fig. 3.2). The position of anatomical landmarks and wheelchair landmarks relative to the marker clusters was determined. In addition, mass and center of pressure (COP) of the participants + wheelchair was measured on a separate 1.0 x 1.0 m custom-made strain gauge force plate (Kingma et al. 1995). Subsequently, participants propelled an all-court sports wheelchair (13.2 kg) on a large motor-driven treadmill

(Bonte, Zwolle, the Netherlands). First, participants propelled at a constant velocity of 1.2 m/s for 90 seconds, while following a metronome of 25 beats/min (to naturally impose effective strokes and keep a constant power per push). Following this, participants accelerated from 1.2 to 1.7 m/s over a 7-second period imposed by gradually increasing treadmill speed. During the treadmill sessions, three-dimensional kinematics were measured using the IMU and MOCAP system. As performing a deceleration test is not feasible on a treadmill, drag tests were used to obtain F_{roll} . After each treadmill session, drag tests were performed at 1.7 m/s while the participants were instructed to sit as still as possible for a period of 30s in six conditions. The (2x3) conditions consisted of sitting with vertical trunk and sitting bent forward while no mass was added, while 10 kg was added at the footrests and while 10 kg was added on the upper legs. Simultaneously, $F_{roll,inst}$ was measured with a S-beam load cell (Revere Transducers, Lisse, the Netherlands).



Fig. 3.2. Overview of the measurement setup. Participants were measured with a MOCAP system with marker clusters (Δ) on the wheelchair frame, trunk (sternum), head, upper arm and lower arm, and IMUs (\square) on the wheel axle and on the center of the wheelchair frame. Both the 3.0 x 5.0m treadmill and the 1.0 x 1.0 force plate (below the treadmill) are visible in the figure.

Data analysis

Based on the landmark positions from the MOCAP system, total body length and mass, the upper body segment lengths and COM's were estimated based on the non-linear regression equations as described by Zatsiorsky (2002). Subsequently, upper body segment COM's, m_{AW} and COP of the wheelchair + participant were used to determine the COP of the lower body + wheelchair with respect to the rear-wheel axes. With this information, the horizontal COM_{AW} position (and COM_{AW} velocity vector as its time derivative) relative to the rear-wheel axes could be determined from MOCAP data during the treadmill sessions. COM_{AW} velocity was obtained by summing this 'relative' COM_{AW} velocity to wheelchair velocity. Wheelchair velocity for all models was determined from the wheel-mounted IMU data, wheel circumference, track width and camber angle according to Rupf et al. (2021) and van der Slikke et al. (2015).

Subsequently, instantaneous normal forces were calculated from the horizontal COM_{AW} position relative to the wheels and vertical COM_{AW} acceleration times total mass. Rolling resistance coefficients were numerically solved based on the drag tests with varying load distributions and Eq. 3.8 (Sauret et al. (2013)). The instantaneous normal forces and rolling resistance coefficients were used to determine the instantaneous rolling resistance ($F_{roll,inst}$) according to Eq. 3.8. $F_{roll,drag}$, determined by a drag test in upright position, was used for \overline{P}_{IMU} .

To compare the three different models ($\overline{P_{IMU}}$, $\overline{P_{AW}}$ and $\overline{P_W}$), data were 2nd order low-pass filtered at 6 Hz, after which the instantaneous rolling resistance, dE_{kin} and instantaneous power values were calculated according to Eq. 3.3, 3.5 and 3.10. Subsequently, pushes were identified by the time instance at which the horizontal position of the wrist relative to the wheelchair reaches its maximum. Accordingly, the average values of three consecutive pushes were calculated and again averaged for each participant per condition. The differences between the models were tested statistically using a Wilcoxon signed-rank test (Shapiro-Wilk test revealed no normal distribution) with a significance level of 0.05.

Results and discussion of results

The instantaneous power graphs of the three models (see Fig. 3.3) show that P_{AW} (i.e., athlete-wheelchair model) has a shape similar to the typical shape reported for force-instrumented push-rims (de Groot et al. 2014), while P_W (i.e., wheelchair model) fluctuated within a push cycle due to mass displacements of the upper body. As expected, P_{IMU} fluctuates similarly to P_W as both are based on wheelchair kinematics, with a larger amplitude for P_{IMU} since m_{AW} (Eq. 3.10) is larger than m_W (Eq. 3.5). The differences between P_{IMU} and P_{AW} are due to differences between the wheelchair velocity and acceleration (which fluctuates substantially due to upper body motion) and that of the COM_{AW} (which fluctuates much less, see Appendix B).

Cycle average power values of $\overline{P_{IMU}}$ were similar to $\overline{P_{AW}}$ during constant velocity and acceleration. However, $\overline{P_W}$ deviated from $\overline{P_{IMU}}$ and $\overline{P_{AW}}$ during acceleration, because in the wheelchair model, the inertial forces of the upper body (in this case accelerating the upper body mass) is incorporated as athlete force instead of changing kinetic energy. As interpretation of $\overline{P_W}$ may thus be confusing when the velocity is not constant, the wheelchair model is not recommended for estimating power during overground wheelchair propulsion.

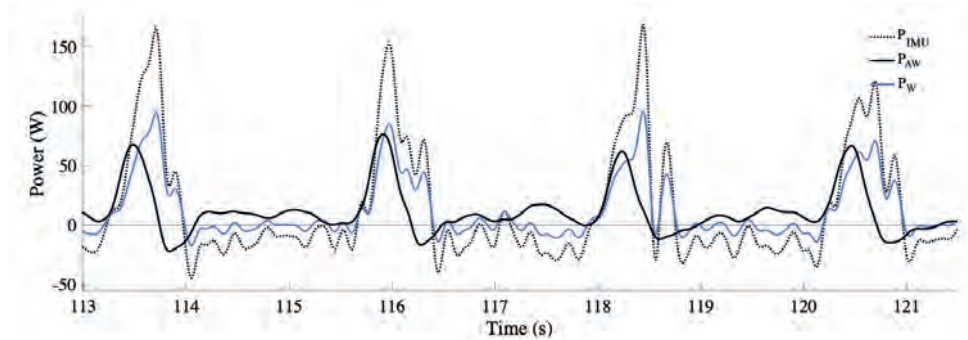


Fig. 3.3. Typical example of the instantaneous power graph of P_{AW} (black solid line), P_W (blue solid line) and P_{IMU} (black dotted line) of approximately four pushes at 1.2 m/s.

However, dE_{kin}/dt differ significantly between $\overline{P_{IMU}}$ and $\overline{P_{AW}}$ (see Table 3.2). As the first assumption must be true over a longer time duration, dE_{kin}/dt differences between $\overline{P_{IMU}}$ and $\overline{P_{AW}}$ should be similar over time. The difference may be caused by the low number (three) consecutive pushes that have been used for calculation. Due to missing data points in the motion capture data, a larger number of consecutive pushes would lead to insufficient data points. Assuming that dE_{kin}/dt differences diminish over several pushes, the accuracy of power output largely depends on the estimated rolling resistance. However, $F_{roll,drag}$ showed an average

underestimation of 0.9% (during acceleration) to 1.7% (at a constant velocity) of the instantaneous rolling resistance. Moreover, at a constant velocity, this underestimation ranged from -0.9% to 4.6% between participants (see Fig. 3.4 and 3.5). As this underestimation might be induced by upper body movements, improving the rolling resistance estimate (e.g., by adding an additional IMU on the trunk to correct for trunk-induced effects (Chenier et al., 2016; Poulet et al., 2022; van Dijk et al., 2021), might eventually improve power estimates as well.

To summarize, \overline{P}_{IMU} seems an acceptable estimation for power. As it depends largely on the accuracy of the rolling resistance estimate, \overline{P}_{IMU} will be slightly underestimated over several pushes and will improve when rolling resistance estimates improve.

Table 3.2.

Mean (S.D.) values and mean (S.D.) differences for power (P), change in kinetic energy ($dE_{kin,i}/dt$) and power loss due to rolling resistance ($P_{roll,i}$, i.e., $F_{roll,i} * v_i$) per cycle averaged over three consecutive pushes. The differences are determined by subtracting the variable of the IMU model from the AW model (e.g., $P_{AW} - P_{IMU}$).

	Absolute values in Watt			Differences		
	IMU model	AW model	W model	in Watt	in % of P_{AW}	p-value
Constant velocity						
P	10.7 (1.0)	10.5 (0.9)	10.8 (0.9)	-.19 (.25)	-1.8%	0.11
$dE_{kin,i}/dt$	-0.1 (0.3)	-0.3 (0.3)	-0.2 (0.3)	-.41 (.30)*	-3.9%	0.02
$P_{roll,i}$	10.4	10.6	10.6	.18 (.14)*	1.7%	0.02
Accelerate						
P	16.4 (2.7)	15.7 (2.6)	13.9 (2.1)	-.71 (.76)	-4.5%	0.05
$dE_{kin,i}/dt$	4.1 (1.3)	3.3 (1.3)	1.5 (1.0)	-.81 (.73)*	-5.2%	0.03
$P_{roll,i}$	12.3 (1.6)	12.4 (1.6)	12.4 (1.6)	.15 (.06)	0.9%	0.08

* p-value < 0.05, ** p-value < 0.01

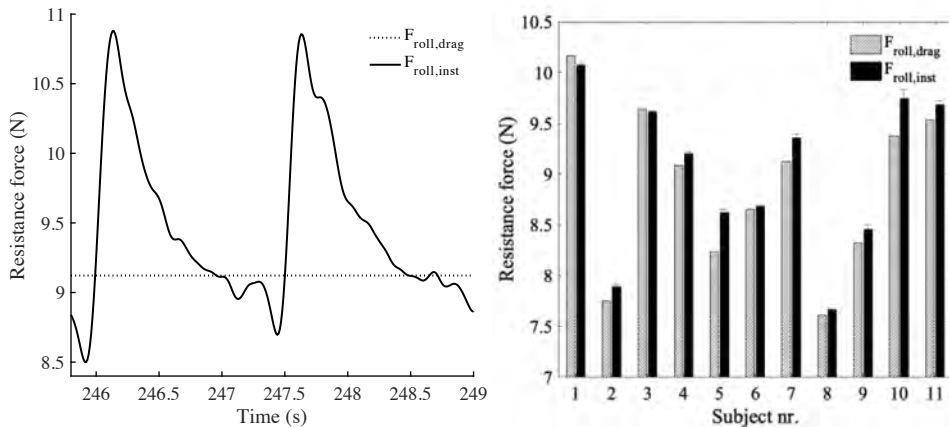


Fig. 3.4 and 3.5. Figure 3.4 (left) shows a typical rolling resistance graph during two pushes. The dotted horizontal line shows the resistance force determined from a drag test ($F_{roll,drag}$), and the black curve shows the instantaneous resistance force ($F_{roll,inst}$), in which intra-cyclical changes are taken into account.

Figure 3.5 (right) shows the differences between the resistance values of the drag test ($F_{\text{roll,drag}}$) and the average values + standard deviations of the instantaneous resistance force ($F_{\text{roll,inst}}$) for each participant. The measurements took place on a treadmill.

Concluding remarks & practical implications

This article proposes a theoretical framework for monitoring mechanical power in wheelchair sports practice. With a well-executed deceleration test and one wheel-mounted IMU, acceptable power estimates can be obtained during wheelchair field and court sports. Based on this feasible approach and the underlying framework, one can elaborate and finetune power estimates for each specific application.

As our results are based on straight-line wheelchair propulsion and rolling resistance usually increases during curves and turns (Chénier et al. 2015; Fallot et al. 2021) one should be aware that the resistance (and thus power) underestimation may be larger when applied in match situations. To accurately monitor power during all match conditions, more knowledge about rolling resistance during turning and trunk inclination is required. External forces due to ball handling and contact with other players will further complicate power estimates. Additionally, accelerations during the experiments were lower than those typically observed during matches. However, as IMUs accurately measure wheelchair accelerations, similar accuracies of power estimates are expected at higher acceleration levels. To apply IMU-based power estimates in wheelchair racing, air resistance and gravity should be included as velocities are usually between 5-10 m/s (Fuss 2009; Poulet et al. 2022) and long distance races might contain slopes. For everyday wheelchair use, the power estimates can already be used.

To conclude, we believe that the theoretical framework and the resulting IMU-model is well suited to estimate mechanical power during straight-line (non-contact) wheelchair propulsion in wheelchair field and court sports. In addition, the framework is an important first step towards feasible power estimates in all wheelchair (sports) situations. As this study is no validation study, the accuracy of \overline{P}_{IMU} may be assessed using force-instrumented push-rims.

References

1. Bakatchina, Sadate, Thierry Weissland, Marjolaine Astier, Didier Pradon, and Arnaud Faupin. 2021. "Performance, Asymmetry and Biomechanical Parameters in Wheelchair Rugby Players." *Sports Biomechanics* 1–14. doi: 10.1080/14763141.2021.1898670.
2. Barbosa, Tiago, Forte, Pedro, Morais, Jorge E., and Coelho, Eduarda. 2014. "Partial Contribution of Rolling Friction and Drag to Total Resistance of an Elite Wheelchair Athlete." in *Advanced Materials for Sports Technology*. Singapore.
3. Chénier, Félix, Ilona Alberca, Dany H. Gagnon, and Arnaud Faupin. 2022. "Impact of Sprinting and Dribbling on Shoulder Joint and Pushrim Kinetics in Wheelchair Basketball Athletes." *Frontiers in Rehabilitation Sciences* 3:863093. doi: 10.3389/fresc.2022.863093.
4. Chénier, Félix, Pascal Bigras, and Rachid Aissaoui. 2015. "A New Dynamic Model of the Wheelchair Propulsion on Straight and Curvilinear Level-Ground Paths." *Computer Methods in Biomechanics and Biomedical Engineering* 18(10):1031–43. doi: 10.1080/10255842.2013.869318.
5. Chenier, Felix, Dany H. Gagnon, Martine Blouin, and Rachid Aissaoui. 2016. "A Simplified Upper-Body Model to Improve the External Validity of Wheelchair Simulators."

- IEEE/ASME Transactions on Mechatronics* 21(3):1641–49. doi: 10.1109/TMECH.2016.2527240.
6. Coe, P. L. 1979. “Aerodynamic Characteristics of Wheelchairs.”
 7. Cooper, Rory A. 1990. “A Systems Approach to the Modeling of Racing Wheelchair Propulsion.” *The Journal of Rehabilitation Research and Development* 27(2):151. doi: 10.1682/JRRD.1990.04.0151.
 8. Cooper, Rory A., and Arthur Jason De Luigi. 2014. “Adaptive Sports Technology and Biomechanics: Wheelchairs.” *PM&R* 6:S31–39. doi: 10.1016/j.pmrj.2014.05.020.
 9. De Groot, S., M. Zuidgeest, and L. H. V. Van Der Woude. 2006. “Standardization of Measuring Power Output during Wheelchair Propulsion on a Treadmill.” *Medical Engineering & Physics* 28(6):604–12. doi: 10.1016/j.medengphy.2005.09.004.
 10. van Dijk, M.P., van der Slikke, R.M.A., Berger, M.A.M., Hoozemans, M.J.M., and H. E. J. Veeger. 2021. “Look Mummy, No Hands! The Effect of Trunk Motion on Forward Wheelchair Propulsion.” *39th ISBS Conference* 4.
 11. van Dijk, Marit P., Manon Kok, Monique A. M. Berger, Marco J. M. Hoozemans, and DirkJan H. E. J. Veeger. 2021. “Machine Learning to Improve Orientation Estimation in Sports Situations Challenging for Inertial Sensor Use.” *Frontiers in Sports and Active Living* 3:670263. doi: 10.3389/fspor.2021.670263.
 12. van Dijk, Marit P., Rienk M. A. van der Slikke, Rob Rufp, Marco J. M. Hoozemans, Monique A. M. Berger, and DirkJan H. E. J. Veeger. 2022. “Obtaining Wheelchair Kinematics with One Sensor Only? The Trade-off between Number of Inertial Sensors and Accuracy for Measuring Wheelchair Mobility Performance in Sports.” *Journal of Biomechanics* 130:110879. doi: 10.1016/j.jbiomech.2021.110879.
 13. Doyle, Matthew M., Andrew Lyttle, and Bruce Elliott. 2010. “Comparison of Force-Related Performance Indicators between Heavyweight and Lightweight Rowers.” *Sports Biomechanics* 9(3):178–92. doi: 10.1080/14763141.2010.511678.
 14. Fallot, Constantin, Joseph Bascou, H el ene Pillet, and Christophe Sauret. 2021. “Manual Wheelchair’s Turning Resistance: Swivelling Resistance Parameters of Front and Rear Wheels on Different Surfaces.” *Disability and Rehabilitation: Assistive Technology* 16(3):324–31. doi: 10.1080/17483107.2019.1675781.
 15. Forte, Pedro, Daniel A. Marinho, Jorge E. Morais, Pedro G. Morou o, and Tiago M. Barbosa. 2018. “The Variations on the Aerodynamics of a World-Ranked Wheelchair Sprinter in the Key-Moments of the Stroke Cycle: A Numerical Simulation Analysis” edited by Y.-K. Jan. *PLOS ONE* 13(2):e0193658. doi: 10.1371/journal.pone.0193658.
 16. Fuss, Franz Konstantin. 2009. “Influence of Mass on the Speed of Wheelchair Racing.” *Sports Engineering* 12(1):41–53. doi: 10.1007/s12283-009-0027-2.
 17. Gl ersen,  yvind, Thomas Losnegard, Anders Malthe-S orensen, Dag Kristian Dysthe, and Matthias Gilgien. 2018. “Propulsive Power in Cross-Country Skiing: Application and Limitations of a Novel Wearable Sensor-Based Method During Roller Skiing.” *Frontiers in Physiology* 9:1631. doi: 10.3389/fphys.2018.01631.
 18. Goosey-Tolfrey, Victoria L., and Andrew D. Moss. 2005. “Wheelchair Velocity of Tennis Players during Propulsion with and Without the Use of Racquets.” *Adapted Physical Activity Quarterly* 22(3):291–301. doi: 10.1123/apaq.22.3.291.
 19. de Groot, Sonja, R. Vegter, C. Vuijk, F. Dijk, C. Plaggenmarsch, M. Sloots, J. Stolwijk-Swaeste, F. Woldring, M. Tepper, and L. Woude. 2014. “WHEEL-I: Development of a Wheelchair Propulsion Laboratory for Rehabilitation.” *Journal of Rehabilitation Medicine* 46(6):493–503. doi: 10.2340/16501977-1812.

20. Halson, S. L. 2014. "Monitoring Training Load to Understand Fatigue in Athletes." *Sports Medicine* 44(S2):139–47. doi: 10.1007/s40279-014-0253-z.
21. Hoffman, Martin D., Guillaume Y. Millet, Anne Z. Hoch, and Robin B. Candau. 2003. "Assessment of Wheelchair Drag Resistance Using a Coasting Deceleration Technique." *American Journal of Physical Medicine and Rehabilitation* 82(11):880–89. doi: 10.1097/01.PHM.0000091980.91666.58.
22. Hogan, Cruz, Martyn J. Binnie, Matthew Doyle, and Peter Peeling. 2022. "Quantifying Sprint Kayak Training on a Flowing River: Exploring the Utility of Novel Power Measures and Its Relationship to Measures of Relative Boat Speed." *European Journal of Sport Science* 22(11):1668–77. doi: 10.1080/17461391.2021.1977393.
23. Holt, Ana C., William G. Hopkins, Robert J. Aughey, Rodney Siegel, Vincent Rouillard, and Kevin Ball. 2021. "Concurrent Validity of Power From Three On-Water Rowing Instrumentation Systems and a Concept2 Ergometer." *Frontiers in Physiology* 12:758015. doi: 10.3389/fphys.2021.758015.
24. van Ingen-Schenau, G. J., and P. R. Cavanagh. 1990. "Power Equations in Endurance Sports." *Journal of Biomechanics* 23(9):865–81.
25. Kingma, Idsart, Huub M. Toussaint, Dianne A. C. M. Commissaris, Marco J. M. Hoozemans, and Michiel J. Ober. 1995. "Optimizing the Determination of the Body Center of Mass." *Journal of Biomechanics* 28(9):1137–42. doi: 10.1016/0021-9290(94)00164-Y.
26. de Koning, Jos. J., Carl Foster, Joanne Lampen, Floor Hettinga, and Maarten F. Bobbert. 2005. "Experimental Evaluation of the Power Balance Model of Speed Skating." *Journal of Applied Physiology* 98(1):227–33. doi: 10.1152/jappphysiol.01095.2003.
27. van der Kruk, E., F. C. T. van der Helm, H. E. J. Veeger, and A. L. Schwab. 2018. "Power in Sports: A Literature Review on the Application, Assumptions, and Terminology of Mechanical Power in Sport Research." *Journal of Biomechanics* 79:1–14. doi: 10.1016/j.jbiomech.2018.08.031.
28. Leo, Peter, James Spragg, Tim Podlogar, Justin S. Lawley, and Iñigo Mujika. 2022. "Power Profiling and the Power-Duration Relationship in Cycling: A Narrative Review." *European Journal of Applied Physiology* 122(2):301–16. doi: 10.1007/s00421-021-04833-y.
29. Macdermid, Paul, and Philip Fink. 2017. "The Validation of a Paddle Power Meter for Slalom Kayaking." *Sports Medicine International Open* 01(02):E50–57. doi: 10.1055/s-0043-100380.
30. Mujika, Iñigo. 2017. "Quantification of Training and Competition Loads in Endurance Sports: Methods and Applications." *International Journal of Sports Physiology and Performance* 12(s2):S2-9-S2-17. doi: 10.1123/ijsp.2016-0403.
31. Ott, Joseph, and Jonathan Pearlman. 2021. "Scoping Review of the Rolling Resistance Testing Methods and Factors That Impact Manual Wheelchairs." *Journal of Rehabilitation and Assistive Technologies Engineering* 8:205566832098030. doi: 10.1177/2055668320980300.
32. Poulet, Yoann, Florian Brassart, Emeline Simonetti, H el ene Pilet, Arnaud Faupin, and Christophe Sauret. 2022. "Analyzing Intra-Cycle Velocity Profile and Trunk Inclination during Wheelchair Racing Propulsion." *Sensors* 23(1):58. doi: 10.3390/s23010058.
33. Refai, Mohamed Irfan Mohamed, Bert-Jan F. Van Beijnum, Jaap H. Buurke, and Peter H. Veltink. 2020. "Portable Gait Lab: Instantaneous Centre of Mass Velocity Using Three Inertial Measurement Units." Pp. 1–4 in *2020 IEEE SENSORS*. Rotterdam, Netherlands: IEEE.

34. Rietveld, Thomas, Barry S. Mason, Victoria L. Goosey-Tolfrey, Lucas H. V. van der Woude, Sonja de Groot, and Riemer J. K. Vegter. 2021. "Inertial Measurement Units to Estimate Drag Forces and Power Output during Standardised Wheelchair Tennis Coast-down and Sprint Tests." *Sports Biomechanics* 1–19. doi: 10.1080/14763141.2021.1902555.
35. Rupf, R., M. C. Tsai, S. G. Thomas, and M. Klimstra. 2021. "Original Article: Validity of Measuring Wheelchair Kinematics Using One Inertial Measurement Unit during Commonly Used Testing Protocols in Elite Wheelchair Court Sports." *Journal of Biomechanics* 127:110654. doi: 10.1016/j.jbiomech.2021.110654.
36. Sauret, C., P. Vaslin, M. Dabonneville, and M. Cid. 2009. "Drag Force Mechanical Power during an Actual Propulsion Cycle on a Manual Wheelchair." *IRBM* 30(1):3–9. doi: 10.1016/j.irbm.2008.10.002.
37. Sauret, Christophe, Philippe Vaslin, François Lavaste, Nicolas de Saint Remy, and Mariano Cid. 2013. "Effects of User's Actions on Rolling Resistance and Wheelchair Stability during Handrim Wheelchair Propulsion in the Field." *Medical Engineering and Physics* 35(3):289–97. doi: 10.1016/j.medengphy.2012.05.001.
38. Schnorenberg, Alyssa J., Brooke A. Slavens, Mei Wang, Lawrence C. Vogel, Peter A. Smith, and Gerald F. Harris. 2014. "Biomechanical Model for Evaluation of Pediatric Upper Extremity Joint Dynamics during Wheelchair Mobility." *Journal of Biomechanics* 47(1):269–76. doi: 10.1016/j.jbiomech.2013.11.014.
39. Silva, L. C. A., F. C. Corrêa, J. J. Eckert, F. M. Santiciolli, and F. G. Dedini. 2017. "A Lateral Dynamics of a Wheelchair: Identification and Analysis of Tire Parameters." *Computer Methods in Biomechanics and Biomedical Engineering* 20(3):332–41. doi: 10.1080/10255842.2016.1233327.
40. van der Slikke, R. M. A., M. A. M. Berger, D. J. J. Bregman, A. H. Lagerberg, and H. E. J. Veeger. 2015. "Opportunities for Measuring Wheelchair Kinematics in Match Settings; Reliability of a Three Inertial Sensor Configuration." *Journal of Biomechanics* 48(12):3398–3405. doi: 10.1016/j.jbiomech.2015.06.001.
41. van der Slikke, R. M. A., M. A. M. Berger, D. J. J. Bregman, and H. E. J. Veeger. 2016. "From Big Data to Rich Data: The Key Features of Athlete Wheelchair Mobility Performance." *Journal of Biomechanics* 49(14):3340–46. doi: 10.1016/j.jbiomech.2016.08.022.
42. van der Slikke, Rienk M. A., Monique A. M. Berger, Daan J. J. Bregman, and Dirkjan H. E. J. Veeger. 2020. "Wearable Wheelchair Mobility Performance Measurement in Basketball, Rugby, and Tennis: Lessons for Classification and Training." *Sensors* 20(12):3518. doi: 10.3390/s20123518.
43. Soligard, Torbjørn, Martin Schwellnus, Juan-Manuel Alonso, Roald Bahr, Ben Clarsen, H. Paul Dijkstra, Tim Gabbett, Michael Gleeson, Martin Häggglund, Mark R. Hutchinson, Christa Janse Van Rensburg, Karim M. Khan, Romain Meeusen, John W. Orchard, Babette M. Pluim, Martin Raftery, Richard Budgett, and Lars Engebretsen. 2016. "How Much Is Too Much? (Part 1) International Olympic Committee Consensus Statement on Load in Sport and Risk of Injury." *British Journal of Sports Medicine* 50(17):1030–41. doi: 10.1136/bjsports-2016-096581.
44. Teran, Efrain, and Jun Ueda. 2017. "Influence of Rolling Resistance on Manual Wheelchair Dynamics and Mechanical Efficiency." *International Journal of Intelligent Robotics and Applications* 1(1):55–73. doi: 10.1007/s41315-016-0007-1.
45. Uddin, Md Zia, Trine M. Seeberg, Jan Kocbach, Anders E. Liverud, Victor Gonzalez, Øyvind Sandbakk, and Frédéric Meyer. 2021. "Estimation of Mechanical Power Output

- Employing Deep Learning on Inertial Measurement Data in Roller Ski Skating.” *Sensors* 21(19):6500. doi: 10.3390/s21196500.
46. vanLandewijck, Y. C., and W. R. Thompson. 2011. *The Paralympic Athlete: Handbook of Sports Medicine and Science*. International Olympic Committee.
47. Veeger, H. E. J., L. A. Rozendaal, and F. C. T. Van Der Helm. 2002. “Load on the Shoulder in Low Intensity Wheelchair Propulsion.” *Clinical Biomechanics* 17(3):211–18. doi: 10.1016/S0268-0033(02)00008-6.
48. Veeger, H. E. J., L. H. V. van der Woude, and R. H. Rozendal. 1991. “Load on the Upper Extremity in Manual Wheelchair Propulsion.” *Journal of Electromyography and Kinesiology* 1(4):270–80. doi: 10.1016/1050-6411(91)90014-V.
49. de Vette, Vera G., DirkJan (H. E. J.). Veeger, and Marit P. van Dijk. 2022. “Using Wearable Sensors to Estimate Mechanical Power Output in Cyclical Sports Other than Cycling—A Review.” *Sensors* 23(1):50. doi: 10.3390/s23010050.
50. de Vries, Wiebe H. K., Rienk M. A. van der Slikke, Marit P. van Dijk, and Ursina Arnet. 2023. “Real-Life Wheelchair Mobility Metrics from IMUs.” *Sensors* 23(16):7174. doi: 10.3390/s23167174.
51. de Witte, Annemarie M. H., Marco J. M. Hoozemans, Monique A. M. Berger, Rienk M. A. van der Slikke, Lucas H. V. van der Woude, and Dirkjan H. E. J. Veeger. 2018. “Development, Construct Validity and Test–Retest Reliability of a Field-Based Wheelchair Mobility Performance Test for Wheelchair Basketball.” *Journal of Sports Sciences* 36(1):23–32. doi: 10.1080/02640414.2016.1276613.
52. van der Woude, L. H. V., H. E. J. Veeger, A. J. Dallmeijer, T. W. J. Janssen, and L. A. Rozendaal. 2001. “Biomechanics and Physiology in Active Manual Wheelchair Propulsion.” *Medical Engineering and Physics* 23(10):713–33. doi: 10.1016/S1350-4533(01)00083-2.
53. Zatsiorsky, Vladimir M. 2002. *Kinetics of Human Motion*. Human Kinetics.

Appendix A

Explanation of the differences between the athlete-wheelchair model and the wheelchair model (and the difference between power estimates based on these models compared to force-instrumented push rims or wheelchair ergometers) when the upper body movements do produce net mechanical power

When the upper body movements do produce net power

When the upper body movements *do* produce net power on the wheelchair seat, for example, when a wheelchair athlete tries to move the wheelchair by using mass displacements only (without touching the rim), this means that $M_{hand,rim}$ from the wheelchair model (see Eq. 3.5) is zero, while $F_{upper\ body,seat} * v_{wc}$ will on average be equal to $F_{propulsion,COM} * v_{COM}$ of the athlete-wheelchair model (see Eq. 3.3). However, when using a force-instrumented push-rim, power won't be measured. In addition, in a wheelchair ergometer, $F_{upper\ body,seat}$ would not be able to produce power since the wheelchair frame is fixed. When we translate this to normal wheelchair propulsion situations, it becomes clear that any (net) propulsive power produced by $F_{upper\ body,seat}$ is neglected by force-instrumented push-rims and wheelchair ergometers. In rowing this phenomenon was also reported and may cause an underestimation of up to 10% (Hofmijster et al. 2018¹). As both the wheelchair and athlete-wheelchair model will not have this problem, we assume that comparing the IMU-based power with the power estimates based on these models is a suitable way to demonstrate the usefulness of IMU-based power estimates.

¹ Hofmijster, Mathijs J., Lotte L. Lintmeijer, Peter J. Beek, and A. J. Knoek van Soest. 2018. "Mechanical Power Output in Rowing Should Not Be Determined from Oar Forces and Oar Motion Alone." *Journal of Sports Sciences* 36(18):2147–53.

Appendix B

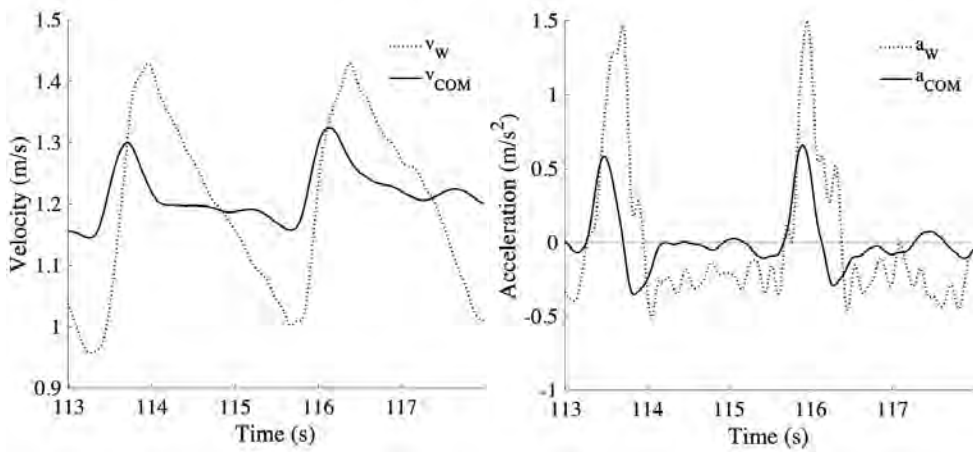
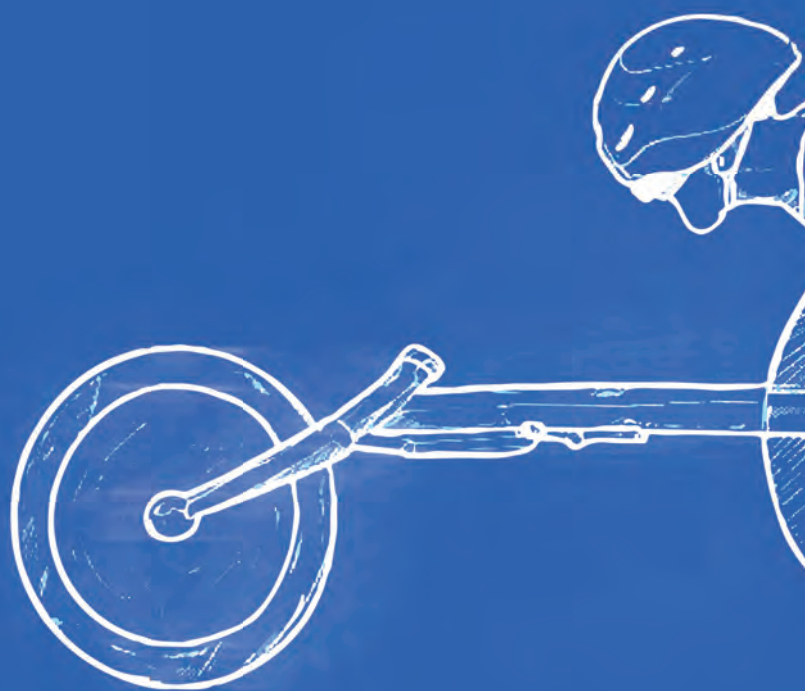


Fig 3.6 and 3.7. Typical velocity (left) and acceleration (right) graphs of the COM_{AW} (based on motion capture data - solid line) and the wheelchair (based on IMU data - dotted line) during steady state wheelchair propulsion for two pushes. v_W and a_W represent the velocity and acceleration of the wheelchair and v_{COM} and a_{COM} represent the velocity and acceleration of the COM_{AW} . Accelerations are calculated by differentiating velocity over time. The velocity and acceleration of the wheelchair vary more than the velocity and acceleration of the COM_{AW} due to the effect of upper body motion. The negative wheelchair acceleration during recovery can be explained by the upper body movements. Immediately after each push, the upper body accelerates backwards (the small a_W peak right after large a_W peak), and consequently decelerates backwards - until the upper body and wheelchair reach the same velocity when the trunk approaches the back rest - to prepare for the next push. This backward deceleration of the upper body, causes a backward acceleration of the wheelchair (i.e., negative acceleration and decreasing velocity) during recovery as is seen between 114 and 115.5 s.





Abstract

In sports, inertial measurement units (IMUs) are often used to measure the orientation of human body segments. A Madgwick (MW) filter can be used to obtain accurate IMU orientation estimates. This filter combines two different orientation estimates by applying a correction of the (1) gyroscope-based estimate in the direction of the (2) earth frame-based estimate. However, in sports situations that are characterized by relatively large linear accelerations and/or close magnetic sources, such as wheelchair sports, obtaining accurate IMU orientation estimates is challenging. In these situations, applying the MW filter in the regular way, i.e. with the same magnitude of correction at all time frames, may lead to estimation errors. Therefore, in the present study, the MW filter was extended with machine learning to distinguish instances at which a small correction magnitude is beneficial from instances at which a large correction magnitude is beneficial, to eventually arrive at accurate body segment orientations in IMU challenging sports situations. A machine learning algorithm was trained to make this distinction based on raw IMU data. Experiments on wheelchair sports were performed to assess the validity of the extended MW filter, and to compare the extended MW filter with the original MW filter based on comparisons with a motion capture-based reference system. Results indicate that the extended MW filter performs better than the original MW filter in assessing instantaneous trunk inclination (7.6° versus 11.7° RMSE), especially during the dynamic, IMU challenging situations with moving athlete and wheelchair. Improvements up to 45% RMSE were obtained for the extended MW filter compared to the original MW filter. To conclude, the machine learning-based extended MW filter has an acceptable accuracy and performs better than the original MW filter for the assessment of body segment orientation in IMU challenging sports situations.

1. Introduction

In sports, inertial measurement units (IMUs) are often used to measure the orientation of human body segments [1]. When an IMU is attached to a body segment, the segment's orientation relative to the earth field can be estimated using an orientation estimation algorithm. Although optical motion capturing is widely accepted as a reference system for kinematic measurements, IMUs are often preferred over optical motion capture systems, since they are generally small, wearable (wireless), cheap and easy to use outside the lab. IMU accuracy has shown its validity for several applications in sports [2–7]. Some examples of this are upper body orientations during walking and running on a treadmill [2], pelvis orientation during swimming [3] and trunk orientation during sports motions that last for only short time periods (<30 s) such as sprint starts, tennis serves and the golf swing [4–7].

An IMU generally consists of an accelerometer, a gyroscope and a magnetometer, which measure the three-dimensional (3D) linear accelerations (including gravity), the angular velocity and the local magnetic field, respectively. To estimate the orientation from these raw IMU signals, the data can be fused together using an Attitude and Heading Reference System (AHRS). A commonly used AHRS method is to first obtain two different orientation estimates which are subsequently combined. First, the orientation of the IMU is estimated by integrating the angular velocity, based on the gyroscope signals. As this orientation estimate is distorted by integration drift, the gyroscope-based orientation is 'corrected' using a second orientation estimate; the IMU orientation estimated relative to the direction of gravity (down; based on the accelerometer) and the direction of the earth's magnetic field (north; based on the magnetometer). The second estimate will be referred to as the 'earth frame-based' orientation estimate. To estimate the earth frame-based orientation, it is assumed that the accelerometer only measures gravity and that the magnetometer only measures the earth's magnetic field, such that the orientation of the sensor relative to the earth frame, i.e., down and north, is obtained.

In many applications, this assumption can be made since linear accelerations in directions other than gravity are much smaller than gravity, such that they have a negligible effect on the direction of the acceleration vector. However, in sports activities characterized by relatively large and continuously present linear accelerations (e.g., every push in speed-skating or in wheelchair propulsion) or by the presence of close magnetic sources (e.g., from a bike or a wheelchair), the accelerations in directions other than gravity affect the direction of the acceleration vector and the close magnetic sources affect the direction of the local magnetic field. Therefore, during these sports activities, the earth frame-based orientation estimate is often incorrect such that the integration drift is corrected in the wrong direction. In the current paper, such sports activities are referred to as 'IMU challenging sports situations'.

Some studies solve this problem by combining data of the IMU sensors with that of other sensor types such as force sensors or GPS [8,9]. These sources provide additional (indirect) information about the sensor orientation. Another (magnetometer-free) solution that is used to detect the direction of gravity without assuming that only gravity is measured, is to attach multiple sensors on connected body segments [10,11]. Although those approaches previously produced accurate orientation estimates [8,9], the benefits of using a single sensor (easy to use and cheap) diminish. Obtaining accurate estimates based on one or two IMUs only is therefore preferred.

To implement the algorithms in already existing sports applications (e.g., smartphones or sports watches) and to enable real-time orientation estimations, the computational efficiency of the algorithms is of interest. A computationally efficient filter that previously provided

accurate results in sport settings based on IMU signals only is the Madgwick (MW) filter [12]. The MW filter is resilient against short-term disturbances [13] and is widely used in sports settings. The filter combines the gyroscope-based estimate and earth frame-based estimate by correcting the gyroscope estimate in the direction of the earth frame-based estimate at each time instance. In this way, the filter corrects for integration drift. The magnitude of this correction, or correction size, is the same at each time instance and its value is therefore crucial to performance [12]. Since the optimal correction size depends on the extent to which integration drift is expected (which depends on the sensor used and the nature of the measurements, i.e. static or dynamic [12]), the correction size should be determined for each sensor and application. Commonly, the correction size is determined based on the smallest difference with a reference system and is maintained henceforth [7,12].

To obtain accurate orientation estimates in IMU challenging sports situations, applying a MW filter in the regular way, i.e., with the same correction size at all time frames, will lead to estimation errors. During these sports situations, the correction will be too small to correct for drift or too large such that drift is corrected in the wrong direction (due to a wrong earth frame-based orientation estimate). Therefore, during instances at which the earth frame-based orientation estimate is likely to be wrong, it may be beneficial to temporarily decrease the correction size, i.e., limit the impact of the earth frame-based estimate. In line with this, the correction size should be increased again when the earth frame-based orientation estimate is correct, such that the drift can be controlled. Adapting the correction size in this way has already led to improved orientation estimates in (aerial) vehicles [14,15]. However, these studies only took the effect of acceleration into account and implemented self-designed filters. To ensure usability in sports settings, we present a proof of concept in which the widely used MW filter is extended with an adaptive correction size to make it applicable in IMU challenging sports situations. Since the combined effect of linear accelerations and magnetic sources is expected to be indirect and non-linear, machine learning was used to predict the right time instances for each correction size.

In the present study, the MW filter is extended with machine learning to distinguish instances at which a *small* correction size (in the direction of the earth frame-based orientation estimate) is advantageous from instances at which a *large* correction size is advantageous, to eventually arrive at accurate body segment orientation in IMU challenging sports situations. To this end, a machine learning model was trained to classify whether or not the earth frame-based estimate is likely to be correct based on raw IMU data. Experiments were performed to assess the validity of the extended MW filter, and to compare the extended with the original MW filter. The experiments involved indoor wheelchair sport activities. The presence of a wheelchair and the accelerate-decelerate nature of this sport makes it a representative IMU challenging sport situation. During wheelchair propulsion, trunk motion is used to prevent the chair from tipping over during large accelerations and may be used to increase stroke length. In addition, trunk motion causes continuous displacements of the center of mass such that e.g., rolling resistance is affected. Therefore, trunk motion is expected to have a significant role in wheelchair propulsion. Since wheelchair kinematics, such as speed and rotational speed, can already be measured accurately using IMUs in wheelchair match settings [16], adding instantaneous IMU-based trunk motion would result in more information about the wheelchair-athlete interaction which is beneficial for training purposes.

The aim of the current study was to investigate whether machine learning-based classification could be used to extend the existing MW filter and, in this way, improve the obtained body segment orientation in IMU challenging sports situations.

2. Methods

2.1 Procedure

Eleven differently skilled participants (Table 4.1) performed a series of wheelchair sport-specific activities with IMUs attached to their wheelchair and trunk, while simultaneously being measured with an optical motion capture (MOCAP) analysis system to serve as reference system. Video recordings were made to distinguish between different activities afterwards. The experiment was approved by the ethical committee of the Technical University of Delft. Prior to the experiment, participants were informed about the aim and procedure of the study and provided a written informed consent.

Based on the obtained data, a machine learning-based classification model was trained to classify for each time instance whether a *small* or *large* correction size is advantageous. This classification was used to extent the MW filter (see section 2.5.1). To assess the validity of the resulting extended MW filter, trunk inclination was calculated based on MOCAP data and IMU data processed with the extended MW filter. Also, comparisons with the original (not extended) MW filter were made.

Table 4.1.

Subject characteristics (mean \pm standard deviation)

Type	N	Age (years)	Class ¹
Elite wheelchair athlete ²	3	25.0 \pm 3.0	3.2 \pm 1.3
Active wheelchair user	3	46.3 \pm 11.0	2.5 \pm 0.5
Non-experienced user	5	25.0 \pm 1.2	-

¹ The classes were indicated by the points as used in (elite) wheelchair basketball.

² Two wheelchair basketball players (premier league) and one wheelchair hockey player (Dutch national team).

2.2 Equipment

Two IMUs (NGIMU, x-io technologies) were used to collect 3D inertial sensor data of the trunk and the wheelchair with a sample frequency of approximately 100 Hz. A ten camera optoelectric MOCAP system (OptiTrack Prime, National Point) with a sampling rate of 120 Hz was used to record the 3D orientation of the segments of interest. The trunk marker cluster frame was constituted of four markers connected to a rigid body, and was attached to the sternum (manubrium sterni). The wheelchair marker cluster frame was constituted of five markers connected to different positions on the wheelchair frame. The video camera (Casio Exilim) recorded the entire track lay-out with a sample frequency of 60 Hz.

2.3 Wheelchair sport-specific activities

The wheelchair sport-specific test session is described in Table 4.2 and Fig. 4.1 and covers the main aspects of wheelchair basketball, tennis, rugby, triathlon and racing. Certain tests were similar to ones used in prior research on wheelchair IMUs [16,17], while tests 1, 10 and 11 in Table 4.2 were added to put more focus on trunk motion. Prior to the session, the tests were explained and participants without wheelchair experience were instructed to ride in the wheelchair for approximately five minutes to familiarize with wheelchair propulsion. The participants were instructed to adopt a neutral pose for at least 20 s at the start and end of the session. All tests were performed in a motion lab.

Table 4.2.

All sport-specific tests, together with a description of each test and the speed at which the participants were instructed to perform the test (see also Fig. 4.1). All tests were carried out in immediate succession.

Test	Speed	Description
1	no	3x flexion/extension, left/right lateral rotations
2	normal	3x sprint with static trunk
	low	3x
	normal	3x
	low	3x
	high	3x
3	high	2x sprint (stop with skidding wheels)
4	normal	around 3 cones (Fig. 4.1B)
	low	
	high	around 3 cones (Fig. 4.1B)
5	normal	(Fig. 4.1C)
	low	
	high	(Fig. 4.1C)
6	normal	180° clockwise turn (Fig. 4.1D)
	low	
	high	180° clockwise turn (Fig. 4.1D)
	normal	180° anti clockwise turn (Fig. 4.1D)
	low	
	high	180° anti clockwise turn (Fig. 4.1D)
7	normal	360° clockwise turn
	low	
	normal	360° anti clockwise turn
	low	
	high	360° clockwise turn
	high	360° anti clockwise turn
8	free	Star wise bi-directional rotation
	free	As previous, combined with back-and-forth movement (Fig. 4.1E)
9	free	2x 2m sprint and collision against a block of 30 kg (Fig. 4.1F)
1	no	Do two service- and two backhand motions with tennis racket
0	no	Pick up ball from the ground (2x) and throw ball away with one hand
1	no	

Figure 4.1 (A to F). Track lay-out with dimensions in cm (A) corresponding to the tests as explained in Table 4.2. Cones and collision block (CB) were removed during test parts in which they were not used. During tests with ‘no’ speed, the wheels of the wheelchair were blocked. This figure was adopted from Van der Slikke et al. [16].

Data pre-processing

Pre-processing of MOCAP data

OptiTrack 3D position data of the frame and trunk markers were acquired in Motive 2.2.0 (Natural Point), converted to a C3D format and imported in MATLAB (R2019b, The Mathworks Inc.). Missing values were interpolated if the duration of the gap was < 0.2 s and subsequently resampled from 120 to 100 Hz using a spline interpolation. Based on the first sample of each time series, the 3D local coordinate frames of the trunk and the wheelchair were determined

based on the positions of the three markers with the lowest number of missing values [18]. The local marker coordinate frames with respect to the global marker coordinate system were tracked over time.

Pre-processing of IMU data

First, the magnetometer (hard iron) offset of the IMU data was corrected [19]. Subsequently, sample frequency deviations were corrected by resampling the data to 100 Hz using a spline interpolation. Given the obtained 3D accelerometer, 3D magnetometer and 3D gyroscope data, the IMU orientation was determined using the MW filter and the correction size [12]. First, an IMU orientation estimate was obtained using the original MW filter to enable time alignment of the IMU and marker data (see next paragraph). For this, a correction size of 0.033 was used as reported by Madgwick et al. [12]. A grid search for different beta values on the current dataset supported the use of this value. Second, the earth frame-only estimate (without gyroscope data) was obtained, which will be used to generate the classification model (see section 2.5). For this estimate, the direction of the acceleration vector was regarded ‘down’ and the direction of the magnetometer vector was regarded ‘north’.

Determining trunk inclination

To convert the IMU- and MOCAP-based orientations into a one-dimensional inclination angle between the trunk and the wheelchair, a helical approach was used. First, the rotation matrix between the proximal (wheelchair) segment and the distal (trunk) segment was obtained. Subsequently, this rotation matrix was represented relative to the first static sample, in which the person was positioned in neutral pose. Neutral pose was considered 0 degrees trunk inclination, in which positive values indicate trunk flexion. Accordingly, the helical angles could be calculated [20]. After obtaining the helical angles of both IMU and MOCAP systems, they were synchronized with respect to time using the cross-correlation of the helical angle time series [21]. After synchronization, the helical angles were determined again to ensure that all orientations were relative to the same static (neutral pose) sample.

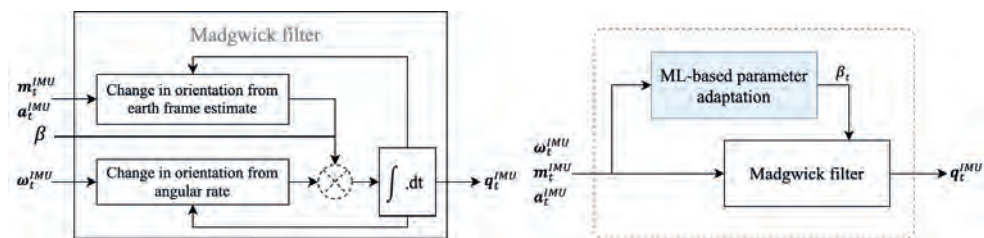


Figure 4.2. A simplified block diagram of the MW filter (left) and a block diagram of the machine learning (ML)-based extended MW filter (right). Within the extended MW filter, the correction size (β) may change over time (i.e. β_t), which differs from the original application of the MW filter. The filters use IMU data consisting of 3D gyroscope data (ω_t^{IMU}), 3D magnetometer data (m_t^{IMU}) and 3D accelerometer data (a_t^{IMU}) as input and IMU orientation (q_t^{IMU}) as output. Note that the white box in the left figure corresponds to the white box in the right figure.

2.4 Data analysis

2.4.1 Filter design

Using the data collected, trunk inclination angles are determined using the original MW filter and the extended MW filter, which are explained in more detail in this section. Fig. 4.2 (left) shows a representation of the original MW filter, which corrects for integration drift on the gyroscope-based estimate ($\Delta \mathbf{q}_{\omega,t}$) based on the earth frame-based estimate. The earth frame-based correction ($\Delta \mathbf{q}_{am,t}$) is determined by a gradient descent algorithm based on the accelerometer and magnetometer data [12]. Subsequently, the correction step is normalized to a pre-determined magnitude, the correction size or β , such that the resulting orientation at time t (\mathbf{q}_t^{IMU}) is calculated according to Eq. 4.1. The correction size is the only parameter to be tuned when using the MW filter.

$$\mathbf{q}_t^{IMU} = \mathbf{q}_{t-1}^{IMU} + (\Delta \mathbf{q}_{\omega,t} - \beta \Delta \mathbf{q}_{am,t}) \Delta t \quad (4.1)$$

Fig. 4.2 (right) shows the proposed extension of the MW filter. Instead of one correction size (β), two different correction sizes were determined for the extended filter; a large correction size for situations at which the earth frame-based estimate is expected to be correct, and a small correction size otherwise. To apply each correction size at the right instance in time, the validity of the earth frame-based estimate should be determined based on the raw IMU data (which is the only available data at this point). Therefore, the MW filter was extended with a machine learning-based classification model, that predicts whether or not the earth frame-based estimate will be correct based on IMU data. Accordingly, this prediction will be used to adapt the correction size (β) to a high value when a correct earth frame-based estimate was predicted (i.e. β_{high}) and to a low value (i.e. β_{low}) otherwise. This ‘decoding’ results in a correction size for each instance in time, i.e., β_t , which is an input of the MW filter (see Fig. 4.2). Fig. 4.3 shows a step-by-step explanation of model generation, implementation and validation.

2.4.2 Model generation

Label samples

To generate the classification model, training samples were created with known input (raw IMU data) and output (labelled *correct* [1] or *in-correct* [0] earth frame-based orientation estimate) data. These output labels were obtained by comparing the ‘earth frame-only’ orientation estimate with the MOCAP-based orientation on a sample-to-sample basis. A sample was labelled ‘correct’ (i.e., 1) if the difference between the ‘earth frame-only’ and the MOCAP-based trunk inclination was < 1 degree + noise, and was labelled ‘incorrect’ (i.e., 0) otherwise. To determine noise, the standard deviation of the difference between the MOCAP-based inclination and the earth frame-only estimate during 20 s neutral pose was assessed for all participants, and accordingly averaged. The labels were saved as ‘EFcorrect’.

Labelling this way, may cause some samples to be falsely labelled ‘correct’ due to coincidental intersections between the MOCAP system and a deviating earth frame-only estimate. Therefore, a second, more conservative, outcome variable was defined in which a sample is labelled ‘correct’ only if the maximal difference of five consecutive samples (that sample, two preceding samples and two following samples) was < 1 degree + noise. These labels were saved as ‘EFcorrect_S5’. The labels of ‘EFcorrect’ and ‘EFcorrect_S5’ were determined for all samples and added to the dataset.

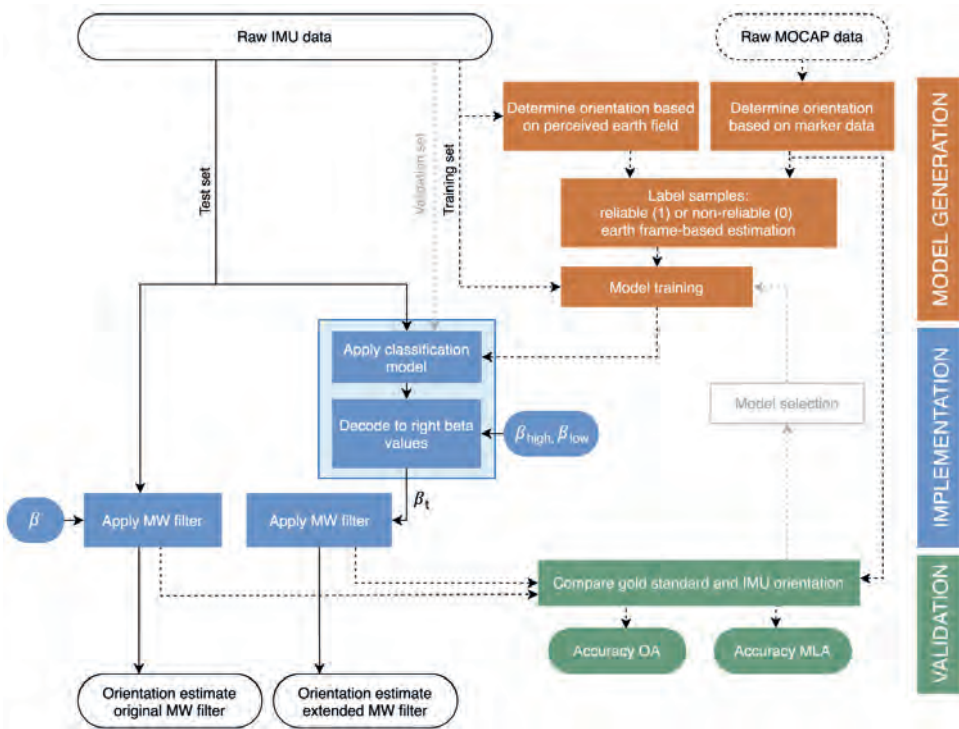


Figure 4.3. Overview of the model generation, implementation and validation steps and corresponding in- and outputs in the current study. Model implementation for the original MW filter (left blue) is compared to that of the extended MW filter (right blue) as proposed in the current study. Model generation and validation is done using MOCAP data and was performed only once. Those steps are therefore indicated by dashed lines (--). Before the classification model was chosen, several models were trained, implemented and compared with MOCAP data, after which the best model was selected (see model selection) using data of the validation set. This loop is indicated by grey dashed lines (---). The solid lines indicate the steps that should be taken each time one wants to estimate the IMU orientation. Note that the light-blue box corresponds to the light-blue box in Fig. 4.2.

Model training

First of all, the participants were divided into a training set, a validation set and a test set (with 6, 3 and 2 participants, respectively [see Fig. 4.3]). The training set included one elite, one active and four non-experienced wheelchair users, the validation set included two active and one non-experienced wheelchair user and the test set included two elite wheelchair athletes. Subsequently, all data were imported in Python (version 3.7, Python Software Foundation) to perform machine learning. Before learning, all input data were standardized using z-normalization [22] and the training data were balanced (by randomly removing samples of the majority class) such that the number of samples labelled 1 was equal to that labelled 0 [23]. Accordingly, the 18 features (2 sensors with each 3D accelerometer, magnetometer and gyroscope [$2 \times 3 \times 3$]) were ranked on importance using recursive feature selection on a Random

Forest classification algorithm [23] with a leave-one-subject-out cross-validation (LOSO-CV) on the training set [23]. Using a LOSO-CV, the model is trained on all-but-one participant of the training set, and accordingly evaluated on the participant that was left out. Subsequently, the feature ranking was used to select the best number of features. The best five sets (based on precision, recall and F1-score of the LOSO-CV) were selected for further model training.

To determine which learning algorithm is the most suitable, four different classification algorithms were trained. Since the data are tabular and relations are expected to be non-linear, a Gaussian Naive bayes algorithm, a logistic regression, a decision tree algorithm, and a random forest algorithm were compared [23]. Also, the two different outcome variables (EFcorrect and EFcorrect_S5) were compared. Since five sets were left from the feature selection procedure, 40 models (four learning algorithms, two outcome variables and five sets of features) were trained.

2.4.3 Implementation

Decode to β_t and apply MW filter

After applying a model, the outcome matrices consist of predicted 1's (correct earth frame-based estimation) and 0's were decoded to β_{high} and β_{low} , respectively. Subsequently, the IMU orientations were calculated by the MW filter and the helical angles were determined (see Fig. 4.3). The best values for β_{high} and β_{low} were chosen by applying the extended MW filter on the EFcorrect labels of the training and validation set. All combinations of β_{low} from 0 to 0.01 (steps of 0.001) and β_{high} from 0.5 to 1 (steps of 0.025) were applied. The root-mean-squared error (RMSE) between the IMU-based trunk inclination and the MOCAP-based trunk inclination was used to determine the final values for β_{high} and β_{low} .

Model selection

After training all 40 models, the best model was selected by comparing the models on the validation data. Therefore, all models were fit to the validation data and trunk inclination angles were determined. The best model was selected based on the lowest mean absolute error (MAE) and RMSE between the IMU-based angles and the MOCAP-based angles. To evaluate the performance of the final classification model, precision, recall and accuracy were reported. Also, the hyperparameters of the particular algorithm were tuned using a random search LOSO-CV on the training set. Subsequently, the final model was trained on the training set and was implemented on the test set to assess its performance.

2.4.4 Validation

To determine the accuracy of trunk inclination based on the extended MW filter and to determine the difference between the extended and the original MW filter, the mean error, RMSE and MAE with respect to the MOCAP-based inclination angles were determined for both filters. Also, the correlation between trunk inclination determined using MOCAP data and the trunk inclination determined using the IMU data with both filters was determined.

To compare the filters for activities with different levels of dynamics, a distinction was made between ‘slow to moderate sprints’ (Table 4.2.2 with speeds ‘normal’ and ‘low’), ‘fast sprints’ (Table 4.2.2 and 4.2.3 with speed ‘high’) and ‘agility exercises’ (Table 4.2.4-4.2.9). The parts were selected manually using the video frames. For each of the three parts, MOCAP-based trunk inclination was plotted against the original and extended MW filter-based trunk inclination to assess eventual angle dependencies. Also, a Bland-Altman analysis [24] was performed on the three parts to compare mean differences and 95% confidence intervals between MOCAP-based trunk inclination angles and those determined by the extended MW filter. To compare situations in which the wheelchair was fixed to the ground, i.e., ‘fixed wheelchair’ part, and in which it was not, sprints and agility exercises were taken together to represent the ‘free wheelchair’ part. Mean error, MAE and RMSE between both filters and the MOCAP-based trunk inclination were determined for both the fixed wheelchair part and the free wheelchair part. In addition, the evolution of trunk inclination over time was presented for isolated trunk rotations (Table 4.2.1) in the fixed wheelchair part and for both star twists (Table 4.2.8) in the free wheelchair part.

To gain more insight into the behaviour of the machine learning model, an analysis was performed of the situations at which small and large correction sizes were applied and their durations.

3 Results

Eleven participants were included (6 in training set, 3 in validation set, 2 in test set) with a mean session duration of 14.6 minutes. Of this, 14.4% of the samples was labelled 1 (<2.27° difference with MOCAP-based trunk inclination) according to the criteria as defined for ‘EFcorrect’ and 12.5% of the samples were labelled 1 for ‘EFcorrect_S5’. After balancing, the training set consisted of 155032 and 133426 samples for EFcorrect and EFcorrect_S5 respectively, with equally represented labels.

3.1 Implementation

Applying the extended MW filter on labelled data for different values for β_{high} and β_{low} yielded the smallest RMSE’s with the reference system when β_{high} ranged from 0.925 to 1, and β_{low} ranged from 0 to 0.003. Therefore, the mean of these values was taken such that $\beta_{\text{high}} = 0.9635$ and $\beta_{\text{low}} = 0.0015$.

Based on feature selection, the final set of features consisted of $\mathbf{a}_{x,\text{trunk}}$, $\mathbf{m}_{y,\text{trunk}}$, $\mathbf{m}_{x,\text{trunk}}$, $\mathbf{m}_{z,\text{wheelchair}}$, $\mathbf{m}_{x,\text{wheelchair}}$ in which x represents the sagittal axis (forward-backward), y represents the transversal axis (left-right) and z represents the longitudinal axis (up-down). Using this feature set, the models were trained and implemented to determine trunk inclination. The IMU-based trunk inclination based on the different models were compared with the MOCAP-based trunk inclination (see Table 4.3). The smallest difference with the MOCAP-based trunk inclination was found for the Random Forest classification with label ‘EFcorrect’. Compared with the labelled data, this model showed a precision, recall and accuracy of 0.90, 0.95 and 0.86, respectively.

Table 4.3.

Performance of the eight models left after selecting the final set of features in terms of mean absolute error (MAE) and root-mean-squared error (RMSE) between MOCAP-based trunk inclination and the trunk inclination of the extended MW filter based on validation data.

Classification algorithm	MAE (°)		RMSE (°)	
	EFcorrect	EFcorrect_S5	EFcorrect	EFcorrect_S5
Decision Tree	9.6	9.2	13.3	13.4
Random Forest	8.9	10.3	13.6	15.8
Naive Bayes	14.2	14.4	23.5	24.0
Logistic Regression	11.7	12.0	18.7	18.9

3.2 Validation

To gain more insight into the performance of the original and the extended MW filter, comparisons were presented for parts in which the wheelchair could move (free wheelchair) and could not move (fixed wheelchair), separately (see Table 4.4). Results indicate that the extended MW filter outperforms the original MW filter, and performs particularly better during ‘free wheelchair’ instances (MAE decreased from 9.5° to 5.9° and RMSE from 11.7° to 7.6°, on average) with improvements up to 47% MAE and 45% RMSE. During ‘fixed wheelchair’ instances, the models show equal performances with average RMSEs of 6.0° and 5.3° for the original and the extended MW filter, respectively. The extended MW filter showed correlations of .86 (fixed wheelchair) and .92 (free wheelchair) with the MOCAP data, which were stronger than those of the original MW filter in all situations.

Fig. 4.4 shows the trunk inclination of the original (blue) and the extended MW filter (red) against the reference system for isolated trunk rotations and star twists (Table 4.2.1 and 4.2.8). Instances at which B_{high} was applied are indicated by the black dots in Fig. 4.4. Fig. 4.5 shows the trunk inclination of both filters against the MOCAP-based inclination for three ‘free wheelchair’ parts of the session. Bland-Altman analyses reveal a mean difference of 3.5° for slow to moderate sprints, 1.4° for fast sprints, and 2.0° for agility exercises between extended MW filter-based and MOCAP-based trunk inclination. The corresponding 95% limits of agreement were -7.6° and 14.6° (slow to moderate sprints), -12.3° and 15.2° (fast sprints), and -13.0° and 16.9° (agility exercises).

Table 4.4.

Comparison of the mean error, mean absolute error (MAE), root-mean-squared error (RMSE) and correlation (r) between the MOCAP data and the original MW filter and between the MOCAP data and the extended MW filter. Results were presented for parts in which the wheelchair could not move (Fixed wheelchair), and for parts in which the wheelchair could move (Free wheelchair) for subject 1 (S1) and subject 2 (S2) of the test set.

Condition	MW filter	Mean error (°)		MAE (°)		RMSE (°)		r	
		S1	S2	S1	S2	S1	S2	S1	S2
Fixed wheelchair	Original	-1.3	0.3	4.5	4.3	5.5	6.5	.88	.95
	Extended	0.0	2.2	4.1	4.0	5.2	5.4	.88	.97
Free wheelchair	Original	-8.2	-5.5	10.2	8.8	12.4	11.0	.72	.80
	Extended	1.6	2.7	5.4	6.5	6.8	8.4	.87	.86

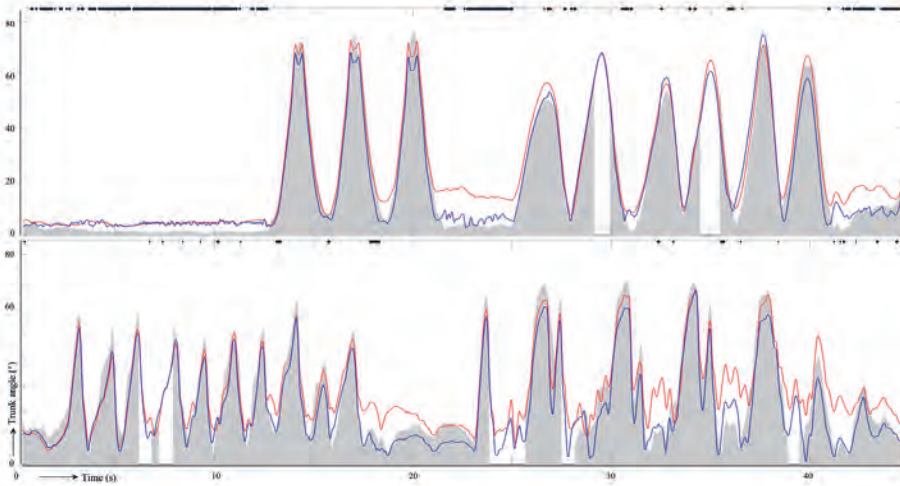


Figure 4.4. Typical plots of the trunk inclination angles over time of the original MW filter (red) and that of the extended MW filter (blue) for the isolated trunk rotations in a static wheelchair, i.e. Test 1, (upper figure) and star twists in a free wheelchair, i.e. Test 8, (lower figure). The MOCAP-based trunk inclination is indicated by the grey surface (which is interrupted at some time frames due to insufficient marker visibility). The black dots indicate time instances at which β_{high} was applied. The data was from an elite wheelchair basketball athlete (classification 3.0).

To gain more insight into the behaviour of this model, the time instances at which large or small correction sizes were applied were analysed. The black dots in Fig. 4.4 indicate that β_{high} was most common in static situations, while β_{low} was most common in dynamic situations. The duration of successive β_{low} -instances had a median of .05 and .03s for subject 1 and 2 in the test set, respectively, and ranged from 0.01 to 15.3s for subject 1 and from 0.01 to 2.05s for subject 2. The median duration of successive β_{high} -instances was .03 and .05s for subject 1 and 2, respectively, and duration ranged from 0.01 to 0.99s for subject 1 and from 0.01 to 34.3s for subject 2.

4 Discussion

The aim of the present study was to explore whether machine learning-based classification could be used to extend the MW filter, to make it applicable for highly dynamic situations (where assumptions on earth-frame based estimates are invalid). We specifically studied our proposed algorithms for estimating the instantaneous trunk inclination in wheelchair sports. Results indicate that the extended MW filter performs better than the original MW filter in assessing instantaneous trunk inclination (7.6° versus 11.7° RMSE), especially during the dynamic, IMU challenging situations with moving athlete and wheelchair. Compared to the extended MW filter, the difference between the original filter and the reference system increased for lower trunk inclination angles. This might be due to the slight underestimation of large trunk inclination angles by the IMU-based approaches, such that deviations due to drift are mainly visible at lower inclination angles, while they diminish at higher angles.

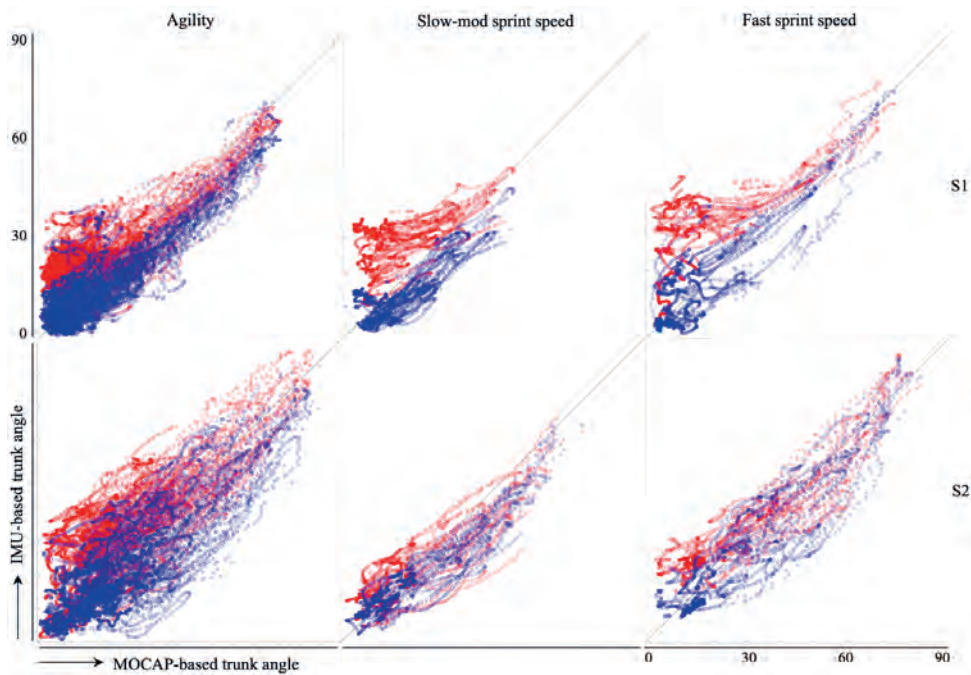


Figure 4.5. Scatter plots of the inclination of the original filter (red) and that of the extended filter (blue) against the MOCAP-based trunk inclination for the ‘agility’ part (left), ‘slow-mod sprint speed’ part (middle) and ‘fast sprint speed’ part (right) of subject 1 (upper three figures) and 2 (lower three figures) in the test set.

To our knowledge, no previous studies investigated the accuracy of IMU-based body segment orientation during wheelchair activities or other dynamic IMU challenging situations. Therefore, only trunk inclination accuracy of the fixed wheelchair parts, i.e., the less dynamic parts, allows for comparison with previous studies. The 5.3° RMSE for trunk inclination in the present study is comparable to the trunk inclination accuracy of 5° RMSE during postural disturbances when walking on a treadmill [2] and the 3.0° to 4.9° RMSEs for the estimation of trunk orientation during dynamic sports motions with both legs on the ground [7]. Although the latter results were more accurate, the measurement duration was much shorter (< 30 s [7]) than the session durations in the present study (~ 15 minutes). Also, some studies reported somewhat better accuracies of the IMU-based estimation of body segment orientations [4,27], but those studies measured for very short periods [4] or studied tasks with a small range of motion [27]. Of the mentioned studies, all studies reported a Kalman filter [2,4,27] or a MW filter [7] as AHRS and all studies validated the IMU-based estimations using an optical motion capture system. Overall, it can be concluded that the better performance of our method for highly dynamic situations has not been gone at the cost of a lower accuracy than that of previously reported results during less dynamic situations.

Since, to our knowledge, trunk inclination accuracy during highly dynamic sports situations is not reported in the literature yet, comparing the present study’s results of the original and the extended MW filter may provide more insight. A major difference between the filters is their performance during dynamic situations; the extended MW filter performed better

than the original MW filter in the dynamic ‘free wheelchair’ situations. This can be explained by the extent to which accelerations were present in these situations. When the wheelchair is propelled, continuous accelerations and decelerations are present and the magnitude of accelerations is determined by the acceleration of the wheelchair plus the acceleration of the trunk relative to the wheelchair. Therefore, the earth frame-based estimate is wrong relatively often during ‘free wheelchair’ instances causing the original filter to deviate, while the extended MW filter remains accurate by reducing the impact of this estimate. A similar trend was obtained from the time evolution of IMU-based trunk inclination in which the filters perform equally well in long-term static pose, while the original MW filter shows an increasing deviation during dynamic instances. Moreover, during static instances following dynamic instances, the extended MW filter immediately increases the correction size to ‘reorient’ towards the earth frame-based estimate such that accumulated drift is corrected at once. For the original filter, this ‘reorientation’ takes much longer, which may be a second explanation for the larger errors observed at smaller inclination angles for the original MW filter.

From the previous paragraphs it may be concluded that the extended MW filter provides considerable improvements compared to the original MW filter. Crucial for this performance is the machine learning-based classification model. To gain more insight into the behaviour of this model, the time instances at which large or small correction sizes were applied were analysed. As expected, β_{low} was most common in dynamic situations such that the orientation estimate was hardly affected by (wrong) earth frame-based estimates, whereas β_{high} was most common in static situations such that the effect of drift was limited. Since the orientation estimates during β_{low} instances rely mainly on integrating the gyroscope signal, integration drift will accumulate for each successive β_{low} instance. Therefore, the duration of successive β_{low} instances should not be too long. According to the durations observed in the present study (maximum durations of 15.3s and 2.05s with only two occurrences > 10s), it is assumed that drift was corrected before it may have caused any noteworthy deviations. In general, this relatively simple machine learning model seems to predict the most ‘advantageous’ correction size at each instance well and seems suitable for AHRS extension. Although the MW filter was used in our study, applying this extension to other orientation estimation filters may be promising as well.

Although the extended MW filter performed better compared to the original MW filter, the question whether the method can be seen as sufficiently accurate depends on its application and the aim that is to be accomplished. McGinley et al. [27] performed a systematic review on the reliability of 3D kinematic gait measurements with regard to clinical interpretation. According to McGinley et al. [27], errors below 5° will be widely considered acceptable to reasonable, while errors exceeding 5° may mislead interpretation. Since gait motions considerably differ from body motions during wheelchair propulsion and the range of trunk motion during wheelchair sports will exceed that of body segments during clinical gait, the minimal acceptable error may be somewhat higher in wheelchair propulsion. Considering the 7.6° RMSE obtained here, and a range of motion of 70 to 80 degrees (see Fig. 4.4 and 4.5) during wheelchair propulsion, the system should be able to differentiate trunk inclinations higher than 11% of the range of motion. For application in wheelchair sports, trunk inclination angle can be used to approximate the center of mass displacement, or to analyse motion patterns. A RMSE of 7.6° or 11% is expected to have an effect on above-mentioned analyses of trunk inclination only to a limited extent and will therefore be regarded acceptable.

In this study, external validity had priority above acquiring the smallest possible error and it was aimed to avoid any unnecessary complexity, such that sports scientists will be able to implement the extended MW filter with limited effort. In this regard, some choices were made

that may have influenced the final results. Some examples that might have produced more accurate results are (1) measuring all participants in the same wheelchair instead of using their own wheelchair, (2) compensate for magnetic distortions in the motion lab by performing a specific ‘mapping’ of the laboratory [28], (3) start a new measurement for each specific exercise, (4) optimize β_{high} and β_{low} after training the final model and (5) add more refinement in β values, instead only β_{high} and β_{low} . To put the focus on external validity and repeatability, these examples were not applied. Therefore, we expect our results to be well translatable and implementable to sports and rehabilitation practice.

Limitations

Although this study provided useful outcomes with regard to orientation estimation in dynamic sports situations, some limitations should be noted. First of all, the trunk markers that were used to determine the MOCAP-based trunk inclination, were placed on the upper sternum (to ensure visibility), while the trunk IMU was attached to a lower location on the sternum using a chest strap (to enhance reproducibility and usability and to limit skin artefacts). Since the sternum is rigid, the use of different locations was assumed to have no effect on the measurements. Second, in the current study, helical angles were used to determine trunk inclination during wheelchair sports activities. Therefore, caution should be exercised in generalizing the present results to situations in which trunk motion is analysed in terms of anatomical angle definitions. Third, a relatively low number of subjects was included in this study. However, since the results of the measurements with the subjects in the test set showed the same trends and was based on over 100k samples, similar results are expected to be obtained when a larger sample of subject was included.

Future perspectives

For measuring trunk inclination in wheelchair sports, the machine learning-based extended MW filter is ready to use. Since differently skilled participants were used in this study, it may be assumed that the extended MW filter works well for trunk inclination estimation in all types of wheelchair-users, for all types of wheelchairs and in both rehabilitation as well as (elite) sports practice. Measuring trunk inclination during on-site wheelchair sports offers many opportunities. When trunk inclination is combined with wheelchair kinematics during wheelchair sports [16], the (simplified) kinematic state of the wheelchair-athlete combination can be obtained. In this way, center of mass displacement can be approximated, and field-based power losses and power production can be more accurately obtained than based on the wheelchair motions only. This enables more insight into training load, fitness and the effect of different push techniques. Also, information about trunk inclination can be fed back directly to the coach and/or athlete for specific training purposes.

For application in other IMU challenging sports situations, it is expected that the extended MW filter will also work. From the raw IMU data, only two simple additional steps; (1) run the classification model on the raw IMU data ($\mathbf{a}_{x,\text{distal segment}}$, $\mathbf{m}_{y,\text{distal segment}}$, $\mathbf{m}_{x,\text{distal segment}}$, $\mathbf{m}_{z,\text{proximal segment}}$ $\mathbf{m}_{x,\text{proximal segment}}$) and (2) decode the outcomes to β_{high} and β_{low} (0.9635 and 0.0015 in the present study), have to be performed to convert the original MW filter into the proposed extended MW filter. These steps are schematically represented on the left side of Fig. 4.3. After obtaining β_i , the MW filter can be executed such that IMU-orientation is obtained. The approach to determine the best values for β_{high} and β_{low} is equal to that in the original MW filter [12] and may differ between sensors and situations. Although the classification model should be verified for other sports, it is expected to

be transferable to other situations since (1) the model was based on raw IMU data only and (2) works on a sample-to-sample basis such that differences in movement pattern should not cause any problems. If only one IMU was used, or accelerations in multiple directions (relative to the IMU) were common, a custom-made random forest classification model is recommended for optimal results.

Conclusion

The extended MW filter with machine learning-based classification improved orientation estimation in sports applications that are challenging for IMU usage. The extended MW filter resulted in accurate trunk inclination angles during wheelchair sport-specific exercises. During exercises in which the wheelchair was moved unrestrictedly, the extended MW filter performed better than the original MW filter. During situations in which the wheelchair was static (by blocking the wheels), both the original and the extended MW filter performed equally well. In conclusion, the extended MW filter is a promising application for the estimation of body segment orientation using IMU's in highly dynamic sports situations and is ready to be used in (elite) wheelchair sports and rehabilitation practice.

References

1. Camomilla V, Bergamini E, Fantozzi S, Vannozzi G. Trends supporting the in-field use of wearable inertial sensors for sport performance evaluation: A systematic review. *Sens Switz.* 2018;18(3).
2. Miller EJ, Kaufman KR. Cross-sectional validation of inertial measurement units for estimating trunk flexion kinematics during treadmill disturbances. *Med Eng Phys.* 2019;70:51–4.
3. Le Sage, T, Conway, P C J, Slawson, S, West, Andrew. A wireless sensor system for monitoring the performance of a swimmer's tumble turn. *J Sports Eng Technol.* 2013;227(3):161–71.
4. Bergamini E, Guillon P, Camomilla V, Pillet H, Skalli W, Cappozzo A. Trunk inclination estimate during the sprint start using an inertial measurement unit: A validation study. *J Appl Biomech.* 2013;29(5):622–7.
5. Ahmadi A, Rowlands DD, James DA. Development of inertial and novel marker-based techniques and analysis for upper arm rotational velocity measurements in tennis. *International Sports Engineering Association.* 2010;12:179–88.
6. Najafi B, Lee-Eng J, Wrobel JS, Goebel R. Estimation of center of mass trajectory using wearable sensors during golf swing. *J Sports Sci Med.* 2015;14:354–63.
7. Brouwer NP, Yeung T, Bobbert MF, Besier TF. 3D trunk orientation measured using inertial measurement units during anatomical and dynamic sports motions. *Scand J Med Sci Sports.* 2020;
8. Zhang Y, Chen K, Yi J, Liu T, Pan Q. Whole-body pose estimation in human bicycle riding using a small set of wearable sensors. *IEEEASME Trans Mechatron.* 2016;21(1):163–74.
9. Brodie M, Walmsley A, Page W. Fusion motion capture: A prototype system using inertial measurement units and GPS for the biomechanical analysis of ski racing. *Sports Technol.* 2008;1(1):17–28.
10. Lee JK, Jeon TH. Magnetic condition-independent 3D joint angle estimation using inertial sensors and kinematic constraints. *Sensors.* 2019;19(24):5522.

11. Weygers I, Kok M, De Vroey H, Verbeerst T, Versteyhe M, Hallez H, Claeys K. Drift-free inertial sensor-based joint kinematics for long-term arbitrary movements. *IEEE Sens J.* 2020;20(14):7969–79.
12. Madgwick SOH, Harrison AJL, Vaidyanathan R. Estimation of IMU and MARG orientation using a gradient descent algorithm. *IEEE Int Conf Rehabil Robot.* 2011;179–85.
13. Kok M, Schon TB. A fast and robust algorithm for orientation estimation using inertial sensors. *IEEE Signal Process Lett.* 2019;26(11):1673–7.
14. Yoo T, Hong S, Yoon H, Park S. Gain-scheduled complementary filter design for a MEMS based attitude and heading reference system. *Sensors.* 2011;11(4):3816–30.
15. Valenti R, Dryanovski I, Xiao J. Keeping a good attitude: A quaternion-based orientation filter for IMUs and MARGs. *Sensors.* 2015;15(8):19302–30.
16. van der Slikke RMA, Berger MAM, Bregman DJJ, Lagerberg AH, Veeger HEJ. Opportunities for measuring wheelchair kinematics in match settings; reliability of a three inertial sensor configuration. *J Biomech.* 2015;48(12):3398–405.
17. Pansiot J, Zhang Z, Lo B, Yang GZ. WISDOM: wheelchair inertial sensors for displacement and orientation monitoring. *Meas Sci Technol.* 2011;22(10):105801.
18. Kontaxis A, Cutti AG, Johnson GR, Veeger HEJ. A framework for the definition of standardized protocols for measuring upper-extremity kinematics. *Clin Biomech.* 2009;24(3):246–53.
19. MathWorks. Navigation Toolbox: User's Guide (R2020b) [Internet]. 2020. Available from: <https://nl.mathworks.com/help/nav/ug/magnetometer-calibration.html>
20. Blankevoort, L., Huiskes, R., De Lange, A. Helical axis of passive knee joint motions. *J Biomech.* 1990;23(12):1219–29.
21. Rhudy M. Time alignment techniques for experimental sensor data. *Int J Comput Sci Eng Surv.* 2014;5(2):14.
22. Goldin DQ, Kanellakis PC. On similarity queries for time-series data: Constraint specification and implementation. *Int Conf Princ Pract Constraint Program.* 1995;137–53.
23. Pedregosa, F; Varoquaux, G; Gramfort, A; Michel, V, Thirion, B; Grisel, O; Blondel, M; Prettenhofer, P, Weiss, R.;Dubourg, V; Vanderplas, J; Passos, A.; Cournapeau, D; Brucher, M; Perrot, M; Duchesnay, E. Scikit-learn: Machine Learning in {P}ython. *J Mach Learn Res.* 2011;12:2825–30.
24. Bland, J.M., Altman, D.G. Statistical methods for assessing agreement between two methods or clinical measurement. *The Lancet.* 1986;307–10.
25. McGinley JL, Baker R, Wolfe R, Morris ME. The reliability of three-dimensional kinematic gait measurements: A systematic review. *Gait Posture.* 2009;29(3):360–9.
26. de Vries WHK, Veeger HEJ, Baten CTM, van der Helm FCT. Magnetic distortion in motion labs, implications for validating inertial magnetic sensors. *Gait Posture.* 2009;29(4):535–41.



Abstract

In wheelchair sports, there is an increasing need to monitor mechanical power in the field. When rolling resistance is known, inertial measurement units (IMUs) can be used to determine mechanical power. However, upper body (i.e., trunk) motion affects the mass distribution between the small front and large rear wheels, thus affecting rolling resistance. Therefore, drag tests - which are commonly used to estimate rolling resistance - may not be valid. The aim of this study was to investigate the influence of trunk motion on mechanical power estimates in hand-rim wheelchair propulsion by comparing instantaneous resistance-based power loss with drag test-based power loss. Experiments were performed with no, moderate and full trunk motion during wheelchair propulsion. During these experiments, power loss was determined based on 1) the instantaneous rolling resistance and 2) based on the rolling resistance determined from drag tests (thus neglecting the effects of trunk motion). Results showed that power loss values of the two methods were similar when no trunk motion was present (mean difference [MD] of $0.6 \pm 1.6\%$). However, drag test-based power loss was underestimated up to $-3.3 \pm 2.3\%$ MD when the extent of trunk motion increased ($r=0.85$). To conclude, during wheelchair propulsion with active trunk motion, neglecting the effects of trunk motion leads to an underestimated mechanical power of 1 to 6% when it is estimated with drag test values. Depending on the required accuracy and the amount of trunk motion in the target group, the influence of trunk motion on power estimates should be corrected for.

Introduction

In manual wheelchair propulsion, wheelchair athletes produce mechanical power to overcome resistance forces and to accelerate their wheelchair (van Dijk et al., 2023; van Ingen-Schenau and Cavanagh, 1990). Mechanical power is therefore crucial to performance in wheelchair sports. In addition, monitoring mechanical power on a regular basis can provide insight into training load, physical capacity, and fatigue, which is useful for coaches, athletes, and sport scientists. During hand-rim wheelchair propulsion, mechanical power can be monitored by determining the power lost due to resistance forces and the change in kinetic energy (de Vette et al., 2022; van Ingen-Schenau & Cavanagh, 1990).

To determine resistance force and, consequently, power during ergometer-, treadmill- and wearable sensor-based measurements of wheelchair propulsion, drag or deceleration tests are commonly used (de Groot et al., 2013; de Klerk et al., 2020; Mason et al., 2014; van der Woude et al., 1986; Veeger, H.E.J. & van der Woude, L.H.V., 1989). However, in our previous study, deviations of -4.6 to 0.9% were found between the drag test-based resistance force and the reference resistance force (van Dijk et al., 2023). Also, deviations were much larger for some participants than for others. As during drag tests, the user is instructed to maintain a static position (Rietveld et al., 2021), while during wheelchair propulsion most wheelchair users incline their upper body - mainly trunk - within a push cycle, these deviations may be due to the (neglected) effects of trunk motion on the rolling resistance (Sauret et al., 2013). In this regard, larger deviations are expected when larger trunk inclinations are observed. However, the relation between trunk motion and deviations in rolling resistance (and thus power) estimates during wheelchair propulsion is not yet known.

During wheelchair propulsion, trunk inclination influences the rolling resistance in two ways. First, rolling resistance coefficients of the small castor wheels on the front are usually larger than that of the - much larger - rear wheels (Sauret et al., 2013). Thus, the rolling resistance increases when the load (or COM) is shifted towards the castor wheels and vice versa. Second, trunk motion causes vertical accelerations of the COM such that the total load on the wheels increases when the COM accelerates upward and vice versa. In practice, forward trunk inclination will thus cause a varying rolling resistance force due to two different mechanisms.

Sauret et al. (2013) investigated the 'effects of users actions on rolling resistance' in everyday wheelchairs and investigated both changes in forward-backward load distribution, and vertical COM accelerations. Based on three participants, they found the total load to vary from 80-130% of the gravitational force, indicating the effect of the vertical acceleration of the COM. In addition, the forward and backward shift of the COM, mainly due to inclination resulted in a castor wheel load ranging from 24-31% (minimal values) to 61-83% (maximal values) of the total load within each push cycle. However, they did not quantify the relative contribution of the two mechanisms. Once this is known, the effects of trunk motion could be corrected for when estimating rolling resistance, such that more accurate power values are obtained. Therefore, the relative contribution of the two mechanisms that cause a varying rolling resistance during wheelchair propulsion should be investigated.

The first aim of this study was to investigate the relation between trunk motion and the difference between the reference power loss (calculated from instantaneous rolling resistance), i.e., P_{IR} , and drag test-based power loss, i.e., P_{drag} , during wheelchair propulsion. The second aim of this study was to quantify the relative contributions of 1) changes in forward-backward load distribution, and 2) vertical COM accelerations, to the difference between P_{IR} , and P_{drag} . To this end, wheelchair propulsion experiments were performed while load on the front wheels

was measured with custom-made load pins, and trunk and wheelchair kinematics were obtained from inertial sensors. P_{IR} and P_{drag} were compared for three levels of trunk motion: no trunk motion, moderate trunk motion and full trunk motion.

Methods

1. Data collection

1.1 Outline of the study

Twenty-four able-bodied individuals (18 females and 6 males, mean age: 25 ± 13 years, mean body mass: 76 ± 13 kg, mean body height: 1.70 ± 0.07 m) without wheelchair experience propelled the hand-rims of a wheelchair on a large treadmill in three different conditions; 'no trunk motion', 'moderate trunk motion' and 'full trunk motion'. During the 'no trunk motion' condition, participants were instructed to keep the trunk static, whereas the other two conditions were imposed by following a metronome making participants to propel with long strokes accompanied by (natural) trunk motion (Goosey et al., 2000). During this experiment, trunk and wheelchair kinematics were measured using three IMUs attached to the participants' sternum, the wheelchair's frame, and right wheel axle. Custom-made load pins in the castor wheel axes measured the vertical load on the castor wheels (see Fig. 5.1). Before the treadmill session, participants received a 10-minute overground wheelchair training to get familiar with the wheelchair, a force plate session in which they stationary performed 'fake' wheelchair strokes on a force plate, and a 10-minute training on the treadmill (see Fig. 5.2). After the treadmill session, drag tests were performed on the treadmill to obtain rolling resistance coefficients of each pair of wheels. Lastly, participants' body mass was determined. All measurements were performed with a rear wheel tire pressure of 5.25 bar.

The study was approved by the ethical committee of the Technical University of Delft (Nr. 1530). Prior to the measurements, participants were informed about the aim and procedure of the study and provided written informed consent. The data used in this study were collected simultaneously with the data of another study (van Dijk et al., 2023).

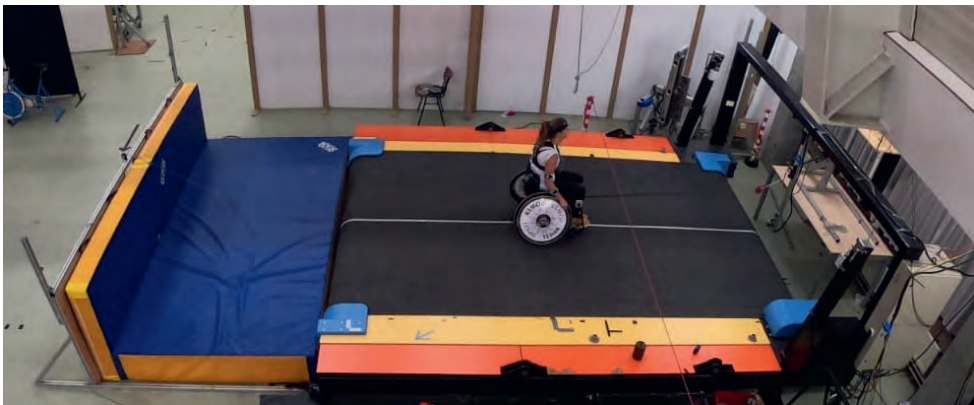




Figure 5.1a-b. Measurement set-up during the treadmill sessions. The custom-made load pins were integrated in each of the castor wheels (normal castor wheel axle were replaced by the load pins)

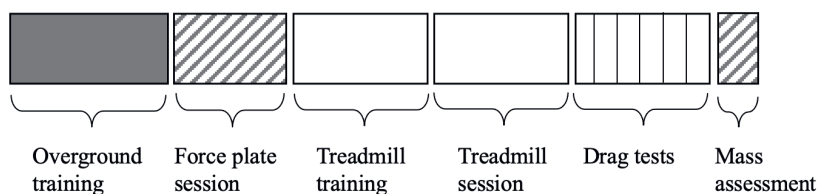


Figure 5.2. Schematic overview of the measurement sessions consisting of overground wheelchair training, a force plate (FP) session, treadmill training and three treadmill sessions which were performed at different rear wheel tire pressure. Within each 3.5-minute treadmill session, participants propelled the wheelchair in three conditions: ‘no trunk motion’, ‘moderate trunk motion’, and ‘full trunk motion’. In addition, drag tests were performed and participants’ body mass was assessed.

1.2 Instrumentation

All treadmill measurements took place on a large (3.0 x 5.0 m) motor-driven treadmill (Bonte, Zwolle, the Netherlands) located at the Vrije Universiteit Amsterdam. A large treadmill was used to make participants feel safe to move forwards, backwards and sideways on the belt. An S-beam load cell (Revere Transducers, Lisse, the Netherlands) was used to measure the horizontal (drag) forces during the drag tests. An RGK Chrome all-courts wheelchair was used for the measurements (see Table 5.1). Wheelchair setup was equal for all participants. Load pins (Batarow Sensorik, Germany) were integrated in the castor wheel axes of the wheelchair to measure the vertical load on the castor wheels. Three IMUs (NGIMU, X-io Technologies, Colorado Springs, CO, United States) were used to collect 3D inertial sensor data with a sample frequency of 100 Hz. In addition, the NGIMU analogue input channels of the frame-mounted sensor were connected to the load pins to act as power source and data logger. Ground reaction forces were measured at 200 Hz using a 1.0 x 1.0 m custom-made strain gauge force plate as described in the study of Kingma et al. (Kingma et al., 1995). The load cell and force plate were

calibrated with known masses at the start of each measurement day. The load pins were calibrated during each force plate session by positioning the castor wheels on the force plate (while rear wheels were positioned at the same height).

Table 5.1.

Wheelchair dimensions of the RGK Chrome all-courts wheelchair that was used for all measurements. The rear wheels had pneumatic tyres. The front wheels were solid rubber castor wheels.

Mass	13.5 kg
Wheel radius (rear)	0.61 m
Wheel radius (front)	0.075 m
Camber angle (rear)	13 degrees
Seat position (horizontal distance between backrest and rear wheel axis)	0.08 m
Distance front-rear wheels	0.39 m

1.3 Treadmill session

The treadmill sessions consisted of 30s familiarization, followed by 60s propelling at a low velocity (1.2 m/s) with no instruction (condition ‘moderate trunk motion’), 60s propelling at a low velocity with the instruction to keep the trunk vertical (condition ‘no trunk motion’) and 60s propelling at a high velocity (1.7 m/s) with no instruction again (condition ‘full trunk motion’). Participants were instructed to maintain a constant stroke frequency indicated by a metronome (set at 25 beats/minute during the first 90s, and 40 beats/minute thereafter). Adherence to the instructions was monitored by observation. Safety was guaranteed by an automatic and a manual security stop.

After each treadmill session, drag tests were performed at 1.7 m/s, while the participants were instructed to sit as still as possible for a period of 30s in six conditions. The (2x3) conditions consisted of sitting with vertical trunk and sitting bent forward while no mass was added, while 10 kg was added at the footrests and while 10 kg was added on the upper legs. Conditions with varying load distributions were required to be able to solve Eq. 5.2 numerically, as front wheel load was measured, and rear wheel load could be determined.

2. Data analysis

Acceleration, gyroscope and load pin force data were 2nd order low-pass filtered at 6 Hz. The gyroscope data of the wheel sensor were used to obtain wheelchair velocity (van der Slikke et al., 2015). Trunk inclination angle relative to the global vertical (in which 0 degrees was assumed vertical) was obtained using an extended Madgwick filter as described by van Dijk et al. (van Dijk, Kok, et al., 2021), with the β -value being 0.0015 (if $|\text{wheelchair acceleration}| < 0.1 \text{ m/s}^2$ for at least 5 consecutive samples) or 0.9635 (otherwise). In addition, vertical trunk acceleration was determined. To this end, the sine of trunk inclination angle was determined to obtain vertical trunk (IMU) displacement, and subsequently differentiated twice.

The drag test-based rolling resistance forces were obtained by averaging the last 10 seconds of the S-beam force data. Subsequently, the rear (r) and front (f) wheel rolling resistance coefficients, c_r and c_f , were determined by solving Eq. 5.2 numerically based on the average S-beam force and average load pin force ($F_{N,f}$) of the series of drag tests. Accordingly, c_f and c_r were used to estimate the instantaneous resistance force (F_{IR}) during all treadmill sessions. Power loss was obtained by multiplying the resistance force with wheelchair velocity.

Knowing c_f , c_r and $F_{N,f}$, the only unknown left to determine F_{IR} during the treadmill sessions is the instantaneous vertical acceleration of the system’s COM ($a_{COM,z}$, see Eq. 5.3). Therefore, $a_{COM,z}$ was estimated from vertical trunk acceleration (see above). The relation

between $a_{COM,z}$ and vertical trunk acceleration was determined using a force plate session in which participants performed a 2-minute protocol consisting of ‘fake’ wheelchair strokes. Simultaneously, vertical trunk acceleration and the $a_{COM,z}$ (calculated from the instantaneous vertical force on the force plate) were measured. A linear regression analysis was performed to predict $a_{COM,z}$ from vertical trunk acceleration for each participant.

$$F_{IR} = c_f * F_{N,f} + c_r * F_{N,r} \quad (5.2)$$

$$F_{N,r} = (m * g + m * a_{com,z}) - F_{N,f} \quad (5.3)$$

$$F_{IR,a=0} = c_f * F_{N,f} + c_r * (m * g - F_{N,f}) \quad (5.4)$$

2.1 Influence of trunk motion on estimation of power loss

To investigate to what extent trunk motion affects IMU-based power estimates during wheelchair propulsion, the resistance force and resulting power loss were estimated for each condition of trunk motion during the treadmill sessions. F_{drag} was obtained from the drag test with vertical trunk and no added mass, which is essentially the same as an overground deceleration test (Ott & Pearlman, 2021) and was subsequently compared with F_{IR} during wheelchair propulsion. Subsequently, the mean differences and mean absolute differences between F_{drag} and F_{IR} (and corresponding power losses, i.e., P_{drag} and P_{IR}) were determined per condition for each participant. To assess the relation between trunk inclination and the difference between P_{drag} and P_{IR} , trunk inclination range was determined for each participant by determining the maximal difference (i.e., maximum-minimum) in trunk angle per push, which were then averaged over the entire trial.

2.2 Relative contribution of changing load distribution and vertical COM accelerations

To determine the mechanism underlying potential deviations between P_{drag} and P_{IR} , the relative contribution of 1) changes in forward-backward load distribution and 2) vertical COM accelerations on the rolling resistance was determined. Therefore, rolling resistance as presented in Eq. 5.2 and 5.3 was compared with the rolling resistance when $a_{com,z}$ was ‘ignored’ by setting it at 0 (see Eq. 5.4). In this way, $F_{IR,a=0}$ only considers the effect of load distribution (note that both the mass distribution as well as horizontal forces of the wheelchair user on the wheelchair can influence this). Subsequently, the percentage of error due to changes in load distribution (i.e., $F_{IR,a=0} - F_{drag} / F_{IR} * 100\%$) and that due to $a_{com,z}$ (i.e., $F_{IR} - F_{IR,a=0} / F_{IR} * 100\%$) were calculated.

3. Statistical analysis

A one-way repeated measures ANOVA was used to assess whether the mean differences between (cycle-average) P_{drag} and (cycle-average) P_{IR} varied significantly between the three conditions of trunk motion. If the Greenhouse-Geisser epsilon ≥ 0.75 , the Huynh-Feldt correction was used, otherwise the Greenhouse-Geisser correction was used. Subsequently, the correlation between trunk inclination range and the difference between (cycle-average) P_{drag} and (cycle-average) P_{IR} were analysed using a repeated measures correlation. A QQ-plot and a Shapiro-Wilks test of the residuals were performed to verify the assumption of normality. This assumption was not violated. Statistical analysis was conducted using software R (R Core Team, 2023). The significance level was set at $p < 0.05$.

Results

In total, 24 treadmill sessions were analysed. During the sessions, the average trunk inclination was 4 to 14 degrees in the ‘no trunk motion’-condition (trunk inclination range (TIR): 7.1 ± 3), 7 to 61 degrees in the moderate trunk motion condition (TIR: 23.5 ± 12) and 9 to 47 degrees (TIR: 25.0 ± 10) in the full trunk motion-condition. The mean absolute trunk angular velocity was 10 deg/s for no trunk motion, 21 deg/s for moderate and 33 deg/s for full trunk motion. The drag tests revealed rolling resistance coefficients of .0147 for the set of castor wheels and .0104 and .0089 (the tires were replaced after 8 participants) for the rear wheels.

Influence of trunk motion on estimation of power loss

Over time, drag test-based resistance force (F_{drag}) and power loss (P_{drag}) differ from the instantaneous resistance-based force (F_{IR}) and power loss (P_{IR}), see Fig. 5.3 and 5.4. On average, P_{drag} is underestimated in both moderate and full trunk motion conditions (see Table 5.2). A one-way repeated measures ANOVA showed a significant effect for the condition ($F(1.6,36.4)=55.1, p<.001$) on the difference between P_{drag} and P_{IR} . Post-hoc Bonferroni test for multiple comparisons showed a significant difference between the conditions no and moderate trunk motion ($p<.001$), no and full trunk motion ($p<.001$) and moderate and full trunk motion ($p<.01$).

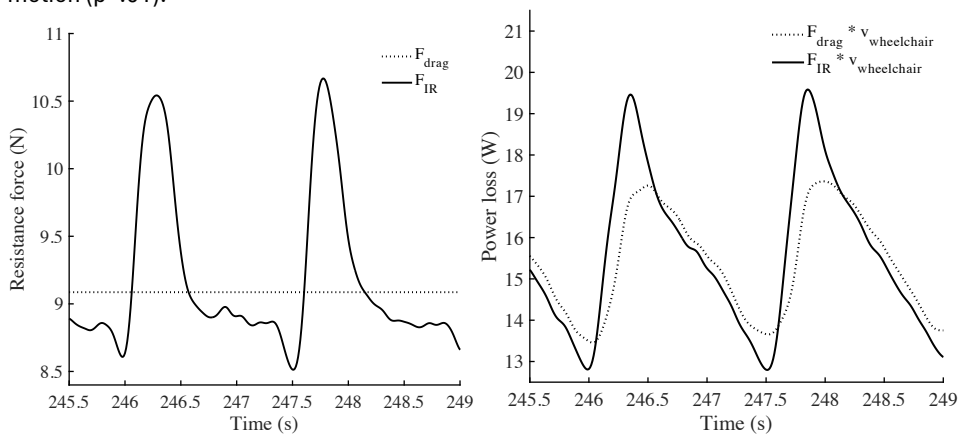


Figure 5.3-5.4. Typical example of resistance force (left figure) and corresponding power loss (right figure) derived from the drag test-based resistance force, i.e., F_{drag} (dotted line), and the instantaneous resistance force, i.e., F_{IR} (solid line). These data are obtained from the condition with full trunk motion for two pushing cycles.

Table 5.2.

Mean (SD) drag test-based and instantaneous resistance-based power (P) and resistance force (F) values for each condition. The mean difference (MD) and the mean absolute difference (MAD) is presented. In addition, the average trunk inclination range is given for each condition.

Condition	Variable	Drag	IR	MD (%)	MAD (%)	Range of trunk inclination (°)
No	F	8.4 (1.3)	8.4 (1.3)	0.6 (1.6)	1.4 (1.0)	7 (3)
	P	10.0 (1.6)	10.0 (1.6)	0.6 (1.6)	1.4 (1.0)	
Moderate	F	8.4 (1.3)	8.6 (1.3)	-2.3 (2.0)	2.5 (1.8)	24 (12)
	P	10.0 (1.6)	10.3 (1.6)	-2.4 (2.0)	2.6 (1.9)	
Full	F	8.4 (1.3)	8.7 (1.3)	-3.2 (2.3)	3.2 (2.3)	25 (10)
	P	14.3 (2.3)	14.8 (2.3)	-3.3 (2.3)	3.3 (2.3)	

Moreover, a negative correlation ($r(47)=-.85, p<.001$) was found between trunk inclination range and the difference between P_{drag} and P_{IR} for all conditions (see Fig. 5.5).

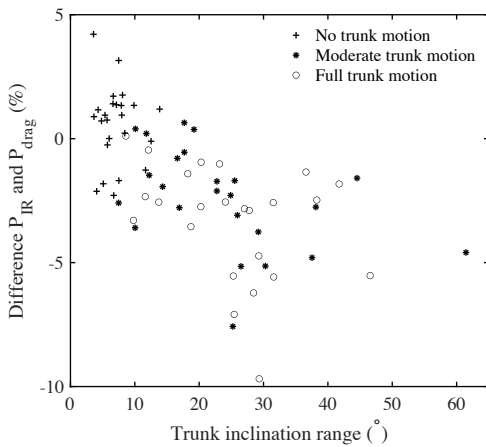


Figure 5.5. Difference between P_{drag} and P_{IR} against the trunk inclination range (i.e., the maximal difference (i.e., maximum-minimum) in trunk angle per push averaged over the entire trial) for all participants and all conditions. The condition with no trunk motion is indicated by '+', the condition with moderate trunk motion is indicated by '*', and the condition with full trunk motion is indicated by 'o'. The difference is determined by $(P_{drag} - P_{IR}) / P_{IR}$.

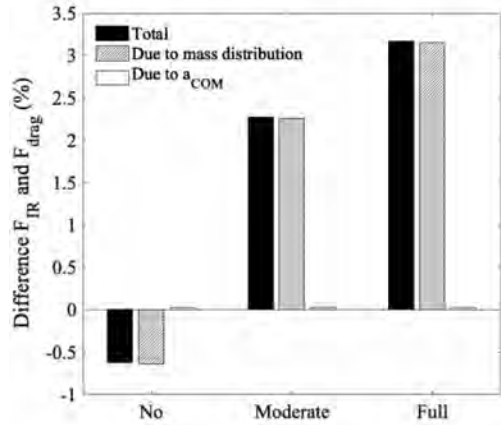


Figure 5.6. The mean difference between F_{drag} and F_{IR} , compared with the mean differences due to (changes in) mass distribution and COM accelerations only. The difference is determined by $(F_{drag} - F_{IR}) / F_{IR}$.

Relative contribution of changing load distribution and vertical COM accelerations

Substantial differences were observed for the relative contribution of changing load distribution and vertical COM accelerations to the differences between F_{drag} and F_{IR} (see Fig. 5.6). For full trunk motion, changes in load distribution caused an underestimation of -0.3 to 9.4% (MD 3.1%), while vertical COM accelerations caused an underestimation of -0.2 to 0.2% (MD 0.02%). From the total difference, 103% (no), 99% (moderate) and 99% (full) is explained by changes in load distribution, compared to negligible effects (-3%, 1% and 1%) for vertical COM accelerations. The deviation between F_{drag} and F_{IR} is thus caused by changes in load distribution only.

Discussion

The first aim of this study was to investigate the relation between trunk motion and the difference between power calculated from instantaneous rolling resistance, i.e., P_{IR} , and drag test-based power loss, i.e., P_{drag} , during wheelchair propulsion. Comparisons between P_{IR} and P_{drag} showed almost no difference for wheelchair propulsion without moving the trunk (mean difference [MD] $0.6 \pm 1.6\%$), and a small underestimation of P_{drag} for wheelchair propulsion with

moderate (MD $-2.4 \pm 2.0\%$) and full (MD $-3.3 \pm 2.3\%$) trunk motion. A significant negative correlation was found between the trunk inclination range and the difference between P_{drag} and P_{IR} , indicating a larger underestimation when trunk motion increases. In addition, the results show that the difference between P_{drag} and P_{IR} (when trunk motion is present) is for 99% caused by changes in forward-backward load distribution, whereas the effects of vertical COM accelerations were negligible.

Compared to previous studies, the rolling resistance coefficients, drag forces and power values as found in the present study were similar to the values reported previously during treadmill and overground wheelchair propulsion (Mason et al., 2014; Rietveld et al., 2021). In addition, the larger relative influence of forward-backward load distribution (compared to vertical COM acceleration, or, total wheel load) was reported by a previous study of de Saint Rémy et al. (2003). However, their results were based on deceleration tests with different (static) masses and mass distributions, and the findings were not related to a measured trunk or upper body motion. The present study is, as far as we know, the first to quantify the relation (and its underlying mechanisms) between trunk motion and the difference between drag test-based rolling resistance and actual rolling resistance during wheelchair propulsion.

The present study found an underestimation of 1 to 6% for the drag test-based power loss when no instructions on trunk motion were given, and a larger underestimation when more trunk motion was measured. This underestimation can be explained by the differences between the small castor wheels (high rolling resistance coefficient, i.e., .0147) and large rear wheels (low rolling resistance coefficient, i.e., .0104 and .0089) in combination with a changing load distribution. Whereas, in the present study, the rear wheel coefficients were 30-40% smaller than the front wheel coefficients, the relative differences between rolling resistance coefficients differ over wheelchairs. In this regard, the underestimation will be smaller when rolling resistance coefficients become more similar, for instance, due to a lower rear wheel tyre pressure (see Appendix A). When interpreting rolling resistance or power (loss) based on drag tests, both trunk motion and the relative difference between rolling resistance coefficients of the rear and castor wheels should thus be considered.

As drag tests are used to determine rolling resistance in many wheelchair measurements based on IMUs, ergometers or treadmills, the results of the present study may impact previously reported results on drag-test based rolling resistance or power loss. For example, Rietveld et al. (2021) reported differences in rolling resistance for different tennis court surfaces, like grass and hardcourt. However, as most wheelchair tennis players propel with considerable trunk movements (Ju et al., 2021), the actual values for rolling resistance during wheelchair propulsion would be higher than reported by Rietveld et al. (2021). Moreover, as a larger rolling resistance is associated with increasing trunk motion (Chow et al., 2000), actual differences between 'resistive' surfaces and 'less resistive' surfaces may also be larger than the ones reported by Rietveld et al. (2021). In addition, results of studies that compared the effect of tyre pressure on rolling resistance based on standard drag tests may not be valid as well (de Groot et al., 2013). As the accuracy of rolling resistance depend on 1) relative differences between rolling resistance coefficients and 2) amount of trunk motion, which are both intentionally or unintentionally altered when rear wheel tyre pressure is changed, making comparisons regarding actual rolling resistance based on drag tests is not valid. Overall, previously reported results regarding rolling resistance or power that were based on drag-test based rolling resistance should be handled with caution.

In wheelchair field sports, the results of the present study may have implications as well. In disciplines like wheelchair basketball or wheelchair rugby, differences are seen in the amount

of trunk motion between athletes from different classifications and between accelerating from standstill versus steady-state wheelchair propulsion (Altmann et al., 2016; van Dijk et al., 2021). Ignoring the effects of trunk motion may thus lead to an underestimation in power for athletes with high classifications compared to athletes with lower classifications. In addition, within a short sprint starting from stand-still, the power during the first pushes will be underestimated more than the power in the later pushes. When monitoring power in wheelchair sports practice, and mainly when comparisons between or within athletes are made, trunk motion should be determined and ideally be corrected for.

For future measurements one may, depending on the extent of trunk motion, correct for this to obtain accurate rolling resistance (and power) estimates. As the load pins used in this study are not convenient to use in daily practice, an additional IMU on the chest - in combination with a proper prediction model - may be used to estimate changing (upper body) mass (and thus load) distribution. This was already done in one of our previous studies by determining rolling resistance based on three different drag tests each having a different (known) trunk angle and, subsequently, determining the relation between trunk angle and drag test-based rolling resistance (van Dijk et al., 2021). However, no gold standard was determined such that the accuracy of this method could not be determined. All in all, the underestimated rolling resistance may be corrected by adding (IMU-based) information on trunk motion.

For the present study, some limitations should be noted. First, all experiments were executed on a treadmill. However, as several precautions were taken to stimulate natural wheelchair propulsion (such as using a large treadmill and a respectable familiarization period), we believe that the relations and conclusions found in this study translate well to the field. Second, in this study, drag tests were used to determine F_{drag} , while, in the field, deceleration tests are more convenient. As drag tests and deceleration tests are both indirect methods to determine F_{drag} , they should result in the same value when circumstances are equal (Ott & Pearlman, 2021). Lastly, this study focused on four-wheeled wheelchairs, whereas in wheelchair racing, another type of wheelchair is used. Because the rolling resistance coefficients of wheelchair racing wheels are more similar, arm movements may have more influence on the resistance force, and velocities are higher, our results are not expected to translate well to wheelchair racing.

Conclusion

During wheelchair propulsion with active trunk movement, ignoring the effects of trunk motion leads to an underestimated mechanical power of 1 to 6% when this is based on drag test values. In addition, more trunk motion was related to a larger underestimation of power. Therefore, depending on the required accuracy of power output and the amount of trunk motion in the target group, the influence of trunk motion should be considered. As the power difference was caused by (trunk motion-induced) changes in load distribution between the front wheels and rear wheels during wheelchair propulsion, future studies should assess changes in forward-backward load distribution to obtain accurate rolling resistance and power values.

To conclude, including trunk motion in the mechanical power estimation improves the accuracy of power output estimations during hand-rim wheelchair propulsion and is crucial to ensure fair comparisons between and within athletes.

Acknowledgements

This work was supported by the Netherlands Organisation for Health Research and Development (ZonMw), project number 546003002. This project, named WheelPower: wheelchair sports and data science push it to the limit is a cooperative effort between TU Delft, UMCG, THUAS, VU Amsterdam and is in cooperation with several sports federations collected under the umbrella of NOC*NSF.

Supplementary material

Load pin and IMU data of the entire experiment is publicly accessible via <https://doi.org/10.4121/bc9a8588-5e50-4dff-aa77-5114ff7626f7>.

References

1. Altmann, V. C., Groen, B. E., Groenen, K. H., Vanlandewijck, Y. C., Van Limbeek, J., & Keijsers, N. L. (2016). Construct Validity of the Trunk Impairment Classification System in Relation to Objective Measures of Trunk Impairment. *Archives of Physical Medicine and Rehabilitation*, 97(3), 437–444. <https://doi.org/10.1016/j.apmr.2015.10.096>
2. Chow, J. W., Millikan, T. A., Carlton, L. G., Chae, W., & Morse, M. I. (2000). Effect of resistance load on biomechanical characteristics of racing wheelchair propulsion over a roller system. *Journal of Biomechanics*.
3. de Groot, S., Vegter, R. J. K., & Van Der Woude, L. H. V. (2013). Effect of wheelchair mass, tire type and tire pressure on physical strain and wheelchair propulsion technique. *Medical Engineering & Physics*, 35(10), 1476–1482. <https://doi.org/10.1016/j.medengphy.2013.03.019>
4. de Klerk, R., Vegter, R. J. K., Veeger, H. E. J., & Van Der Woude, L. H. V. (2020). Technical Note: A Novel Servo-Driven Dual-Roller Handrim Wheelchair Ergometer. *IEEE Transactions on Neural Systems and Rehabilitation Engineering*, 28(4), 953–960. <https://doi.org/10.1109/TNSRE.2020.2965281>
5. de Saint Rémy, N. de S., Vaslin, P., Dabonneville, M., Martel, L., & Gavand, A. (2003). Dynamique de la locomotion en fauteuil roulant manuel: Influences de la masse totale et de sa répartition antéropostérieure sur la résultante des forces de freinage. *Science & Sports*, 18(3), 141–149. [https://doi.org/10.1016/S0765-1597\(03\)00076-5](https://doi.org/10.1016/S0765-1597(03)00076-5)
6. de Vette, V. G., Veeger, D. (H. E. J.), & van Dijk, M. P. (2022). Using Wearable Sensors to Estimate Mechanical Power Output in Cyclical Sports Other than Cycling—A Review. *Sensors*, 23(1), 50. <https://doi.org/10.3390/s23010050>
7. Goosey, V. L., Campbell, I. G., & Fowler, N. E. (2000). Effect of push frequency on the economy of wheelchair racers: *Medicine & Science in Sports & Exercise*, 174. <https://doi.org/10.1097/00005768-200001000-00026>
8. Ju, Y.-Y., Chu, W.-T., Shieh, W.-Y., & Cheng, H.-Y. K. (2021). Sensors for Wheelchair Tennis: Measuring Trunk and Shoulder Biomechanics and Upper Extremity Vibration during Backhand Stroke. *Sensors*, 21(19), 6576. <https://doi.org/10.3390/s21196576>
9. Kingma, I., Toussaint, H. M., Commissaris, D. A. C. M., Hoozemans, M. J. M., & Ober, M. J. (1995). Optimizing the determination of the body center of mass. *Journal of Biomechanics*, 28(9), 1137–1142. [https://doi.org/10.1016/0021-9290\(94\)00164-Y](https://doi.org/10.1016/0021-9290(94)00164-Y)
10. Mason, B., Lenton, J., Leicht, C., & Goosey-Tolfrey, V. (2014). A physiological and biomechanical comparison of over-ground, treadmill and ergometer wheelchair

- propulsion. *Journal of Sports Sciences*, 32(1), 78–91. <https://doi.org/10.1080/02640414.2013.807350>
11. Ott, J., & Pearlman, J. (2021). Scoping review of the rolling resistance testing methods and factors that impact manual wheelchairs. *Journal of Rehabilitation and Assistive Technologies Engineering*, 8, 205566832098030. <https://doi.org/10.1177/2055668320980300>
 12. R Core Team. (2023). R: A Language and Environment for Statistical Computing. *R Foundation for Statistical Computing*, 2023. <https://www.R-project.org/>
 13. Rietveld, T., Mason, B. S., Goosey-Tolfrey, V. L., van der Woude, L. H. V., de Groot, S., & Vegter, R. J. K. (2021). Inertial measurement units to estimate drag forces and power output during standardised wheelchair tennis coast-down and sprint tests. *Sports Biomechanics*, 1–19. <https://doi.org/10.1080/14763141.2021.1902555>
 14. Sauret, C., Vaslin, P., Lavaste, F., de Saint Remy, N., & Cid, M. (2013). Effects of user's actions on rolling resistance and wheelchair stability during handrim wheelchair propulsion in the field. *Medical Engineering and Physics*, 35(3), 289–297. <https://doi.org/10.1016/j.medengphy.2012.05.001>
 15. van der Slikke, R. M. A., Berger, M. A. M., Bregman, D. J. J., Lagerberg, A. H., & Veeger, H. E. J. (2015). Opportunities for measuring wheelchair kinematics in match settings; reliability of a three inertial sensor configuration. *Journal of Biomechanics*, 48(12), 3398–3405. <https://doi.org/10.1016/j.jbiomech.2015.06.001>
 16. van der Woude, L. H. V., Groot, G. D., Hollander, A. P., Schenau, G. J. V. I., & Rozendal, R. H. (1986). Wheelchair ergonomics and physiological testing of prototypes. *Ergonomics*, 29(12), 1561–1573. <https://doi.org/10.1080/00140138608967269>
 17. van Dijk, M. P., Hoozemans, M. J. M., Berger, M. A. M., & Veeger, D. H. E. J. (2023). *From Theory to Practice: Monitoring Mechanical Power Output During Wheelchair Field and Court Sports Using Inertial Measurement Units* [Preprint]. *Journal of Biomechanics*. <https://doi.org/10.2139/ssrn.4414741>
 18. van Dijk, M. P., Kok, M., Berger, M. A. M., Hoozemans, M. J. M., & Veeger, D. H. E. J. (2021). Machine Learning to Improve Orientation Estimation in Sports Situations Challenging for Inertial Sensor Use. *Frontiers in Sports and Active Living*, 3, 670263. <https://doi.org/10.3389/fspor.2021.670263>
 19. van Dijk, M. P., van der Slikke, R.M.A., Berger, M.A.M., Hoozemans, M.J.M., & Veeger, H. E. J. (2021). Look mummy, no hands! The effect of trunk motion on forward wheelchair propulsion. *39th ISBS Conference*, 4.
 20. van Ingen-Schenau, G. J., & Cavanagh, P. R. (1990). Power equations in endurance sports. *Journal of Biomechanics*, 23(9), 865–881.
 21. Veeger, H.E.J. & van der Woude, L.H.V. (1989). The effect of rear wheel camber in manual wheelchair. *The Journal of Rehabilitation Research and Development*, 26(2), 37–46.

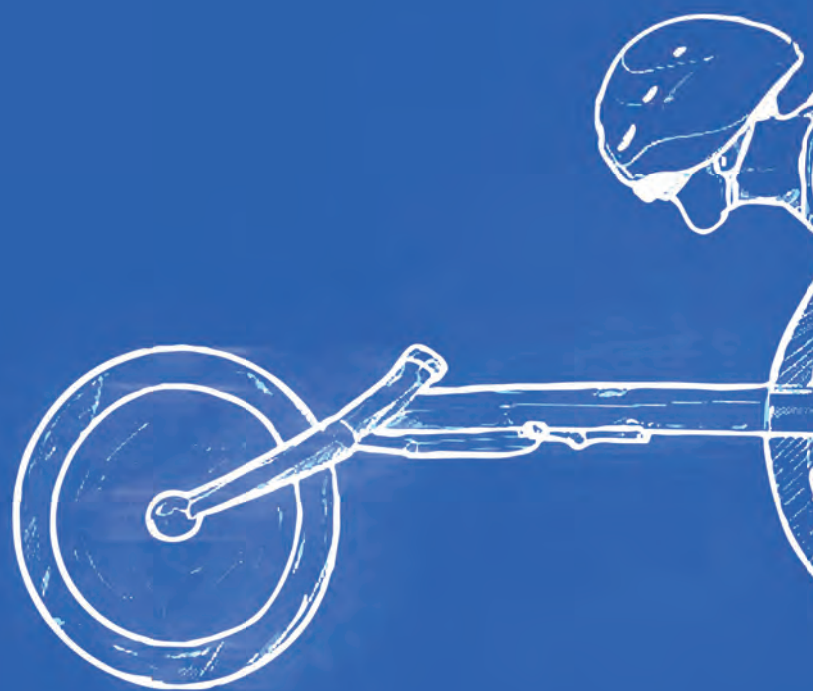
Appendix A

To assess to what extent the differences between F_{drag} and F_{IR} depend on the relative difference between front- and rear-wheel rolling resistance coefficients, the treadmill session and drag tests were repeated two more times with different tire pressures (immediately after the first set of drag tests). Based on these data, differences between F_{drag} and F_{IR} were determined for the two additional situations in which the tyre pressure of the rear wheel tyres was lowered with 33% (to 3.5 bar) and 76% (to 1.75 bar), respectively. Table 5.3 shows that when the relative difference between front- and rear-wheel rolling resistance coefficients becomes smaller, F_{drag} and F_{IR} become more similar.

Table 5.3.

Mean (S.D.) drag force and mean difference (MD) for the three conditions and for different tyre pressures of the rear wheels are presented. The corresponding rolling resistance coefficients (i.e., c) of the rear and castor (or front) wheels is given. Due to a tyre change after the 9th participant, the first value for c_{rear} corresponds to the participant 1-9, the second value to participant 10-25.

	c_{front}	c_{rear}	F_{drag} (N)	MD (%)	MD (%)	MD (%)
Trunk motion				No	Moderate	Full
Normal	.0147	.0104 – .0089	8.4 (1.3)	0.6 (1.6)	-2.3 (2.0)	-3.2 (2.3)
Tire pressure -33%	.0147	.0112 – .0100	9.0 (1.4)	0.5 (1.1)	-0.9 (4.7)	-2.2 (2.4)
Tire pressure -76 %	.0147	.0139 – .0123	10.6 (1.6)	0.3 (0.4)	-0.6 (0.6)	-0.9 (0.8)



POWER FOR ALL
**MEETING THE DEMANDS OF
DIFFERENT WHEELCHAIR USER
POPULATIONS**





Abstract

Accurate assessment of rolling resistance is important for wheelchair propulsion analyses. However, the commonly used drag and deceleration tests are reported to underestimate rolling resistance up to 6% due to the (neglected) influence of trunk motion. The first aim of this study was to investigate the accuracy of using trunk and wheelchair kinematics to predict the intracyclical load distribution, and more particularly front wheel loading, during hand-rim wheelchair propulsion. Secondly, the study compared the accuracy of rolling resistance determined from the predicted load distribution with the accuracy of drag test-based rolling resistance. Twenty-five able-bodied participants performed hand-rim wheelchair propulsion on a large motor-driven treadmill. During the treadmill sessions, front wheel load was assessed with load pins to determine the load distribution between the front and rear wheels. Accordingly, a machine learning model was trained to predict front wheel load from kinematic data. Based on two inertial sensors (attached to the trunk and wheelchair) and the machine learning model, front wheel load was predicted with a mean absolute error (MAE) of 3.8% (or 1.8 kg). Rolling resistance determined from the predicted load distribution (MAE: 0.9%, mean error: 0.1%) was more accurate than drag test-based rolling resistance (MAE: 2.5%, mean error: -1.3%).

Introduction

Rolling resistance is an important resistive force in hand-rim wheelchair propulsion and can be very different between wheelchairs, tyres and surface types [1–4]. Accurately assessing the rolling resistance is crucial to estimate power output [1, 5] or to optimize wheelchair settings [2]. For this assessment, a drag or deceleration test is commonly used. During a drag test, the force required to pull a wheelchair across a surface is measured. Likewise, during a deceleration test, the wheelchair is accelerated to an initial velocity (at which air resistance can still be assumed negligible) and subsequently passively decelerated. When the deceleration is known and the wheelchair user does not move, the rolling resistance can be determined from this deceleration and the total mass. However, recent studies [5, 6] report a difference between rolling resistance during propulsion and that obtained during these commonly-used tests.

The difference between rolling resistance during propulsion and that obtained during drag or deceleration tests can be explained by considering a four-wheeled wheelchair which is typically used for court sports or everyday use (neglecting the anti-tip wheels which only sporadically hit the ground) and a wheelchair user that actively moves the upper body during propulsion. As, in such wheelchairs, the front wheels are smaller than the rear wheels, the front wheels have a higher rolling resistance. Due to this difference, inclining the (relatively heavy) trunk - which will shift the mass forward and accelerates the centre of mass vertically - causes the rolling resistance to vary within a push cycle. In addition to upper body motion, a backward ‘tipping over’ moment – that mainly occurs during wheelchair acceleration [7] – may also influence the load distribution between the rear and front wheels. Since intra-cyclical changes in load distribution are neglected by drag and deceleration tests, rolling resistance estimates based on these tests have been found to deviate up to 6% from the actual rolling resistance [6, 8] (see Fig. 1). *Note that the extent of upper body movement during wheelchair propulsion varies greatly among wheelchair users due to differences in trunk impairment [9] or environmental demands. Therefore, the above-mentioned deviation is only present and relevant for users and athletes that actively move their trunk during wheelchair propulsion.*

As previous studies reported that a 30% difference in tyre pressure in wheelchair tennis resulted in a 3.3% difference in rolling resistance [3], and a power difference (determined from rolling resistance times velocity) up to 7% between different wheel configurations [10], a deviation of 6% is too much to accurately calculate power output or optimal wheelchair settings. Therefore, more accurate rolling resistance estimates are needed.

To estimate rolling resistance accurately, a continuous determination of load distribution is required. This might be done by measuring the vertical force on the (front and/or rear) wheelchair wheels. However, implementing force sensors is complex, expensive, and not sufficiently robust for wheelchair (sports) practice. An alternative is to measure kinematics and derive the instantaneous load distribution from that. Whereas marker-based motion capturing has previously been used for this [5, 11], inertial sensors (IMUs) are preferred as they are less invasive, inexpensive, and readily used in wheelchair (sports) practice. Upper body motions can be approximated by IMU-based trunk motion (ignoring arm movements) and wheelchair kinematics can be obtained from a wheel-mounted IMU [12–14]. However, a model that predicts load distribution from (IMU-based) trunk and wheelchair kinematics is yet to be developed.

The first aim of this study was to investigate the accuracy of using trunk and wheelchair kinematics to predict the instantaneous load distribution, and more particularly front wheel loading, during straight-line hand-rim wheelchair propulsion in a four-wheeled wheelchair. With this prediction, a more accurate (and instantaneous) estimate of rolling resistance may be

obtained. Therefore, the second aim of this study was to compare the accuracy of rolling resistance determined from the predicted load distribution with the accuracy of drag test-based rolling resistance. In addition, the robustness of this method was investigated for variations in wheelchair and subject characteristics and trunk use. If the method appears to be accurate and robust, it can be applied in each wheelchair (sport) situation to obtain accurate rolling resistance estimates and, eventually, e.g. power output.

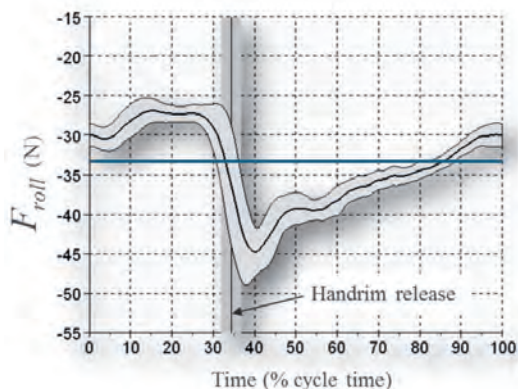


Figure 6.1. Image of ‘actual’ rolling resistance (black line) and rolling resistance based on a static drag test (blue line). This image is adapted from the image reported by Sauret et al. [1]. Note that – in this example – the drag test-based rolling resistance is similar to the average ‘actual’ rolling resistance. However, depending on the upper body pose during deceleration or drag test, this value may be higher or lower.

Materials and methods

Data collection protocol

Experimental data from a previous study on wheelchair propulsion were used in this study [6]. Twenty-five able-bodied participants (19 females, mean (S.D.) age 30 (11) years, mean body mass 68 (11) kg, body height 170 (7) cm) with no wheelchair experience were included in the study. Participants propelled the hand-rims of a wheelchair on a large (3.0 x 5.0 m) motor-driven treadmill, while their kinematics were measured with three IMUs (attached to the participant’s sternum, the wheelchair’s frame, and right wheel axle) and the front-wheel load was measured using custom-made load pins (in both front wheel axes). Before the treadmill sessions, participants received a 10-minute overground wheelchair training to get familiar with the wheelchair and a 10-minute training on the treadmill (see Fig. 6.2). In addition, drag tests were performed on the treadmill to obtain rolling resistance coefficients of the (small) front and (large) rear wheels.

To simulate different wheelchair characteristics and pushing styles, the treadmill session was repeated six times with different tire pressures (1.75 bar, 3.5 bar, 5.25 bar) [16] or added mass (0 kg, 5 kg, 15 kg) [17], see Fig. 6.2, and with three pushing styles (no trunk motion at 1.2 m/s [style 1], unrestricted trunk motion at 1.2 m/s [style 2], unrestricted trunk motion at 1.7 m/s [style 3] [18, 19]). By following a metronome (25 beats/min in pushing style 2 and 40 beats/min in pushing styles 1 and 3), participants were encouraged to make effective pushes, which – in style 2 and 3 - were accompanied by forward-backward trunk motion. Each treadmill session consisted of 30s familiarization to the new situation, after which participants propelled 60s in each pushing style. In this way, a dataset was composed of eighteen (three pushing styles and six treadmill sessions) 60s-time trials per participant. The order of the treadmill sessions differed per participant.

Drag tests were performed at 1.7 m/s, while the participants were instructed to sit as still as possible for a period of 30s in six conditions to evoke varying load distributions. The drag test conditions consisted of sitting with an upright trunk and sitting bent forward while no mass was added, while 10 kg was added at the footrests and while 10 kg was added on the upper legs. The drag test-based rolling resistance forces, measured by an S-beam load cell, were obtained by averaging the final ten seconds of each drag test condition. Subsequently, the rear (r) and front (f) wheel rolling resistance coefficients, c_r and c_f , were numerically determined by solving Eq. 6.2 based on the average drag force (which equals F_{IR} in static situations) and average load pin force ($F_{N,f}$) of the series of drag tests which is similar to previous studies [20, 21]. Accordingly, c_f and c_r were used to estimate the gold standard rolling resistance during all treadmill sessions. $F_{N,tot}$ was assumed equal to total mass times 9.81 m/s^2 .

This study was approved by the ethical committee of Delft University of Technology (Nr. 1530) and written informed consent was obtained from all participants prior to data collection.

$$F_{N,tot} = F_{N,f} + F_{N,r} \tag{6.1}$$

$$F_{IR} = c_f * F_{N,f} + c_r * F_{N,r} \tag{6.2}$$

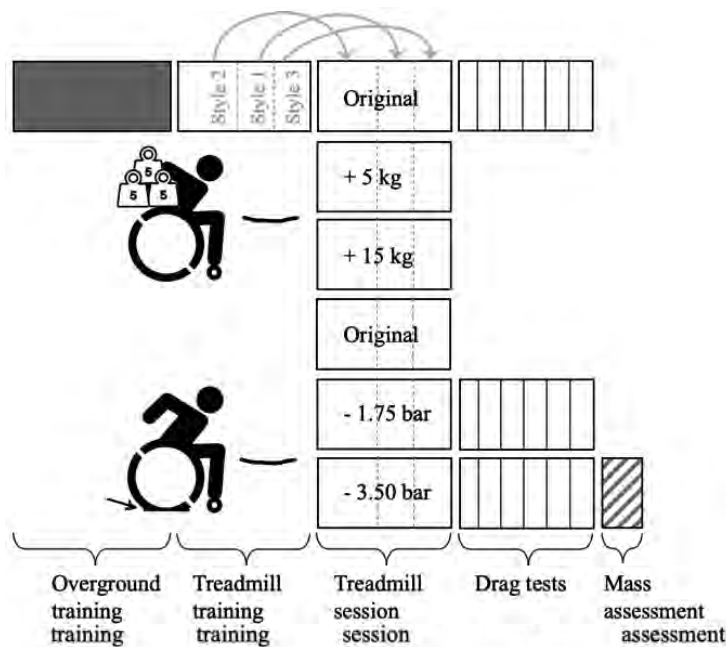


Figure 6.2. Schematic overview of measurements during different sessions. The 'original' treadmill session refers to the condition with no added mass (0 kg) and fully inflated rear wheel tyres (5.25 bar). Mass (i.e., total mass of participant and wheelchair) was assessed on a 1.0 x 1.0 m force plate.

Instrumentation

All treadmill measurements took place on a large (3.0 x 5.0 m) motor-driven treadmill (Bonte, Zwolle, the Netherlands) at the Vrije Universiteit Amsterdam. A large treadmill was used to make participants feel safe to move forwards, backwards and sideways on the belt. An S-beam load cell (Revere Transducers, Lisse, the Netherlands) was used to measure the horizontal (drag) forces during the drag tests. An RGK Chrome all-courts wheelchair (13.5 kg, camber angle of 13°) was used for the measurements. Load pins (Batarow Sensorik, Germany) were integrated in the

front wheel axes of the wheelchair to measure the vertical load on the front wheels. Three IMUs (NGIMU, X-io Technologies, Colorado Springs, CO, United States) were used to collect 3D inertial sensor data with a sample frequency of 100 Hz. In addition, the NGIMU analogue input channels of the frame-mounted sensor were connected to the load pins to act as power source and data logger. The load cell was calibrated with known masses at the start of each measurement day. The load pins were calibrated before each measurement session by positioning the front wheels on a 1.0 x 1.0 m custom-made strain gauge force plate (while the rear wheels were positioned on a dummy plate at the same height) [22].

Predicting load distribution between front- and rear wheels

Preprocessing

After data collection, the force plate calibration data were used to convert voltage of the two individual load pins to vertical force. Subsequently, the summed vertical force on the front wheels was normalized to percentage of the total vertical force on all four wheels (i.e., total mass times gravitational force). As vertical accelerations of the upper body were previously shown to have no effect on rolling resistance [15], vertical accelerations were assumed to be zero.

In addition, predictor features that represented different aspects of trunk and wheelchair motion were generated based on IMU data (see Table 6.1). Subsequently, all data were 2nd order low-pass filtered with a cut-off frequency of 3 Hz. This cut-off frequency was chosen based on the assumption that load is influenced mainly by trunk motion, which has a maximal frequency of around 2 Hz. The last 60s in each pushing style were analyzed.

Table 6.1.

Overview of the abbreviations and calculation method of all predictor features and outcome feature that were used in the predictive model.

	<i>Predictor feature</i>	<i>Determined by</i>
v_{wc}	Wheelchair velocity in m/s	(Gyroscope signal of IMU around wheel axis · rear wheel diameter · π) / 360 [13] ¹
a_{wc}	Wheelchair acceleration in m/s ²	Derivative of v_{wc}
φ_{tr}	Trunk inclination angle in rad	Based on extended Madgwick filter [8] with β -value being 0.0015 (if wheelchair acceleration < 0.1 m/s ² for at least 5 consecutive samples) or 0.9635 (otherwise)
$\dot{\varphi}_{tr}$	Angular velocity of trunk (around sagittal axis) in rad/s	Gyroscope signal (around sagittal axis) of trunk-mounted IMU
$\ddot{\varphi}_{tr}$	Angular acceleration of trunk (around sagittal axis) in rad/s ²	Derivative of $\dot{\varphi}_{tr}$
$a_{tr,\perp}$	Trunk acceleration perpendicular to the frontal plane of the trunk in m/s ²	Acceleration signal (directed perpendicular to frontal plane) of trunk-mounted IMU
$a_{tr,\parallel}$	Trunk caudal-cranial acceleration in m/s ²	Acceleration signal (in caudal-cranial direction) of trunk-mounted IMU
$ a_{tr} $	Magnitude of trunk acceleration vector in m/s ²	Euclidean norm of the three-dimensional acceleration signal of the trunk-mounted IMU subtracted by 9.81
	<i>Outcome feature</i>	<i>Determined by</i>
$\hat{F}_{N,f}$	normalized relative front wheel-load in %	Force data from the front wheels' load pins, calculated as $F_{N,f} / F_{N,tot} * 100\%$

¹In case of curves and turns, the linear velocity obtained from the wheel should be corrected for turning using the algorithm described by van der Slikke et al. [13]

To generate the final dataset, all treadmill session data were sequenced into one large dataset consisting of the ‘outcome’ feature (relative front wheel load, or $\hat{F}_{N,f}$), ‘predictor’ features (v_{wc} , a_{wc} , φ_{tr} , $\dot{\varphi}_{tr}$, $\ddot{\varphi}_{tr}$, $a_{tr,\perp}$, $a_{tr,\parallel}$, $|a_{tr}|$), and ‘descriptive’ variables (participant number, pushing style and session-type) (see Table 1). The outcome and predictor features were standardized to a z-score. Since the best predictive model could contain linear or non-linear relations, both linear methods as well as (non-linear) machine learning methods were examined for predicting the relative front wheel load from the predictor features.

Training, validation and test set

From the full dataset, three random participants and two test configurations (+5 kg and -1.75 bar, see Fig. 6.2) were removed to act as ‘test’ set for model evaluation in a later stage. The reduced dataset based on 22 subjects and four configurations was split randomly - while each treadmill session was kept in the same set - a training set (80% or 66 treadmill sessions) and a validation set (20% or 17 treadmill sessions). The training set was used to determine the best set of predictive features to predict the relative front wheel load ($\hat{F}_{N,f}$), and to ‘train’ all models. The validation set was used to select the best model and the best model hyperparameters. Finally, the test set was used once the final model was obtained to determine how well the model performs on unseen data (i.e., data that was not previously used to train the model or to make decisions). This was done by comparing the predicted relative front wheel load (and resulting rolling resistance) with the measured relative front wheel load (and resulting rolling resistance). The test set was assumed to be representative for any new dataset.

Feature, model and hyperparameter selection

As the inclusion of outcome-unrelated features may result in overfitting, a feature selection was performed to select the best feature combination. In this study, an exhaustive feature selection method based on a random forest regressor and 7-fold cross validation (leaving 1/7th of the subsets out during each iteration) was used. A random forest regressor was used as this model is fast and robust to overfitting. According to the results of the exhausting feature selection, the best trade-off between maximal accuracy (more features) and chance of overfitting (less features) was found with three features: linear wheelchair velocity, linear wheelchair acceleration and linear acceleration perpendicular to the trunk (i.e., v_{wc} , a_{wc} , and $a_{tr,\perp}$, see Table 6.1).

With the above-mentioned three-feature combination, five different model types were trained on the training set: a simple linear regression model (LR), a random forest regressor (RFR), a multiple layer perceptron (MLP), a long short-term memory (LSTM) and a gate recurrent unit (GRU) model. The LR model was used to investigate whether a linear relation may be used to solve the relation between trunk and wheelchair motion, and front wheel-load. The RFR has been known as a robust and fast algorithm and may therefore be suitable to predict front wheel-load. In addition, three (deep) neural networks have been tested. The long short-term memory (LSTM) and gate recurrent unit (GRU) models both take previous time samples into account, which might yield good results as well. MLP, LSTM and GRU have all been proved useful to predict ground reaction forces from IMU data in walking and running [23]–[28]. After training, the most predictive model was selected by applying the five models to the validation set data and determining the mean error (ME; i.e. the mean difference between the observed and predicted relative front wheel load), mean absolute error (MAE), and root-mean-squared error (RMSE). The model with the overall best performance was assumed the best model type. To maximize performance of the final model, hyperparameters were tuned based on the validation set. Lastly,

the best model type with selected hyperparameters was trained again based on all data from the training set. The predictions from the final model were evaluated hereafter. Based on the final model, the relative front wheel load was predicted for all test set data.

Evaluating predicted load distribution

1 – How well does the final model predict relative front wheel load?

To determine the accuracy of the model predictions, the relative front wheel load was predicted for all test set data and compared with the measured relative front wheel load. Differences between the two values were expressed in ME, MAE and RMSE. To assess whether the model was prone to overfitting, a second version of the final model was obtained based on the training dataset and a Gaussian noise layer that was added to the original model architecture. A large difference between the results of both models indicates that the model's output is influenced by white noise on the input data, and thus overfits the data.

2 - Does adding a trunk-mounted IMU and a prediction model result in a more accurate rolling resistance estimate than drag test-based rolling resistance estimates?

To convert proportions (%) to absolute normal forces, the proportions were multiplied by $F_{N,tot}$, and subsequently, rolling resistance was calculated according to Eq. 6.1 and 6.2. To evaluate whether the model improves the rolling resistance estimates, the predicted rolling resistance was compared to the 'gold standard' load pin-based rolling resistance. Secondly, the predicted rolling resistance was compared to the drag test-based rolling resistance. Therefore, the drag test-based rolling resistance was determined based on the rolling resistance coefficients that were determined previously, and the load distribution corresponding to the drag tests in upright position.

3 - Is the model robust for different wheelchair characteristics and pushing styles?

To evaluate model robustness, the final prediction model was used to predict load distribution in situations that were not used to train the model with *only* the participants that were not used to train the model (i.e., unseen conditions and unseen subjects, so 6 treadmill sessions). Subsequently, these load distributions were used to determine rolling resistance force. ME, MAE and RMSE were reported for different propulsion styles and for different wheelchair configurations (averaged over three 'unseen' participants).

Results

In the present study, 143 treadmill sessions were included of which 83 were used to train and select the final machine learning model (i.e., training and validation set) and 60 were used to evaluate the results (i.e., the test set). Seven sessions were left out due to incompleteness (caused by empty batteries or connection errors). As expected, the largest variation (and largest value) in front wheel load was found for the 3rd pushing style that was characterized by the largest trunk motion (see Table 6.2 and Fig. 6.3). The average front wheel load differed considerably between participants (see 'Range' in Table 6.2). The total mass (participant + wheelchair) in the test set was on average 76.9 ± 9.1 kg. Overall, the test set seems a decent reflection of the training dataset.

1 – How well does the final model predict relative front wheel load?

Exhaustive feature selection resulted in wheelchair velocity, wheelchair acceleration and trunk acceleration (perpendicular to the frontal plane of the trunk) to be the most predictive features for relative front wheel loading. With these features, five different model types were trained. Overall, LSTM turned out to yield the most accurate predictions (see Table 6.3). The hyperparameter combination that resulted in the lowest MAE value consisted of one hidden layer, 50 neurons, learning rate of 0.01, batch size of 128, drop out-rate of 0.1, and 20 time steps. This final model showed an MAE of $3.8 \pm 1.8\%$ relative front wheel load corresponding with about ($68 \text{ kg} * 3.8 =$) $2.6 \pm 1.2 \text{ kg}$ on average compared to the actual measured load on the front wheels, and an RMSE of $4.4 \pm 1.6\%$ (see Table 6.3).

The final model and the second version of the final model in which a Gaussian noise layer was added resulted in comparable accuracies (see right side of Table 6.3), indicating that the model does not overfit the data.

Table 6.2.

Mean (variation) and range of relative front wheel loads (expressed as percentage (%) of the total load) for all participants per pushing style (characterized by the amount of trunk motion, i.e., TM) in the training & validation and test set. The range consists of the average front wheel load of the participant with the lowest load and the average front wheel load of the participant with the highest load. The variation is determined by the average of the standard deviations per person. The values are based on 60s of propulsion per pushing style per person.

	Style 1: No trunk motion	Style 2: Moderate trunk motion	Style 3: Full trunk motion
Mean (training & validation set) (%)	20.0 (4.9)	24.9 (6.9)	27.1 (9.2)
Range (training & validation set) (%)	12.8 – 26.3	14.0 – 32.1	17.5 – 35.4
Mean (test set) (%)	20.7 (4.4)	24.0 (6.4)	24.9 (7.6)
Range (test set) (%)	15.2 – 26.2	16.3 – 31.5	17.0 – 31.2

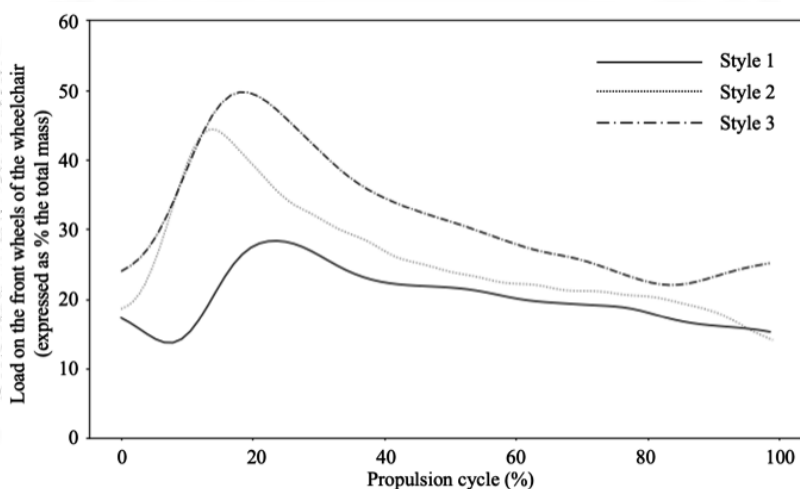


Figure 6.3. Typical example of the relative load on the front wheels of the wheelchair (expressed as % the total mass of the wheelchair and user) of a representative subject in the original wheelchair condition during one propulsion cycle (0% representing the start of the push) for propulsion style 1 (no trunk motion at 1.2 m/s), style 2 (normal trunk motion at 1.2 m/s), and style 3 (normal trunk motion at 1.7 m/s).

Table 6.3.

The results in terms of mean error (ME), mean absolute error (MAE), and root-mean-squared error (RMSE) of the five model types that were trained to predict the front wheel load as a percentage of the total mass of wheelchair and user (i.e., RFWL). Models were trained on the training set (with default hyperparameters) and evaluated on the validation set for which the results are shown.

	Evaluated on validation set					Evaluated on test set		
	LR	RFR	MLP	LSTM	GRU	LSTM (final)	LSTM (final) + noise	
ME (RFWL)	1.9	1.8	1.6	1.0	1.2	0.5	0.5	
MAE (RFWL)	4.4	3.8	3.4	2.7	2.9	3.8	3.8	
RMSE (RFWL)	5.9	5.1	4.6	3.5	3.6	4.4	4.4	
Comp. time E ⁻⁰³ (s)	0.0	0.1	0.4	1.8	1.8	-	-	

2 - Does adding a trunk-mounted IMU and a prediction model result in a more accurate rolling resistance estimate than drag test-based rolling resistance estimates?

As the third pushing style (full trunk motion) showed larger variations in normal force and has previously been shown to deviate more from drag test-based rolling resistance estimates, data are reported for the third pushing style in Table 6.4. The rolling resistance estimates based on the final (LSTM) model had a similar shape as those based on the gold standard load pin force (Fig. 6.4). Whereas drag test-based rolling resistance tend to be underestimated (ME of -1.3), with application of the prediction model these underestimations were absent (ME of 0.1). A similar trend was seen for MAE and RMSE (see Table 6.4).

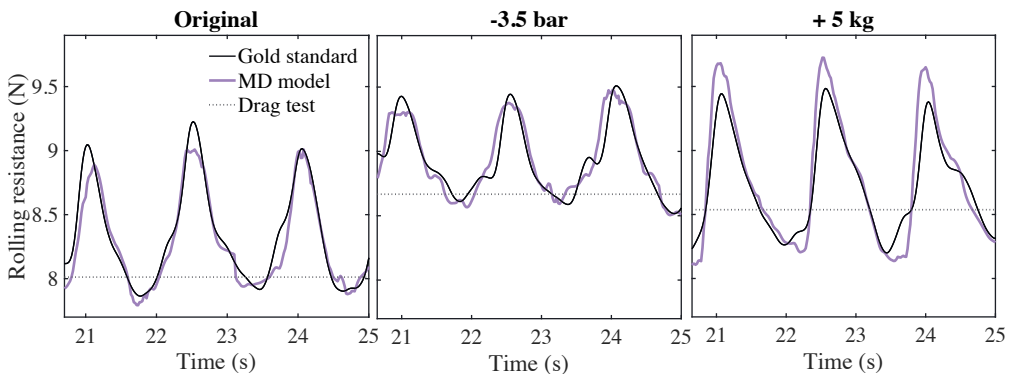


Figure 6.4a-c. Gold standard rolling resistance (black line), load distribution model-based rolling resistance (purple line) and drag test-based rolling resistance (dotted line) for the 'original' condition, condition with -3.5 bar tire pressure and condition with + 5 kg added mass.

3 - Is the model robust for different wheelchair characteristics and pushing styles?

Looking at different wheelchair characteristics and pushing styles, again, the deviations with the gold standard are considerably smaller for the prediction model compared to the drag test-based rolling resistance (see Fig. 6.4 and Table 6.5). The errors are similar for the different conditions. Therefore, the model seems to be robust for different unseen characteristics.

Table 6.4.

Comparisons between the accuracies of the load distribution model-based rolling resistance ($F_{\text{roll,LD model}}$) and the drag test-based rolling resistance ($F_{\text{roll,drag}}$) based on the ‘original’ condition-data from the test set (pushing style: full trunk motion). Accuracies were determined by comparison with the ‘gold standard’ load pin-based rolling resistance ($F_{\text{roll,gold standard}}$) and expressed in mean error (ME), mean absolute error (MAE) and root-mean-squared error (RMSE). The actual gold standard rolling resistance values were reported as well. The measures are given for each subject in the test set.

	$F_{\text{roll,gold standard}}$ (N)	$F_{\text{roll,LD model}} - F_{\text{roll,gold standard}}$ (%)			$F_{\text{roll,drag}} - F_{\text{roll,gold standard}}$ (%)		
		ME	MAE	RMSE	ME	MAE	RMSE
Subject 1	8.6 (1.0)	0.5	0.7	0.9	-1.1	1.4	1.8
Subject 2	9.9 (1.0)	-0.4	1.0	1.3	-0.4	3.3	4.0
Subject 3	9.4 (0.9)	0.3	1.0	1.4	-2.3	2.8	3.9
Mean	9.3	0.1	0.9**	1.2*	-1.3	2.5	3.2

* $p < 0.05$, ** $p < 0.01$

Table 6.5.

Comparisons between the accuracies of the load distribution model-based rolling resistance ($F_{\text{roll,LD model}}$) and the drag test-based rolling resistance ($F_{\text{roll,drag}}$) based on the ‘-3.5 bar’ and ‘+5 kg’ condition-data from the test set (for each pushing style). Accuracies were determined by comparison with the ‘gold standard’ load pin-based rolling resistance ($F_{\text{roll,gold standard}}$) and expressed in mean error (ME), mean absolute error (MAE) and root-mean-squared error (RMSE). The actual gold standard rolling resistance values were reported as well.

Pushing style	$F_{\text{roll,gold standard}}$ (N)	$F_{\text{roll,LD model}} - F_{\text{roll,gold standard}}$ (%)			$F_{\text{roll,drag}} - F_{\text{roll,gold standard}}$ (%)		
		ME	MAE	RMSE	ME	MAE	RMSE
-3.5 bar condition							
Style 1	8.5 (0.7)	-0.5	0.8	1.0	0.4	1.5	1.9
Style 2	8.7 (0.8)	-0.4	1.0	1.3	-1.1	2.3	2.8
Style 3	8.7 (0.8)	-0.1	1.0	1.3	-1.2	2.7	3.4
+5 kg condition							
Style 1	8.4 (0.5)	0.2	1.1	1.3	1.6	2.7	3.3
Style 2	8.5 (0.5)	-0.1	1.5	2.0	-0.2	3.2	3.8
Style 3	8.6 (0.6)	0.2	1.4	1.8	-0.9	3.7	4.5

Discussion

The aim of this study was to investigate the accuracy of using trunk and wheelchair kinematics to predict the instantaneous load distribution, and more particularly front wheel loading, during hand-rim wheelchair propulsion, such that – eventually – rolling resistance estimates could be improved. Based on two inertial sensors (one at the trunk and one at the wheelchair wheel), and a machine learning model (which is publicly accessible – see Appendix A), the front wheel load could be predicted up to 2.6% (or 1.8 kg) accuracy (MAE). When this front wheel load is subsequently used to estimate rolling resistance, rolling resistance estimates have an accuracy of about 0.9% (MAE) and a mean error of 0.1%, which was significantly lower than the rolling resistance estimates without the model. Moreover, the robustness of the model was tested for different wheelchair characteristics and pushing styles. As the accuracy did not differ between

different wheelchair characteristics and pushing styles (i.e., MAE ranging from 0.8 to 1.5 and ME ranging from -0.5 to 0.2), we assumed the model to be robust for different circumstances.

The average front wheel loads in the present study ($24.9 \pm 6.9\%$) were lower than the average front wheel loads of about 40% reported by Sauret et al. [8] and Brubaker [29]. This may have to do with the different types of wheelchairs used. In wheelchairs designed for everyday use, stability of the wheelchair (not falling over) is often regarded more important than the rolling resistance of the wheelchair (by limiting the weight on the front wheels), such that the seat (and thus the centre of mass) is put more forward deliberately. Hence, sports wheelchairs typically exhibit lower rolling resistances in comparison to everyday use wheelchairs. Besides these differences, the front wheel load development over a push cycle in the present study is similar to those reported by Sauret et al. [8]. Overall, our results are well in line with previously reported values and patterns of front wheel load.

Based on the results of the present study, the front wheel load can continuously be determined during wheelchair propulsion. In this way, the effects of upper body motion and wheelchair accelerations on rolling resistance can be incorporated such that accurate rolling resistance estimates can be obtained. As the presented model makes the rolling resistance values sensitive to different circumstances (i.e., large vs small upper body motions and high vs low accelerations), the estimates are more accurate and more individualized than rolling resistance values determined based on drag or deceleration tests.

An important implication of this higher accuracy and more individualized rolling resistance is that comparisons between and within wheelchair athletes are much fairer. Traditional drag test-based estimates lead to unfair comparisons, especially when trunk motion varies between athletes. For instance, during a sprint, the initial pushes involve higher rolling resistance due to acceleration and larger trunk inclination, contrasting with periods of constant velocity with less trunk inclination. Ignoring these variations (as is done during deceleration or drag tests) results in inaccurate power comparisons within a wheelchair sports team. The present load distribution model offers more accurate estimates of rolling resistance and power, ensuring fairer comparisons between and within wheelchair users and athletes compared to traditional drag test-based methods.

For wheelchair (sports) practice, the presented method is ready to be applied. When trunk and wheelchair kinematics are obtained (e.g., using inertial sensors), and a set of deceleration tests is performed to obtain the rolling resistance coefficients, accurate estimates of rolling resistance can be determined. Subsequently, accurate rolling resistance estimates can be used to monitor mechanical power or to optimize wheelchair setup and/or tire pressure. However, it should be noted that the improved rolling resistance estimates with the prediction model comes with extra information that is required about trunk motion and a machine learning model that should be executed. As the error based on drag or deceleration tests only – without incorporating changes in load distribution – is on average 3% (see right side of Table 4), and differs from 1 to 6% (as reported in our previous study [6]) this may be accurate enough for some purposes such as for recreational wheelchair sports or everyday wheelchair use. Therefore, depending on the required accuracy one may choose to base the rolling resistance on drag- or deceleration tests only – instead of applying the load distribution model – and accept some inaccuracies.

Limitations

For this study, some limitations should be noted. First, wheelchairs with different front- to rear-wheel distances or different seat positions were not tested in the present study. However, as

front- to rear-wheel distances are assumed to differ <20 cm in general, and a similar front wheel load pattern was observed in the study of Sauret et al. (2013) with a 'general use' wheelchair, we assume the model is suitable for other wheelchair dimensions. Second, the participants that were tested in the present study had no disabilities. The model should ideally be tested with wheelchair users with different movement strategies or different physique (e.g., missing body parts) to assess whether the model is robust for movement strategies (e.g., non-symmetrical trunk motion) used by this group. Lastly, participants in this study had no wheelchair experience which may affect their propulsion technique. However, the estimation of load distribution is expected to be independent of propulsion technique as it reflects trunk motion and the resulting centre of mass displacement. Therefore, the experience level of participants will not influence the translatability of our model to experienced wheelchair users.

Conclusion

In hand-rim wheelchair propulsion, the estimation of the continuous intra-cyclic load distribution between front and rear wheels could be determined with an accuracy of 3.8% MAE (or 1.8 kg) based on two inertial sensors and a machine learning model. Rolling resistance determined from the predicted load distribution (MAE: 0.9%, mean error: 0.1%) was more accurate than the rolling resistance based on drag tests only (MAE: 2.5%, mean error: -1.3%). Since the model is based on a relatively large number of participants, a considerable variation in front wheel load between participants, and different wheelchair characteristics and pushing styles, the model is considered valid to estimate rolling resistance in a wide range of wheelchair (sports) situations and for a wide range of wheelchair users.

Acknowledgements

The authors gratefully acknowledge the department of Human Movement Sciences (VU Amsterdam) and their staff for making their laboratory, 'Loopzaal', and software available. The authors would also like to thank Vera de Vette, Thomas Keijsers and Jesper Brabander for their valuable contribution to this work.

Data availability statement

The raw data supporting the conclusions of this article are publicly available on [10.4121/bc9a8588-5e50-4dff-aa77-5114ff7626f7.v2](https://doi.org/10.4121/bc9a8588-5e50-4dff-aa77-5114ff7626f7.v2). The machine learning model, including instructions how to use it are available on [10.4121/14883927.v1](https://doi.org/10.4121/14883927.v1).

Funding

This work was supported by ZonMw under project number 546003002. This project, named WheelPower: wheelchair sports and data science push it to the limit is a cooperative effort between TU Delft, UMCG, THUAS, VU Amsterdam and is in cooperation with several sports federations collected under the umbrella of NOC*NSF.

Disclosure statement

The authors report no conflict of interest.

References

1. de Klerk R, Vegter RJK, Leving MT, De Groot S, Veeger DHEJ, Van Der Woude LHV (2020) Determining and Controlling External Power Output During Regular Handrim Wheelchair Propulsion. *J Vis Exp* 60492
2. Ott J, Pearlman J (2021) Scoping review of the rolling resistance testing methods and factors that impact manual wheelchairs. *J Rehabil Assist Technol Eng* 8:205566832098030
3. Rietveld T, Mason BS, Goosey-Tolfrey VL, van der Woude LHV, de Groot S, Vegter RJK (2021) Inertial measurement units to estimate drag forces and power output during standardised wheelchair tennis coast-down and sprint tests. *Sports Biomech* 1–19
4. van der Woude L, Geurts C, Winkelman H, Veeger H (2003) Measurement of wheelchair rolling resistance with a handle bar push technique. *J Med Eng Technol* 27:249–258
5. Van Dijk MP, Hoozemans MJM, Berger MAM, Veeger DHEJ (2024) From theory to practice: Monitoring mechanical power output during wheelchair field and court sports using inertial measurement units. *J Biomech* 112052
6. van Dijk MP, Hoozemans MJM, Berger MAM, Veeger DHEJ (2024) Trunk motion influences mechanical power estimates during wheelchair propulsion. *J Biomech* 163:111927
7. van Dijk MP, van der Slikke, R.M.A., Berger, M.A.M., Hoozemans, M.J.M., Veeger HEJ (2021) Look mummy, no hands! The effect of trunk motion on forward wheelchair propulsion. 39th ISBS Conf 4
8. Sauret C, Vaslin P, Lavaste F, de Saint Remy N, Cid M (2013) Effects of user's actions on rolling resistance and wheelchair stability during handrim wheelchair propulsion in the field. *Med Eng Phys* 35:289–297
9. Altmann VC, Hart AL, Vanlandewijck YC, Van Limbeek J, Van Hooff ML (2015) The impact of trunk impairment on performance of wheelchair activities with a focus on wheelchair court sports: a systematic review. *Sports Med - Open* 1:22
10. Mason BS, Lemstra M, Van Der Woude LHV, Vegter R, Goosey-Tolfrey VL (2015) Influence of wheel configuration on wheelchair basketball performance: Wheel stiffness, tyre type and tyre orientation. *Med Eng Phys* 37:392–399
11. Chénier F, Marquis E, Fleury-Rousseau M (2023) Tracking the whole-body centre of mass of humans seated in a wheelchair using motion capture. *J Biomech* 156:111675
12. van Dijk MP, Kok M, Berger MAM, Hoozemans MJM, Veeger DHEJ (2021) Machine Learning to Improve Orientation Estimation in Sports Situations Challenging for Inertial Sensor Use. *Front Sports Act Living* 3:670263
13. van Dijk MP, van der Slikke RMA, Rupf R, Hoozemans MJM, Berger MAM, Veeger DHEJ (2022) Obtaining wheelchair kinematics with one sensor only? The trade-off between number of inertial sensors and accuracy for measuring wheelchair mobility performance in sports. *J Biomech* 130:110879
14. van der Slikke RMA, Berger MAM, Bregman DJJ, Lagerberg AH, Veeger HEJ (2015) Opportunities for measuring wheelchair kinematics in match settings; reliability of a three inertial sensor configuration. *J Biomech* 48:3398–3405
16. de Groot S, Vegter RJK, Van Der Woude LHV (2013) Effect of wheelchair mass, tire type and tire pressure on physical strain and wheelchair propulsion technique. *Med Eng Phys* 35:1476–1482

17. van der Slikke RMA, de Witte AMH, Berger MAM, Bregman DJJ, Veeger DJHEJ (2018) Wheelchair Mobility Performance enhancement by changing wheelchair properties: What is the effect of grip, seat height, and mass? *Int J Sports Physiol Perform* 13:1050–1058
18. Marie JC, Morgan K, Stephens CL, Standeven J, Engsborg J (2014) Trunk and neck kinematics during overground manual wheelchair propulsion in persons with tetraplegia. *Disabil Rehabil Assist Technol* 9:213–218
19. Veeger D (H. EJ), van der Woude LHV, Rozendal RH (1989) Wheelchair propulsion technique at different speeds. *Scand J Rehabil Med* 21:197–203
20. Bascou J, Sauret C, Pillet H, Vaslin P, Thoreux P, Lavaste F (2013) A method for the field assessment of rolling resistance properties of manual wheelchairs. *Comput Methods Biomech Biomed Engin* 16:381–391
21. Sauret C, Bascou J, Rmy NDS, Pillet H, Vaslin P, Lavaste F (2012) Assessment of field rolling resistance of manual wheelchairs. *J Rehabil Res Dev* 49:63
22. Kingma I, Toussaint HM, Commissaris DACM, Hoozemans MJM, Ober MJ (1995) Optimizing the determination of the body center of mass. *J Biomech* 28:1137–1142
23. Alcantara RS, Edwards WB, Millet GY, Grabowski AM (2022) Predicting continuous ground reaction forces from accelerometers during uphill and downhill running: a recurrent neural network solution. *PeerJ* 10:e12752
24. Davidson P, Virekunnas H, Sharma D, Piché R, Cronin N (2019) Continuous Analysis of Running Mechanics by Means of an Integrated INS/GPS Device. *Sensors* 19:1480
25. Leporace G, Batista LA, Metsavaht L, Nadal J (2015) Residual analysis of ground reaction forces simulation during gait using neural networks with different configurations. In: 2015 37th Annu. Int. Conf. IEEE Eng. Med. Biol. Soc. EMBC. IEEE, Milan, pp 2812–2815
26. Leporace G, Batista LA, Nadal J (2018) Prediction of 3D ground reaction forces during gait based on accelerometer data. *Res Biomed Eng* 34:211–216
27. Pogson M, Verheul J, Robinson MA, Vanrenterghem J, Lisboa P (2020) A neural network method to predict task- and step-specific ground reaction force magnitudes from trunk accelerations during running activities. *Med Eng Phys* 78:82–89
28. Sharma D, Davidson P, Müller P, Piché R (2021) Indirect Estimation of Vertical Ground Reaction Force from a Body-Mounted INS/GPS Using Machine Learning. *Sensors* 21:1553
29. Brubaker CE (1986) Wheelchair prescription : an analysis of factors that affect mobility and performance. *J Rehabil Res Dev* 23:19–26

Appendix A: Instruction on how to apply the LD model on kinematic data

Step-by-step explanation on how to collect and pre-process IMU data, use the LD model to predict load distribution, and export the full dataset to a csv-file. The dataset that was used for the current study is publicly available via: [10.4121/bc9a8588-5e50-4dff-aa77-5114ff7626f7.v2](https://doi.org/10.4121/bc9a8588-5e50-4dff-aa77-5114ff7626f7.v2).

1. Download model from: [10.4121/14883927.v1](https://doi.org/10.4121/14883927.v1)
2. Collect kinematic data
 - of coast-down tests with different (known) load distributions
 - of the situation / actions of interest (if IMUs are used to collect the data: Attach one IMU to the wheelchair wheel axle, one IMU to the center of the wheelchair frame and one IMU around the chest against the sternum)
3. Determine from the data:
 - The rolling resistance coefficients per pair of wheels
 - The acceleration vector perpendicular to the trunk
 - The wheelchair velocity
 - The wheelchair acceleration
 - Time
4. Save the above-mentioned variables in the following order:
i.e., `df["samples","time","v_wc", "a_wc", "trunk_acc_3"]`
5. Run the code below in Python
6. Done



Abstract

This study examined associations between wheelchair sprint and anaerobic power (measured in the lab) and wheelchair mobility performance (measured in the field) among wheelchair tennis players. Additionally, construct validity was assessed for all tests. Nine amateur and nine elite wheelchair tennis players performed a Sprint and Wingate test on a wheelchair ergometer in the lab and a Sprint, Illinois and Spider test in the field, with inertial measurement units mounted on their wheelchairs. Associations were assessed using regression analyses, while construct validity was assessed with an independent t-test (elite vs. amateur). The strongest associations were observed between lab outcomes and field sprint power output ($R^2 > 90\%$), followed by peak linear velocity and test duration ($R^2 = 77-85\%$), while peak rotational velocity showed the lowest associations with lab outcomes ($R^2 = 69-80\%$). The elite group outperformed the amateur group on all test outcomes. Despite differences in lab- and field-testing methodologies (e.g., trunk influence, linear/rotational components, skill involvement), the strong associations indicate overlap in measured constructs. While field testing provides valuable insight in practical performance, lab testing allows a broad additional array of in-depth biomechanical and physiological analyses. Furthermore, all tests could effectively discriminate between elite and amateur wheelchair tennis players.

1 Introduction

Wheelchair tennis has been incorporated in the programs of all four Grand Slam tennis tournaments and the Paralympics Games. Wheelchair tennis distinguishes from able-bodied tennis, using a wheelchair and a second allowed bounce before contact. Wheelchair tennis demands linear velocities, accelerations and rotations of the wheelchair-user combination.¹ The anaerobic energy system is assumed to be crucial for this short-term work and wheelchair skills are required for high velocities and rotations.^{2,3} To gain insights into their performance, wheelchair tennis players and their coaches can monitor these characteristics through testing, either in a standardized laboratory or natural field environment.⁴⁻⁶

Lab testing offers researchers standardized conditions to collect detailed physiological, kinetic or kinematic data.⁷ Wheelchair sprint and anaerobic power are commonly assessed using Sprint and Wingate tests on a computer-controlled wheelchair ergometer.⁸ Such a wheelchair ergometer accommodates the player's sports wheelchair and measures mechanical power output.⁹ To achieve velocities similar to those experienced on court, the Sprint test is performed against a resistance that aims to mimic realistic overground conditions. Conversely, a Wingate test is performed against a higher resistance, which decreases rim velocity, thereby limiting upper-body coordination difficulties at higher velocities, allowing higher power production.¹⁰

Field-testing is conducted on-court, is easier to perform and is suggested to enhance external validity.⁶ Wheelchair mobility performance, i.e., the wheelchair player's ability on-court, can be systematically tested using a 10m straight Sprint test, Illinois agility test and Spider manoeuvrability test.⁵ Attaching inertial measurement units (IMUs) to the wheelchair enables assessment of dynamic aspects like linear and rotational accelerations and velocities.¹¹ Recent work by van Dijk et al. (2023) showed that, using the same IMU set-up, with one additional IMU on the trunk, power output per push during straight-line sprinting can be determined.^{12,13} The Sprint test gives insight in linear velocities and power output, the Illinois test assesses linear and rotational velocities and the Spider test focuses on rotational velocities. These field tests are construct-valid, meaning that they can distinguish between elite and youth athlete performances.⁵

Tests conducted under lab and field conditions are thought to be complementary, allowing us to benefit from their respective strengths. The previous discussed lab and field tests clearly show overlap in their tested constructs. All tests are of short duration (< 40s), implying they mostly rely on anaerobic power output.² Moreover, all tests are performed in the player's own sports wheelchair, without altering the wheelchair-user interface.¹⁴ Additionally, with exception of the Wingate test, all tests are performed with a racket and high (linear or rotational) velocities are achieved that require a certain skill level. Besides similarities, differences exist. During wheelchair propulsion in the field, the athlete's weight constantly shifts between the smaller front wheels and the larger rear wheels, leading to fluctuating rolling resistances (with the smaller wheels experiencing more resistance).¹⁵ Conversely, in a lab setting, the large rear wheels of the wheelchair are strapped onto the rollers of the wheelchair ergometer, resulting in a more constant rolling resistance. Furthermore, when fixed on the wheelchair ergometer, the

influence of the player's trunk is constrained, rotational aspects cannot be assessed and there is no need for small steering adjustments to prevent or correct directional errors. Conversely, in the field, trunk motion has a greater impact, rotational movements are involved, and immediate self-correction is essential to address directional errors.^{15,16}

These similarities and differences lead to the question whether both testing environments together provide a more in-depth understanding of the players performance. Assuming a degree of overlap between the test environments, detailed power output analyses in the lab can directly be used for on-court training, for example, an inefficient stroke pattern with high negative and peak powers can be distilled from lab testing and should be a focus point for training.¹⁷ To our knowledge, only one study associated the performance (mean and peak power) on a wheelchair-specific Wingate test with time needed to perform a 20 meter Sprint and an agility test, and found good associations in wheelchair basketball players.¹⁸

The current study aims to examine associations between wheelchair sprint and anaerobic power, assessed in a standardized lab-environment, and wheelchair mobility performance, assessed in the field, among experienced wheelchair tennis players. It is hypothesised that the strongest associations will be found between the power output and velocity of lab tests (Sprint and Wingate) and the power output, velocity, and test duration of the field Sprint test. Weaker associations are expected between the power output and velocity of lab tests (Sprint and Wingate) and the peak linear velocity, peak rotational velocity and test duration of the Illinois and the Spider test. Furthermore, construct validity will be assessed comparing an elite and amateur adult wheelchair tennis group. It is expected that, in line with Rietveld et al. (2019), elite athletes will achieve a higher power output and linear and rotational velocities in the field, resulting in faster end times.⁵ In the lab, elite athletes are expected to achieve higher power output and velocities, compared to amateur players.

2 Material and methods

2.1 Participants

Wheelchair tennis players (elite and amateur players) were included in this cross-sectional study between May 2022 and July 2023. Inclusion criteria were to practise wheelchair tennis on a regular basis (at least one time a week) and the absence of medical contra-indications according to the Physical Activity Readiness Questionnaire (PAR-Q, ACSM: 2009). The local ethics committee of the Centre for Human Movement Sciences, University Medical Centre Groningen, University of Groningen, the Netherlands approved the study protocol (202000455). All participants gave their written consent prior to participation.

2.2 Measurement set-up

Lab measurements were performed in two different laboratories with similar facilities (University Medical Centre Groningen and Reade Rehabilitation centre Amsterdam). Field tests were performed at different training facilities (National Tennis Centre Amstelveen, Drachtster Lawn Tennis Club Drachten and Tennis and Squashclub Haren) on the same acrylic hardcourt surface. There was a minimum period of two days and a maximum of one month between lab and field

measurements. For both testing modalities (lab and field), players used their own sports wheelchair and racket. Before testing, tires of the wheelchair were inflated up to their recommended pressure.

2.2.1 Standardized lab testing

The computer-controlled Esseda wheelchair roller ergometer was available at both testing locations and used for testing (Fig. 7.1, Lode BV, Groningen, The Netherlands). This commercial dual-roller wheelchair ergometer provides an accurate individual simulation of inertia and resistance, while allowing for accurate measurements (100 Hz) of both left and right-hand propulsion characteristics.⁹ Before each test, the individual-wheelchair combination was calibrated on the ergometer to account for static and dynamic friction.⁹

2.2.2 On-court field testing

Inertial Measurement Units (IMU) were placed on the hub of both wheels, the frame of the wheelchair and the chest of the participant (Fig. 7.2).¹¹ The IMUs consist of a gyroscope, accelerometer and magnetometer. The three IMUs on the wheelchair allow measurements of covered distance, and linear and rotational velocities over time. The IMU on the chest was used to calculate the orientation of the trunk with respect to the global earth frame, which was used to determine power output with more accuracy.¹⁵ All data were collected at 200Hz via Wi-Fi, which enabled all four IMUs to collect data synchronously.

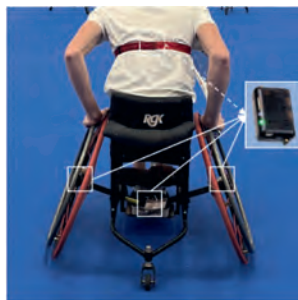


Figure 7.1 (left). Wheelchair tennis player in sports wheelchair on Esseda wheelchair ergometer

Figure 7.2 (right). Placement of three Inertial Measurement Units on wheelchair and a 4th on the player's chest

2.3 Test protocols

2.3.1 Standardized lab testing

After a familiarisation period of five minutes, participants were asked to perform three tests on the wheelchair ergometer: 1) an isometric strength test without racket, 2) a 10s Sprint test with racket and, 3) a 30s Wingate test without racket. These test protocols are extensively described by Janssen et al (2022).⁴ In short, regarding the isometric strength test, players are instructed to exert maximum force on the hand rim three times with both hands for a duration of 5s, pushing along the tangential direction of the hand rim. The 10s Sprint test from a standstill was performed on a resistance resembling the resistance typically found on an average gym court (resistance coefficient = 0.012). Because the current test was part of a larger standardized test battery for

wheelchair athletes of multiple sports, resistance was not similar to an indoor tennis court, which has a slightly lower resistance coefficient of 0.008.¹⁹ Lastly, the 30s Wingate test, also from a standstill, was performed against a high individualized resistance, based on their performance on the isometric strength test.⁴ In the current study, the isometric strength test was solely used to calculate the Wingate resistances but was not used as outcome measure in the current study.

2.3.2 On-court field testing

Participants were asked to complete three field tests: a 10m Sprint test, an Illinois test and a Spider test, all with racket. Each test was performed twice. These tests are specifically developed for wheelchair tennis and extensively described by Rietveld et al. (2019) (Fig. 7.3). Although analysing the average of the two attempts is considered the most reliable approach for these field tests⁵, not all included players showed consistent performance in the two tests, resulting in instances where two good attempts were not achieved. Consequently, the test with the fastest end time was chosen for further analyses. Before every test, players stood still with the castor wheels behind the starting line and completed the trajectory as fast as possible. After each trial there was a resting period of at least 2 minutes.

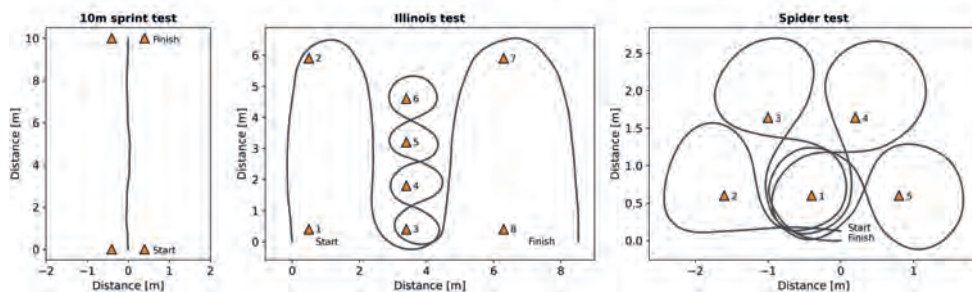


Figure 7.3. Lay-out of set up and trajectory of the three field tests.

To be able to determine power output during the 10m Sprint test, four coast-down trials were performed to determine drag forces.²⁰ Players were instructed to push the wheelchair with two pushes, place their hands on their knees, sit as still as possible and let the wheelchair decelerate naturally for a minimum of two seconds. The first two trials were performed in an upright position during deceleration, and in the last two trails, players were instructed to bend forward during deceleration. This was performed to evoke a variance in load distribution, such that the rolling resistance coefficients of each pair of wheels could numerically be solved.²¹

2.4 Data analyses

All analyses were done with custom-written Python scripts, all used functions can be found in the following two packages: Worklab and Wheeltennis.^{22,23}

2.4.1 Standardized lab testing

Torque and velocity data were directly measured from the wheelchair ergometer and filtered using a fourth order low-pass Butterworth filter with a cut-off frequency of 10Hz.²⁴ The instantaneous mechanical power output (PO [W]) at each side was calculated from the measured torque (M [Nm]), wheel radius (r_w [m]) and wheel velocity (v_w [$m \cdot s^{-1}$]):

$$PO = M * r_w^{-1} * v_w \quad (7.1)$$

Regarding the 10s Sprint test, only data of the first 10m was analysed for more resemblance with the 10m Sprint test in the field. Sprint peak velocity (v_{peak} [$m \cdot s^{-1}$]) was calculated over the average of left and right wheel velocity, as the highest peak sample. Average Sprint power output (PO_{mean} [$W \cdot kg^{-1}$]) and Wingate anaerobic power (P30 [$W \cdot kg^{-1}$]) were calculated as the sum of left and right wheel, averaged over 10m or 30s, respectively, and divided by body mass.

2.4.2 On-court field testing

Start time for every test was defined as when initial linear velocity exceeded $0.1 m \cdot s^{-1}$. End time for the 10m Sprint test was defined as the moment when the average distance covered by both wheels was 10m. For the Illinois and Spider test, end times were set based on analyses of plots created in Python (Fig. 7.2). A zero line was set at the starting point, when this line was crossed at the end of the trial, time was automatically defined.⁵

The three-dimensional gyroscopes of the four attached IMUs were used to derive all variables. Data was filtered with a low-pass second order recursive Butterworth filter with a cut-off frequency of 10Hz.¹¹ Due to the camber angle and horizontal rotations of the sports wheelchair, angular wheel velocity was first corrected using the sinus of the camber angle and the gyroscope data of the frame sensor in the Z-direction (Eq. 7.2).²⁵ Linear velocity (v_{lin} [$m \cdot s^{-1}$]) was subsequently calculated from angular wheel velocity (v_{ang} [$^{\circ} \cdot s^{-1}$]) and wheel circumference (WC [m]) (Eq. 7.3). Rotational velocity (v_{rot} [$^{\circ} \cdot s^{-1}$]) was directly obtained from the GyroZframe.²⁶

$$v_{ang} = (GyroY_{wheel} + \sin(\text{camber})) * GyroZ_{frame} \quad (7.2)$$

$$v_{lin} = WC / 360^{\circ} * v_{ang} \quad (7.3)$$

Cycle-average mechanical power (PO [W]) was determined by summing the power losses due to resistive force and the change in kinetic energy. As the wheelchair is assumed to have no angular rotations during the sprint, air resistance is assumed negligible, and the floor is assumed flat, PO was determined by summing the power loss due to rolling resistance (F_{roll} [N]) and the change in kinetic energy (Eq. 7.4). F_{roll} was determined from the coast-down tests and corrected for trunk inclination to obtain realistic rolling resistance forces.^{16,21} The change in kinetic energy was determined from wheelchair velocity (v_{lin} [$m \cdot s^{-1}$]) and total mass of wheelchair and user (m_{total} [kg]).¹² Cycle time is represented by T [s]. To obtain cycle-average power output, the weighted average of power output per cycle was calculated.

$$PO = (1/T) * \int_0^T -F_{roll} * v_{lin} + \frac{1}{dt} (0.5 * m_{total} * v_{lin}^2) \quad (7.4)$$

Mean power output (PO_{mean} [W]) was only calculated for the Sprint test. Peak linear velocity ($v_{peak-lin}$ [$m \cdot s^{-1}$]) was calculated for the Sprint and Illinois test and peak rotational velocity ($v_{peak-rot}$ [$^{\circ} \cdot s^{-1}$]) for the Illinois and Spider test. Test duration [s] was an outcome measure for all three field tests.

Table 7.1.

Participant characteristics	N or mean (SD)	
	Elite group	Amateur group
Men / woman (N)	5/4	5/4
Age (years)	23 (7)	42 (18)
Body mass (kg)	61 (7)	81 (21)
Wheelchair tennis experience (years)	10 (8)	13 (13)

2.5 Statistical analyses

All statistical analyses were done using Python 3.8 (Python Software Foundation). Average and standard deviation for the outcomes were calculated, separately for elite and amateur players. All data were normally distributed (Shapiro-Wilk test). To check for systematic differences between elite and amateur players (e.g., construct validity), an independent t-test with Bonferroni correction was performed. This implies that the chosen alpha level (0.05) was divided by the amount of t-tests (i.e., eleven for construct validity).²⁷ Significance level for the t-test was thus set at $0.05/11 = 0.0045$.

Linear or curvilinear regression analyses were performed between outcome variables from standardized lab tests versus the outcome variables from on-court field tests. The regression (linear or curvilinear) with the highest explained variance (R^2) was reported. Lastly, since mean power output and peak linear velocity were identical variables for lab and field sprints, a dependent t-test was used to check for systematic differences.

3 Results

All participants completed all lab and field tests, which led to a total of eighteen wheelchair tennis players in this study, nine elite and nine amateur players (Table 7.1). Due to technical issues of the wheelchair ergometer two participants had missing data for the 10s Sprint lab tests, and one participant had missing data for the Wingate test. Power output of the 10m field Sprint test was missing for six players. Three elite players did not perform the coast-down tests, two amateur players had pushes in their coast-down tests and for one amateur player, the data file was corrupted. Table 7.2 reports the main test outcomes and typical examples of the lab and field tests results are displayed in Fig. 7.4. The independent t-test showed that the elite group performed consistently better on all tests, compared to the amateur group (Table 7.2, $p < 0.001$).

Table 7.2

Primary test outcomes for the Sprint and Wingate test in the lab, and for the Sprint, Illinois and Spider test in the field. Differences between the amateur group and elite group are significant ($p < 0.001$) for all tests.

		Amateur group		Elite group	
		<i>N</i>	Mean (SD)	<i>N</i>	Mean (SD)
Lab tests					
<i>Sprint test</i>					
PO_{mean} [$W \cdot \text{kg}^{-1}$]	Average power over 10m	8	1.1 (0.5)	8	2.2 (0.6)
V_{peak} [$\text{m} \cdot \text{s}^{-1}$]	Peak velocity over 10m	8	2.6 (0.4)	8	3.5 (0.4)
<i>Wingate test</i>					
$P30$ [$W \cdot \text{kg}^{-1}$]	Average power over 30s	8	1.2 (0.5)	9	2.5 (0.4)
Field tests					
<i>10m Sprint test</i>					
PO_{mean} [$W \cdot \text{kg}^{-1}$]	Average power output	6	0.8 (0.3)	6	2.3 (0.4)
$V_{\text{peak-lin}}$ [$\text{m} \cdot \text{s}^{-1}$]	Peak linear velocity	9	3.2 (0.6)	9	4.6 (0.4)
Test duration [s]	Total time needed	9	4.9 (0.6)	9	3.5 (0.2)
<i>Illinois test</i>					
$V_{\text{peak-lin}}$ [$\text{m} \cdot \text{s}^{-1}$]	Peak linear velocity	9	2.8 (0.4)	9	4.0 (0.4)
$V_{\text{peak-rot}}$ [$^{\circ} \cdot \text{s}^{-1}$]	Peak rotational velocity	9	173 (17)	9	240 (21)
Test duration [s]	Total time needed	9	31.3 (6.7)	9	18.9 (1.3)
<i>Spider test</i>					
$V_{\text{peak-rot}}$ [$^{\circ} \cdot \text{s}^{-1}$]	Peak rotational velocity	9	176 (24)	9	260 (23)
Test duration [s]	Total time needed	9	24.4 (3.8)	9	15.6 (1.2)

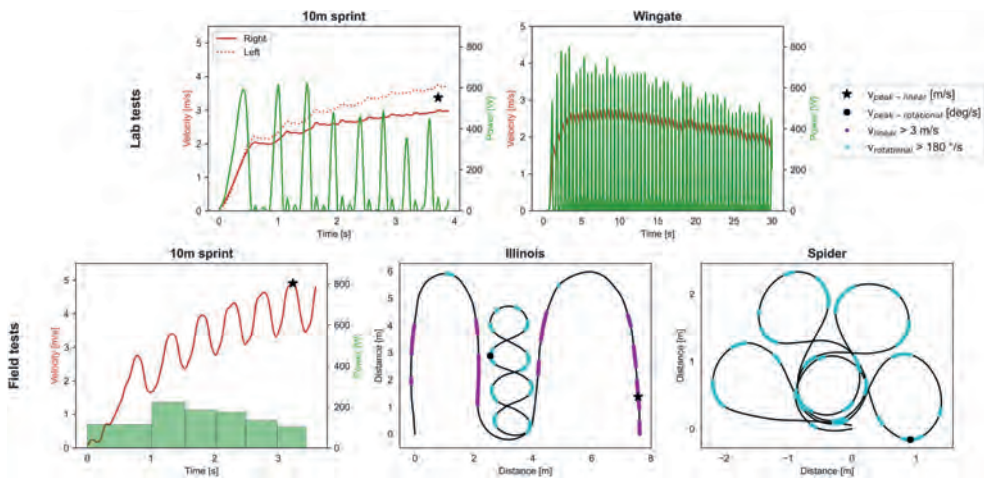


Figure 7.4. Typical example of outcomes from lab (top row) and field tests (row below). Velocity is shown in red, power output in green and completed trajectory in black. Peak linear and rotational velocity is annotated and the Illinois and Spider test are highlighted when linear velocity is above 3 m/s (purple) or rotational velocity is above 180 °/s (light blue).

3.1 Associations among lab and field tests

All associations were determined with seventeen or sixteen individual data points, except for the power output of the field sprint with the lab tests; those three regressions were constructed with only eleven individuals.

The strongest associations ($R^2 > 90\%$) were found for the power output in the field Sprint test with all three lab outcomes. Peak linear velocity and time needed for all field tests showed slightly lower explained variances ($R^2 = 77\text{--}85\%$) with the three lab outcomes. Peak rotational velocity showed the lowest explained variances ($R^2 = 69\text{--}80\%$) with lab outcomes. Fig. 7.5 shows the associations between the lab and field test outcomes.

Peak linear velocity and average power output were both measured in the lab and field sprints and a line of identity is shown in these two plots in Fig. 7.5 (dotted line). Peak linear velocity was on average significantly $26 \pm 14\%$ higher in the field sprint ($p < 0.001$) and mean power output was not significantly different in the field sprint ($p = 0.31$), compared to the sprint in the lab.

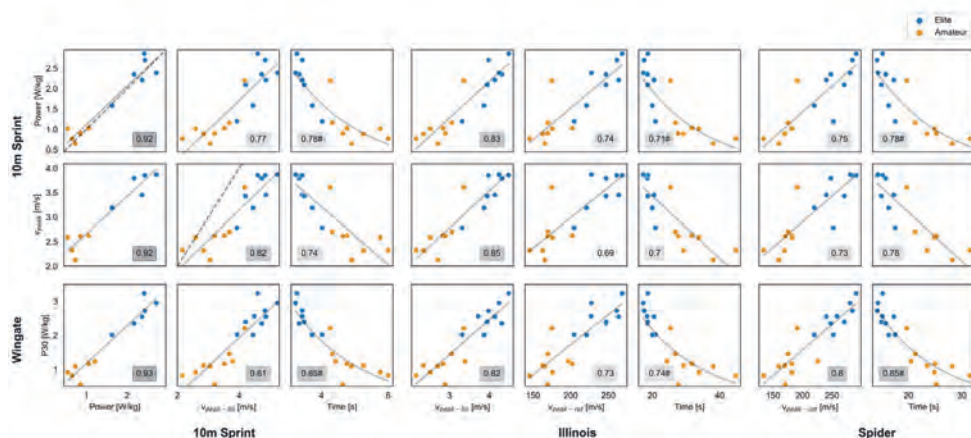


Figure 7.5. Association between lab and field test outcomes. Lab tests are displayed at the vertical axis, field tests at the horizontal axis. Plots are annotated with the explained variance (R^2), if the curvilinear regression gave the best fit, an # is added to the R^2 . Two plots show the line of identity (dotted line) because PO_{mean} and v_{peak} were measured in both lab and field sprints. Orange dots designated the amateur players and blue dots are elite players.

4 Discussion

The associations between wheelchair sprint and anaerobic power, assessed within a lab setting, and wheelchair mobility performance, evaluated on the field, are strong for experienced wheelchair tennis players. As expected, the field Sprint test outcomes showed the strongest associations with the lab Sprint and Wingate test outcomes. However, the Illinois and the Spider test outcomes, which mainly focused on rotational velocities and require different skills, also showed strong associations with the lab tests outcomes. Thus, although there are some

differences in set up between lab and field testing (i.e., influence of trunk, linear or rotational components, skill involvement), the strong associations show that these tests partly measure the same construct (i.e., sprint performance, anaerobic power and wheelchair mobility). Furthermore, the expected construct validity of both lab and field tests was confirmed, as all tests outcomes differentiated between elite and amateur players.

Associations between results of the wheelchair-specific lab and field test battery were strong. As far as we know, only one previous study reported wheelchair-specific associations between a Wingate test and field sprint test among wheelchair basketball players and found comparable associations ($R^2 = 86\%$ in their study, compared to 85% in this study).¹⁸ No wheelchair-specific studies investigated the relation with more-rotational based tests, like the Illinois and the Spider test, but the strong associations in the current study showed that there is overlap in test requirements. In contrast, studies using an arm-crank ergometer for the Wingate test exhibited weaker associations with linear field wheelchair sprints ($R^2 = 48\%$) and wheelchair agility field tests ($R^2 = 32\%$).^{28,29} The stronger associations between wheelchair-specific testing modalities highlights the need for wheelchair-specific lab testing methodologies, instead of arm-cranking.

The current study additionally showed the construct validity of both lab and field tests, which means that a distinction can be made between amateur and elite players. This validation aligns with findings reported by Rietveld et al. (2019) on wheelchair tennis field tests and extends it to lab testing.⁵ Although groups differed significantly from each other, regression analyses were conducted on the entire group of players without playing level as confounder, due to the small sample size. To examine the influence of playing level on the associations, a larger sample size should be included. The current study already showed some curvilinear relations (Fig. 7.5), suggesting an influence of playing level. Curvilinear associations were found between test duration of the 10m field Sprint, Illinois and Spider tests with the lab Sprint and Wingate test (Fig. 7.5), indicating that amateurs perform relatively better in the lab but require more time for the field tests. The higher skill level of elite players becomes more apparent in field tests. After making an error when pushing the hand rim, immediate correction is needed in the field, whereas these adjustments are not necessarily required on the wheelchair ergometer.

Graphs for sprint velocity between lab and field differ in amount of deceleration after every push (Fig. 7.4). In the lab, the wheelchair is fixed to the wheelchair ergometer and allows no movement in relation with the trunk. Conversely, in the field, the wheelchair counteracts with the movement of the trunk and thus exaggerates the actual velocity of the total wheelchair-user combination, both in a positive and negative direction. Moreover, rolling resistance is assumed close to constant on the wheelchair ergometer (rear wheels are strapped onto the rollers), but fluctuating in the field because the mass of the user shifts between the smaller front castor-wheels (that have a larger rolling resistance) and the larger rear wheels. Not only deceleration after every push differed, peak velocity was also significantly higher in the field ($26 \pm 14\%$). This can at least partly be explained by the lower resistance coefficient of 0.008 on hard-court, compared to 0.012 used on the wheelchair ergometer.¹⁹ Future studies should use similar resistances to better isolate and investigate the impact of trunk motion.

In contrast to velocity, mean power output did not differ significantly between lab and field sprints. Power output also showed a strong association between lab and field ($R^2 = 92\%$). Caution is warranted in the interpretation of the association due to the limited data for power output in the field ($N=11$) and clustering among players in the scatter plot, i.e., amateur players are in the lower left corner, elite players in the upper right corner (Fig. 7.5). The analysed players exhibited values closely aligned with the line of identity (indicating similar values in both lab and field sprints, as shown by the dotted line in Fig. 7.5) and did not show a significant difference in PO_{mean} ($p = 0.31$). Therefore, it is expected that any missing values in the current study (specifically, six out of eighteen values were missing for field power output) would also fall near this line of identity, thereby preserving the strong association. Wheelchair tennis players may encounter varying levels of rolling resistance, arising from different surfaces or slight disparities in tyre pressure, that will influence the achieved velocity.¹⁹ In contrast, while power output takes rolling resistance and velocity into account, it emerges as a more objective measure to utilize.

Practical implications

Strong associations suggest that detailed biomechanical analyses from lab testing can guide training to improve player's wheelchair mobility on-court. Lab testing offers unique advantages, including detailed power output, independent left-right measurements, and its suitability for tests against higher resistances. Detailed power output can, for example, be used to analyse negative and peak power output during wheelchair propulsion with a tennis racket, which has led already to the development of a new, more efficient hand rim for wheelchair tennis.¹⁷ The lab setting, without the need for immediate corrections due to directional errors, provides players with more insights into their maximal capacities for the left and right arm separately.³⁰ Lastly, higher resistance tests in the lab can be used to measure anaerobic power and to construct force-velocity curves, informing whether players should prioritize training on force or velocity.³

Where lab tests can give a deeper understanding of the biomechanics behind a sprint, field tests show the wheelchair mobility on-court, including linear and rotational aspects. An earlier study distracted six key mobility components during wheelchair tennis matches and found that four of them were based on rotations, that can only be tested in the field.¹ Moreover, field tests are also more similar to match situations, as it is performed on the same court as matches, resulting in a higher ecological validity. Lastly, field testing demands immediate correction when deviating from the desired trajectory and requires thus more skill compared to lab testing.³¹

Furthermore, combining both testing environments will give a complete overview of the players' performance and it can also provide direction for training. Lab and field tests outcomes showed strong associations, but there also remains an unexplained variance ($1 - R^2$), due to test-retest variation and to the different focus of the tests.³² Because elite players are often seeking for the last few percentages to improve their performance, they will benefit from both lab and field testing, while for amateur players, field tests may also be sufficient to track performance. Additionally, looking at the constructed regression lines, those to the right of the 'rotational velocity-anaerobic power trend line' excel in rotational skills, suggesting power-focused training,

whereas those with higher power but less rotational skills could benefit more from rotational (skill) training.

To track wheelchair performance, it is recommended to adopt the field test battery, which is easier to perform, regularly throughout the season (e.g., four times a year). Lab testing should complement this regimen for more in-depth biomechanical analyses. Due to the strong associations between lab and field outcomes and the increased effort required for lab visits, the frequency of lab testing may be less frequent, such as twice a year. Lab tests are ideally performed around the same time as the field tests, or conducted when specific biomechanical questions arise.

Future research

The current research focused on standardized wheelchair performance testing. However, the actual performance takes place during competition what requires a holistic integration of all skills such as sprinting, rotating, racket handling, and tactical decisions.^{33,34} A next step would be to investigate how much these standardized lab and field tests contribute to wheelchair tennis match performance. Additionally, current methods for determining power output are established for straight-line sprints. As turning involves unknown factors such as rotational inertia and increased rolling resistance due to e.g. slipping, the accuracy of IMU-based power estimation during turning is yet to be determined.³⁵ Further developments are necessary to extent power monitoring to turning, enabling objective assessments in tests, training sessions, and competitions for a comprehensive understanding of the players' workload throughout their season.

Conclusion

Associations between wheelchair lab sprint and anaerobic power with wheelchair mobility field performance are strong among a group of experienced wheelchair tennis players. Although there are some differences between lab- and field-testing methodologies (i.e., influence of trunk motion, linear and rotational velocity profile, skill involvement), the strong associations indicate overlapping measured constructs (i.e., sprint performance, anaerobic power and wheelchair mobility). This implies that field testing provides us with valuable wheelchair mobility insights, and lab testing gives a broad additionally array of in-depth biomechanical and physiological analyses. Construct validity of both lab and field tests was confirmed, as all tests outcomes differentiated between elite and amateur players.

References

1. Rietveld T, Vegter RJK, van der Slikke RMA, Hoekstra AE, van der Woude LH V, de Groot S. Six inertial measurement unit-based components describe wheelchair mobility performance during wheelchair tennis matches. *Sport Eng.* 2023;26(32). doi:<https://doi.org/10.1007/s12283-023-00424-6>
2. Gastin P. Energy system interaction and relative contribution during maximal exercise. *Sport Med.* 2001;31(10):725-741.
3. Janssen RJF, de Groot S, Van der Woude LHV, Houdijk H, Goosey-Tolfrey VL, Vegter RJK.

- Force–velocity profiling of elite wheelchair rugby players by manipulating rolling resistance over multiple wheelchair sprints. *Scand J Med Sci Sport*. 2023;33(8):1531-1540. doi:10.1111/sms.14384
4. Janssen RJF, Vegter RJK, Houdijk H, Van der Woude LHV, de Groot S. Evaluation of a standardized test protocol to measure wheelchair-specific anaerobic and aerobic exercise capacity in healthy novices on an instrumented roller ergometer. *PLoS One*. 2022;17(9):e0274255. doi:10.1371/journal.pone.0274255
 5. Rietveld T, Vegter RJK, van der Slikke RMA, Hoekstra AE, van der Woude LHV, De Groot S. Wheelchair mobility performance of elite wheelchair tennis players during four field tests: Inter-trial reliability and construct validity. *PLoS One*. 2019;14(6). doi:10.1371/journal.pone.0217514
 6. Van der Slikke RMA, Sindall P, Goosey-Tolfrey VL, Mason BS. Load and performance monitoring in wheelchair court sports: A narrative review of the use of technology and practical recommendations. *Eur J Sport Sci*. Published online 2022. doi:10.1080/17461391.2021.2025267
 7. de Klerk R, Vegter RJK, Goosey-Tolfrey VL, et al. Measuring handrim wheelchair propulsion in the lab: A critical analysis of stationary ergometers. *IEEE Rev Biomed Eng*. 2020;13:199-211. doi:10.1109/RBME.2019.2942763 LK
 8. van der Woude LHV, Houdijk HJP, Janssen TWJ, et al. Rehabilitation: mobility, exercise & sports; a critical position stand on current and future research perspectives. *Disabil Rehabil*. 2021;43(24):3476-3491. doi:10.1080/09638288.2020.1806365
 9. de Klerk R, Vegter RJK, Veeger HEJ, van der Woude LHV. Technical note : a novel servo-driven dual-roller handrim wheelchair ergometer. *IEEE Trans Neural Syst Rehabil Eng*. 2020;28(4):1-9. doi:10.1109/TNSRE.2020.2965281
 10. Bar-Or O. The Wingate Anaerobic Test An Update on Methodology, Reliability and Validity. *Sport Med*. 1987;4(6):381-394. doi:10.2165/00007256-198704060-00001
 11. van der Slikke RMA, Berger MAM, Bregman DJJ, Lagerberg AH, Veeger HEJ. Opportunities for measuring wheelchair kinematics in match settings; reliability of a three inertial sensor configuration. *J Biomech*. 2015;48(12):3398-3405. doi:10.1016/j.jbiomech.2015.06.001
 12. van Dijk MP, Hoozemans MJM, Berger MAM, Veeger HEJ. From theory to practice: monitoring mechanical power output during wheelchair field and court sports using inertial measurement units. *J Biomech*. 2023;(January).
 13. van Dijk MP, Kok M, Berger MAM, Hoozemans MJM, Veeger DJHEJ. Machine Learning to Improve Orientation Estimation in Sports Situations Challenging for Inertial Sensor Use. *Front Sport Act Living*. 2021;3(August). doi:10.3389/fspor.2021.670263
 14. Mason BS, Van Der Woude LHV, Goosey-Tolfrey VL. The ergonomics of wheelchair configuration for optimal performance in the wheelchair court sports. *Sport Med*. 2013;43(1):23-38. doi:10.1007/s40279-012-0005-x
 15. Van Dijk MP, Van Der Slikke RMA, Berger MAM, Hoozemans MJM, Veeger HEJ. Look Mummy, No Hands! the Effect of Trunk Motion on Forward Wheelchair Propulsion. *39th Int Soc Biomech Sport Conf Canberra, Aust*. Published online 2021:312-315. <https://commons.nmu.edu/isbs/vol39/iss1/80>
 16. Dijk MP Van, Hoozemans MJM, Berger MAM, Veeger DHEJ. Trunk motion influences mechanical power estimates during wheelchair propulsion. *J Biomech*. 2024;163(January):111927. doi:10.1016/j.jbiomech.2024.111927
 17. Rietveld T, Vegter RJK, van der Woude LHV, de Groot S. A newly developed hand rim for

- wheelchair tennis improves propulsion technique and efficiency in able-bodied novices. *Appl Ergon.* 2022;104(January):103830. doi:10.1016/j.apergo.2022.103830
18. Vanlandewijck YC, Daly DJ, Theisen DM. Field test evaluation of aerobic, anaerobic, and wheelchair basketball skill performances. *Int J Sports Med.* 1999;20(8):548-554. doi:10.1055/s-1999-9465
 19. Rietveld T, Mason BS, Goosey-Tolfrey VL, van der Woude LHV, de Groot S, Vegter RJK. Inertial measurement units to estimate drag forces and power output during standardised wheelchair tennis coast-down and sprint tests. *Sport Biomech.* 2021;00(00):1-19. doi:10.1080/14763141.2021.1902555
 20. de Klerk R, Vegter RJK, Leving MT, de Groot S, Veeger DHEJ, van der Woude LH V. Determining and Controlling External Power Output During Regular Handrim Wheelchair Propulsion. *J Vis Exp.* 2020;(156). doi:10.3791/60492
 21. Sauret C, Vaslin P, Lavaste F, de Saint Remy N, Cid M. Effects of user's actions on rolling resistance and wheelchair stability during handrim wheelchair propulsion in the field. *Med Eng Phys.* 2013;35(3):289-297. doi:10.1016/j.medengphy.2012.05.001
 22. De Klerk R, Rietveld T, Janssen RJF, Braaksma J. Worklab: a wheelchair biomechanics mini-package. Published online 2023. doi:https://doi.org/10.5281/zenodo.8362963
 23. Rietveld T. Wheeltennis: a wheelchair tennis data analysis package. Published online 2022.
 24. Cooper R, DiGiovine C, Boninger C, Shimada S, Robertson R. Frequency analysis of 3-dimensional pushrim forces and moments for manual wheelchair propulsion. *Automedica.* 1998;16:355-365.
 25. Van Der Slikke RMA, Berger MAM, Bregman DJJ, Veeger HEJ. Wheel skid correction is a prerequisite to reliably measure wheelchair sports kinematics based on inertial sensors. *Procedia Eng.* 2015;112(0):207-212. doi:10.1016/j.proeng.2015.07.201
 26. Pansiot J, Zhang Z, Lo B, Yang GZ. WISDOM: Wheelchair inertial sensors for displacement and orientation monitoring. *Meas Sci Technol.* 2011;22(10). doi:10.1088/0957-0233/22/10/105801
 27. Sedgwick P. Multiple significance tests: The Bonferroni correction. *BMJ.* 2012;344(7841):1-2. doi:10.1136/bmj.e509
 28. Molik B, Laskin JJ, Kosmol A, Marszatek J, Morgulec-Adamowicz N, Frick T. Relationships between anaerobic performance, field tests, and functional level of elite female wheelchair basketball athletes. *Hum Mov.* 2013;14(4):366-371. doi:10.2478/humo-2013-0045
 29. Marszatek J, Kosmol A, Morgulec-Adamowicz N, et al. Laboratory and non-laboratory assessment of anaerobic performance of elite male wheelchair basketball athletes. *Front Psychol.* 2019;10:1-10. doi:10.3389/fpsyg.2019.00514
 30. Goosey-Tolfrey VL, Vegter RJK, Mason BS, et al. Sprint performance and propulsion asymmetries on an ergometer in trained high- and low-point wheelchair rugby players. *Scand J Med Sci Sport.* 2018;28(5):1586-1593. doi:10.1111/sms.13056
 31. Bakatchina S, Weissland T, Astier M, Pradon D, Faupin A. Performance, asymmetry and biomechanical parameters in wheelchair rugby players. *Sport Biomech.* 2021;00(00):1-14. doi:10.1080/14763141.2021.1898670
 32. Zaghlul N, Goh SL, Razman R, Danaee M, Chan CK. Test-retest reliability of the single leg stance on a Lafayette stability platform. *PLoS One.* 2023;18(1 January):1-12. doi:10.1371/journal.pone.0280361
 33. Sánchez-Pay A, Martínez-Gallego R, Crespo M, Sanz-Rivas D. Key physical factors in the

- serve velocity of male professional wheelchair tennis players. *Int J Environ Res Public Health*. 2021;18(4):1-11. doi:10.3390/ijerph18041944
34. Abuwarda K, Akl AR. Changes in Electromyographic Activity of the Dominant Arm Muscles during Forehand Stroke Phases in Wheelchair Tennis. *Sensors (Basel)*. 2023;23(20). doi:10.3390/s23208623
 35. Caspall JJ, Seligsohn E, Dao PV, Sprigle S. Changes in inertia and effect on turning effort across different wheelchair configurations. *J Rehabil Res Dev*. 2013;50(10):1353-1362.



Abstract

In wheelchair sports, the use of Inertial Measurement Units (IMUs) has proven to be one of the most accessible ways for ambulatory measurement of wheelchair kinematics. A three-IMU configuration, with one IMU attached to the wheelchair frame and two IMUs on each wheel axle, has previously shown accurate results and is considered optimal for accuracy. Configurations with fewer sensors reduce costs and could enhance usability, but may be less accurate. The aim of this study was to quantify the decline in accuracy for measuring wheelchair kinematics with a stepwise sensor reduction. Ten differently skilled participants performed a series of wheelchair sport specific tests while their performance was simultaneously measured with IMUs and an optical motion capture system which served as reference. Subsequently, both a one-IMU and a two-IMU configuration were validated and the accuracy of the two approaches was compared for linear and angular wheelchair velocity. Results revealed that the one-IMU approach show a mean absolute error (MAE) of 0.10 m/s for absolute linear velocity and a MAE of 8.1 degrees/s for wheelchair angular velocity when compared with the reference system. The two-IMU approach showed similar differences for absolute linear wheelchair velocity (MAE 0.10 m/s), and smaller differences for angular velocity (MAE 3.0 degrees/s). Overall, a lower number of IMUs used in the configuration resulted in a lower accuracy of wheelchair kinematics. Based on the results of this study, choices regarding the number of IMUs can be made depending on the aim, required accuracy and resources available.

Introduction

In wheelchair court sports, kinematic variables like forward acceleration and angular velocity are important for the quantification of the athlete's wheelchair mobility performance (van der Slikke et al., 2018), which is an important aspect of overall game performance. In wheelchair racing, the relationship between wheelchair kinematics and overall performance is even more profound, with the highest average speed resulting in the best race time. Therefore, the ability to measure wheelchair kinematics using inertial sensors offers multiple opportunities for many wheelchair sports.

Van der Slikke et al. (2015) used inertial measurement units (IMUs) attached to the rear wheels and frame to measure wheelchair kinematics on the court. By using the gyroscope data of the wheel-mounted IMUs to obtain wheel speed, and those of the frame IMU to obtain frame rotation speed, wheelchair kinematics could be assessed with relative ease. To further increase accuracy in vigorous sports conditions, van der Slikke et al. (2015) developed a skid detection algorithm to correct for misinterpretations due to wheel skidding. This three-IMU configuration was validated using an optical motion capture system and provides accurate linear- and angular wheelchair displacement and speed (van der Slikke et al., 2015).

Although the three-IMU configuration might be considered optimal for accuracy, a two-IMU configuration (with IMUs attached to the frame and right wheel) is more accessible by reducing cost and enhance usability. A two-IMU configuration still allows for the same calculations as described by van der Slikke (2015), except for wheel skid correction. As wheel speed was initially determined by a weighted average of the two wheel-mounted IMUs, wheel speed may be less accurate in the two-IMU configuration.

Recently, Rupf et al. (2021) developed an IMU-based method that enables detection of wheelchair kinematics using only a single IMU. This method used a single IMU mounted on the wheel to derive both frame rotation and angular speed. Frame rotation was obtained by fusing the accelerometer and gyroscope data such that the attitude of the sensor was determined in a global reference frame. Although this one-IMU configuration is promising and was already tested and compared to the three-IMU configuration, validation with an optical motion capture system has yet to be performed.

The aim of this study is to quantify the decline in accuracy for measuring wheelchair kinematics using a stepwise sensor reduction. Errors in outcome parameters due to skidding may affect the results of one- and two-IMU configurations, whereas additional errors may be introduced in the one-IMU configuration as rotation is measured at the wheel instead of the frame center. It is therefore hypothesized that a lower number of IMUs would result in a lower accuracy of the measured wheelchair kinematics. To test this hypothesis, the one-IMU and two-IMU configurations were validated in a wheelchair sport specific test setting. Secondly, the accuracy of the two approaches was compared for linear and angular wheelchair velocity.

Methods

Procedure

Ten differently skilled participants (Table 8.1) performed a series of wheelchair sport-specific activities, while simultaneously being measured with two IMUs on their wheelchair and a marker-based optical motion capture system serving as reference. Calculated outcomes based on the one-IMU configuration, two-IMU configuration and reference system were compared to test the accuracy. Prior to the measurements, participants were informed about the aims and procedures of the study and provided written informed consent. The study was approved by the Human Research Ethics Committee of the Technical University of Delft (nr. 1530).

Table 8.1.
Subject characteristics (mean ± standard deviation)

Type	N	Age (years)	Class ¹	Wheel base	Camber angle	Wheel diameter
Elite wheelchair athlete ²	3	25.0 ± 3.0	3.2 ± 1.3	0.75 ± 0.05	18, 18	0.63 ± 0.02
Active wheelchair user	3	46.3 ± 11.0	2.5 ± 0.5	0.62 ± 0.23	18, 2, 3	0.62 ± 0.02
Non-experienced user	4	24.5 ± 0.6	-	0.62 ± 0.11	18, 4, 4, 4	0.61 ± 0.01

¹ The classes were indicated by the point scores as used in elite wheelchair basketball classification.

² Two wheelchair basketball players (premier league) and one wheelchair hockey player (Dutch national team).

System overview

Two IMUs (NGIMU, x-io technologies) were used to collect 3D inertial sensor data (100 Hz) of the right wheel and the wheelchair frame. A ten-camera optical motion capture system (OptiTrack Prime, National Point) with a frame rate of 100 Hz was used to record the 3D orientation and position of the wheelchair. The wheelchair marker cluster frame consisted of five retro-reflective markers attached to the front and back of the wheelchair frame.

Wheelchair sport-specific activities

The measurement session (see Table 8.2 and Figure 8.1) included sprints and agility exercises that represent some main aspects of wheelchair basketball, tennis, and rugby games (Pansiot et al., 2011; van der Slikke et al., 2015; van Dijk et al., 2021). At the start and end of each session, participants were instructed to keep a static posture for 20 seconds. Wheelchair athletes performed the session in their own wheelchair if feasible, whereas untrained participants used an ADL (Progeo) or all court sports (Quickie) wheelchair and were instructed to familiarize themselves with the chair (Vegter et al., 2014).

Optical motion capture analysis

OptiTrack three-dimensional position data of the wheelchair markers were acquired in Motive 2.2.0 (Natural Point), converted to a C3D format and imported in MATLAB (R2019b, The Mathworks Inc.). Missing values were interpolated if the duration of the gap was < 1/6 of a second. Accordingly, the rotation matrix and translation vector of the wheelchair segment relative to the first (static) sample was determined using the singular value decomposition described by Söderkvist & Wedin (1993). This required position data of at least three markers at both time instants. The derivative of the angle in the sagittal plane was determined and low-pass filtered at 6 Hz (Cooper et al., 2002) to obtain wheelchair angular velocity. The translation vectors were filtered at 10 Hz (van der Slikke et al., 2015) to filter marker positioning noise. Linear wheelchair velocities were determined according to Eq. 8.1, with x and y being the positions in the horizontal plane.

$$\left| \sqrt{(ds_x/dt)^2 + (ds_y/dt)^2} \right| \quad (8.1)$$

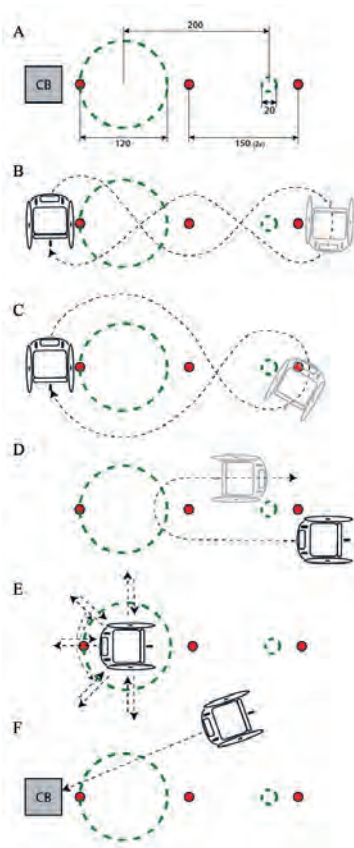


Table 8.2.

All sport-specific tests, together with a description of each test and the speed at which the participants were instructed to perform the test (see also Fig. 8.1). All tests were carried out in immediate succession.

Test	Speed	Description	
1	Straight 5 m	normal	3x sprint with static trunk
	Straight 5 m	low	3x
	Straight 5 m	normal	3x
	Straight 5 m	high	3x
2	Straight skid	high	2x sprint (stop with skidding wheels)
3	Slalom	normal	around 3 cones (Fig. 8.1B)
	Slalom	high	around 3 cones (Fig. 8.1B)
4	Figure 8	normal	(Fig. 8.1C)
	Figure 8	high	(Fig. 8.1C)
5	U turn	normal	180° clockwise turn (Fig. 8.1D)
	U turn	high	180° clockwise turn (Fig. 8.1D)
	U turn	normal	180° anti clockwise turn (Fig. 8.1D)
	U turn	high	180° anti clockwise turn (Fig. 8.1D)
6	Turn on spot	normal	360° clockwise turn
	Turn on spot	normal	360° anti clockwise turn
	Turn on spot	high	360° clockwise turn
	Turn on spot	high	360° anti clockwise turn
7	Star twist	free	Star wise bi-directional rotation
	Star twist	free	As previous, combined with back-and-forth movement (Fig. 8.1E)
8	Collision	free	2x 2m sprint and collision against a block of 30 kg (Fig. 8.1F)

Figure 8.1 (A to F). Track lay-out with dimensions in cm (A) corresponding to the tests as explained in Table 8.2. Cones and collision block (CB) were removed during test parts in which they were not used. This figure was adopted from Van der Slikke et al. (van der Slikke et al., 2015).

Two-IMU analysis

Wheelchair linear and angular velocity based on the two-IMU configuration were calculated as reported by van der Slikke et al. (2015). Wheelchair angular velocity was directly measured by the gyroscope signal around the vertical axis of the frame IMU, and low-pass filtered at 6 Hz. Wheelchair linear velocity was determined based on the gyroscope signal around the wheel axis of the wheel IMU (see Eq. 8.2.1-2.4 in Appendix A). Wheel angular velocity was low-pass filtered at a 10 Hz cut-off frequency, corrected for camber angle (Eq. 8.2.1; Pansiot et al., 2011; van der Slikke et al., 2015) and multiplied by the wheel circumference (Eq. 8.2.2) to obtain linear velocity of the wheel. To obtain the linear velocity of the frame center instead, an additional correction was performed (Eq. 8.2.4).

One-IMU analysis

To analyze the one-IMU configuration, only data from the wheel-mounted IMU were used. A Madgwick filter (Madgwick et al., 2011), with a tuning parameter set at 0.03 (Rupf et al., 2021), was used to derive the attitude of the sensor. The resulting Euler angles were differentiated with respect to time (Rupf et al., 2021) and low-pass filtered at 6 Hz. Wheelchair angular velocity was defined by the angular velocity in the horizontal plane. Since the sensor orientation was obtained relative to the global earth frame, no correction for camber angle was required. Wheelchair linear

velocity was derived in the same way as for the two-IMU configuration (see Eq. 8.2.1-8.2.4 in Appendix A).

Comparisons

IMU data and reference data were synchronized with respect to time using a cross-correlation of the angular velocity. Mean error, mean absolute error (MAE), root mean squared error (RMSE), maximal error and the 95% confidence intervals of the difference between different sensor configurations and reference data were reported for linear (absolute linear velocity > 0.1 m/s) and rotational (angular velocity > 5 °/s or < -5 °/s) wheelchair movements. Further, the start and end of each exercise of interest was selected manually based on the plots.

Results

Table 8.2 shows the error measures for the two different configurations compared to the reference system. Table 8.3 shows characteristics and error measures per subject group as defined in Table 8.1. Figure 8.2 and 8.3 show typical examples of the linear and angular velocities measured by the one-IMU configuration, two-IMU configuration and reference system.

Table 8.2.

Differences between the given sensor configuration and the reference system expressed as mean absolute error (MAE), root-mean-squared error (RMSE), mean error, maximal error, and upper and lower bound of the confidence interval (CI). The mean (SD) of the outcome measures over all participants was reported.

Config.	MAE	RMSE	Mean error	Max error	CI lower bound	CI upper bound
Angular velocity in deg/s						
One IMU	8.1 (2.5)	11.2 (3.3)	-0.1 (0.3)	55.6 (22.1)	-0.2 (0.3)	0.0 (0.3)
Two IMUs	3.0 (3.3)	4.6 (4.9)	-0.2 (0.3)	23.9 (15.3)	-0.2 (0.3)	-0.1 (0.3)
Linear velocity in m/s						
One IMU	.10 (.06)	.19 (.11)	-.03 (.05)	1.55 (1.52)	-.03 (.05)	-.03 (.05)
Two IMUs	.10 (.05)	.20 (.10)	-.02 (.05)	1.44 (1.47)	-.02 (.05)	-.01 (.05)

Table 8.3.

Mean and maximal values of the angular and linear velocities, and differences between the one- and two IMU configurations and the reference system expressed as MAE and RMSE averaged for each subject group.

Group*	Sensors	Angular velocity in deg/s				Linear velocity in m/s			
		Mean	Max	MAE	RMSE	Mean	Max	MAE	RMSE
EA	IMU1vsOpti	17.5	450	7.1	9.8	0.41	3.51	.15	.28
EA	IMU2vsOpti	-	-	2.5	3.8	-	-	.14	.28
EU	IMU1vsOpti	18.2	328	8.8	12.5	0.41	3.15	.10	.21
EU	IMU2vsOpti	-	-	6.3	9.3	-	-	.10	.22
NU	IMU1vsOpti	15.0	272	8.3	11.2	0.36	2.75	.07	.12
NU	IMU2vsOpti	-	-	1.0	1.7	-	-	.06	.11

*EA = Elite Athlete, EU = Experienced wheelchair user, NU = non-experienced user

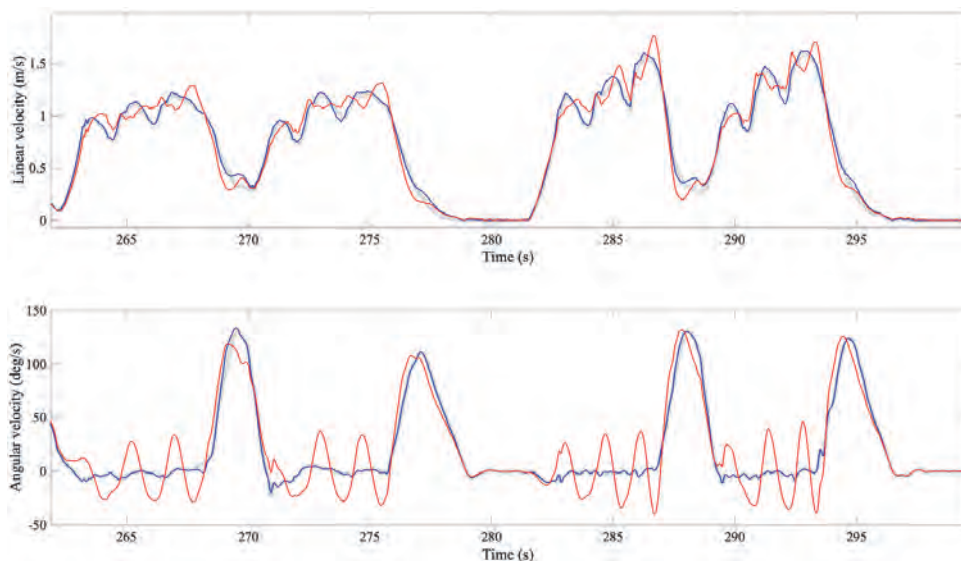


Figure 8.2. Typical examples of the angular velocity and linear velocity during two linear sprints at low speed and two linear sprints at normal speed (see Table 8.2, test 1). The results from the two-IMU analysis are indicated in blue, One-IMU analysis are indicated in red, and those of the optical motion capture system were indicated in grey. Although both IMU configurations match the patterns of the reference system, striking differences for the one-IMU frame angular velocity show in sinusoidal deviations in straight forward motion.

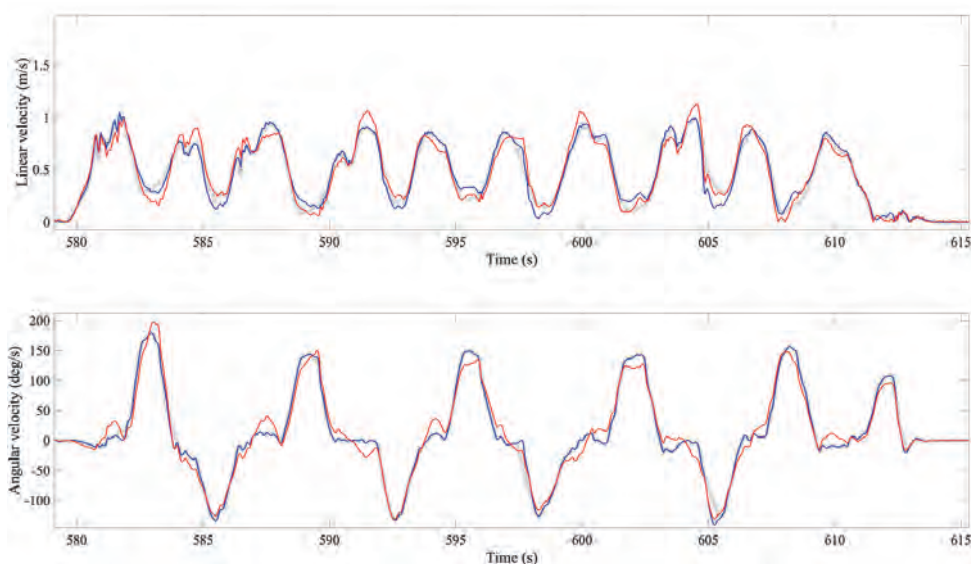


Figure 8.3. Typical examples of the angular velocity and linear velocity during a bidirectional star twist (see Table 8.2, test 7). The results from the two-IMU analysis are indicated in blue, one-IMU analysis are indicated in red, and those of the optical motion capture system were indicated in grey.

Discussion

The aim of this study was to quantify the decline in accuracy for measuring wheelchair kinematics using a stepwise sensor reduction. Compared to the reference system, the one-IMU

approach show a MAE of 0.10 m/s for wheelchair linear velocity and a MAE of 8.1 degrees/s for angular velocity. The two-IMU approach showed similar differences for linear wheelchair velocity (MAE 0.10 m/s), and smaller differences for angular velocity (MAE 3.0 degrees/s). Plots to compare the different approaches show a small sinusoidal deviation for the one-IMU approach which is mainly visible in angular wheelchair velocity.

To put the present results into perspective, the accuracy obtained for linear and angular velocity were compared with those previously reported for wheelchair sports. Van der Slikke et al. (2015) validated the three-IMU configuration with an optical motion capture system and reported an average RMSE of 0.07 m/s (ranging from 0.03 to 0.27 m/s) for linear velocity, which is smaller than the 0.19 and 0.20 m/s for the one and two-IMU configurations in this study, respectively. The increased accuracy of the three-IMU configuration is likely due to skid-correction. As skidding causes a mis-match between wheel rotation and frame displacement, larger errors in frame displacement occur when skidding is not identified. Since the skid-detection algorithm is based on two wheel-mounted sensors, this can only be applied in the three-IMU algorithm. However, further development of IMU analyses in the global reference frame may enable skid correction with less than three IMUs as well.

Regarding angular velocity, van der Slikke et al. (2015) reported an average RMSE of 4.8 degrees/s (ranging from 3.1 to 6.8 degrees/s) among different wheelchair specific tests. This error is smaller than the 11.2 degrees/s RMSE for the one-IMU configuration and similar to the 4.6 degrees/s RMSE for the two-IMU configuration which were found in our study. One explanation for the larger error and the sinusoidal deviation (see Fig. 8.2), found for the one-IMU configuration, may come from the way the IMU was mounted around the wheel axle. Due to the wheel camber angle and a non-zero axle diameter, a small lateral displacement relative to the frame center was induced with each wheel rotation. Since the one-IMU algorithm determines the IMU attitude with respect to the global reference frame (Rupf et al., 2021), these lateral displacements may be interpreted as small wheelchair rotations. Better results might be obtained by attaching the IMU to the lateral side of the wheel axle or by correcting for the lateral displacement induced by wheel rotation. Another possibility is to lower the cut-off frequency of the low-pass filter as done by Rupf et al. (2021). Eventually, optimization of the sensor fusion tuning parameter may further enhance the potential of one-IMU analyses (van Dijk et al., 2021).

Practical implications and limitations

Overall, the hypothesis that a lower number of IMUs would result in less accurate wheelchair kinematics was confirmed by this study. Given the mean error (0.03 m/s) with regard to linear wheelchair velocity for the one-IMU configuration, this configuration may well be used to determine average velocity or distance covered over a certain time interval (e.g., over a 3-minute interval at 1.4 m/s [low-point player], the distance covered deviates approximately 2%, or 5m, over 250m). However, to assess wheelchair (angular) velocity at the push level or to accurately determine field position, the three-IMU configuration is advised. Depending on the intended accuracy and resources available, fewer than three sensors may be used to obtain wheelchair kinematics.

Although this study provides a clear overview on the trade-off between number of sensors and accuracy regarding wheelchair kinematics, a few limitations should be noted. The number of wheelchair athletes was relatively low and top speeds that were achieved during the measurements were lower than during wheelchair sports matches due to the limited measurement area. Still, the results of this study are expected to be well transferable to wheelchair match settings since all subject groups showed similar trends, most participants

performed the measurements in their own wheelchair and a wide variety of wheelchair sport-specific situations were included.

Conclusion

The present study aimed to quantify the trade-off between the number of sensors and accuracy for measuring wheelchair kinematics in wheelchair court sports. Results revealed that a lower number of IMUs used in the configuration would result in a lower accuracy of wheelchair kinematics. While one IMU seems sufficient to determine average wheelchair velocity, three IMUs are advised to analyze wheelchair kinematics on a push level. Based on the present results, choices regarding the number of IMUs can be made depending on the aim, required accuracy and resources available.

Conflict of interest statement

No potential conflict of interest was reported by the authors.

Acknowledgements

This work was supported by ZonMw under project number 546003002. This project, named WheelPower: wheelchair sports and data science push it to the limit is a cooperative effort between TU Delft, UMCG, THUAS, VU Amsterdam and is in cooperation with several sports federations collected under the umbrella of NOC*NSF.

Appendix A

$$AV_{wheel,corrected} = AV_{wheel} + \tan(\varphi_{camber}) * \text{Frame angular velocity} * \cos(\varphi_{camber}) \quad (8.2.1)$$

$$LV_{wheel} = AV_{wheel,corrected} * \text{WheelCircumference} \quad (8.2.2)$$

$$d_{axle,center} = \text{WheelBase} / 2 - \sin(\varphi_{camber}) * 0.5 * \text{WheelDiameter} \quad (8.2.3)$$

$$\text{Frame linear velocity} = LV_{wheel} - (\tan(\text{Frame angular velocity} / fs) * d_{axle,center}) * fs \quad (8.2.4)$$

In which, AV_{wheel} the angular wheel velocity, φ_{camber} is the camber angle of the wheels, LV_{wheel} is the linear wheel velocity and $d_{axle,center}$ is the distance from the wheel axle to the frame center. For clarity purposes, wheelchair angular and linear velocity (as indicated in the text) are referred to as *frame* angular and *frame* linear velocity. The calculations are based on the approach as described by van der Slikke et al. (2015).

References

1. Cooper, R.A., DiGiovine, C.P., Boninger, M.L., Shimada, S.D., Koontz, A.M., Baldwin, M.A., 2002. Filter frequency selection for manual wheelchair biomechanics. *J. Rehabil. Res. Dev.* 39, 323-36. PMID: 12173753
2. Madgwick, S.O.H., Harrison, A.J.L., Vaidyanathan, R., 2011. Estimation of IMU and MARG orientation using a gradient descent algorithm. *IEEE Int. Conf. Rehabil. Robot.* 179–185. <https://doi.org/10.1109/ICORR.2011.5975346>
3. Pansiot, J., Zhang, Z., Lo, B., Yang, G.Z., 2011. WISDOM: wheelchair inertial sensors for displacement and orientation monitoring. *Meas. Sci. Technol.* 22, 105801. <https://doi.org/10.1088/0957-0233/22/10/105801>
4. Rupf, R., Tsai, M.C., Thomas, S.G., Klimstra, M., 2021. Original article: Validity of measuring wheelchair kinematics using one inertial measurement unit during commonly used testing protocols in elite wheelchair court sports. *J. Biomech.* 127, 110654. <https://doi.org/10.1016/j.jbiomech.2021.110654>

5. Söderkvist, I., Wedin, P.-Å., 1993. Determining the movements of the skeleton using well-configured markers. *J. Biomech.* 26, 1473–1477. [https://doi.org/10.1016/0021-9290\(93\)90098-Y](https://doi.org/10.1016/0021-9290(93)90098-Y)
6. van der Slikke, R.M.A., Berger, M.A.M., Bregman, D.J.J., Lagerberg, A.H., Veeger, H.E.J., 2015. Opportunities for measuring wheelchair kinematics in match settings; reliability of a three inertial sensor configuration. *J. Biomech.* 48, 3398–3405. <https://doi.org/10.1016/j.jbiomech.2015.06.001>
7. van der Slikke, R.M.A., de Witte, A.M.H., Berger, M.A.M., Bregman, D.J.J., Veeger, D.J.H.E.J., 2018. Wheelchair Mobility Performance enhancement by changing wheelchair properties: What is the effect of grip, seat height, and mass? *Int. J. Sports Physiol. Perform.* 13, 1050–1058. <https://doi.org/10.1123/ijsp.2017-0641>
8. van Dijk, M.P., Kok, M., Berger, M.A.M., Hoozemans, M.J.M., Veeger, D.H.E.J., 2021. Machine Learning to Improve Orientation Estimation in Sports Situations Challenging for Inertial Sensor Use. *Front. Sports Act. Living* 3, 670263. <https://doi.org/10.3389/fspor.2021.670263>
9. Vegter, R.J.K., Lamothe, C.J., de Groot, S., 2014. Inter-Individual Differences in the Initial 80 Minutes of Motor Learning of Handrim Wheelchair Propulsion. *PLOS ONE* 9, 10. <https://doi.org/10.1371/journal.pone.0089729>

In 2023, the World Health Organization has released their Wheelchair Provision Guidelines [1], in which they aim 'to support improved access to appropriate wheelchairs' and describe an 'overall strategy for strengthening assistive technology capacity in any context' for wheelchair users. Moreover, in this document, the first recommendation towards wheelchair provision includes to define an individual assessment based on physical, functional, environment and lifestyle needs and preferences.

To stimulate a healthy wheelchair population, the ability to monitor push technique and track physical activities over time may be helpful [2]. However, monitoring push technique, joint load or force and, e.g., energy expenditure, is not straight-forward. Whereas force-instrumented push-rims can determine those variables by measuring the force applied on the push-rim [3], [4], such a system is expensive and not accessible to wheelchair users. Inertial measurement units (IMUs) are accessible, but in one of our previous studies, we concluded that some crucial parameters, such as push and recovery phase, and force applied, cannot be determined based on IMUs only [5]. Therefore, a system able to distinguish push and recovery phase, while still being inexpensive and lightweight, is required.

In the same study, a preliminary design of such a system, called the RHIDE (rim hit detection) system, was presented. The design consisted of two strips of conductive tape, closely parallel to each other along the perimeter of the push-rim. A voltage was applied to one of the strips to detect a short circuit in the system due to hand contact. Since this system was automatically synchronized with the IMU data, it proved to be very useful. Validation based on visual video images revealed an average underestimation of contact time of 0.03s. Despite the success of this system, it was not usable when hands or rims were wet (e.g. due to sweat) and installing the tape on the rim was relatively time-consuming. The idea of combining existing push-rim covers with the electronics required for the RHIDE system then led - after several design iterations - eventually to the current version of the RHIDE system. The current system can be easily installed around the push-rim of a wheelchair, is robust in wet conditions, and works with (thin) gloves, and it has therefore developed in a suitable system to determine push- and recovery phase during overground wheelchair propulsion. Because it has remained affordable and lightweight, the system would be accessible for all wheelchair users, athletes, coaches, scientists, and therapists, and may serve as a smart watch for wheelchair users. However, some developments still need to be made to translate the current version into a marketable product.

Recognizing the RHIDE system's potential to strengthen assistive wheelchair technology and offer insights into individual physical and functional capabilities within wheelchairs, the invention has been patented. This chapter elucidates the RHIDE system's design, presents its output parameters, and reports the corresponding patent publication, marking a significant step towards stimulating further development and market introduction.

System design: Mechanical and Electronic design

After several design iterations, the latest version of the system consists of two sensing systems, a capacitive sleeve with integrated sensor array to detect the angular position and time instant of each hand (or limb) contact, and a wireless IMU to measure wheelchair kinematics.

The first component is a capacitive sleeve (see Fig. 9.1a and 9.2), similar to already existing push-rim covers that have been used to increase grip, comfort or aesthetics. The sleeve consists of a 2 mm rubber PVC hose, with the same length as the circumference of the wheelchair rim, on which 24 (10 x 3 cm) copper tapes are attached. The hose is cut in the length

direction so it can be clamped around the rim. The copper tapes are connected to a capacitive touch sensor module (MPR121), such that the proximity of hands (and other limbs) can be detected. Subsequently, the micro-controller (see Fig. 9.1b) was set in such a way that only touching the rim (i.e., proximity equal to the thickness of the copper-covering layer) would lead to a detectable signal.

The second component is the IMU (NGIMU, X-io Technologies, Colorado Springs, United States [used in Prototype I]; 100 Hz; see Fig. 9.1c), which is a lightweight sensor that measures three-dimensional angular velocity and three-dimensional linear acceleration. With these measures, the wheelchair's acceleration, velocity, covered distance and rotations can be obtained as described in a previous study [6]. Data of the capacitive sleeve can be saved to the IMU (which sends all data to a laptop via WIFI-connection and X-io Technologies software).

In the most recent prototype (March 2024) the two components are integrated in an 'integrated unit design' making the system easier to install, more robust and lighter weight. To increase compatibility and avoid wireless connection errors, data are saved to an SD-card (see Fig. 9.3).



Figure 9.1a-c. The RHIDE system [prototype version November 2022] and its different components. Fig. 9.1a (left) shows the capacitive sleeve attached to a wheelchair push-rim, Fig. 9.1b (middle) shows how the cables from the capacitive sleeve connect with the left side of the microcontroller unit (black square) and the cable of the IMU (around the wheel axis) is connected via a red wire to the microcontroller unit. Fig. 9.1c (right) shows the IMU.

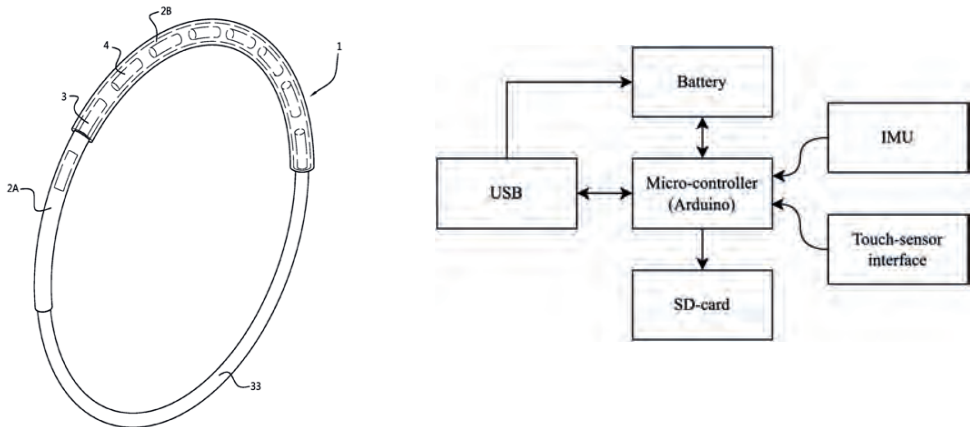


Figure 9.2 (left) and 9.3 (right). Fig. 9.2 is a schematic figure of a wheelchair push-rim (nr. 33) – which is not part of the RHIDE system, the inner sleeve (nr. 2A), two separated capacitive sensors (nr. 3 and 4) and an outer layer (nr. 2B). Fig. 9.3. Block diagram of the integrated unit design of the RHIDE system.

Output: contact time & duration

The output data of the RHIDE system consists of an electric potential for each capacitive sensor (i.e., for each of the 24 pieces of copper tape) over time (see Fig. 9.4a and 9.4b). Based on this, contact time and contact duration can be assessed. Since the RHIDE system is synchronized with the IMU data, contact information can easily be coupled to wheelchair velocity, wheelchair acceleration and other IMU-based variables.

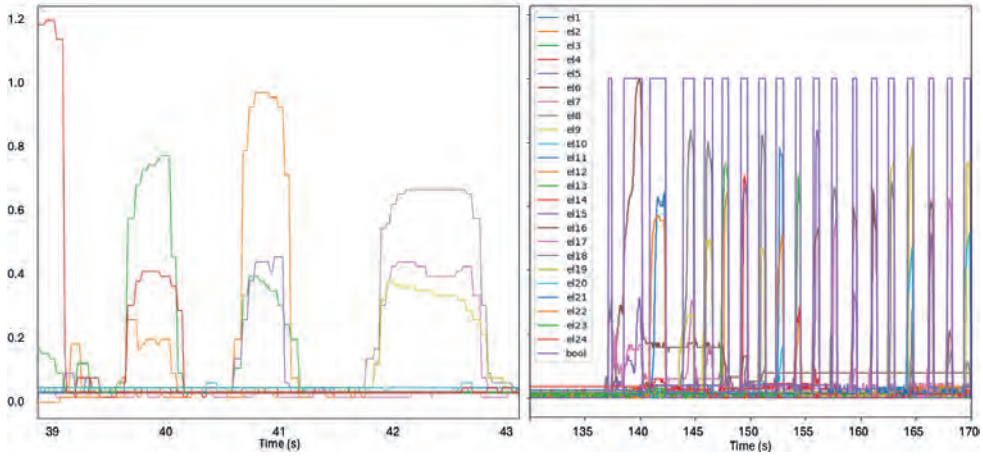


Figure 9.4a-b. In Fig. 9.4a (left) the raw signal of the RHIDE system is visualized. During one touch, multiple capacitive sensors – each represented by a different color - can be ‘touched’ simultaneously. In Fig. 9.4b (right) the signal of each conductive element is transferred to a ‘contact Boolean’ in which 1 represents ‘contact’ and 0 represents ‘no contact’.

Output: contact position

Once the relative position of (at least) one electrode with respect to the wheel-mounted IMU is known, the IMU orientation [6] can be used to obtain information about the position of touch as well. In this way, initial contact angle, contact release angle and push angle can be obtained (see Fig. 9.5).

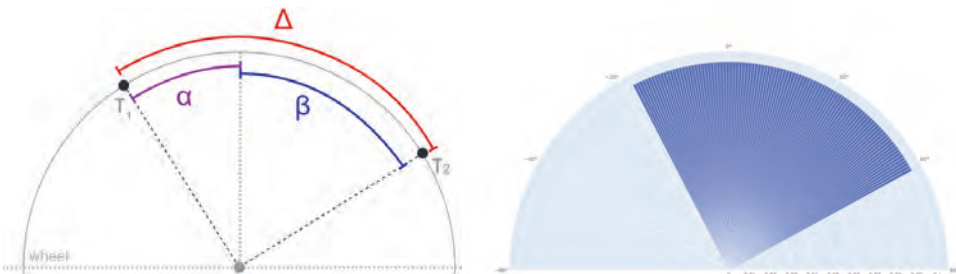


Figure 9.5a-b. In Fig. 9.5a (left) the definitions of push angle (Δ), initial contact angle (α) and contact release angle (β) are indicated. The time duration between the time instant of initial contact (i.e., T_1) and contact release (i.e., T_2) is referred to as contact time. Fig. 9.5b (right) shows a way of visualizing these data.

Accuracy

The accuracy was assessed by comparing the RHIDE data (contact time and contact location) with video data. Mean differences between the two systems are 0.00 ± 0.01 s for contact time and around -0.5 ± 14.0 degrees for contact location (either initial contact angle or hand release angle). More details will be published as soon as a manuscript about this validation of the RHIDE system is ready. The writing is currently in progress.

Conclusion

This chapter outlines the aim and design underlying the patent publication (reported below) of the RHIDE system. As the system seems to be accurate in determining push time, duration, and push angle, it has great potential to become a wheelchair-suitable activity tracker. When the system is combined with an IMU on the wheelchair wheel, it could be used to monitor and give feedback regarding push- and recovery phase, contact angles and, eventually, (tangential) force applied to the rim. Future research should investigate the accuracy of these variables. In addition, the usability and acceptance of the system in daily practice is yet to be investigated.

Acknowledgements

The authors would like to thank Rienk van der Slikke, Oscar Bliet, Jeroen Koot, Sander Roux, Puck Willemse, Wouter Gregoor, Giel Hermans, and Hans van der Does for their valuable contributions to the system.

Funding

This work was supported by the combined health and sports idea accelerator grant 'Technology that makes people move' assigned by TU Delft Health Initiative and TU Delft Sports Engineering Institute. The project was named: 'Fitrim: Wheelchair power to the people'.

References

1. (2023) Wheelchair Provision Guidelines. World Health Organization, Geneva
2. van der Woude L.H.V., Veeger H.E.J., Dallmeijer A.J., Janssen T.W.J., Rozendaal L.A. (2001). Biomechanics and physiology in active manual wheelchair propulsion. *Med Eng Phys* 23:713–733
3. de Groot S., Vegter R., Vuijk C., Dijk .F, Plaggenmarsch C., Sloots M., Stolwijk-Swaeste J., Woldring F., Tepper M., Woude L. (2014). WHEEL-I: Development of a wheelchair propulsion laboratory for rehabilitation. *J Rehabil Med* 46:493–503
4. Chénier F., Pelland-Leblanc J-P., Parrinello A., Marquis E., Rancourt D. (2021). A high sample rate, wireless instrumented wheel for measuring 3D pushrim kinetics of a racing wheelchair. *Med Eng Phys* 87:30–37
5. van Dijk M.P., van der Slikke, R.M.A., Berger, M.A.M., Hoozemans, M.J.M., Veeger H.E.J. (2021). Look mummy, no hands! The effect of trunk motion on forward wheelchair propulsion. 39th ISBS Conf 4
6. van Dijk M.P., van der Slikke R.M.A., Rupf R., Hoozemans M.J.M., Berger M.A.M., Veeger H.E.J. (2022). Obtaining wheelchair kinematics with one sensor only? The trade-off between number of inertial sensors and accuracy for measuring wheelchair mobility performance in sports. *J Biomech* 130:110879

Patent publication

Family: [WO2023033646 \(A1\)](#) - A METHOD FOR AUTOMATICALLY MEASURING A PROPULSIVE POWER APPLIED TO A PUSHRIM OF A WHEELCHAIR BY A USER OF THE WHEELCHAIR

Uitvinder(s): VAN DIJK MARIA PETRONELLA [NL]; BLIEK OSCAR [NL]; VAN DER SLIKKE RIENK MICHIEL ARJEN [NL] ± (VAN DIJK, Maria Petronella, ; BLIEK, Oscar, ; VAN DER SLIKKE, Rienk Michiel Arjen)

Aanvrager(s): UNIV DELFT TECH [NL] ±

Classificatie:

- international: [A61G5/02](#)
- cooperative: [A61G5/022 \(EP\)](#); [A61G5/028 \(EP\)](#)

Aanvraagnummer: WO2022NL50493 20220830 [Global Dossier](#)

Prioriteitsnummer(s): [NL20212029083](#) [20210831](#)

Ook gepubliceerd als: [NL2029083 \(B1\)](#)

https://nl.espacenet.com/publicationDetails/originalDocument?CC=WO&NR=2023033646A1&KC=A1&FT=D&ND=3&date=20230309&DB=&locale=nl_NL





- (51) International Patent Classification:
A61G 5/02 (2006.01)
- (21) International Application Number:
PCT/NL2022/050493
- (22) International Filing Date:
30 August 2022 (30.08.2022)
- (25) Filing Language: English
- (26) Publication Language: English
- (30) Priority Data:
2029083 31 August 2021 (31.08.2021) NL
- (71) Applicant: TECHNISCHE UNIVERSITEIT DELFT
[NL/NL], Stevinweg 1, 2628 CN DELFT (NL).
- (72) Inventors: VAN DIJK, Maria Petronella; TU Delft, Innovation & Impact Centre, Postbus 5, 2600 AA DELFT (NL). BLIEK, Oscar; TU Delft, Innovation & Impact Centre, Postbus 5, 2600 AA DELFT (NL). VAN DER SLIKKE, Rienk Michiel Arjen; TU Delft, Innovation & Impact Centre, Postbus 5, 2600 AA DELFT (NL).
- (74) Agent: ALGEMEEN OCTROOI- EN MERKENBU-
REAU B.V., P.O. Box 645, 5600 AP EINDHOVEN (NL).
- (81) Designated States (unless otherwise indicated, for every kind of national protection available): AE, AG, AL, AM,

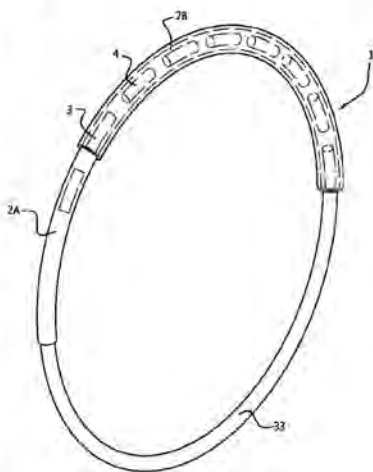
AO, AT, AU, AZ, BA, BB, BG, BH, BN, BR, BW, BY, BZ, CA, CH, CL, CN, CO, CR, CU, CV, CZ, DE, DJ, DK, DM, DO, DZ, EC, EE, EG, ES, FI, GB, GD, GE, GH, GM, GT, HN, HR, HU, ID, IL, IN, IQ, IR, IS, IT, JM, JO, JP, KE, KG, KH, KN, KP, KR, KW, KZ, LA, LC, LK, LR, LS, LU, LY, MA, MD, ME, MG, MK, MN, MW, MX, MY, MZ, NA, NG, NI, NO, NZ, OM, PA, PE, PG, PH, PL, PT, QA, RO, RS, RU, RW, SA, SC, SD, SE, SG, SK, SL, ST, SV, SY, TH, TJ, TM, TN, TR, TT, TZ, UA, UG, US, UZ, VC, VN, WS, ZA, ZM, ZW.

- (84) Designated States (unless otherwise indicated, for every kind of regional protection available): ARIPO (BW, GH, GM, KE, LR, LS, MW, MZ, NA, RW, SD, SL, ST, SZ, TZ, UG, ZM, ZW), Eurasian (AM, AZ, BY, KG, KZ, RU, TJ, TM), European (AL, AT, BE, BG, CH, CY, CZ, DE, DK, EE, ES, FI, FR, GB, GR, HR, HU, IE, IS, IT, LT, LU, LV, MC, MK, MT, NL, NO, PL, PT, RO, RS, SE, SI, SK, SM, TR), OAPI (BF, BJ, CF, CG, CI, CM, GA, GN, GQ, GW, KM, ML, MR, NE, SN, TD, TG).

Published:
— with international search report (Art. 21(3))

(54) Title: A METHOD FOR AUTOMATICALLY MEASURING A PROPULSIVE POWER APPLIED TO A PUSHRIM OF A WHEELCHAIR BY A USER OF THE WHEELCHAIR

Fig. 2B



(57) Abstract: A computer-implemented method for measuring a propulsive power exerted on a pushrim of a wheelchair by a user of said wheelchair, comprising: determining a wheelchair energy state at a first moment, F1, and determining a wheelchair energy state at a second moment, F2, the energy states determined based upon a mass and a velocity and/or a mass and an acceleration of the wheelchair; estimating a mean resistance force acting on the wheelchair in between the first and second instance, Ff; determining a distance covered in between the first, F1, and the second, F2, instance, s; automatically determining a duration of contact between a limb of the user and a pushrim of the wheelchair in between the first, F1 and the second, F2, time instance, t; and determining the propulsive power exerted on the pushrim of the wheelchair by said user based on F1, F2, Ff, s and t





CHAPTER 10

General discussion

The aim of this dissertation was to enable non-invasive and inexpensive mechanical power monitoring during overground hand-rim wheelchair propulsion, mainly in the context of wheelchair sports. Based on the well-founded theoretical framework for wheelchair propulsion (Chapters 2 and 3), a method was developed to monitor power output in straight-line wheelchair field- and court sports by placing one IMU on the wheel axis and one IMU on the wheelchair frame. With these two sensors, a deceleration test in the environment of interest (see Fig. 10.1), and a known rear wheel diameter and total mass, mechanical power can be monitored with an average accuracy of 2.4% (Chapter 5) for situations in which air resistance can be assumed negligible (i.e., velocity < 2.5 m/s). The accuracy, however, is reduced to 6% for wheelchair users that show considerable forward-backward trunk motion during wheelchair propulsion (Chapters 4 and 5). These inaccuracies can be corrected up to 0.5% by adding an additional IMU attached to the chest in combination with a (machine learning-based) prediction of load distribution (Chapter 6). When the power output correction was applied during 10m overground sprints of amateur and elite wheelchair tennis players, mean power outputs were comparable with mean power output of 10m sprints on a wheelchair ergometer (Chapter 7). As the demands of different wheelchair populations differ, depending on the required accuracy, only one IMU on the wheel axle can be used to obtain wheelchair kinematics and thus power (Chapter 8). A rim hit detection (RHIDE) system can be used to distinguish push and non-push phases, and to obtain contact angle (Chapter 9). To summarize, depending on the wheelchair user demands, one may use one, two or three IMUs (with or without RHIDE system) for on-field monitoring of mechanical power during straight-line wheelchair propulsion in wheelchair (sports) practice (see Table 10.1).

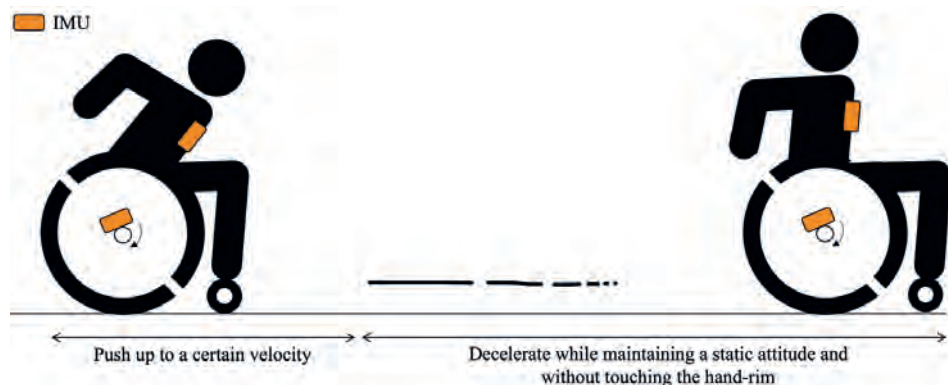







Figure 10.1. Overview of a deceleration test of a wheelchair athlete with the advised sensor set, i.e., one IMU attached at the trunk and one around the wheel axle. A third IMU can be placed on the wheelchair frame (not visible in the present figure) to determine wheelchair rotations.

Table 10.1.

An overview of the accuracies for different kinematic variables during wheelchair propulsion obtained from different sensor configurations and for different type of sensors. The accuracies are obtained from Chapter 8 (1 and 2 IMUs), van der Slikke et al. [12] (3 IMUs) and Chapter 9 (RHIDE). Errors of the RHIDE system were calculated based on manual comparisons with video data. Errors of the IMUs are based on comparisons with optical motion capture data.

	Linear velocity (m/s)	Ang. Velocity (deg/s)	Contact time (s)	Contact angle (deg)	Initial contact angle (deg)
					
Mean error					
1 IMU	-0.03 (0.05)	-0.1 (0.3)	-	-	
2 IMU's	-0.02 (0.05)	-0.2 (0.3)	-	-	
3 IMU's	-0.01 - 0.01	-0.22 - 0.14	-	-	
RHIDE	-	-	.008 +- .085	-4.8 +- 17.6	-0.5 +- 14.0
RMSE					
1 IMU	0.19 (0.11)	11.2 (3.3)	-	-	
2 IMU's	0.20 (0.10)	4.6 (4.9)	-	-	
3 IMU's	0.02 - 0.09	3.1 - 6.8	-	-	
RHIDE	-	-	.085	18.2	14.0

Putting into perspective – choices made and consequences for interpretation

Before interpreting the results of this dissertation, some considerations are discussed. Firstly, to create the power balance and to validate IMU-based power calculations (as explained in Chapters 2, 3, and 5) we used a model in which the athlete-wheelchair combination is considered a rigid body (athlete-wheelchair model, see Chapter 3) or the wheelchair is considered a rigid body (wheelchair model, see Chapter 3). However, both models are a simplification of the reality, because manually propelling the rear wheels of a wheelchair obviously results from moving (body) parts relative to each other. Although moving these body parts will cost (muscle) force and thus power [1], this energy is disregarded in the external, or mechanical power, due to the assumption that the ‘bodies’ are rigid. One should thus be aware of this assumption, when interpreting power values. In wheelchair rugby, for example, overcoming a ‘block’ of opponents may cost a lot of energy (mainly due to muscle power), but as long as the wheelchair is blocked, and the wheels of the wheelchair are thus not moving (velocity = 0), no power is transferred to the environment, and mechanical power is zero given the two models as described in Chapter 3. However, when considering propulsive power, we believe that the rigid body models as presented in Chapter 3 are the most suitable for monitoring power and provide a solid foundation to build upon in future studies.

Secondly, both the reference mechanical power and the IMU-based power were calculated based on the same drag tests (the drag tests to determine F_{drag} used in the IMU-model was used to determine the rolling resistance coefficients for the gold standard power values as well). A measurement error in F_{drag} would therefore not result in a decreased accuracy. Given that previous studies found a standard deviation of 16% in the IMU-based deceleration during standardized coast-down tests on different surfaces [2], the actual deviation of our power

estimates might be larger than the values found in Chapters 3 and 5. This means that an error of $(2.4\% * 1.16 =) 2.8\%$ for moderate trunk motion and $(3.3\% * 1.16 =) 3.8\%$ for full trunk motion may be realistic. Assuming an average error of 4% will be thus safe. Chapter 5 reveals that the degree of trunk inclination is related to the ‘underestimation’ of rolling resistance. In addition, during the first pushes from stand-still, a wheelchair athlete (with sufficient trunk function) inclines his or her torso 60-70 degrees (Chapter 4). A realistic maximum error will thus be around $(8\% * 1.16 =) 9.3\%$.

A third design choice in the present dissertation was to use a large (3.0 x 5.0m) treadmill to validate our IMU-based estimates. The treadmill is a suitable medium 1) to gain insight into wheelchair propulsion dynamics and the influence of upper body movements, 2) to validate power estimates based on gold standard motion capture data [3], and 3) is more similar to regular overground wheelchair propulsion compared to wheelchair ergometers or force-instrumented push-rims. However, small differences exist between treadmill-based wheelchair propulsion and overground wheelchair propulsion, as air friction during treadmill measurements is minimal - velocity relative to the air is almost zero - and accelerating from stand-still cannot well be replicated. Despite these remarks, van der Woude et al. [4] reported that ‘treadmill wheelchair propulsion is mechanically realistic, showing a natural form of wheelchair propulsion’. Treadmill-based validations were thus considered the best choice for this phase of power monitoring development. This choice is supported by a recent study of Maier et al. [3] that used a similar method to assess the accuracy of cycling power meters based on a mechanical model of treadmill cycling. Nevertheless, additional validation of our IMU-based model could have been performed with measurement wheels. Despite adding unrealistic masses - which leads to unrealistic wheelchair dynamics - and invalid values in situations where the upper body adds power to the system, these measurement wheels could help to demonstrate the validity of the IMU-based power once again during (real) overground wheelchair propulsion.

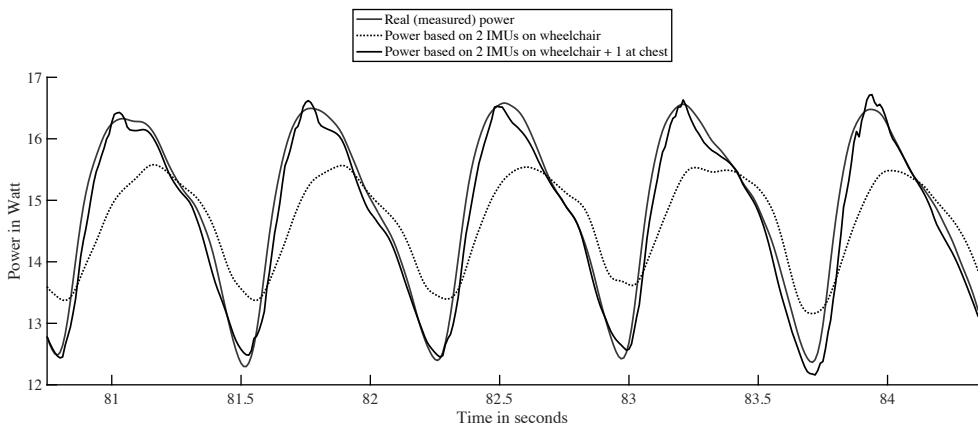


Figure 10.2. Comparison between measured mechanical power (blue), power estimated with two IMUs on the wheelchair (black dotted line, see Chapters 3 and 5), and power estimated with two IMUs on the wheelchair and one IMU at the chest (black solid line, see Chapter 6).

Comparison with other state-of-the-art power meters

Given a safe margin of 4% accuracy for power estimates with a maximal deviation of 9.3%, the next question is: What do these numbers actually mean? Therefore, comparisons with other state-of-the-art power meters were done. For wheelchair sports, Vegter et al. [5] performed measurements with two types of instrumented wheels during a 4-minute block of hand-rim wheelchair propulsion on a motor-driven treadmill. They reported an average difference of -0.03 W for different intensities and participants. However, the mean absolute error between the reported values of the two systems was 7% over 4 minutes, and for the participant in which the largest deviations were found a 14% difference was reported. In road cycling, power meters are reported to deviate on average 0.9-3.2% [3]. For rowing, errors of 8-17% were found for the most accurate power meters [6], which was similar to the 11.6% found for (user-independent) power in roller ski skating [7]. Given these numbers, the accuracies of the IMU-based power estimates as reported in this dissertation can be assumed to be at least comparable to other power measurement systems.

Practical implications: New possibilities for monitoring power in wheelchair (sports) practice

In the introduction, the drawbacks of previous systems that measure power during wheelchair propulsion were discussed. Whereas the wheelchair ergometer imposes unrealistic wheelchair dynamics which differ from overground propulsion, the force-instrumented push-rims affect propulsion dynamics by their heavy mass. With the newly developed method to estimate power from IMU data, both drawbacks are overcome since IMUs are lightweight and can be used during overground wheelchair propulsion. Moreover, IMUs are much cheaper (ca. €60,-) than an ergometer device (> €50.000,-) or force-instrumented push-rims (> €20.000,-). Unlike other systems, IMU-based power monitoring is non-invasive and inexpensive.

The IMU-based method therefore allows athletes to be monitored on a daily basis and to get feedback on mechanical power from the coaching staff. Consequently, coaches can use the information to monitor and enhance athlete performance, to track fitness and fatigue and to, eventually, reduce the risk of injuries. In addition, to support the interpretation of power data an athlete power profile can be developed in which the physical capacities of athletes are objectively represented. One example of a power profile that has been used in cycling is a diagram in which the maximal power that can be obtained per time duration is given (e.g., maximal power that an athlete can maintain for 1-5 seconds versus the maximal power that an athlete can obtain for 0.5-1 hour) [8, 9], see Fig. 10.3. Such a power profile may be used to identify strengths and weaknesses, and to individualize the training programs based on this. Lastly, as high associations were found between lab and field tests (see Chapter 7), the salient (power-related) features that were identified in the field may subsequently be analyzed in more detail during periodic lab-based ergometer measurements. These analyses may result in recommendations for training. For example, when lab analyses point out that less force can be produced at high wheelchair velocities, i.e., an athlete has a steep force-velocity curve [10], the recommendation could be: 'practice power production at a high velocity'. Subsequently, IMUs can be used to monitor the athlete's progression during daily practice in the field.

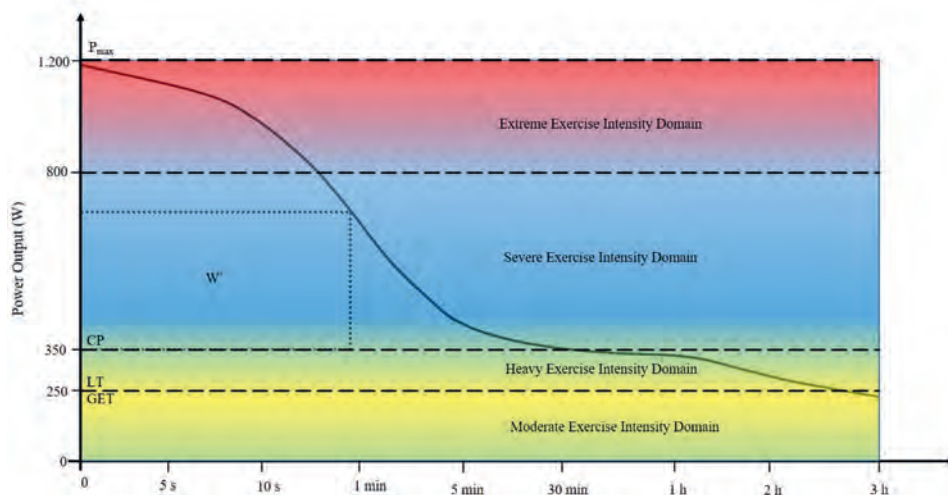


Figure 10.3. Example of a power profile as reported in the study of Leo et al. [8].

In addition to power, athletes and coaches can obtain information about push technique using the RHIDE system as explained in Chapter 9. As the system measures hand contact angle and push duration, useful push characteristics can be obtained. Coaches can compare push techniques between athletes or between fit and fatigue states and can, in this way, gain more insight into the most effective push technique. This will be mainly beneficial in wheelchair racing as push technique is crucial in this discipline, but may also be used for wheelchair tennis, basketball, and rugby. In addition, the RHIDE system can be used in rehabilitation practice, as hand contact angle has been associated with shoulder loading [11]. Lastly, tracking push characteristics and performance can act as an additional motivator for both novel as well as experienced wheelchair users and athletes to maintain a healthy lifestyle.

The results of the present dissertation led to an accessible and ambulatory power monitoring system. Therefore, the IMU-based methods can be used to collect wheelchair propulsion data on a larger scale for many different objectives. For example, more insight could be gained into wheelchair propulsion technique, the development of injuries, different power requirements between field positions in ball sports like wheelchair basketball, the influence of different training modalities on power gains (and losses), and differences between classifications in different wheelchair sports.

Lastly, the new insights on wheelchair propulsion technique and, e.g., the intra-cyclic and inter-cyclic variations in rolling resistance during wheelchair propulsion, may be used to improve the interpretation of ergometer data. As, with a trunk-mounted IMU, the instantaneous load distribution between the front- and rear wheels during propulsion can be estimated (see Chapter 6), a realistic load profile can be obtained. Currently, wheelchair ergometers have a static resistance force programmed, which becomes *lower* when a wheelchair user inclines the trunk (less load on the rollers located below the rear wheels) and *higher* when a user has an upright position (more load on the rollers). With the instantaneous load distribution prediction from Chapter 6, a realistic resistance force may be imposed depending on the upper body movements of the wheelchair user. In this way, wheelchair dynamics might be made more realistic and better translatable to overground wheelchair propulsion.

The missing pieces of the power puzzle

Despite the wealth of new possibilities regarding measuring mechanical power during wheelchair propulsion with our novel method, still some pieces of the puzzle need to be found.

First, the presented methodology is only tested during straight-line wheelchair propulsion. As turning involves unknown factors such as rotational inertia and increased rolling resistance due to e.g. slip [12], the IMU-based power estimations are not yet valid for turning. This implies that information on power should be gained during the straight-line propulsion parts of a training or competition, which can be identified from IMU-based frame rotation [13]. This still provides useful data for wheelchair basketball and rugby, although for wheelchair tennis - which is characterized by continuous rotations - selecting straight-line propulsion parts may yield limited information. Further development of the current methodology for turning would allow power to be monitored during an entire training session or competition of wheelchair field sports, such that more complete picture can be obtained, and specific power aspects could be distinguished.

Second, power monitoring is not yet available for wheelchair racing. The velocities during wheelchair racing are much higher compared to wheelchair field sports, such that air resistance plays a considerable role and cannot be ignored like in indoor field sports (see Chapter 2). Moreover, air resistance varies with relative wind velocity and direction (which might change any moment), such that resistance values should ideally be updated every minute. In addition, during outdoor training sessions or competitions (outside the track), the surface - and thus rolling resistance - may change continuously as well. Therefore, monitoring power during situations in which the circumstances continuously change will lead to biased estimates.

Third, to make the application of power monitoring using IMUs even more feasible, standardized deceleration tests should be made redundant. To this end, multiple attempts were made to estimate (rolling) resistance forces based on short deceleration periods during a training routine or competition, which are so-called non-standardized deceleration tests. Also, (rolling) resistance forces have been estimated during the recovery phase of a single push. Below some (unpublished) results are presented based on the World Championships Wheelchair Rugby in 2022. Rolling resistance estimates based on standardized deceleration tests (as proposed in this dissertation) and non-standardized deceleration tests were compared for periods in which the wheelchair decelerated in a (more or less) linear trajectory. Unfortunately, the results show that rolling resistance estimated from non-standardized deceleration tests are not sufficiently accurate for power estimates (see Fig. 10.4). It is likely that athletes actively brake during deceleration, or make turns, or move the upper body, such that the values obtained from these non-standardized deceleration periods are not accurate enough for power monitoring. For now, regardless of the type of sport, standardized deceleration tests should thus still be included in the warming-up or cooling-down routine to ensure accurate power estimates.

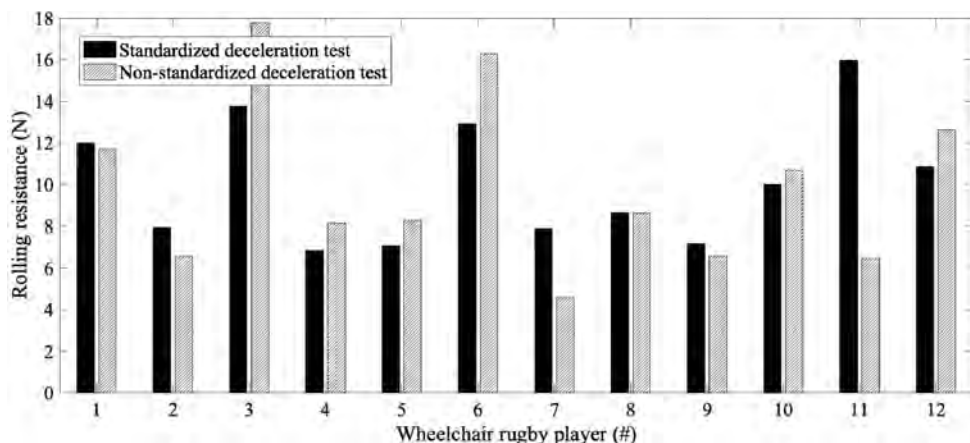


Figure 10.4. (Rolling) resistance forces estimated from ‘standardized’ deceleration tests (as proposed in Chapter 3 – in black) versus ‘non-standardized’ deceleration tests (striped) for periods in which the wheelchair decelerated in a (more or less) linear trajectory. Data were collected during the World Championships Wheelchair Rugby in 2022.

Future directions for power in wheelchair propulsion

The present dissertation adds valuable information to both wheelchair (sports) practice as well as in wheelchair-related scientific research. Future studies can build upon the results and algorithms presented in this dissertation. Some suggestions for future directions are presented below.

Resulting from the ‘impossibilities’ mentioned in the previous section, the first goal to improve power monitoring in wheelchair practice in the future will be to investigate the power balance during turning or cornering. Second, enabling power monitoring in situations with changing circumstances, for instance because of wind or different surfaces, is desired. When an ‘adaptive’ resistance value can be determined, power monitoring can be applied in wheelchair racing as well. The reason for this is that, in wheelchair basketball, rugby or tennis, the surface will not change during a training or competition (such that rolling resistance parameters remain more or less constant), while in wheelchair racing, both the surface as well as the wind velocity and wind direction – affecting air resistance – are likely to change. Our first attempt in a preliminary study to determine this ‘adaptive’ resistance value during the recovery phases in wheelchair racing yielded unrealistic predictions, likely because the trunk and arms move a lot during wheelchair racing. Third, more research is required to make standardized deceleration tests redundant. To this end, the results of Chapter 6 may be useful as variations in rolling resistance play a key role in predicting the rolling resistance coefficients.

In addition, the IMU-based method presented in this dissertation gives a cycle-average mechanical power, which is the average power over both push and recovery phase. Extending the methodology with the estimation of peak power and push-phase power might be a valuable addition, since peak power is a commonly used performance measure [14, 15], and ‘push’ power may be easier to interpret as this measure is commonly given by wheelchair ergometers and force-instrumented push-rims [16, 17]. Push-phase power can already be determined, by combining the RHIDE system (see Chapter 9) - distinguishing ‘push’ and ‘recovery’ phases - with the cycle average power. When the RHIDE system is also combined with the predicted front

wheel load from Chapter 6, instantaneous power and thus peak power can be estimated as well. Future studies should investigate how accurate these estimates will be.

Lastly, new developments in the field of power measuring in wheelchair propulsion are continuously presented. Recently, two novel force-instrumented push-rims have been developed that, with less mass, can measure power during wheelchair propulsion [18, 19]. In addition, artificial intelligence has been used throughout the present dissertation to solve pieces of the puzzle that could not easily be solved using classic mechanics. If the application of AI is chosen wisely, it will yield many more solutions in the field of wheelchair sports.

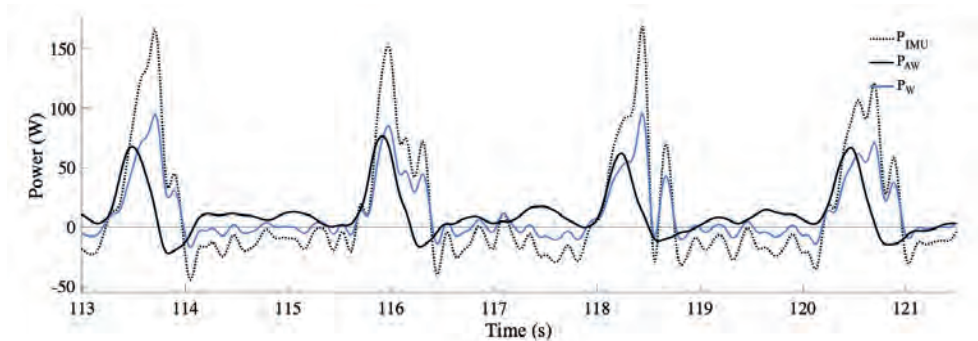


Figure 10.5. Typical example of the instantaneous power graph of power determined from optical motion capture data according to the athlete-wheelchair model described in Chapter 3 (black solid line), according to the wheelchair model described in Chapter 3 (blue solid line) and the IMU-based mechanical power (black dotted line). The data is of approximately four pushes on a treadmill at 1.2 m/s.

Conclusion

With two IMUs attached to the wheelchair (attached to the wheelchair wheel and frame), a proper deceleration test in the environment of interest, and a known rear wheel diameter and total mass, mechanical power can be monitored relatively accurate during straight-line hand-rim propulsion in indoor wheelchair field- and court sports. For daily wheelchair users and recreational-level athletes, the use of one IMU will suffice for decent power estimates. In addition, for 1) a more accurate power estimation, 2) situations with considerable trunk motion or 3) determining peak power, the use of an additional wearable (i.e., a trunk-mounted IMU and/or a hand-rim touch-detection [RHIDE] system) is advised. IMUs and/or a RHIDE system are suitable to enhance performance and reduce injury risk in a non-invasive and inexpensive way. As these power estimates assume that air resistance is negligible, some additional steps are required to make the method valid for wheelchair racing as well.

References

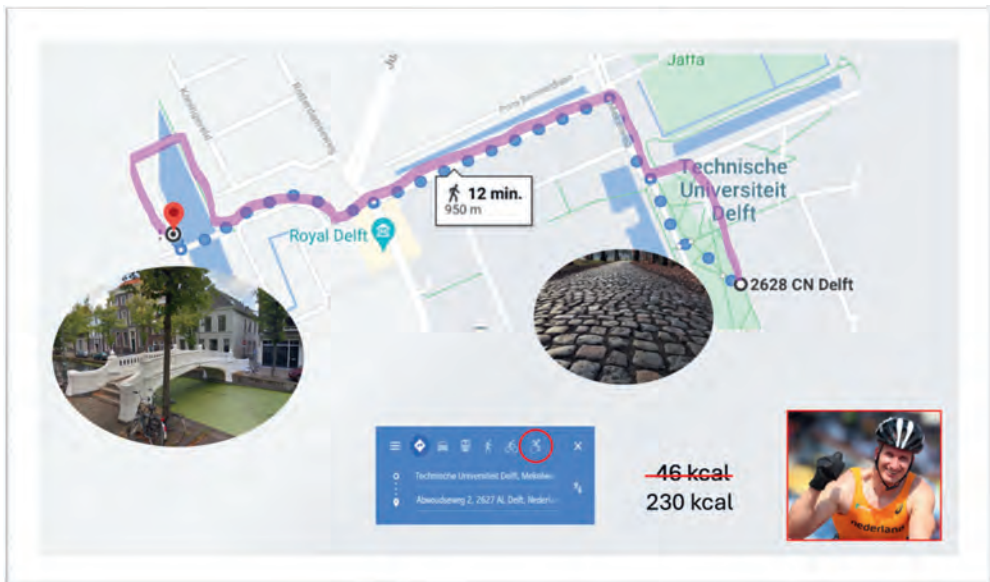
1. van Ingen-Schenau GJ, Cavanagh PR (1990) Power equations in endurance sports. *J Biomech* 23:865–881
2. Rietveld T, Mason BS, Goosey-Tolfrey VL, van der Woude LHV, de Groot S, Vegter RJK (2021) Inertial measurement units to estimate drag forces and power output during standardised wheelchair tennis coast-down and sprint tests. *Sports Biomech* 1–19
3. Maier T, Schmid L, Müller B, Steiner T, Wehrin J (2017) Accuracy of Cycling Power Meters against a Mathematical Model of Treadmill Cycling. *Int J Sports Med* 38:456–461
4. van der Woude LHV, Veeger HEJ, Dallmeijer AJ, Janssen TWJ, Rozendaal LA (2001) Biomechanics and physiology in active manual wheelchair propulsion. *Med Eng Phys* 23:713–733
5. Vegter RJK, Lamoth CJ, De Groot S, Veeger DHEJ, Van Der Woude LHV (2013) Variability in bimanual wheelchair propulsion: Consistency of two instrumented wheels during handrim wheelchair propulsion on a motor driven treadmill. *J NeuroEngineering Rehabil* 10:1–1
6. Holt AC, Hopkins WG, Aughey RJ, Siegel R, Rouillard V, Ball K (2021) Concurrent Validity of Power From Three On-Water Rowing Instrumentation Systems and a Concept2 Ergometer. *Front Physiol* 12:758015
7. Uddin MZ, Seeberg TM, Kocbach J, Liverud AE, Gonzalez V, Sandbakk Ø, Meyer F (2021) Estimation of Mechanical Power Output Employing Deep Learning on Inertial Measurement Data in Roller Ski Skating. *Sensors* 21:6500
8. Leo P, Spragg J, Podlogar T, Lawley JS, Mujika I (2022) Power profiling and the power-duration relationship in cycling: a narrative review. *Eur J Appl Physiol* 122:301–316
9. Pinot J, Grappe F (2011) The Record Power Profile to Assess Performance in Elite Cyclists. *Int J Sports Med* 32:839–844
10. Janssen RJF, De Groot S, Van der Woude LHV, Houdijk H, Goosey-Tolfrey VL, Vegter RJK (2023) Force–velocity profiling of elite wheelchair rugby players by manipulating rolling resistance over multiple wheelchair sprints. *Scand J Med Sci Sports* 33:1531–1540
11. Requejo PS, Mulroy SJ, Ruparel P, Hatchett PE, Haubert LL, Eberly VJ, Gronley JK (2015) Relationship Between Hand Contact Angle and Shoulder Loading During Manual Wheelchair Propulsion by Individuals with Paraplegia. *Top Spinal Cord Inj Rehabil* 21:313–324
12. Caspall JJ, Seligsohn E, Dao PV, Sprigle S (2013) Changes in inertia and effect on turning effort across different wheelchair configurations. *J Rehabil Res Dev* 50:1353–1362
13. van der Slikke RMA, Berger MAM, Bregman DJJ, Lagerberg AH, Veeger HEJ (2015) Opportunities for measuring wheelchair kinematics in match settings; reliability of a three inertial sensor configuration. *J Biomech* 48:3398–3405

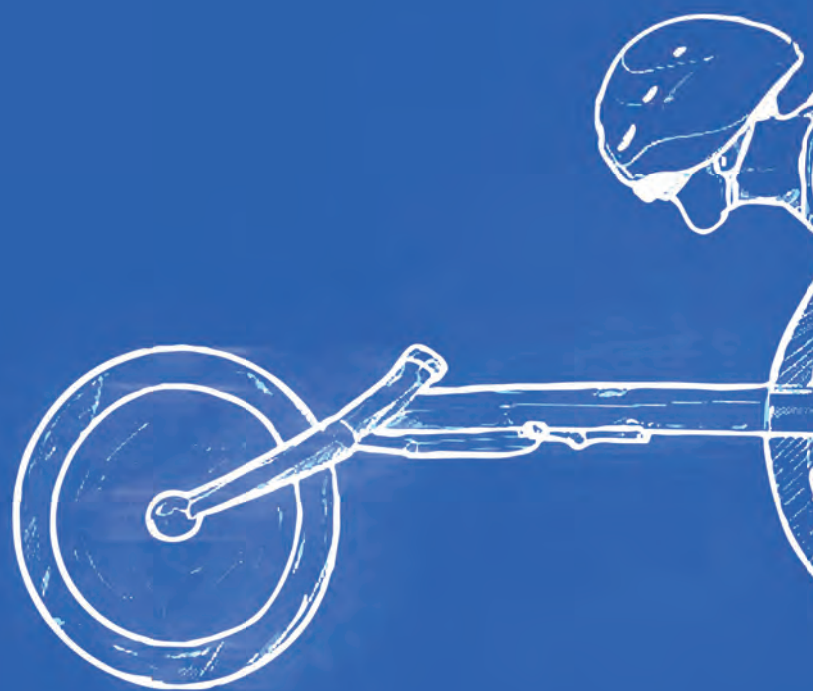
14. Churton E, Keogh JW (2013) Constraints influencing sports wheelchair propulsion performance and injury risk. *Sports Med Arthrosc Rehabil Ther Technol* 5:3
15. Chaikhot D, Reed K, Petroongrad W, Athanasiou F, Van Kooten D, Hettinga FJ (2020) Effects of an Upper-Body Training Program Involving Resistance Exercise and High-Intensity Arm Cranking on Peak Handcycling Performance and Wheelchair Propulsion Efficiency in Able-Bodied Men. *J Strength Cond Res* 34:2267–2275
16. de Groot S, Vegter R, Vuijk C, Dijk F, Plaggenmarsch C, Sloots M, Stolwijk-Swaeste J, Woldring F, Tepper M, Woude L (2014) WHEEL-I: Development of a wheelchair propulsion laboratory for rehabilitation. *J Rehabil Med* 46:493–503
17. Janssen RJF, Vegter RJK, Houdijk H, Van Der Woude LHV, De Groot S (2022) Evaluation of a standardized test protocol to measure wheelchair-specific anaerobic and aerobic exercise capacity in healthy novices on an instrumented roller ergometer. *PLOS ONE* 17:e0274255
18. Chénier F, Pelland-Leblanc J-P, Parrinello A, Marquis E, Rancourt D (2021) A high sample rate, wireless instrumented wheel for measuring 3D pushrim kinetics of a racing wheelchair. *Med Eng Phys* 87:30–37
19. Togni R, Müller M, Plüss S, Taylor WR, Zemp R (2023) A 2D lightweight instrumented wheel for assessing wheelchair functionality/activity. *J Rehabil Assist Technol Eng* 10:205566832311551

Power to the wheelchair people

Whereas the present dissertation mainly focused on wheelchair sports, the findings are also applicable to everyday wheelchair use. The results presented in this dissertation indicate that power can be monitored relatively accurately using just one or two IMUs, and that the RHIDE system can readily give feedback on push- and recovery phase, push length and push angle. This valuable information can be integrated into an activity tracker. Given that the wearables proposed in this dissertation are non-invasive, user-friendly, and affordable, we are on the brink of making wheelchair activity tracking accessible to every wheelchair user.

In a perfect world, the RHIDE system could serve as the next-generation smartwatch, or rather 'smart-rim', designed specifically for wheelchair users. This innovative system would provide timely reminders like "Time to take a break" when your shoulders are at risk of overuse, offer accurate calorie tracking for various activities, and count pushes instead of steps. The wealth of data collected through this smart-rim could help identify wheelchair-accessible routes, enhancing Google Maps with a dedicated 'wheelchair' icon. Perhaps the best part of it all? Say goodbye to bumpy roads and grassy terrain, and compete with your peers to become the reigning King of the rolling Mountain."





APPENDICES
SUMMARY
SAMENVATTING
DANKWOORD
LIST OF PUBLICATIONS
CURRICULUM VITAE



SAMENVATTING

Vanuit de rolstoelsportpraktijk is er een groeiende behoefte om feedback te geven over vermogen. Vermogen kan namelijk worden gebruikt om o.a. de fitheid en vermoeidheid van sporters te monitoren en daarmee overtraining en evt. blessures te voorkomen, om training programma's te individualiseren en te analyseren, en het is bovendien een objectieve maat voor inspanning of intensiteit. Het bepalen van mechanisch vermogen gebeurt bij voorkeur zonder dat sporters of coaches hier hinder van ondervinden. Deze dissertatie is daarom gefocust op het ontwikkelen van een non-invasieve en betaalbare methode om mechanisch vermogen te monitoren in de dagelijkse rolstoel(sport)praktijk. We richten ons met name op rolstoelbasketbal, rolstoeltennis, rolstoelrugby en rolstoelraces, ook wel wheelen genoemd.

From theory to practice: Estimating mechanical power during in-field wheelchair propulsion

Om niet het wiel opnieuw uit te vinden, beginnen we in Hoofdstuk 2 met een samenvatting van de literatuur over het schatten van vermogen met behulp van draagbare sensoren in cyclische sporten. Hieruit komt naar voren dat vermogensmeters in veel cyclische sporten al goed geïntegreerd zijn, maar dat dit voor rolstoelsporten nog niet het geval is. Daarnaast missen we een volledige en beknopte uiteenzetting over het bepalen van mechanisch vermogen tijdens rolstoel rijden. In Hoofdstuk 3, hebben we daarom een theoretisch raamwerk ontwikkeld, waarin de vermogensvergelijking voor rolstoel rijden wordt gedefinieerd en stap voor stap uitgelegd. In het kort komt het erop neer dat vermogen tijdens rolstoel veldsporten, zoals rolstoeltennis, rolstoelbasketbal en rolstoelrugby, kan worden berekend uit 1) de snelheid en versnelling van de rolstoel en 2) de rolweerstand van de sporter en rolstoel samen. In dit hoofdstuk wordt uitgelegd hoe draagbare (inertiële) sensoren, IMUs, kunnen worden gebruikt om vermogen per push te bepalen. Rolweerstand wordt hierbij bepaald met behulp van de veelgebruikte uitroltest. Tijdens deze test laat men de rolstoel vanuit een beginsnelheid passief uitrollen, en wordt de gemeten vertraging gebruikt om rolweerstand te berekenen. Op basis van metingen op een gemotoriseerde loopband, wordt IMU-gabaseerd vermogen per cyclus vergeleken met de schattingen van een referentie systeem. Hieruit blijkt dat het vermogen kan worden geschat met behulp van IMUs, maar dat de rolweerstand tijdens de uitroltest voor sommige personen afwijkt van de rolweerstand tijdens het rolstoel rijden. Mogelijk wordt dit veroorzaakt door de bewegingen van het bovenlichaam. Meer inzicht in de invloed van de romp(beweging) tijdens rolstoelrijden zou dus interessant zijn.

Pushing further: The role of trunk motion on estimating power during wheelchair propulsion

Om de invloed van de romp(beweging) tijdens rolstoelrijden beter te begrijpen, ontwikkelen we in Hoofdstuk 4 een methode om de romp-inclinationehoek tijdens het rolstoelrijden te meten met behulp van IMUs. Een IMU op de borst wordt gebruikt om de oriëntatie van de romp te bepalen. Met slimme wiskundige trucjes kunnen we uit de IMU data op ieder moment bepalen wat de oriëntatie van de IMU - en dus de romp - is ten opzichte van de aarde. Echter, deze wiskundige trucjes worden misleid tijdens het rolstoelrijden, omdat er continu versnellingen en vertragingen in het signaal zijn, en het magnetische veld wordt verstoord door het materiaal van de rolstoelen. In dit artikel hebben we daarom machine learning gebruikt om op de juiste momenten de orientatie-schatting te resetten en zo toch een goede schatting te maken van de IMU-orientatie en dus de romphoek. Nu rompbeweging gemonitord kan worden met een extra IMU op de borst, gaat Hoofdstuk 5 dieper in op de invloed van rompbeweging op rolweerstand. De essentie van dit artikel is het beter begrijpen van de invloed die bewegingen van het bovenlichaam hebben op

de rolweerstand tijdens hand-aangedreven rolstoelrijden. Veel rolstoelgebruikers buigen hun bovenlichaam namelijk naar voren en achteren tijdens het rijden. Omdat in de meeste rolstoelen de voorwielen kleiner zijn dan de achterwielen, hebben de voorwielen een hogere rolweerstand. Door dit verschil zorgt het buigen van de (relatief zware) romp - waardoor de massa naar voren verschuift - ervoor dat de rolweerstand binnen een push-cyclus varieert. We hebben experimenten gedaan met veel, weinig en geen beweging van de romp tijdens het rolstoelrijden, en hebben gekeken naar de invloed van de mate van rompbeweging op de schatting van de rolweerstand. En wat blijkt? Bij weinig rompbeweging komen de rolweerstand tijdens rolstoelrijden en de rolweerstand tijdens de uitroltest overeen. Echter, hoe meer de romp beweegt, hoe groter het verschil tussen deze twee, en dus hoe slechter de schatting van de veelgebruikte uitroltest. Met andere woorden: uitroltesten negeren het effect rompbeweging en dit is daardoor geen nauwkeurige methode om rolweerstand tijdens het rolstoelrijden te bepalen. Corrigeren voor de verandering in gewichtsverdeling tussen voor- en achterwielen is dus nodig om een nauwkeurigere rolweerstand, en dus vermogen, te bepalen.

Power for all: Meeting the demands of different wheelchair user populations

Uit de vorige alinea volgt dat een betere schatting van rolweerstand mogelijk is als de gewichtsverdeling tussen voor- en achterwielen bekend is, zodat hiervoor kan worden gecorrigeerd. Hoofdstuk 6 presenteert daarom een methode om de gewichtsverdeling te voorspellen op basis van IMU data van de romp en rolstoel. Hiervoor hebben we deelnemers laten rolstoelrijden op een loopband waarbij we de gewichtsverdeling tussen voor- en achterwielen continu hebben gemeten met speciale krachtsensoren. Vervolgens werd een machine learning model getraind om de kracht op de voorwielen te voorspellen uit alleen IMU data. Dit resulteerde in een nauwkeurige voorspelling van de gewichtsverdeling. De rolweerstand die hieruit volgde was veel nauwkeuriger (gemiddelde fout: 0,1%) dan de rolweerstand op basis van de uitroltest. In Hoofdstuk 7 wordt bovenstaande informatie samengevoegd om het mechanisch vermogen van rolstoeltennissers te schatten tijdens een 10m sprint in het veld met uitsluitend IMUs. En wat blijkt? Deze is vergelijkbaar met het mechanisch vermogen wat sporters leveren in het lab. Ten slotte wordt in Hoofdstuk 8 en 9 aandacht besteed aan het toegankelijker maken van metingen voor de alledaagse rolstoelpraktijk. Hoofdstuk 8 wordt de trade-off tussen het aantal IMU-sensoren en nauwkeurigheid onderzocht. Hieruit blijkt dat met slechts één IMU op het wiel, de rolstoelsnelheid, versnelling en rotaties bijna net zo nauwkeurig zijn als met twee of drie IMUs. Ten slotte wordt in Hoofdstuk 9 een contact-detectie-systeem, het RHIDE-systeem, gepresenteerd. Door elektronica, ingebouwd in een hoes welke over de push-rim kan worden geplaatst, kan dit systeem timing en positie van handcontact meten. Het systeem is goedkoop en makkelijk in gebruik en daarmee een mooie voorzet voor rolstoelvriendelijk 'activity trackers'.

Al met al kan, met twee IMU's op de rolstoel en een goede uitroltest in de betreffende omgeving, het mechanische vermogen relatief nauwkeurig worden gemeten tijdens rechtlijnig rolstoelrijden in indoor rolstoelveld- en baansporten. Voor dagelijkse rolstoelgebruikers en recreatieve atleten is het gebruik van één IMU voldoende voor fatsoenlijke schattingen van het vermogen. Daarnaast wordt voor 1) een nauwkeurigere vermogensschatting, 2) situaties met een aanzienlijke rompbeweging of 3) het bepalen van push techniek het gebruik van een extra wearable (d.w.z. een op de romp gemonteerde IMU en/of een contact-detectiesysteem [RHIDE]) geadviseerd. IMU's en/of RHIDE-systemen zijn daarom geschikt om de prestaties te verbeteren en het risico op blessures te verminderen op een niet-invasieve en goedkope manier.

SUMMARY

From the perspective of wheelchair sports practice, there is a growing need to provide feedback on power output. Power can be used to monitor athletes' fitness and fatigue levels, thereby preventing overtraining and potential injuries, to individualize and analyze training programs, and it is also an objective measure of effort or intensity. Determining mechanical power preferably occurs without inconveniencing athletes or coaches. Therefore, this dissertation focuses on developing a non-invasive and affordable method to monitor mechanical power in daily wheelchair (sports) practice. We specifically target wheelchair basketball, wheelchair tennis, wheelchair rugby, and wheelchair racing, also known as wheeling.

From theory to practice: Estimating mechanical power during in-field wheelchair propulsion

To avoid reinventing the wheel, Chapter 2 begins with a literature review summarizing power estimation using wearable sensors in cyclic sports. It reveals that power meters are well-integrated in many cyclic sports but not yet in wheelchair sports. Additionally, there is a lack of comprehensive and concise explanation regarding determining mechanical power during wheelchair propulsion. Therefore, in Chapter 3, we develop a theoretical framework defining the power equation for wheelchair propulsion and explain it step by step. In essence, power during wheelchair field sports, such as wheelchair tennis, basketball, and rugby, can be calculated from 1) the wheelchair's speed and acceleration and 2) the combined rolling resistance of the athlete and wheelchair. This chapter explains how wearable (inertial) sensors, IMUs, can be used to determine power per push. Rolling resistance is determined using the commonly used deceleration test, where the wheelchair is passively rolled from an initial speed, and the measured deceleration is used to calculate rolling resistance. Based on measurements on a motorized treadmill, IMU-based power per cycle is compared with estimates from a reference system. It shows that power can be estimated using IMUs, but rolling resistance during the deceleration test deviates for some individuals from rolling resistance during wheelchair propulsion. This might be caused by upper body movements. Therefore, gaining more insight into the influence of trunk (movement) during wheelchair propulsion would be interesting.

Pushing further: The role of trunk motion in estimating power during wheelchair propulsion

To better understand the influence of trunk (movement) during wheelchair propulsion, we develop a method in Chapter 4 to measure trunk inclination angle using IMUs. An IMU on the chest is used to determine trunk orientation. With clever mathematical techniques, we can determine the orientation of the IMU - and thus the trunk - relative to the ground at any given moment from the IMU data. However, these mathematical techniques are misled during wheelchair propulsion due to continuous accelerations and decelerations in the signal, and the magnetic field is disturbed by the wheelchair materials. In this article, we thus use machine learning to reset the orientation estimation at the right moments and thus make a good estimation of the IMU orientation and hence the trunk angle. Now that trunk movement can be monitored with an additional IMU on the chest, Chapter 5 delves into the influence of trunk movement on rolling resistance. The essence of this article is to better understand the influence of upper body movements on rolling resistance during manual wheelchair propulsion. Many wheelchair users lean their upper body forward and backward while driving. Because in most wheelchairs, the front wheels are smaller than the rear wheels, the front wheels have higher rolling resistance. Due to this difference, the bending of the (relatively heavy) trunk - which shifts the mass forward - causes rolling resistance to vary within a push cycle. We conducted

experiments with full, moderate, and no trunk movement during wheelchair propulsion and examined the influence of the degree of trunk movement on the estimation of rolling resistance. And what did we find? With little trunk movement, rolling resistance during wheelchair propulsion matches rolling resistance during the deceleration test. However, the more the trunk moves, the greater the difference between these two, and thus the worse the estimation of the commonly used deceleration test. In other words, deceleration tests ignore the effect of trunk movement, making it an inaccurate method to determine rolling resistance during wheelchair propulsion. Therefore, correcting for the change in weight distribution between front and rear wheels is necessary to determine more accurate rolling resistance, and thus power.

Power for all: Meeting the demands of different wheelchair user populations

From the previous paragraph, it is evident that a better estimation of rolling resistance can be obtained when the weight distribution between front and rear wheels is known, allowing for correction. Therefore, Chapter 6 presents a method to predict weight distribution based on IMU data from the trunk and wheelchair. For this, we had participants drive wheelchairs on a treadmill while measuring the weight distribution between front and rear wheels with special force sensors. Subsequently, a machine learning model was trained to predict the force on the front wheels based solely on IMU data from the trunk and wheelchair. This resulted in highly accurate predictions of weight distribution, and the rolling resistance determined from this was much more accurate (average absolute error: 0.9%, average error: 0.1%) than rolling resistance based on the deceleration test. In Chapter 7, the above information is combined to estimate the mechanical power of wheelchair tennis players during a 10m sprint on the field. With this information from only IMUs, we estimated power per push. After comparison with power generated by the athletes in the lab, we found comparable values. Finally, Chapters 8 and 9 focus on making measurements more accessible for everyday wheelchair practice. Chapter 8 focuses on reducing the number of required IMU sensors and their influence on the accuracy of wheelchair measurements. We demonstrate in this chapter that with just 1 IMU on the wheel axis, wheelchair speed, acceleration, and rotations are almost as accurate as with 2 or 3 IMUs. Finally, Chapter 9 presents a contact detection system, the RHIDE system. By embedding electronics in a cover that can be placed over the wheel rim (or push rim), this system can measure the timing, duration, and position of hand contact. The system is inexpensive and easy to use, making it a great addition for a wheelchair-friendly 'activity tracker'.

Overall, with two IMUs on the wheelchair and a good deceleration test in the respective environment, mechanical power can be measured relatively accurately during straight-line wheelchair propulsion in indoor wheelchair field and track sports. For daily wheelchair users and recreational athletes, the use of one IMU is sufficient for decent power estimates. Additionally, for 1) a more accurate power estimate, 2) situations with significant trunk movement, or 3) determining push technique, the use of an additional wearable (i.e., an IMU mounted on the trunk and/or a contact detection system [RHIDE]) is recommended. IMUs and/or RHIDE systems are therefore suitable for improving performance and reducing the risk of injuries in a non-invasive and inexpensive manner.

DANKWOORD

Wow, wat een jaar. Wat een hoge pieken en wat een diepe dalen. Wat begon als een voortvarend vierjarenplan met hoge ambities, eindigde in een rollercoaster waar het belang van de wetenschappelijke artikelen ver naar de achtergrond verdween. Wat een begon als een mooi avontuur - werken binnen de muren van het indrukwekkende TU Delft - werd al snel werken binnen de muren van een kleine studio in Eindhoven en eindigt op wonderbaarlijke wijze in een kleine studentenkamer in mijn eigen geboortestad Rotterdam. De afgelopen vier jaar kenmerken zich door grote veranderingen, een steile leercurve, en een hoop verschillende thuishavens. Het werk dat voor u ligt is geschreven op werkplekken in Eindhoven, Amsterdam (VU), Den Haag (HHS), De Heen, Vollenhove, Woerden, Rotterdam, Hoeven, Utrecht, Zwitserland en natuurlijk Delft. Op al deze plekken voelde ik me gesteund, geliefd en geïnspireerd. Via deze weg wil ik iedereen bedanken die hier een bijdrage aan heeft geleverd.

DirkJan, vanaf het begin had ik meteen een klik met jou. Bedankt voor je luisterend oor, je steun, je begrip, je vertrouwen, het meedenken wat goed voor *mij* is, het afmaken van m'n zinnen ;), en de koffietjes, autoritjes en zelfs ski-tochtjes in Zwitserland. Toen ik jou mailde dat ik even een week niet wilde werken, heb je me meteen opgebeld. Je hebt me alle ruimte en vertrouwen gegeven en hebt me geholpen waar je kon. Ik heb veel van je geleerd, zowel over de wetenschap als over het leven, en je weet vaak de vinger op de zere plek te leggen. Onze samenwerking liep als een trein, dat ga ik echt missen. Ik had me geen betere mentor kunnen wensen.

Marco en Monique, bedankt voor alle uurtjes sparren over rolstoelonderzoek en over andere dingen (schuttingen, omgezaagde bomen, kapotte verwarmingen, vroeger, mijn nieuwe vriend en natuurlijk... de was – welke wel of niet hing te drogen op de achtergrond bij Marco). Tijdens de discussies over mijn artikelen of experimenten werd jullie tegenspraak niet altijd direct in dank afgenomen, maar gelukkig konden we daar achteraf altijd om lachen. Marco, bedankt dat je altijd beschikbaar bent en de tijd neemt. Bedankt voor je luisterend oor en voor de aandachtige en grondige feedback op al m'n stukken. Monique, bedankt voor je betrokkenheid, vrolijkheid en enthousiasme. Je bent een voorbeeld voor hoe ik mijn ideale werk-privéleven zou willen leiden.

Knoek, door jou ben ik biomechanica echt leuk gaan vinden, en heb ik ontdekt dat dit bij me past. Jij en Peter geloofden in me en enthousiasmeerden me voor het doen van onderzoek. Bedankt! BWSB'ers en docenten, bedankt voor de uitdagingen en gezelligheid, ik ben nog altijd trots op het zijn van een BWSB'er. Roald, Sander, InnoSportLab, bij en van jullie ik heb zo veel geleerd! Bedankt voor alle kansen die jullie me gaven en de geweldige tijd. Medical Delta, ondanks dat ik maar kort bij jullie heb gewerkt, heb ik hier geleerd wat collegialiteit echt inhoudt. Wat een fijne mensen zijn jullie. WheelPower team, rolstoelsporters, en coaches, jullie enthousiasme en gedrevenheid zijn een grote inspiratiebron. Rowie, m'n WheelPower-PhD-zusje, wat fijn dat jij er was. We konden samen onze struggles delen, hebben leuke congressen bezocht, veel te veel betaald voor een hotelkamer waarin we maar één uur hebben geslapen, en uiteindelijk toch nog een gezamenlijk paper geschreven. DEMO, bedankt voor de prettige samenwerking en het meedenken bij het ontwikkelen van het RHIDE-systeem. Wiebe, het was een eer om je te leren kennen. Bedankt voor het opnemen in jullie groep, de leuke eet-avondjes en gezamenlijke zwemsessies in Zwitserland.

Beste studenten, Robert, Ganesh, Twan, Nathalie, Victor, Marije, het was leerzaam om jullie te begeleiden tijdens jullie afstudeeronderzoek en ieder van jullie heeft op zijn manier bijgedragen aan nieuwe inzichten, kennis of onderzoek. Thomas, Jesper, wat een energie leverden jullie. Jullie kregen een super ambitieus project om krachtsensoren in de voorwielen te maken, met de opdracht om direct te beginnen vanwege het krappe tijdschema. Binnen 10 weken hebben jullie een 3D-model van de voorwielsensor gemaakt, prototypes geprint, getest, problemen opgelost, opnieuw geprint, getest, en een bedrijf gevonden om dit te leveren. Jullie samenwerking is voor mij hét voorbeeld van de wederzijdse versterking tussen de aanpakkers- en 'trial-and-error' mentaliteit van het toegepast onderwijs en berekenende modelmatige aanpak van de universiteit. Vera en Louise, dreamteam. Letterlijk bloed, zweet en tranen heeft het ons gekost om de loopbandmetingen tot een goed einde te brengen. Louise, jij nam het stokje van Jesper en Thomas over door de sensoren te leren bedienen. Wat je ook moest doen, je deed het met veel enthousiasme. Je hebt een ontzettend goed oog voor detail, blijft nadenken over het grote geheel en neemt feedback razendsnel op. Tijdens de metingen zat jij uren op de grond met 'jouw' sleutel 10 om de schroeven aan te draaien of de sensoren te resetten. Als we weer nieuwe stappen bedachten voor in het protocol, noteerde je alles, en voor we het wisten had jij een uitgebreid stappenplan opgezet om te voorkomen dat we iets zouden vergeten tijdens de metingen. Later heb je dit weer ingekort, om te voorkomen dat we de draad kwijtraakten in alle kleine stappen die we inmiddels hadden geautomatiseerd. Vera, jouw inzet, gedrevenheid, punctualiteit en stabiliteit waren onmisbaar voor zo'n groot meetproject als dit. Als ik aan iemand de systemen toe durfde te vertrouwen ben jij het. Waar ik soms alle kanten op kan schieten, bleef jij rustig en zorgde je voor de veiligheid van de proefpersonen. Ook was je altijd scherp en kritisch op de biomechanica achter wat we deden, en als ik even begon te twijfelen, plande ik een brainstormsessie met jou in. Met jullie twee was ik dan ook niet in paniek toen ik de eerste meetweek door COVID thuis moest blijven. Jullie konden dit. Uiteindelijk hebben we vier weken aan experimenten, met een killer-planning en de meest uiteenlopende errors zonder al te veel problemen uitgevoerd en is dit de basis voor vele artikelen in dit proefschrift. Meiden, bedankt voor de geweldige tijd en het keiharde werk! Puck, jouw nieuwsgierigheid is aanstekelijk. Dankzij jou heeft het RHIDE-systeem zijn laatste zetje gehad. Je hebt de data nauwkeurig geanalyseerd en weet je waar je mee bezig bent. Hopelijk resulteert dit in twee mooie artikelen. Charlie, Neal, Wendy, Oscar, en Sander, het was een eer jullie te mogen begeleiden tijdens jullie stages in uiteenlopende richtingen. Jeroen, neefje, ik heb altijd al gehoopt een keer met jou samen te mogen werken aan een project, en wat leuk dat dit werkelijkheid werd! Omdat jij een stage zocht en ik iemand met een mechatronica-achtergrond kwam dit samen. Het was bijzonder om samen te brainstormen en elkaars werelden wat beter te leren kennen. Wellicht ooit nog eens!

Liefste collega's van Kantoor 1, tegenwoordig doorontwikkeld tot Office 1, bedankt voor alle leuke momenten. Bart, filosoof op hardloopschoenen, van SportCie tot InnoSportLab tot TU Delft, we blijven elkaar steeds tegenkomen en ik vind het gek om me voor te stellen dat dit misschien stopt. Bedankt voor alle inzichten, het brainstormen, voor onze high-speed sportcultuur-reis in Japan, de slappe lach en nog veel meer! Martijn, we hebben veel goede gesprekken gevoerd en uren gebrainstormd over het ontwerp van een duw-rolstoel, nieuwe toepassingen voor jouw stuurbare naalden, en later over de MDR. Bedankt voor deze ontspanmomentjes tussen het harde werken door! Marco, Teddy, Ton, Anton, Christoff, Sam, Gabrielle, Hassan, het was gezellig om met jullie op kantoor te werken, te padellen of te kletsen over gele auto's (toch Teddy?), de kleur geel (Fayence oid), fietsen of Italiaans eten. Teddy, bedankt voor de dans-inspiratie, de grapjes en nutteloze feitjes. Ton, bedankt voor al het lachen!

Chris, ik ga onze dagelijkse Nederlands-koffieleut-half uurtjes missen. Suus, m'n enige vrouwelijke kantoor 1 maatje. Ondanks dat we elkaar bijna continu afwisselden met onze buitenlandreisjes was het altijd fijn om even te sparren over de dagelijkse issues en samen interessante (en minder interessante) bijeenkomsten te bezoeken. Dance Team, Monika, Vera, Jette, Niko, it was a pleasure to dance with you. We hebben zo veel gelachen om de dansspasjes, Neil, 'Come to live elegantly' of gewoon zomaar. Lieve (pirates of the Carib)BME'ers bedankt voor de fantastische zeiltocht op het IJsselmeer, gezellige pauzes, borrels, zeldzame stapnachten en het bijschaven van m'n Engels. Haagse hogeschool collega's, Daniel, Melle, Carlijn, bedankt voor jullie betrokkenheid, hulp, het meedenken, de pepernoten OF paaseitjes en de heerlijke sfeer! Daniel, je bent speciaal voor mij tijdens Corona naar de HHS gegaan om me bij alle metingen te helpen. Hoofdstuk 4 ligt er mede dankzij jouw inzet, bedankt! En dan nog alle lieve bewegingswetenschappers, waar ik als adoptie-bw'er vaak toch nog even binnen sneakte. Bij jullie blijf ik me toch het allermeeste thuis voelen. Vanuit Rotterdam is het reizen niet meer zo handig, maar het was fijn om af en toe onderdeel van jullie te mogen zijn. Bedankt voor de leuke feestjes, bruiloftsweekend in limburg, ECR-weekenden, vrijmibo's, zaalvoetbalpartijen, lunches en koffiemomentjes. Ik blijf jullie vast zien. Dear Phutsal Doctors, thanks for the fun, laughs, drinks and great phutsal play!

Lieve familie, ik ben dankbaar dat ik deel mag uitmaken van zo'n lieve, betrokken en gezellige familie als van Dijk. Pap, bedankt voor je betrokkenheid, luisterend oor, nuchterheid, het meedenken over bandenspanningsmetingen van mijn rolstoelwielen en voor je trots. Mariette, Rob, bedankt voor de fijne gesprekken, lekkere etentjes en voor jullie stralende aanwezigheid. Familie Koot, wat een inspiratie, zelfstandigheid en ambitie is hier aanwezig. Marc, Marja, bedankt voor de steun en geborgenheid. Oma Koot, ik koester alle momenten en de diepe connectie die we samen hadden. Ik ben ongelooflijk trots op u. Oma van Dijk, ik ben eindelijk afgestudeerd! Bedankt voor alle liefde, knuffels, goede gesprekken, en de momentjes gewoon lekker samen liggen en naar het plafond kijken. Lieve oma's, jullie zijn mijn grootste voorbeeld. Annet, Carlo, Renee, bedankt voor het warme welkom.

Isabelle, wat een avonturen hebben wij al samen meegemaakt. Van pioniers op de amstel gold race (toen het nog bijzonder was om twee jonge vrouwen alleen op de racefiets te zien), tot schaatsen op de nieuwkoopse plassen, zware trainingen of toertochten waarbij ik altijd nét iets te vroeg juich dat we het hebben gehaald en trailruns waarbij we achteraf complimenten krijgen hoe wij toch 'let-ter-lijk de vol-le-di-ge 16 kilometer aan één stuk door kunnen lopen kletsen'. Bedankt voor de lach, traan, luchtige en diepe gesprekken en alle sportieve uitdagingen! Lies, Marloes, mede PhD-aapies, wat fijn dat jullie als één van de weinigen niet-collega's wél begrijpen waarom een PhD doen leuk is. Enjoy the trip! Sel, ik mis jouw projectjes op Uilenstede, waarbij ik de hele dag achter je aan kon lopen en m'n dagelijkse perikelen kon vertellen. Ik hou van jouw rust, creativiteit en relativering. Simon, je was m'n eerste BW-vriendinnetje, en tegenwoordig zie ik je gelukkig weer veel. Je hebt me door het afgelopen jaar heen gesleept, we hebben veel gelachen en we begrijpen elkaar goed. Ik ga je heel erg missen in Rotterdam, maar we blijven elkaar zien! Lieve Suus, ik ken niemand die vriendinnen hoger op de prioriteitenlijst heeft staan dan jij. Bedankt voor alle liefde, luchtigheid, gieter-avondjes, goede wijn en leuke momenten samen. Iet, wij kunnen elkaar maanden (en soms zelfs langer) niet spreken, maar het is altijd meteen weer als vanouds. Je bent m'n favoriete turn-, zeil-, snoepverzamelings-, windsurf- en bovenal n/lepel-maatje. Lee, ik vind het zo leuk dat we elkaar weer meer zien! Bedankt voor het meedenken met de voorkant, alle slappe lachen en goede gesprekken. Puck, Niels, het is altijd

heerlijk om bij jullie te zijn. Of we nu een berg beklimmen met enkelpijn, BWSB-verhalen ophalen of de schaatspodcast nabespreken, met jullie is het altijd goed! Yvonne, bedankt voor alle museumbezoekjes en patisserie-bijtscholing. Franka, ik ben zo blij met jou als huisgenootje en kijk alweer uit naar onze koffie-ochtendjes en klusprojecten. Lidia, wat heerlijk om met jou samen te wonen. ik had me geen betere tijdelijke vervanger van Franka kunnen wensen!

Lieve Olaf, wat hebben wij mooie momenten beleefd. Ik word nog steeds emotioneel als ik bedenk wat je voor me betekent. Bedankt voor je rust, avontuur, luisterend oor en je onmisbare steun het afgelopen jaar.

Lieve Simon, Lies, Daan. Een reisje naar Korea, wigwamvakantie, met 40 graden op een zolderkamertje slapen in Leuven, of alle K2 zoekt K3 afleveringen (inclusief bonusmateriaal) terugkijken, met jullie is het altijd één groot feest. Lieve Simon, ons hele leven loopt onbewust steeds samen en ik zou niet willen dat dat anders was. Jij zorgt voor humor en bent onze mama als het nodig is. Lieve Lies, jij houdt ons, net als juffrouw Marion, in balans als we gaan kleuteren en bent de beste kritische vragensteller die ik ken. Liesje, Simon, of we nu met z'n drieën in Salou op een slaapkamer liggen te chapnatten of in een 120m-bedje in Londen lepeltje-lepeltje de hipste vloggers bekijken, jullie houden me up-to-date en leren me te relaxen. Lieve Daan, ondanks dat je sinds een paar jaar in Londen woont, duurt een gemiddeld telefoongesprek tussen ons zo'n 1,5u. Je kunt precies de goede dingen zeggen. Met jou is alles leuker en krijg ik instant de slappe lach. Bedankt voor alle fietskilometers, boerencake met slagroom en M&M's, logeerpartijtjes, fireman, (werk)weekjes vakantie en meer. Op naar veel meer avonturen samen!

Lieve Thijs, nog nooit heb ik iemand ontmoet met zó weinig interesse in biomechanica als jij. Je opent een nieuwe wereld voor me, laat me in mezelf geloven, haalt me uit m'n bewegings-wetenschappenbubbel en laat mijn vooroordelen over psychologen verdwijnen (lees: neemt sinds kort de trap). We vullen en voelen elkaar perfect aan. Bedankt voor je vrolijkheid, vertrouwen, stomme grapjes, liefde, zorgzaamheid, sprong in het diepe en je eeuwige geduld ♥

Mam, je bent de meest pure, liefdevolle en coolste persoon die ik ken en de belangrijkste vrouw in m'n leven. Ik ben ongelooflijk trots op je. Love you loads!

LIST OF PUBLICATIONS

van Dijk, M.P., Willemse, P., de Vries, W.H.K., Hoozemans, M.J.M., Veeger, H.E.J. (submitted). Validating instantaneous power output based on a wearable sensor system that measures inertial characteristics and hand-rim contact during wheelchair propulsion.

van Dijk, M.P., Heringa, L.I., Berger, M.A.M., Hoozemans, M.J.M., Veeger, H.E.J. (2024). Towards an accurate rolling resistance: Estimating intra-cycle load distribution between front- and rear wheels during wheelchair propulsion, *Journal of Sports Science*, doi: 10.1080/02640414.2024.2353405 ☆

Ferlinghetti, E.[†], **van Dijk, M.P.**[†], Willemse, P., Veeger, H.E.J., Vegter, R.J.K., Lancini, M. (submitted). How we RhIDE the wheelchair: Cross-validation of two feasible and inexpensive systems that detect time and position of hand contact during wheelchair propulsion
[†] *these authors contributed equally*

Janssen, R.J.F., **van Dijk, M.P.**, Rietveld, T., de Groot, S., van der Woude, L.H.V., Houdijk, H., Vegter, R.J.K. (under review). The combined strength of standardized lab sprint testing and wheelchair mobility field testing for wheelchair tennis players, *Sports Biomechanics* ☆

Janssen, R.J.F., **van Dijk, M.P.**, Rietveld, T., de Groot, S., van der Woude, L.H.V., Houdijk, H., Vegter, R.J.K. (2024). COMPARISON BETWEEN OUTCOMES OF A SPRINT TEST ON A WHEELCHAIR ERGOMETER AND ON-COURT AMONG WHEELCHAIR TENNIS PLAYERS, ISBS Proceedings Archive.

van Dijk, M.P., Hoozemans, M.J.M., Berger, M.A.M., Veeger, H.E.J. (2024). From theory to practice: Monitoring mechanical power output during wheelchair field and court sports using inertial measurement units, *Journal of Biomechanics*, <https://doi.org/10.1016/j.jbiomech.2024.112052> ☆

van Dijk, M. P., Hoozemans, M. J. M., Berger, M. A. M., & Veeger, D. J. H. E. J. (2024). Trunk motion influences mechanical power estimates during wheelchair propulsion. *Journal of Biomechanics*, 163, Article 111927. <https://doi.org/10.1016/j.jbiomech.2024.111927> ☆

de Vries W.H.K., van der Slikke R.M.A., **van Dijk M.P.**, Arnet U. (2023). Real-Life Wheelchair Mobility Metrics from IMUs. *Sensors*; 23(16):7174. <https://doi.org/10.3390/s23167174>

van Dijk M.P., van der Slikke R.M.A., Rupf R., Hoozemans M.J.M., Berger M.A.M., Veeger H.E.J. (2022). Obtaining wheelchair kinematics with one sensor only? The trade-off between number of inertial sensors and accuracy for measuring wheelchair mobility performance in sports. *J Biomech. Jan*;130:110879. doi: 10.1016/j.jbiomech.2021.110879 ☆

De Vette, V. G., Veeger, H. E. J., & **van Dijk, M. P.** (2022). Using Wearable Sensors to Estimate Mechanical Power Output in Cyclical Sports Other than Cycling: A Review . *Sensors*, 23(1), Article 50. <https://doi.org/10.3390/s23010050> ☆

van Dijk, M. P.; van der Slikke, R. M. A.; Berger, M. A.M.; Hoozemans, M. J.M.; and Veeger, H.E.J. (2021). LOOK MUMMY, NO HANDS! THE EFFECT OF TRUNK MOTION ON FORWARD WHEELCHAIR PROPULSION, ISBS Proceedings Archive: Vol. 39: Iss. 1, Article 80. Available at: <https://commons.nmu.edu/isbs/vol39/iss1/80>

van Dijk, M.P., Blik, O., and van Der Slikke, R.M.A. (2021). Patent: “A Method For Automatically Measuring a Propulsive Power Applied to a Pushrim of a Wheelchair by a User of the Wheelchair”. [NL2029083B1](https://patents.google.com/patent/NL2029083B1); WO2023033646A1

van Dijk M.P., Kok M., Berger M.A.M., Hoozemans M.J.M., Veeger H.E.J. (2021). Machine Learning to Improve Orientation Estimation in Sports Situations Challenging for Inertial Sensor Use. *Front Sports Act Living*. Aug 3;3:670263. doi: 10.3389/fspor.2021.670263. PMID: 34414370; PMCID: PMC8369156 ☆

van Dijk M.P., Beek P.J., van Soest A.J. (2020). Predicting dive start performance from kinematic variables at water entry in (sub-)elite swimmers. *PLoS ONE* 15(10): e0241345. <https://doi.org/10.1371/journal.pone.0241345>

van Dijk, M., Treur, J. (2018). Physical Activity Contagion and Homophily in an Adaptive Social Network Model. In: Nguyen, N., Pimenidis, E., Khan, Z., Trawiński, B. (eds) *Computational Collective Intelligence. ICCCI 2018. Lecture Notes in Computer Science*, vol 11055. Springer, Cham. https://doi.org/10.1007/978-3-319-98443-8_9



Curriculum Vitae

MARIT VAN DIJK

13-03-1994 Born in Rotterdam, the Netherlands

WORK EXPERIENCE

jan 2020-may 2024 **PhD researcher** – BioMechanical Engineering, TU Delft, Delft
may 2022-feb 2023 **Innovation Manager** – Medical Delta, Delft
jun 2019-jul 2019 **Software developer & project lead** – UNIMAS Universiti Sarawak, Malaysia
aug 2016-Mar 2019 **Embedded scientist Biomechanics** – KNZB / InnoSportLab, Eindhoven
feb 2016-jul 2016 **Research intern gait adaptability** – DNO (Reade), Amsterdam
jan 2015-jan 2017 **Swimming instructor** – Sportbedrijf Amstelveen, Amstelveen

EDUCATION

nov 2023-dec 2023 **Innovation Ecosystem & Business Design** – EIT Manufacturing, Tartu, Estonia
jan 2017-nov 2020 **MSc Artificial Intelligence (cum laude)** – Vrije Universiteit, Amsterdam
aug 2017-mar 2019 **MSc Human Movement Sciences (cum laude)** – Vrije Universiteit, Amsterdam
sep 2012-jul 2016 **BSc Bewegingswetenschappen** - Vrije Universiteit, Amsterdam
aug 2006-jun 2012 **VWO Natuur & Techniek** – Roncalli, Bergen op Zoom

AWARDS & GRANTS

2021 **Patent: Method for automatically measuring propulsive power** - NL2029083
2021 **Grant: Technology that makes people move (12.5k)** – TU Delft HI and SEI
2019 **AISS master thesis award 2019** – Amsterdam Institute of Sport Sciences

